



HAL
open science

Discovery of mosquito molecular factors modulating arbovirus infection in *Aedes aegypti*

Élodie Couderc

► **To cite this version:**

Élodie Couderc. Discovery of mosquito molecular factors modulating arbovirus infection in *Aedes aegypti*. Microbiology and Parasitology. Sorbonne Université, 2024. English. NNT : 2024SORUS199 . tel-04739370

HAL Id: tel-04739370

<https://theses.hal.science/tel-04739370v1>

Submitted on 16 Oct 2024

HAL is a multi-disciplinary open access archive for the deposit and dissemination of scientific research documents, whether they are published or not. The documents may come from teaching and research institutions in France or abroad, or from public or private research centers.

L'archive ouverte pluridisciplinaire **HAL**, est destinée au dépôt et à la diffusion de documents scientifiques de niveau recherche, publiés ou non, émanant des établissements d'enseignement et de recherche français ou étrangers, des laboratoires publics ou privés.

Sorbonne Université

Ecole doctorale 515 "Complexité du Vivant"

Unité Interactions Virus-Insectes, Institut Pasteur, CNRS UMR2000, Paris

Discovery of mosquito molecular factors modulating arbovirus infection in *Aedes aegypti*

Par Elodie Couderc

Thèse de Doctorat de Virologie

Dirigée par Louis Lambrechts & Sarah Merkling

Présentée et soutenue publiquement le 6 septembre 2024

Devant un jury composé de :

Dr. Jean-Luc Imler, Professeur	Rapporteur
Dr. Kevin Maringer, Associate Professor	Rapporteur
Dr. Pascal Miesen, Assistant Professor	Examineur
Dr. Allison Bardin, Directrice de Recherche	Examinatrice, Présidente du jury
Dr. Anna-Bella Failloux, Professeure	Membre invitée
Dr. Louis Lambrechts, Directeur de Recherche	Directeur de thèse
Dr. Sarah Merkling, Chargée de Recherche	Co-encadrante de thèse



ABSTRACT

Arthropod-borne viruses (arboviruses) significantly impact global health, causing diseases with high morbidity and mortality. Mosquito-borne flaviviruses, notably dengue (DENV) and Zika (ZIKV) viruses, are of particular concern. These viruses are primarily transmitted by the *Aedes aegypti* mosquito, which is expanding its range due to global changes. Currently, there are no globally approved vaccines or specific antivirals for these viruses, and traditional vector control methods are hindered by insecticide resistance.

Concerns about the future of vector control have led to alternative strategies aimed at manipulating the biology of vectors to reduce their vector competence, *i.e.*, the ability of mosquitoes to become infected and transmit pathogens. The release of modified mosquitoes that cannot transmit pathogens is a potential strategy to reduce the incidence of human disease. Thus, there is a growing need to identify optimal targets for modification, and mosquito molecular factors that modulate arbovirus transmission are promising candidates.

However, much of the knowledge on mosquito vector competence derives from studies in the insect model *Drosophila melanogaster* and does not fully recapitulate mosquito responses. Therefore, implementation of mosquito-specific approaches is essential to investigate intrinsic factors underlying vector competence.

In this context, this PhD thesis presents three *in vivo* approaches to investigate molecular factors that influence flavivirus infection, dissemination, and transmission in *Aedes aegypti*.

The **first chapter** is dedicated to the functional characterization of a *Vago*-like gene, *VLG-1*, in *Ae. aegypti* in the context of flavivirus infection. Arthropod *Vago* genes are often described as analogs of mammalian cytokines with antiviral functions. Strikingly, a *VLG-1* mutant line generated by CRISPR/Cas9-mediated gene editing revealed that in *Ae. aegypti*, *VLG-1* promotes DENV and ZIKV dissemination within the mosquito, challenging the idea that *Vago*-like genes are conserved antiviral factors. Tissue-specific transcriptome analysis indicated that *VLG-1* affects biological processes potentially linked to viral replication, such as the oxidative stress response.

The **second chapter** focuses on the discovery of a novel non-canonical antiviral factor, cytochrome *P450 4g15*, associated with a natural DENV resistance phenotype in a field-derived *Ae. aegypti* population. Induction of cytochrome *P450 4g15* in the midgut after bloodmeal ingestion hinders DENV infection. Polymorphisms in this gene's promoter sequence control its expression level and the probability of successful DENV infection, marking the first report of natural gene variants impacting DENV resistance in *Ae. aegypti*.

ABSTRACT

The **third chapter** examines candidate DENV receptors in *Ae. aegypti*, with a specific emphasis on *prohibitin-2*. This study demonstrated a proviral effect of *prohibitin-2* on DENV replication in mosquito bodies. Nevertheless, despite employing a range of experimental techniques, *prohibitin-2* did not exhibit a substantial role in DENV entry into mosquito midguts *in vivo*. These findings indicate that *in vitro* identification of viral receptors may not necessarily translate to *in vivo* confirmation of their role in viral entry.

Overall, this PhD thesis contributes to advancing our understanding of mosquito-virus interactions, identifying new targets for vector control strategies, and highlighting the complexity of the molecular mechanisms underlying vector competence. This work emphasizes the necessity for *in vivo* research and underscores the value of exploiting the natural genetic diversity of field-derived mosquito populations to gain insights into the complex mechanisms governing mosquito vector competence for flaviviruses and to develop innovative strategies for controlling mosquito-borne diseases.

Keywords: *Aedes aegypti*, dengue virus, flavivirus, vector competence, host dependency factors, host restriction factors.

RÉSUMÉ EN FRANÇAIS

Les virus transmis par les arthropodes (arbovirus) impactent significativement la santé humaine à l'échelle mondiale, causant des maladies avec une morbidité et une mortalité élevées. Les flavivirus transmis par les moustiques, notamment les virus de la dengue (DENV) et Zika (ZIKV), sont particulièrement préoccupants. Ces virus sont principalement transmis par le moustique *Aedes aegypti*, dont la répartition géographique s'étend en raison des changements globaux. Actuellement, il n'existe pas de vaccins approuvés à grande échelle ni d'antiviraux spécifiques pour ces virus, et les méthodes traditionnelles de contrôle des vecteurs sont entravées par la résistance aux insecticides.

Face à ces défis, des stratégies alternatives ont été développées pour manipuler la biologie des vecteurs afin de réduire leur compétence vectorielle, c'est-à-dire leur aptitude à être infectés et à transmettre des pathogènes. Une stratégie potentielle est de relâcher de moustiques modifiés incapables de transmettre des agents pathogènes. Il est donc crucial d'identifier des cibles optimales pour ces modifications, et les facteurs moléculaires des moustiques qui modulent la transmission des arbovirus sont des candidats prometteurs.

Cependant, une grande partie des connaissances actuelles sur la compétence vectorielle des moustiques provient d'études sur l'insecte modèle *Drosophila melanogaster*, qui ne reproduit pas entièrement les réponses des moustiques. Des approches spécifiques aux moustiques sont donc essentielles pour étudier les facteurs intrinsèques de leur compétence vectorielle.

Cette thèse de doctorat présente trois approches *in vivo* pour étudier les facteurs moléculaires influençant l'infection, la dissémination et la transmission des flavivirus chez *Aedes aegypti*.

Le **premier chapitre** traite de la caractérisation fonctionnelle *in vivo* d'un gène *Vago-like*, *VLG-1*, chez *Ae. aegypti* dans le contexte de l'infection par les flavivirus. De façon surprenante, une lignée mutante de *VLG-1* générée par CRISPR/Cas9 a montré que chez *Ae. aegypti*, *VLG-1* favorise la dissémination de DENV et ZIKV dans le moustique, remettant en question le dogme affirmant que les gènes *Vago-like* sont des facteurs antiviraux conservés chez les arthropodes. Une analyse transcriptomique organe-spécifique a révélé que *VLG-1* affecte des processus biologiques potentiellement liés à la réplication virale, tels que la réponse au stress oxydatif.

Le **deuxième chapitre** rapporte la découverte d'un nouveau facteur antiviral non canonique, le cytochrome *P450 4g15*, associé à une résistance naturelle à DENV dans une population d'*Ae. aegypti*. L'induction de ce gène dans le tube digestif après un repas sanguin entrave l'infection par DENV. Des polymorphismes dans la séquence promotrice de ce gène contrôlent

son expression et la probabilité d'infection par DENV. Cette étude est la première à démontrer l'impact de variants naturels d'un gène sur la résistance d'*Ae. aegypti* à DENV.

Le **troisième chapitre** décrit la caractérisation *in vivo* de potentiels récepteurs de DENV chez *Ae. aegypti*, en particulier *prohibitin-2*. Malgré un effet proviral de *prohibitin-2* sur la réplication de DENV dans le corps du moustique, ce gène n'a pas montré de rôle significatif dans l'entrée de DENV dans le tube digestif du moustique *in vivo*. Ces résultats indiquent que l'identification *in vitro* de récepteurs viraux ne garantit pas la confirmation *in vivo* de leur rôle dans l'entrée virale.

En résumé, cette thèse de doctorat contribue à faire avancer notre compréhension des interactions moustiques-virus, à identifier de nouvelles cibles pour le contrôle des vecteurs et à mettre en lumière la complexité des mécanismes moléculaires de la compétence vectorielle. Elle met en avant la nécessité de la recherche *in vivo* et l'importance d'exploiter la diversité génétique naturelle des populations de moustiques pour développer des stratégies innovantes de contrôle des maladies transmises par les moustiques.

Mots clés : *Aedes aegypti*, virus de la dengue, flavivirus, compétence vectorielle, facteurs de dépendance à l'hôte, facteurs de restriction.

TABLE OF CONTENTS

ABSTRACT	2
RÉSUMÉ EN FRANÇAIS	4
TABLE OF CONTENTS	6
LIST OF FIGURES & TABLES	8
<u>-GENERAL INTRODUCTION- REVEALING THE MOSQUITO'S ASSETS: DISCOVERY OF MOSQUITO MOLECULAR FACTORS MODULATING ARBOVIRUS INFECTION IN <i>Aedes aegypti</i> MOSQUITOES</u>	10
I- MOLECULAR INTERACTIONS BETWEEN MOSQUITOES AND ARBOVIRUSES	11
I.A) ARBOVIRUS TRANSMISSION BY <i>Aedes</i> MOSQUITOES	11
I.B) ANTIVIRAL RESPONSE OF <i>Aedes</i> MOSQUITOES TO MOSQUITO-BORNE FLAVIVIRUSES	18
I.C) FLAVIVIRUS HOST DEPENDENCY FACTORS IN <i>Ae. aegypti</i> MOSQUITOES	23
I.D) GENETIC BASIS OF MOSQUITO-ARBOVIRUS INTERACTIONS	25
II- APPROACHES FOR DISCOVERY OF MOSQUITO MOLECULAR FACTORS MODULATING ARBOVIRUS INFECTION & TRANSMISSION	27
II.A) FORWARD GENETIC APPROACHES: FROM OBSERVATION OF THE MOSQUITO PHENOTYPE TO IDENTIFICATION OF HOST MOLECULAR FACTORS	27
II.B) REVERSE GENETIC APPROACHES: FROM GENE EXPRESSION TO INFECTION PHENOTYPE	32
CONCLUSION	36
REFERENCES	38
<u>-CHAPTER 1- A VAGO-LIKE GENE ENHANCES DENGUE AND ZIKA VIRUS DISSEMINATION IN <i>Aedes aegypti</i></u>	54
ABSTRACT	55
INTRODUCTION	56
RESULTS	57
<i>VLG-1</i> IS A VAGO-LIKE GENE EXCLUSIVELY FOUND IN THE CULICINAE	57
<i>VLG-1</i> IS PERSISTENTLY INDUCED BY BLOODMEAL INGESTION IN <i>Ae. aegypti</i>	60
<i>VLG-1</i> PROMOTES SYSTEMIC DISSEMINATION OF DENV AND ZIKV IN <i>Ae. aegypti</i>	64
<i>VLG-1</i> AND <i>VLG-2</i> HAVE NON-ADDITIVE PROVIRAL EFFECTS ON DENV IN <i>Ae. aegypti</i>	67
THE TRANSCRIPTIONAL LANDSCAPE OF <i>VLG-1</i> MUTANTS IS BROADLY ALTERED	67
DISCUSSION	71
ACKNOWLEDGEMENTS	73
AUTHOR CONTRIBUTIONS	73
METHODS	74
SUPPLEMENTARY FIGURES	82
SUPPLEMENTARY TABLES	88
REFERENCES	95

-CHAPTER 2- CYTOCHROME P450 4G15 POLYMORPHISM MEDIATES DENGUE VIRUS SUSCEPTIBILITY IN A FIELD-DERIVED Aedes Aegypti POPULATION **100**

ABSTRACT	101
INTRODUCTION	102
I- NATURAL RESISTANCE PHENOTYPE LEADS TO IDENTIFICATION OF A NOVEL ANTIVIRAL FACTOR	102
II- KNOWN FUNCTIONS OF CYTOCHROMES P450	105
RESULTS	105
I- P450 4G15 IS A MIDGUT ANTIVIRAL RESPONSE FACTOR DURING EARLY DENV INFECTION	105
II- CORRELATION BETWEEN P450 4G15 PROMOTER HAPLOTYPES AND EXPRESSION LEVELS	113
DISCUSSION	117
METHODS	119
SUPPLEMENTARY FIGURES	126
SUPPLEMENTARY TABLES	129
ACKNOWLEDGEMENTS	130
REFERENCES	131

-CHAPTER 3- IN VIVO CHARACTERIZATION OF A CANDIDATE DENGUE VIRUS RECEPTOR, PROHIBITIN-2, IN Aedes Aegypti MOSQUITO MIDGUTS **134**

ABSTRACT	135
INTRODUCTION	136
I- DEFINITION OF VIRUS RECEPTORS	136
II- APPROACHES FOR DISCOVERY OF DENV RECEPTORS IN MOSQUITOES	137
RESULTS	141
I- SCREENING OF DENV CANDIDATE RECEPTORS IN <i>Ae. Aegypti</i>	141
II- INVESTIGATION OF THE PROVIRAL ACTIVITY OF THE DENV CANDIDATE RECEPTOR <i>PROHIBITIN-2</i>	144
DISCUSSION	156
ACKNOWLEDGEMENTS	158
METHODS	159
SUPPLEMENTARY MATERIALS	165
REFERENCES	167

-GENERAL DISCUSSION- **172**

I- LESSONS LEARNT	173
A) CHAPTER 1: A VAGO-LIKE GENE ENHANCES DENGUE AND ZIKA VIRUS DISSEMINATION IN Aedes Aegypti	173
B) CHAPTER 2: CYTOCHROME P450 4G15 POLYMORPHISM MEDIATES DENV SUSCEPTIBILITY IN A FIELD-DERIVED Aedes Aegypti POPULATION	174
C) CHAPTER 3: IN VIVO CHARACTERIZATION OF A CANDIDATE DENGUE VIRUS RECEPTOR, PROHIBITIN-2, IN Aedes Aegypti MOSQUITO MIDGUTS	175
II- CHOOSING THE RIGHT APPROACH AND MATERIAL	175
III- WHAT'S MORE AND WHAT'S NEXT	176
REFERENCES	179

OTHER SCIENTIFIC WORK **181**

LIST OF FIGURES & TABLES

INTRODUCTION

Figure 1. Structure of flavivirus genome and virion.	12
Figure 2. Global arbovirus presence.	13
Figure 3. Ecological transmission cycles of <i>Aedes</i> -borne flaviviruses.	14
Figure 4. Distribution of <i>Ae. aegypti</i> presence.	15
Figure 5. Arbovirus transmission by mosquitoes.	16
Figure 6. Innate immune pathways in mosquitoes.	22
Figure 7. Historical timeline of approaches and technologies used for the discovery of <i>Ae. aegypti</i> genetic determinants of vector competence towards arboviruses.	35

-CHAPTER 1-

Figure 1. <i>VLG-1</i> is a <i>Vago</i> -like gene specific to the Culicinae subfamily.	59
Figure 2. <i>VLG-1</i> is persistently induced by bloodmeal ingestion and DENV exposure in non-midgut tissues of <i>Ae. aegypti</i> .	61
Figure 3. <i>VLG-1^A</i> mutants are viable and fertile without major fitness defects.	63
Figure 4. <i>VLG-1</i> promotes systemic DENV dissemination in <i>Ae. aegypti</i> .	65
Figure 5. <i>VLG-1</i> promotes systemic ZIKV dissemination in <i>Ae. aegypti</i> .	66
Figure 6. The transcriptome of <i>VLG-1^A</i> mutants is broadly altered.	69
Supplementary Figure S1. Phylogenetic tree of <i>Vago</i> -like gene homologs among Culicinae and <i>Drosophila</i> species.	82
Supplementary Figure S2. Evidence of <i>VLG-1</i> loss of function in mutant <i>Ae. aegypti</i> .	83
Supplementary Figure S3. <i>AaeVLG-2</i> knockdown reduces the proportion of DENV-positive heads.	84
Supplementary Figure S4. Overlap of differentially expressed genes in <i>VLG-1^A</i> mutants compared to wild-type controls on days 5 and 9 post bloodmeal.	85
Supplementary Figure S5. Volcano plots of differentially expressed genes in <i>VLG-1^A</i> mutants compared to wild-type controls in the DENV-exposed condition.	86
Supplementary Figure S6. Transcription factor binding motifs found in the <i>Ae. aegypti</i> <i>VLG-1</i> promoter sequence.	87
Supplementary Table 1. Proposed updated designation of <i>Vago</i> and <i>Vago</i> -like genes.	88
Supplementary Table 2. <i>Vago</i> -like gene homologs used in the gene phylogeny.	89
Supplementary Table 3. Results of dN/dS analysis in CODEML.	90
Supplementary Table 4. GO terms.	90
Supplementary Table 5. Oligonucleotide sequences.	91
Supplementary Table 6. Hits for transcription factor DNA binding motifs from HOCOMOCO H12CORE in the promoter of <i>VLG-1</i> .	93

-CHAPTER 2-

Figure 1. <i>P450 4g15</i> is an antiviral factor associated with natural DENV resistance in the midgut.	104
Figure 2. <i>P450 4g15</i> is transiently induced in midguts within the first 24 hours after bloodmeal ingestion.	106
Figure 3. Midgut exposure to blood and DENV affects <i>P450 4g15</i> subcellular localization.	108
Figure 4. Early DENV infection of midgut cells is associated with higher levels of <i>P450 4g15</i> expression <i>in situ</i> .	111
Figure 5. Midgut-specific ectopic expression of <i>P450 4g15</i> hampers DENV infection in mosquitoes.	113
Figure 6. <i>P450 4g15</i> promoter haplotypes determine its expression level.	115
Supplementary Figure S1. <i>P450 4g15</i> is not induced in carcasses after bloodmeal ingestion.	126
Supplementary Figure S2. <i>P450 4g15</i> antibody specificity assay.	127
Supplementary Figure S3. RNAscope imaging for <i>in situ</i> quantification of <i>P450 4g15</i> RNA levels in midguts.	128
Supplementary Table 1. Oligonucleotide sequences.	129

-CHAPTER 3-

Figure 1. <i>phb2</i> has a proviral effect on DENV infection in <i>Ae. aegypti</i> .	143
Figure 2. Structure of the <i>Ae. aegypti</i> <i>phb2</i> protein.	144
Figure 3. The <i>phb2</i> protein is expressed in <i>Ae. aegypti</i> midguts.	146
Figure 4. Lack of <i>phb2</i> proviral activity in ZIKV- or CHIKV-infected <i>Ae. aegypti</i> .	147
Figure 5. Lack of <i>phb2</i> proviral activity in Aag2 cells during DENV infection.	149
Figure 6. Heterozygous <i>phb2</i> mutants show similar levels of DENV replication than wild-type mosquitoes.	151
Figure 7. <i>Ex vivo</i> virus binding assay on midguts.	152
Figure 8. Absence of demonstrated role of <i>phb2</i> in DENV early infection steps in <i>Ae. aegypti</i> midguts.	154
Supplementary Table 1. Oligonucleotide sequences.	165

-GENERAL INTRODUCTION-

Literature review

Revealing the mosquito's assets: discovery of mosquito molecular factors modulating arbovirus infection in *Aedes aegypti*

GENERAL INTRODUCTION

Revealing the mosquito's assets: discovery of mosquito molecular factors modulating arbovirus infection in *Aedes aegypti*.

I- Molecular interactions between mosquitoes and arboviruses

I.A) Arbovirus transmission by *Aedes* mosquitoes

I.A.1) Definition of arboviruses

Arthropod-borne viruses, or arboviruses, are viruses that are transmitted between vertebrate hosts through the bite of an arthropod vector [2, 3]. Over 500 arboviruses have been identified, a hundred of which are pathogenic to humans [4, 5]. Arboviruses can cause a variety of diseases in humans, ranging from mild fevers to severe illnesses, including encephalitis and hemorrhagic fevers. They are a heterogeneous group which mainly encompasses members of the *Flaviviridae*, *Togaviridae* and *Bunyaviridae* families [2, 6-8]. Vectors of arboviruses include ticks, sandflies, black flies and biting midges, but the majority of medically significant arboviruses are transmitted by mosquitoes [7]. Among mosquito-borne viruses, members of the *Flavivirus* genus have spread remarkably during the past 70 years and many classify as emerging and re-emerging pathogens [8-11].

I.A.2) Mosquito-borne flaviviruses

Flaviviruses are positive single-stranded RNA viruses of the *Flaviviridae* family (Figure 1) and are the etiological agents of many human and veterinary diseases [9].

Among the culprits of the global flaviviral burden, **dengue viruses** (DENV) are the most prevalent mosquito-borne viral pathogens worldwide. They are responsible for approximately 400 million human infections each year, with about 100 million clinically manifested cases [10]. While about 80% of dengue infections are clinically inapparent, dengue disease can be debilitating and associated with high fever, headache, muscle and joint pains or rash. Occasionally, in less than 0.5% of cases, dengue disease can develop into a severe form of dengue hemorrhagic fever or dengue shock syndrome [12, 13]. More than a quarter of the world's population lives in areas where DENV is endemic, and more than half the world's population is estimated at risk for dengue disease [11]. DENV can be found in tropical and subtropical countries (Figure 2), where it exists as four serotypes, DENV-1 to -4, which are genetically divergent and loosely antigenically distinct [14, 15].

Another typical example of the expanding flaviviral burden is **Zika virus (ZIKV)**, which has emerged in 89 countries in the past 15 years [16, 17] (Figure 2). The largest ZIKV outbreak

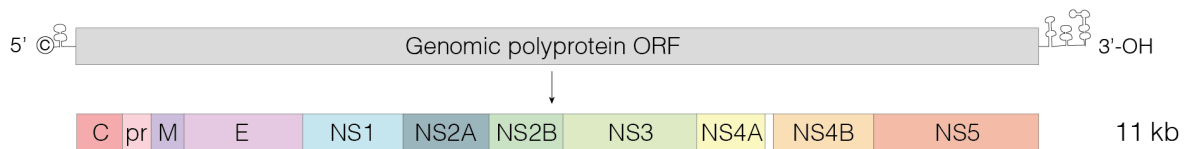
-GENERAL INTRODUCTION-

was reported in Brazil in 2015-2016 with between 400,000 and 1,300,000 estimated cases [18]. Even though most adult infections are asymptomatic, ZIKV can cause symptoms similar to dengue disease, but more importantly, neurological pathologies such as Guillain-Barré syndrome and brain developmental defects in fetuses of infected mothers [16]. ZIKV disease is one of the most important infectious diseases linked to birth defects [19] and was declared Public Health Emergency of International Concern in 2016 by WHO [20].

Mosquito-borne flaviviruses also include West Nile virus, yellow fever virus or Japanese encephalitis virus, which are less prevalent worldwide than DENV and ZIKV [6, 9].

To this day, no globally approved vaccines or specific antiviral treatment are available for DENV and ZIKV [21, 22].

A



B

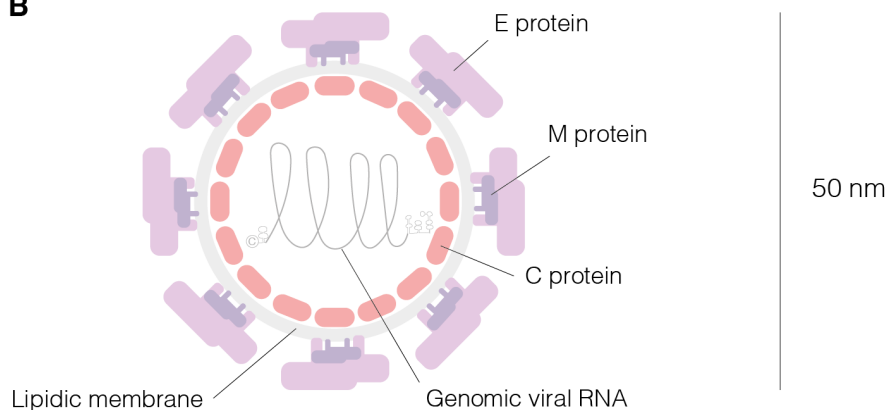


Figure 1. Structure of flavivirus genome and virion. (A) Positive-sense single-stranded RNA flaviviral genome. The flavivirus genome (~11 kilobases (kb)) has a methylated nucleotide cap in its 5' end, and a non-polyadenylated loop structure in its 3' end. It contains a single open reading frame (ORF) encoding for a large polyprotein, which is processed by cellular and viral proteases into 10 mature proteins. They include three structural proteins (capsid (C), envelope (E) and pre-membrane (prM)) and seven non-structural proteins (NS1, NS2A, NS2B, NS3, NS4A, NS4B and NS5). (B) Structure of flavivirus virions. The surface of the enveloped spherical virion is composed of surface proteins (E and M) arranged in an icosahedral-like symmetry.

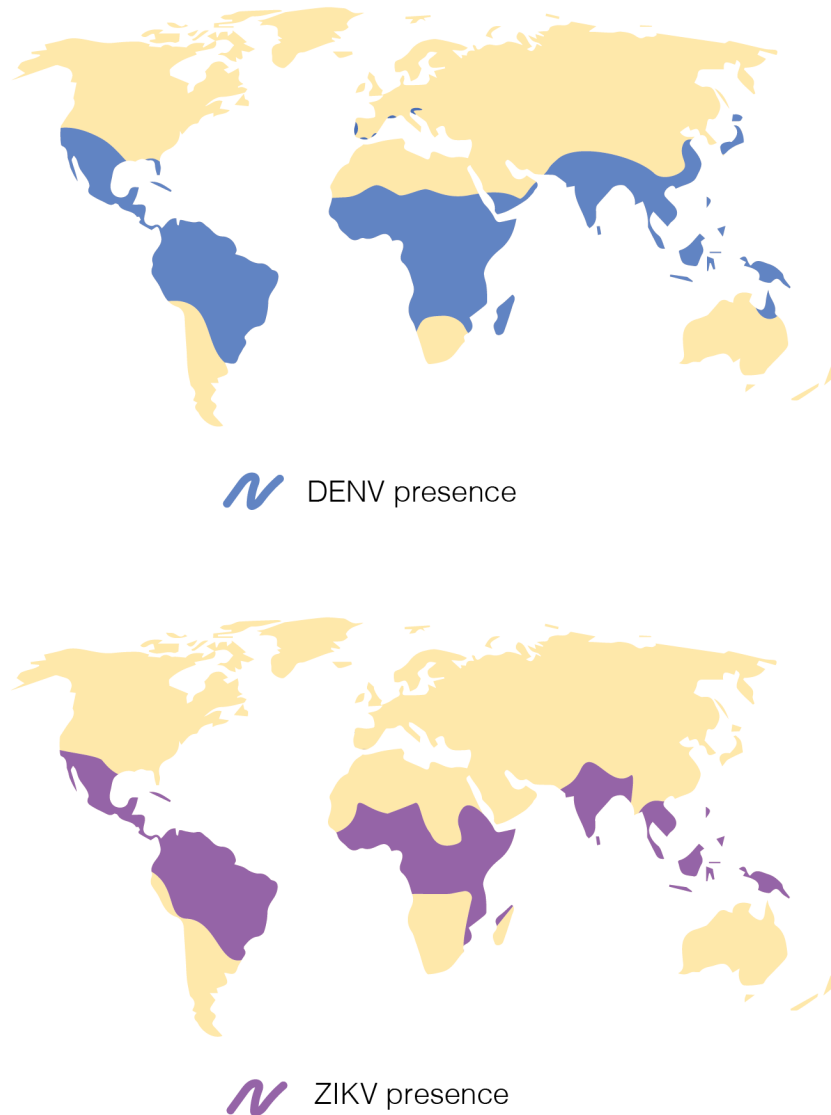


Figure 2. Global arbovirus presence. Regions with previous or current presence of DENV (A) and ZIKV (B) reported are represented in blue and purple respectively. Data are combined and adapted from WHO, CDC and PAHO reports and reviews from [23, 24].

I.A.3) Mosquito vectors of flaviviruses

Mosquito-borne flaviviruses like DENV and ZIKV are maintained in two ecologically distinct transmission cycles: a sylvatic cycle and a human cycle. The sylvatic cycle involves non-human vertebrates and sylvatic mosquitoes, while the human cycle involves human populations and anthropophilic domestic mosquitoes [13, 25] (Figure 3). Human transmission of all known mosquito-borne viruses is sustained by **mosquitoes of the Culicinae subfamily** (with the exception of O'nyong-nyong virus, transmitted by anopheline mosquitoes) [23]. Flaviviruses like DENV or ZIKV are transmitted to humans by mosquitoes of the *Aedes* genus, namely *Aedes aegypti* and *Aedes albopictus* [26-29]. ***Aedes aegypti* (*Ae. aegypti*)**, also known

as the yellow fever mosquito, originated in Africa but spread throughout the world in tropical, subtropical and temperate regions. It is now among the most widespread mosquito species worldwide [27] (Figure 4). *Ae. aegypti* is the primary vector of DENV, ZIKV, yellow fever virus and chikungunya virus, among other epidemiologically significant viruses [27, 30-32]. *Ae. aegypti* has a stronger host preference for humans than *Ae. albopictus* and is a more efficient vector of transmission [33]. Yet, *Ae. albopictus* has been a driving force of arbovirus expansion in more temperate regions due to its ability to overwinter [27, 34]. *Ae. aegypti* consists of two subspecies, the native *Ae. aegypti formosus*, an ecological generalist found in both sylvatic and urban habitats of sub-Saharan Africa, and the globally invasive *Ae. aegypti aegypti*, a human specialist that spread from Africa to the rest of the world in the last few centuries [35-37].

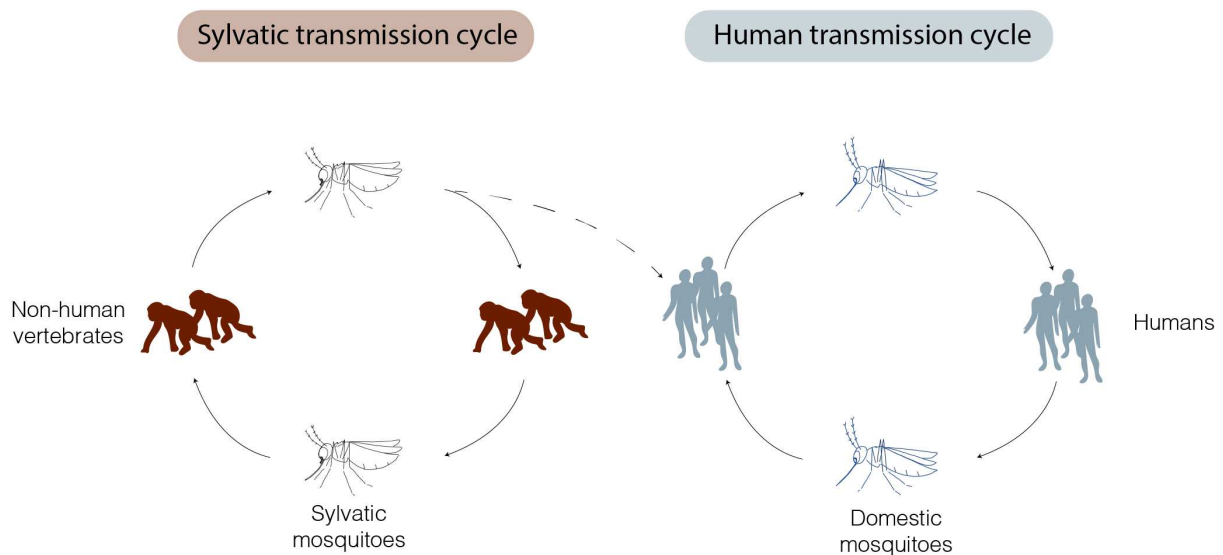
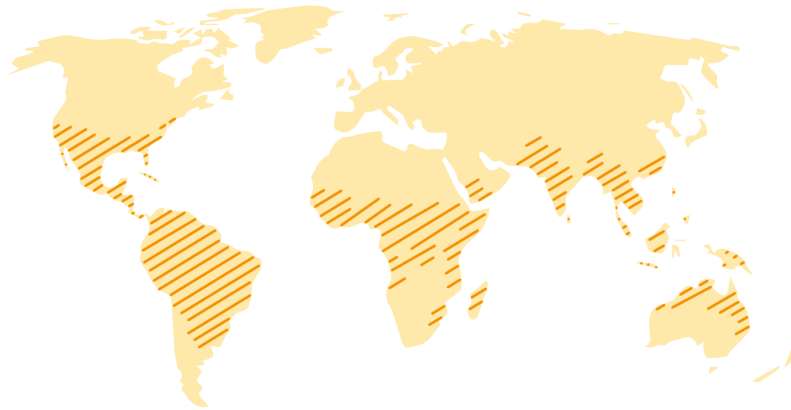


Figure 3. Ecological transmission cycles of *Aedes*-borne flaviviruses. *Aedes* mosquito-borne flaviviruses like DENV and ZIKV are maintained in two ecologically distinct cycles: a sylvatic cycle and a human cycle. The sylvatic cycle involves non-human vertebrates and arboreal mosquitoes, while the human cycle involves human populations and anthropophilic domestic mosquitoes.



////// *Aedes aegypti* presence (reported and predicted)

Figure 4. Distribution of *Ae. aegypti* presence, reported and predicted. Adapted from [25, 288, 289].

Because efficient human-centered treatments of arboviral diseases are yet to be discovered, the fight against mosquito-borne pathogens has been mostly directed towards vector control [40]. Traditional vector control methods are based on the use of insecticides, which are no longer sustainable now that insecticide resistance has emerged and spread in wild mosquito populations [41]. Concerns for the future of vector control have prompted the development of alternatives strategies aiming at manipulating vector biology to regulate their ability to transmit pathogens [42]. The release of modified mosquitoes that are refractory to viral transmission offers one potential strategy for reducing the incidence of human diseases [43, 44]. Thus, there is a growing need to identify optimal targets for modification and mosquito molecular factors which modulate virus transmission are promising candidates [42].

I.A.4) Stages of arbovirus infection in the mosquito

Arbovirus infection in the mosquito can be broken down into three distinct stages: midgut infection, systemic dissemination and transmission (Figure 5). Mosquitoes are hematophagous insects, meaning that females need to feed on blood to sustain the vitellogenesis process and reproduce. When feeding on a viremic human, female mosquitoes can incidentally acquire viral pathogens. The bloodmeal containing viral particles is digested in the mosquito midgut, where the virus infects epithelial cells and establishes infection [45, 46]. Then, viral particles cross the midgut epithelium and disseminate in the hemocoel. Dissemination to secondary organs, such as fat body, ovaries and muscle tissues, likely occurs through infection of circulatory hemocytes [1, 47, 48]. The virus eventually infects salivary glands and is released in the mosquito saliva [49]. During a subsequent bloodmeal, the female mosquito injects virus-containing saliva into the skin of the next naïve human host, leading to pathogen transmission [1].

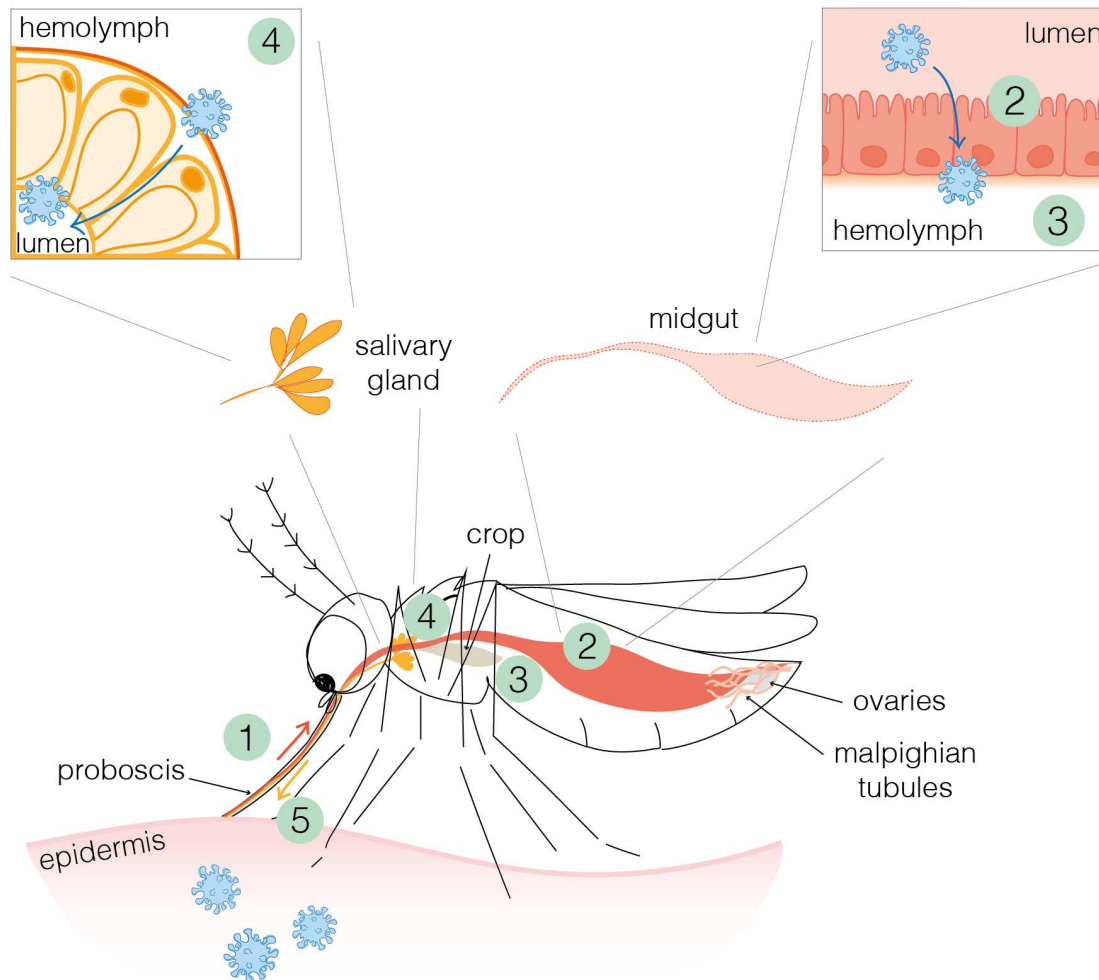


Figure 5. Arbovirus transmission by mosquitoes. A mosquito acquires an arbovirus when biting and blood feeding on a viremic vertebrate host (1). The bloodmeal is processed in the digestive tract, more specifically in the midgut. The virus infects midgut epithelial cells (2) and crosses the midgut tissue barrier to disseminate into the hemolymph (3). Subsequently, the virus infects secondary organs including the fat body and hemocytes. Eventually, the virus reaches the salivary glands and is then released into the salivary gland lumen, in the saliva. Upon the next bloodmeal on a naïve host, the mosquito injects a small amount of infectious saliva in the epidermis and thus leads to arbovirus transmission [1].

I.A.5) Vector competence and vectorial capacity

Mosquitoes are not passive transporters of arboviruses. Instead, mosquitoes actively replicate and amplify arboviruses prior to transmission. Moreover, saliva-associated components enhance intradermal infection and consequent spreading in the human host [50, 51]. The **vector competence** of a mosquito can be defined as its physiological ability to acquire an infectious agent and support its transmission [52-54]. Vector competence is governed by intrinsic and extrinsic factors that influence the ability of a vector to transmit a pathogen [29,

54-56]. Despite the proposal of a standardized procedure to quantitatively assess vector competence [57], most available studies employ inconsistent terminology and use disparate assays to report on this phenomenon. Indices such as infection rate, dissemination rate and transmission rate are often used as proxies to assess vector competence [29]. **Susceptibility** refers to the ability of the mosquito to acquire and sustain infection, at least in the midgut, while **resistance** refers to refractoriness to infection upon virus exposure.

Vector competence is a component of vectorial capacity. **Vectorial capacity** refers to all of the environmental, behavioral, cellular, and biochemical factors that influence the interactions between the vector, the pathogen, and the vertebrate host [52, 58-60]. Vectorial capacity (V) is classically defined by the following formula:

$$V = \frac{ma^2bp^n}{-\ln(p)}$$

where m is the vector density, a the rate of biting, b the vector competence, p the probability of vector daily survival and n is the extrinsic incubation period (*i.e.*, the time between pathogen ingestion and transmission in the saliva) of the pathogen [60].

I.A.6) Intrinsic determinants of vector competence

Vector competence is influenced by a variety of **intrinsic and extrinsic factors**.

Intrinsic determinants of vector competence are the mosquito's inner drivers of its ability to be infected, disseminate and subsequently transmit a pathogen. They typically encompass genetically encoded fixed traits as well as the mosquito's microbiota. Hence, this definition includes, but is not limited to, immune pathways, metabolic processes, cellular components, bacterial and viral microbiota, infection history, and tissue barriers [54, 56, 61, 62].

Tissue barriers were among the first intrinsic factors to be investigated. The notion that viruses need to overcome physical barriers, namely the midgut infection barrier (MIB), the midgut escape barrier (MEB), the salivary gland infection barrier (SGIB) and the salivary gland escape barrier (SGEB) (Figure 5) [1, 62], was explored in the early history of vector competence studies [63]. In the midgut tissue, the MIB determines the initiation of infection and successful replication in the midgut epithelium. The MEB regulates the release of viral particles from the midgut into the hemolymph. In the salivary glands, the SGIB controls the success of viral entry and replication in this organ, and the SGEB defines the ability of the virus to be secreted into the salivary duct, allowing for horizontal transmission via injection of

-GENERAL INTRODUCTION-

infectious saliva [1]. For the mosquito vector to be competent, the virus must overcome all these physical barriers.

Furthermore, **extrinsic factors** such as environmental temperature or nutrition can impact the mosquito's vector competence [64-66], but are beyond the scope of this thesis.

This thesis work focuses on **molecular factors, encoded in the mosquito's genome**, which modulate, either positively or negatively, the infection and transmission of flaviviruses in *Aedes aegypti* mosquitoes.

I.B) Antiviral response of *Aedes* mosquitoes to mosquito-borne flaviviruses

This section reviews the current knowledge on the antiviral response in mosquitoes of the *Aedes* genus, with a particular focus on the response mechanisms of *Ae. aegypti* to flavivirus infection for which experimental evidence is available.

I.B.1) Cellular and humoral responses

I.B.1.a) Immune-specialized cells and tissues

Hemocytes are key components of the mosquito immune system, with roles in pathogen recognition, immune signaling and wound healing [67-69]. Hemocytes are circulating or sessile macrophage-like cells which can act through phagocytosis, lysis or melanization processes. They were shown to accumulate in DENV-infected midguts, and their phagocytic capacity was involved in the control of systemic DENV infection [48]. Other indication for the involvement of hemocytes in antiviral defenses mostly comes from data in *Drosophila* [70-72]. On the other hand, several studies indicated that viral dissemination is supported by infection of circulating hemocytes [45, 47, 48, 73, 74]. Mosquito hemocytes also express a variety of **Pathogen-Associated Molecular Pattern (PAMP) Recognition Receptors (PRR)** [75] which, upon recognition of a pathogen, can act as opsonins, recognizing invading particles and facilitating their phagocytosis, or trigger immune pathways including phagocytosis, encapsulation and nodulation [76]. A class of PRR designated thioester-containing proteins (TEPs) can sustain resistance to flaviviral infections in *Ae. aegypti*, as exemplified by the antiviral activity of TEP1, TEP2, AaMCR, and AaSR-C [77, 78]. It has been suggesting that these PRR's antiviral activity is mediated by a consequent activation of inducible immune pathways (described in section I.B.2) and cellular responses (listed in section I.B.1.c).

The **fat body** is the main organ responding to microbial infection, notably by secreting antimicrobial peptides (AMPs) such as defensins or cecropins, C-type lectins and peptidoglycan recognition proteins (PGRPs) [79]. Its immune functions have mostly been

described in the context of bacterial and parasitic invasions [80, 81]. Yet, considering the established role of AMPs in antiviral defense of *Ae. aegypti* (detailed in section I.B.2.b), it is suggested that the fat body's response is also important against viral infections. A study showed that fat body-specific overexpression of JAK-STAT components enhanced *Ae. aegypti*'s resistance to certain arboviruses only [82], nuancing the assumption of an undistinguished antiviral response of this tissue.

I.B.1.b) Humoral factors

Antimicrobial peptides (AMPs) are conserved humoral effectors among insects. Hemocytes express most known AMPs, such as cecropins and defensins, which have demonstrated antiviral activity (detailed in section I.B.2.b) [72, 75, 83-85].

Hemocyte-derived secreted **PRR**, described in section I.B.1.a, are also important humoral factors involved in the control of viral infections.

Reactive Oxygen Species (ROS) are oxygen-containing radicals and compounds which can act as signaling molecules generated upon stress. ROS-mediated activation of inducible immunity might help control DENV in *Wolbachia*-infected *Ae. aegypti* [83]. ROS-associated genes are induced during DENV infection and could participate in the response against this virus [76].

Finally, **prophenoloxidase (PPO)** is produced exclusively by hemocytes, and its processing mediates **melanization**, *i.e.*, the formation of melanin around invading pathogens [81, 86]. Inhibition of the PPO cascade has been associated with higher titers of arboviruses in *Ae. aegypti* [86].

I.B.1.c) Cellular mechanisms

Phagocytosis is a form of programmed cell death (similarly to apoptosis and autophagy) and was found to hamper systemic dissemination of arboviruses in *Ae. aegypti* [48, 87]. **Apoptosis** has been clearly associated with antiviral response to arboviruses [88-90]. The role of **autophagy** in the defense against flaviviruses has been shown *in vitro* but with variable impact depending on the method used to manipulate this pathway and remains to be established *in vivo* [90-92].

I.B.2) Intracellular antiviral response

I.B.2.a) The JAK-STAT pathway

The Janus kinase-signal transducers and activators of transcription pathway, or **JAK-STAT** pathway, is an antiviral signal transduction cascade, initially identified in mammals [93]. The detailed molecular players of this pathway are described in Figure 6. There is compelling evidence that the JAK-STAT pathway has antiviral activity, in particular against DENV in *Ae. aegypti*. *Dome* knockdown led to increased DENV titers [94] and transgenic expression of *Dome* and *Hop* reduced DENV midgut load and systemic dissemination [82]. Yet, *Hop* overexpression did not affect ZIKV titers, suggesting that JAK-STAT activation through this mechanism is not broadly antiviral. Knocking-down the negative regulator *PIAS* decreased DENV and ZIKV titers [95, 96]. Interestingly, in mosquitoes, the identity of the UPD ligands of the Dome receptor is yet to be established. A secreted protein of the **Vago** family has been proposed as an extracellular activator of the JAK-STAT pathway in *Culex* mosquitoes [97, 98]. The antiviral activity of *Vago* was dependent on Hop and STAT components of the JAK-STAT pathway but did not involve the Dome receptor. Several studies suggested that *Vago* might mediate a crosstalk between the RNA interference pathway and NF- κ B pathways [97-99]. **The role of Vago genes upon flavivirus infection in *Ae. aegypti* is the focus of the Chapter 1 of this thesis.**

I.B.2.b) Toll and IMD pathways

Nuclear factor κ B (NF- κ B) pathways in mosquitoes include the Toll and the immune deficiency (IMD) pathways. The **Toll pathway**, detailed in Figure 6, leads ultimately to the activation of Toll-regulated genes, which include AMPs. A substantial body of evidence supports the involvement of the Toll pathway in the antiviral response of *Ae. aegypti* against arboviruses. The antiviral function of *MyD88* against DENV has been robustly demonstrated [84, 95, 100]. Additionally, activation of Toll pathway by knocking down the negative regulator *Cactus* led to decreased DENV and ZIKV loads in *Ae. aegypti* [84, 95, 96, 100]. Notably, the specificity of the antiviral function of the Toll pathway against flaviviruses and alphaviruses is controversial [101-103].

The mechanisms of **IMD pathway** activation in mosquitoes remain to be established. The IMD pathway components are described in Figure 6. In *Ae. aegypti*, the IMD pathway seems to play a very minor role (if any) in the response against arboviruses. IMD expression seems to reduce DENV titers only in a mosquito-strain specific manner [95]. Evidence for a role of other IMD pathway components during antiviral responses in *Ae. aegypti* is very limited [96, 100, 101]. In other mosquito species, data is scarce and only indicates a minor effect of the pathway in

controlling arbovirus infection [104, 105]. Limited consistency between available studies (virus strain, host models, infection routes) adds significant variability in the observed response and complicates the overall vision of the antiviral effect of this pathway.

AMPs have initially been described as anti-bacterial and anti-fungal effectors. Yet, studies have shown that AMPs also have antiviral activities, notably in mosquitoes. Silencing of AMPs such as defensins, cecropins, as well as the antimicrobial effector lysozyme increased DENV ability to replicate in *Ae. aegypti* [83-85, 106]. Consistently, fat body-specific overexpression of cecropins or defensins impairs DENV replication [83]. Viral antagonism of AMP expression has also been observed in *Ae. aegypti* and provides additional indication of their proviral activity [107-110]. Nevertheless, the mechanism of action of AMPs to hamper viral infection, as well as how regulation of AMP is shared between both NF- κ B pathways in mosquitoes, remain unclear.

I.B.2.c) The RNA interference pathway

In insects, **RNA interference** (RNAi) has long been considered the major player of antiviral defense. Description of this pathway is provided in Figure 6. Experimental evidence supports the antiviral function of *Dcr2* in mosquitoes against several flaviviruses [95, 111-115]. A paralog of *R2D2* and *Loqs-PA*, *Loqs2*, was shown to be necessary for small interfering RNA (siRNA)-pathway-mediated antiviral response in *Ae. aegypti* [116]. However, the importance of *Dcr2* in the antiviral response of *Ae. aegypti* *in vivo* might have been overestimated. Recent studies revealed that despite restricting viral infection dynamics, *Dcr2*'s overall impact on vector competence is modest, and rather suggest its involvement in virus tolerance, *i.e.*, control of pathogenic effects of sustained viral infections [112, 117]. *Ago2* was also shown to control arbovirus infection and protect *Ae. aegypti* from virus-induced mortality [118].

I.B.2.d) Non-canonical antiviral processes

Other **non-canonical intracellular processes** have been linked to antiviral activity in *Ae. aegypti*. The antiviral activity of the **Delta-Notch** pathway, mainly involved in developmental processes, was reported in the context of DENV infection in *Ae. aegypti* [119]. The role of the **autophagy** pathway and **transcriptional pausing** in the antiviral response of mosquitoes is largely unexplored [91, 120], especially *in vivo*, despite some indications of their importance in flies and conservation of these processes among dipteran insects [120-123]. Mitogen activated protein kinase (**MAPK**) kinase pathways (including the nutrient-responsive extracellular signal-regulated kinase (ERK) pathway and the c-Jun N-terminal kinase (JNK) pathway) are also hypothesized to be functionally conserved in mosquitoes, with limited experimental evidence

of their antiviral activity *in vivo* [103, 124, 125]. **Apoptosis** has been reported to limit arbovirus replication in *Ae. aegypti* [89, 90, 126, 127] and was described as an antiviral process in RNAi-defective mosquitoes [118]. However, apoptosis was also shown to correlate with susceptibility to infection [128], hence the antiviral nature of this mechanism is controversial.

Various **non-canonical molecular factors**, with no established link with the immune mechanisms mentioned previously, have been described as restriction factors [111, 129-133]. Their molecular nature and their mode of action -when deciphered- is extremely varied. For instance, Dhx15, an RNA-binding protein, indirectly represses virus replication by controlling cellular glycolysis [130]. Ub3881 targets DENV envelope (E) protein for degradation and consequently limits the number of virions released [133]. aBravo was found associated with Dicer2 but provides its antiviral activity independently of the RNAi pathway [111]. **An example of discovery of a novel non-canonical antiviral factor is presented in Chapter 2 of this thesis.**

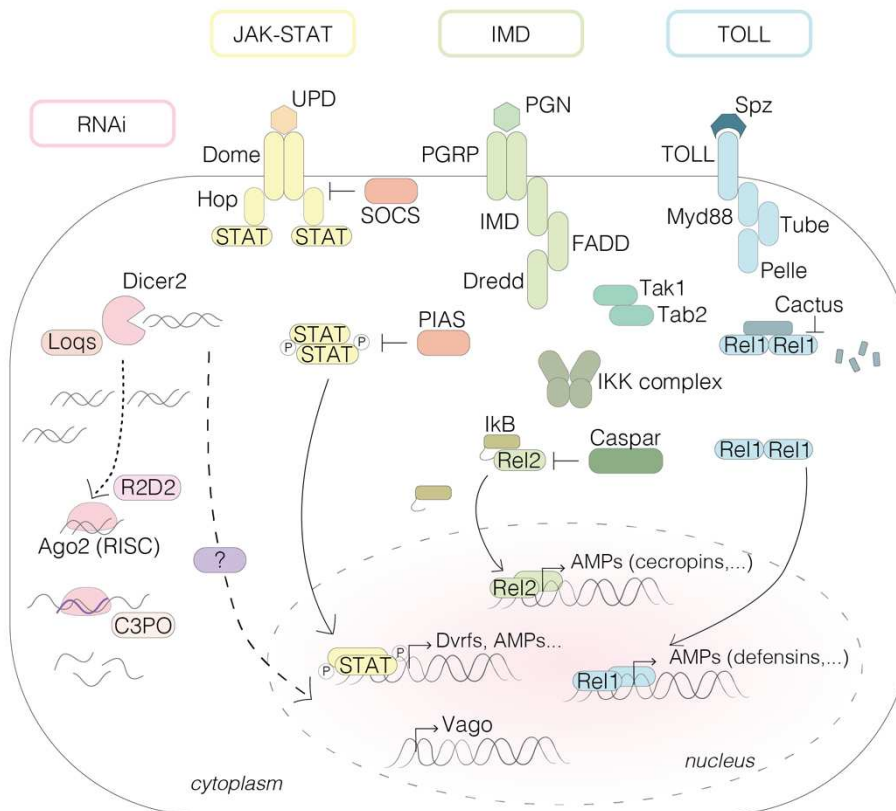


Figure 6. Innate immune pathways in mosquitoes. In the mosquito **JAK-STAT** pathway (shown in yellow), activation of the receptor Dome and the Janus kinase Hop is the trigger of the pathway [134, 135]. The UPD ligands that bind to Dome have not been identified in mosquitoes. Upon triggering, STAT transcription factors (AaSTAT1 in *Ae. aegypti*) translocate into the nucleus and activate the transcription of JAK-STAT regulated genes such as *Dvrf-1*, *Dvrf-2*, *vir-1*, etc. [82, 94, 136]. Negative regulators of the pathway include SOCS (which inhibits signaling at the level of receptor Dome) and PIAS (which inhibits STAT phosphorylation) [94]. In *Drosophila*, the **Toll pathway** (shown in blue) is induced by binding of the

ligand Spätzle (Spz) to the Toll receptor. In mosquitoes, several orthologs of these proteins exist but it is unclear which ligand-receptor association is responsible for the induction of the Toll pathway [134]. Upon receptor activation, the two adaptor proteins Myd88 and Tube are recruited to the cytoplasmic domain of Toll in a complex with Pelle kinase. Phosphorylation of the negative regulator Cactus by Pelle leads to its degradation and releases transcription factor Rel1 complexes to translocate to the nucleus [134, 136]. Rel1 then activates the expression of Toll-regulated genes [137], including AMPs. The **IMD pathway** (shown in green) activation in mosquitoes remains to be described. Mosquitoes encode for several peptidoglycan recognition receptors (PGRP) orthologous to *Drosophila*'s PGRP-LE and PGRP-LC, which are involved upstream of the IMD pathway [138]. The adaptor molecules IMD and FADD interact with the caspase Dredd, which activates IMD. Tak1 kinase, Tab2 adaptor protein and IκB kinase (IKK) complex are then recruited to IMD. The IKK phosphorylates Rel2, which is then cleaved and activated by Dredd and translocated into the nucleus [134, 136]. The negative regulator Caspar inhibits Rel2 translocation. Once in the nucleus, Rel2 upregulates IMD-dependent genes such as AMPs [139]. In the **RNAi pathway** (shown in pink), double-stranded RNA (dsRNA) resulting from viral replication is recognized by Dicer2 (Dcr2), which cleaves it into siRNA duplexes of 21 nucleotides using Loqs-PA. These siRNA are loaded onto the Argonaute-2 (Ago2)-containing RISC complex by R2D2. After loading on Ago2, one of the siRNA is degraded by Ago2 together with the endonuclease C3PO. The remaining guide strand is stabilized on RISC and allows recognition of complementary viral RNA for cleavage and degradation by Ago2 [140, 141]. Induction of the secreted factor Vago is mediated by Dcr2, via an undefined activation pathway [98, 99].

I.C) Flavivirus host dependency factors in *Ae. aegypti* mosquitoes

As obligatory parasites, viruses hijack cellular factors to support the replication of their genome and the translation of the protein components of the virions [142]. Such cellular factors with a proviral activity are called **host dependency factors**. This section focuses on host dependency factors described in *Ae. aegypti* in the context of flavivirus infection.

I.C.1) Entry and trafficking factors

The initial step of **virus entry**, which includes attachment, receptor binding and entry, has been investigated in mosquito cells with the aim of identifying mosquito **receptors** of flaviviruses, but with little success. Several putative receptors of DENV have been identified, without robust (if any) functional *in vivo* confirmation of their biological relevance [143-150]. **The topic of virus receptor investigation in mosquitoes is more extensively discussed in the Chapter 3 of this thesis.**

Nevertheless, some **entry factors** have been identified, such as clathrin or actin filaments, shedding light on the endocytosis mechanism supporting flavivirus entry in mosquito cells [151-

-GENERAL INTRODUCTION-

154]. Intriguingly, a potentializing factor, scavenger receptor B1-like, involved in non-structural protein 1 (NS1) internalization, renders mosquito cells more susceptible to infection [155, 156].

Subsequent **trafficking** of the internalized viral particle relies on a number of cytoskeleton components such as actin, myosin and myosin-associated kinases [157]. **RNA uncoating** is assisted by endoplasmic reticulum (ER) proteins which then address the capsid protein for proteosomal degradation [158].

I.C.2) Factors supporting viral replication and virion production

Viral genome **replication** occurs in replication organelles, also designated viral factories, which are double-membrane vesicles, derived from ER membrane rearrangements [159]. The Loquacious protein, a factor of the RNAi pathway, is recruited to replication organelles, interacts with replication intermediates and facilitates viral RNA replication [160, 161].

Lipids are broadly manipulated by DENV during infection of mosquito cells, ranging from lipidic membrane components to lipid droplets. Among others, the fatty acid synthase [162-164], AGPAT1, ethanolamine, members of the phospholipid biosynthesis pathway [165, 166], the cardiolipin synthase [131], the sterol regulatory element binding protein (SREBP) [167] and the sphingolipid desaturase [168] have been attributed proviral activity during DENV infection of *Ae. aegypti* cells.

Little is known about the mosquito cellular factors mediating **virion progeny production or release**. Septins have been hypothesized as scaffold molecules for immature virions prior to egress [169]. The caveolin chaperone complex was found associated with NS1 during its secretion but is not involved in virion release [170]. Additionally, host-specific glycosylation patterns on NS1 and E proteins are required for productive virion release in mosquito and mammalian cells [171-173].

I.C.3) Miscellaneous host dependency factors

Some host dependency factors indirectly support viral infection by **negatively modulating antiviral defense mechanisms**. For instance, some lipid binding proteins and epigenetic regulators impair activation of IMD and Toll pathways and are thought to support DENV infection in this manner [174, 175]. A midgut factor associated with the peritrophic matrix controls ROS levels upon bloodfeeding and showed proviral activity in mosquito midguts infected with flaviviruses [176]. Similarly, the gut *catalase* gene, an antioxidant factor upregulated after blood intake, favors DENV infection establishment in *Ae. aegypti* midguts, potentially by maintaining redox homeostasis and limiting production of antiviral ROS [177].

Finally, **miscellaneous** host factors of diverse nature (ribosomal proteins, histones, ligases...) have showed proviral activity towards flaviviruses in *Aedes* mosquitoes, but the mechanism underlying their ability to favor viral infection remain unknown [158, 178, 179]. Some of them exert a **tissue-specific** proviral activity, in the midgut or the salivary glands [167, 176, 177, 180]. Interestingly, some human orthologs of these factors showed proviral activity in human cells with the same viruses, suggesting that certain host dependency factors are conserved among species [181].

Overall, this review highlights the broad variety of genetically encoded modulators of arbovirus infection in *Ae. aegypti*. Naturally, the understanding of the genetic basis of mosquito-arbovirus interactions is a relevant starting point for studying the molecular interface between virus and vector.

I.D) Genetic basis of mosquito-arbovirus interactions

I.D.1) Natural genetic variation in *Ae. aegypti* and dengue viruses

Natural genetic variation can be observed in both flaviviruses and mosquitoes. Flaviviruses have a single-stranded, positive-sense RNA genome of about 11 kilobases (kb) (Figure 1). Like most RNA viruses, important genetic diversity can be found among DENV strains [182]. For each of the four DENV serotypes, many different lineages exist and keep increasing in number [183, 184]. This genetic diversity in DENV also translates phenotypically, as lineages are associated with variable virulence [185].

Ae. aegypti has a large genome of about 1.3 gigabases (Gb) [186], with substantial genetic variation at both global and local geographical scales [187].

I.D.2) Mosquito-virus compatibility patterns

When it comes to susceptibility to DENV, not all mosquitoes are created equal: different mosquito strains can exhibit differential vector competence for a given DENV lineage [46, 188, 189]. Reciprocally, different DENV lineages can have differential infectivity potential in a given mosquito population [190-192]. Furthermore, the outcome of infection is determined by the specific combination of virus and mosquito genotypes, referred to as genotype-by-genotype (GxG) interactions. Several examples of these GxG interactions in DENV and *Ae. aegypti* have been documented [190, 191, 193-195]. In plants, host-virus interactions are often governed by “gene-for-gene” compatibility, whereby one host resistance allele confers resistance to all pathogens expressing the corresponding “avirulence” factor [196]. **Mosquito-virus compatibility patterns** are more consistent with the “matching-allele” model, whereby

successful infection requires an exact match between multiple host and pathogen genes or loci. Universal host resistance or viral infectivity is not possible in this model [197, 198]. Indeed, no universally resistant mosquito has been identified, and no universally successful virus either. Even complete refractoriness to a single arbovirus is typically not observed because successful infection can generally be achieved by increasing the infectious dose [193, 199-201].

I.D.3) Quantitative genetics of vector competence

A **quantitative trait locus** (QTL) is a region of the genome which correlates with variation of a quantitative trait, *e.g.*, a measurable phenotype that depends on the cumulative actions of genes and environment. In our context, QTL refer to loci which condition a susceptible or resistant phenotype. **Quantitative genetics** correspond to the study of quantitative traits, *i.e.*, mosquito vector competence for arboviruses. Assessment of vector competence relies on measurement of quantitative variables, such as midgut infection titers, or viral prevalence in heads for dissemination (as reviewed in [29, 202]). Mapping GxG interactions means statistically associating mosquito genome regions or even genetic markers with virus strain-specific resistance or susceptibility. **Foundational quantitative genetic studies** of DENV vector competence in *Ae. aegypti* examined the genetic basis of tissue barriers by measuring the heritability of midgut infection and viral dissemination phenotypes [63]. It became later clear that vector competence is a multigenic trait, whereby variability in vector competence is conditioned by genetic variation at multiple genes acting jointly [203-205]. Further QTL mapping studies confirmed the multigenic nature of DENV vector competence, including QTL underlying GxG interactions [63, 186, 191, 206-208].

Overall, elucidating the **genetic architecture** of *Ae. aegypti* susceptibility is inherently ambitious, given that it is likely to vary depending on the genotype of the host and the virus, as evidenced by a meta-analysis of QTL studies [209]. The subsequent pessimistic conclusion is that the investigation of the genetic basis of mosquito susceptibility to viruses is a highly complex undertaking. To this day, the exact genes responsible for the phenotypic variations observed have not been characterized or even identified. The innate immune system in the mosquito is now recognized as mostly limiting viral pathogenesis but does not determine vector competence. Nevertheless, a variety of other genetic conditioners have been identified. Recent approaches based on novel technologies have identified several mosquito genes with pro- or antiviral activity, sometimes even supported by characterization of the molecular mechanism underlying their ability to modulate the virus cycle in the mosquito. The next section recapitulates the different approaches for discovery of mosquito molecular determinants of vector competence.

II- Approaches for discovery of mosquito molecular factors modulating arbovirus infection & transmission

Novel vector control strategies rely on genetic engineering of mosquitoes which are incapable of transmitting pathogens [43, 44]. An entry point of such a strategy is the identification of mosquito genes which determine the outcome of infection [42]. Hence, deciphering the genetic modulators of the mosquito-virus interface has generated great enthusiasm in the past few decades. Here, we review the methodological approaches implemented for the discovery of mosquito molecular factors which modulate arbovirus infection and transmission, with a specific focus on the interaction between *Ae. aegypti* and flaviviruses (Figure 7). Only approaches for discovery of genetic factors *stricto sensu* (*i.e.*, mosquito protein-coding genes that affect arbovirus infection) will be discussed in this review; other types of intrinsic factors, such as non-protein coding genetic elements, microbiota or any other intrinsic factors are outside the scope of this study.

II.A) Forward genetic approaches: from observation of the mosquito phenotype to identification of host molecular factors

II.A.1) Exploiting the natural variation in mosquito vector competence

II.A.1.a) Foundational genetic approaches

Even though the concept of vector-borne pathogen transmission emerged at the end of the 19th century, the **hypothesis of the genetic basis of mosquito susceptibility** to human pathogens was only formalized in the 1930s for *Anopheles* mosquitoes and malaria parasites [210], and in the 1950s for *Aedes* and arboviruses [211-213]. This notion was then extended to other mosquito-borne pathogens [63, 214-216]. In the 1970s, studies have formally established that different *Ae. aegypti* populations display **variable vector competence** towards arboviruses [46, 217, 218].

Initial exploration of the genetic determinants of vector competence was supported by the generation of **linkage and physical maps** of the *Ae. aegypti* genome. A genetic linkage map describes the position of genetic markers in terms of recombination frequency, instead of physical distance, along each chromosome. The more recombination occurs between two markers, the further apart they are estimated to be. The first linkage maps of the *Ae. aegypti* genome were generated in the 1960s [219-224]. Physical maps were then correlated with linkage maps, using *in situ* hybridization probes to *Ae. aegypti* chromosomes [225, 226]. Additional physical landmarks of the genome were also obtained using expressed-sequence tags and sequence-tagged sites [227]. In parallel, the examination of the genetic structure of

mosquito populations was facilitated by development of RAPD-PCR markers [228] and single-strand conformation polymorphism analysis on mitochondrial DNA [229].

In the late 1990s, **controlled genetic crosses** [63, 204, 205] were conducted to investigate the genetic basis of *Ae. aegypti* vector competence for flaviviruses. For instance, crosses between the two *Ae. aegypti* subspecies demonstrated that genetic loci determine susceptibility to DENV and, more specifically, the outcome of midgut infection (*i.e.*, the MIB) and head dissemination (*i.e.*, the MEB) [63]. From this study, at least two loci were suspected to be involved in the control of the MIB and MEB. The observation of additive genetic effects also led to the hypothesis that vector competence is a complex trait, driven by a sum of genetic factors which vary continuously, potentially like the midgut pH, proteolytic enzymes, or thickness of the tissues.

Further studies continued the efforts of **mapping resistance loci**, based on genetic crosses of mosquito populations which presented with differential susceptibility to DENV, and segregation of the genetic variants associated with resistance [206-208]. In this way, it was suggested that the MIB was determined by two independent loci, which act additively both within each QTL and between QTL, accounting for about 30% of the phenotypic variance [207, 208]. It was then hypothesized that the additive pattern was reflective of differences in density in virus receptors on midgut cells, or in abundance of proviral and antiviral factors [207]. Studies focusing on the MEB enumerated at least 9 different QTL determining the viral dissemination potential from the midgut [206-208]. It became clear that a multitude of cellular processes, influenced by numerous genetic factors, regulate the competence of *Ae. aegypti* for DENV.

The **molecular underpinnings** of the susceptibility loci identified in QTL-mapping studies were later investigated, allowing to connect susceptibility site mapping with molecular functions of host factors. For instance, a mapping study evidenced that the *early trypsin* locus was determinant for DENV infection in the midgut [207]. Functional investigation of the *early trypsin* gene during midgut infection revealed that early trypsin activity is involved blood digestion which is needed for efficient infection of the midgut [230]. A finer association mapping study finally led to the identification of quantitative trait nucleotides (QTN), that is, sites within the *early trypsin* candidate gene which are responsible for the phenotypic variation observed [231].

Yet, the **power of QTL mapping studies** is inherently limited by several parameters. First, the low recombination rate of the *Ae. aegypti* genome [232, 233] drastically limits the mapping resolution. Moreover, this approach does not distinguish protein-coding sequences from non-coding regions, which are abundant in *Ae. aegypti* [186] and complexifies the search for

genetic factors *stricto sensu*. Additionally, this type of mapping only relies on statistical associations and not functional evidence. Furthermore, genetic mapping can only identify mosquito genes involved in vector competence if genetic variants of these very genes are associated with phenotypic variation. Also, most QTL mapping studies used laboratory strains of mosquitoes and ignored the broad genetic diversity inherent to wild mosquito populations. Finally, most of them overlooked the potential influence of the virus strain used, even though certain QTL driving virus dissemination in the vector were shown to be strain-specific [191], thus calling for higher throughput methods to increase the probability of identifying universal host molecular factors.

Consequently, the limitations of QTL mapping studies have prompted the development of other approaches with a broader scope of detection and finer resolution, which also capitalize on the genetic diversity of natural mosquito populations.

II.A.1.b) Technological advances & natural population surveys

The publication of the first **whole genome sequence** of *Ae. aegypti* in 2007 [234], followed by incremental updates and annotations until the last-to-date published version in 2018 [186] provided better foundations to identify genetically encoded molecular factors underlying vector competence. In parallel, the development of **transcriptomic tools** allowed first, identification of individual transcripts with expressed-sequence tags or single-target RT-PCR and later, profiling of a broader range of transcripts with micro-arrays and eventually RNA-sequencing. Transcriptomic approaches for the discovery of host factors are described in section II.A.2.a). The combination of expanding annotations and implementation of **databases and online resources** gathering data on *Ae. aegypti* genome, transcriptome and proteome [235-237] now facilitates the exploration of candidate factors and can guide functional characterization studies.

An alternative to crossing-based mapping studies is to **survey unmanipulated mosquito populations** to identify genetic variants associated with virus susceptibility or resistance. For instance, an exome-wide association study (EWAS) identified gene sets underlying DENV serotype-specific resistance in field-derived *Ae. aegypti* populations [238]. To our knowledge, genome-wide association studies (GWAS) have never been implemented to map vector competence genes in *Ae. aegypti*, although they have been for instance used to identify genetic variants associated with insecticide resistance in mosquitoes [239, 240]. Similarly, a genome-wide description of cis-regulatory elements also analyzed mosquito genetic variation contributing to differential susceptibility among mosquito colonies [241]. **Field-derived mosquito colonies** are great tools to explore and exploit the natural genetic diversity of

mosquito populations. In contrast, early QTL mapping studies often used **laboratory strains** of mosquitoes which have been established in labs sometimes decades before [242, 243]. They have since been used extensively for research around the world [242], but do not fully recapitulate the genetic diversity found in wild populations [244].

All these approaches benefitted from expanding annotations of the genome and transcriptome respectively, and expression profiling of susceptible or resistant phenotype in mosquitoes has been successfully carried out [191, 238, 241].

II.A.2) Exploring the mosquito response to flavivirus infection

II.A.2.a) Transcriptomic approaches

To decipher how mosquitoes respond to viral invasions, either supporting or fighting infection, transcriptomic profiling has provided a wealth of information. Initially, transcriptomic analyses consisted in **microarray analyses**, performed in mosquito cell lines [110] or *in vivo* [245]. These studies allowed to compare responses between tissues, viruses, and over time.

RNA sequencing later allowed to broaden the spectrum of transcripts detected, in an untargeted manner, and was applied to *Ae. aegypti in vivo* studies [246-249]. Identification of genes differentially regulated upon infection can pave the way for further functional characterization. For instance, a study analyzed the transcriptome of mosquito populations which presented with various susceptibility to DENV depending on their midgut mycobiota. RNA sequencing of these mosquitoes allowed to decipher how midgut fungi influence the mosquito physiology, through modulation of gut trypsin activity, to render them more permissive to DENV [248].

Tissue-specific transcriptomic datasets also participated in assessing heterogeneity in immune responses, helping to characterize the response of key tissues for mosquito infection and viral transmission, such as the midgut [237, 250], hemocytes [251, 252] or salivary glands [253, 254].

More recently, the development of **single-cell transcriptomic** approaches allowed to obtain **cell atlases** [252, 255-259] which revealed striking transcriptional heterogeneity at the cellular resolution. Single-cell RNA sequencing has namely been used to describe tissular cell composition, identify new cell types or define hemocyte differentiation trajectories [252]. This paves the way for a refined description of the response to viral infections at the scale of individual cells, yet this technology is yet to be implemented in virus-infected models.

Additionally, attempts at describing **intrinsic features of genes associated with resistance** or susceptibility to DENV have been made based on transcriptomic profiling. Features such as gene context, intron presence, codon usage bias, paralogy, or derivation from the ancestral origin were shown to have marginal effects in the definition of genes responsive to DENV infection. Nevertheless, non-responsiveness to DENV infection was associated with high codon usage bias, and intron-less or *Aedes*-specific genes (without *Culex* or *Anopheles* orthologs) were more associated with responsiveness to DENV [260, 261].

II.A.2.b) Interactomic and proteomic approaches

The implementation of techniques to describe the interactome of viral components was primarily motivated by the need to **identify viral receptors for flaviviruses in mosquitoes**. Conventional virus-overlay protein binding assays (VOPBA), which rely on electrophoresis of cellular components followed by “probing” with virus, were historically used to identify putative viral receptors [143, 262, 263]. Protein candidates were then purified by affinity column purification and used for further experimental confirmation of their interaction with viral components. However, the identification of the viral interactors was based on the protein molecular weight only, leading to uncertain identification. Combination of VOPBA assays with matrix-assisted laser desorption/ionization time-of-flight mass spectrometry (MALDI-TOF MS) later allowed to identify protein candidates with more accuracy [144]. Alternatively, affinity column chromatography with DENV E protein as a ligand [264] or tandem affinity purification assay of DENV E protein [157] have been successfully used.

More recently, wider exploration of the interactome of DENV in mosquito cells has been performed using **high throughput interactomic approaches** focusing on interactants of NS1, NS2A and NS2B, NS5 and capsid proteins [157, 158, 160, 265]. Two hybrid screening also provided additional insights in the network of physical DENV-mosquito protein-protein interactions [266, 267], with the finding of interactants common to both human and mosquito hosts.

With regards to the description of the mosquito response to infection, **proteomics studies** are complementary to transcriptomic profiling and have for instance allowed the identification of antiviral factors, *e.g.*, virus-specific and broad antiviral factors of mosquito salivary glands [103].

II.A.2.c) Metabolomic approaches

Metabolomics studies have proven to be valuable approaches to understand key features of mosquito response to viral infections (as reviewed in [268]). Since they can provide information

-GENERAL INTRODUCTION-

on the link between metabolites, metabolic pathways and viral components, metabolomics broaden the spectrum of routes manipulated by viral pathogens which are left to explore.

Metabolome profiling of DENV infected mosquito has been very predominantly focused on the **mosquito lipidome** [131, 165, 166, 168, 269], with much remaining to be investigated. Notably, further research is required in the areas of amino acid homeostasis, sugar metabolism, and iron usage, which have been shown to be essential for DENV infection modulation in mosquito cells [65, 270-273]. In addition, the tissue-specific metabolic response of the midgut has been investigated, whereas the response of the fat body has been largely overlooked when it is considered as a major metabolic and immune organ in mosquitoes.

II.A.2.d) Computational studies of interaction networks

In silico approaches offer a more comprehensive understanding of DENV molecular partners during the infection cycle in the mosquito. Computational generation of interaction networks combining multiple biologically relevant high-throughput screen datasets [274] or *in silico* prediction of interactions based on structural similarity [275] provide a promising basis for functional investigation of DENV-mosquito protein-protein interactions.

II.B) Reverse genetic approaches: from gene expression to infection phenotype

II.B.1) Sniper mode enabled: candidate-based approaches

Candidate-based approaches consist in testing the pro- or antiviral function of genes whose importance is suspected *a priori*. For vector studies, putative candidate factors are usually inferred from knowledge in *Drosophila*, whose immune system has been extensively studied, or from human data, and thus rely on the assumption of potentially conserved function across hosts.

II.B.1.a) Reverse genetic tools

Reverse genetic approaches allow to determine a gene's function by analyzing the phenotypic consequences of genetically silencing or inactivating this gene. Nowadays, two methods are commonly used, RNAi technics, and CRISPR/Cas9-mediated gene editing.

RNA interference (previously described in section I-2-c) can be exploited as a technique for reverse genetic studies in mosquitoes (as reviewed in [276]). It can be triggered by double-stranded RNA (dsRNA), or other forms of interfering RNA, targeting a gene of interest and supplied by intrathoracic injection or oral supplementation [277-280]. RNAi results in a transient silencing of the target transcript and has been used successfully for reverse genetic studies in a variety of contexts [116, 281-283].

CRISPR/Cas9-mediated gene editing is a precise genome edition tool, which can be used to mutate, knock-out or knock-in a target gene in the genome. Genome editing can result in transmission of the mutant alleles in the germline, allowing the generation of stable mutant lines [284]. Mutagenesis in mosquitoes was initially done using TALEN (TAL-effector nucleases), ZFN (zinc finger nucleases) or homing endonuclease genes [285-289] but CRISPR/Cas9 systems allows site-specific genome edition [284] and are now increasingly used.

II.B.1.b) Inferring knowledge from drosophila immunity

The majority of mosquito genes involved in innate immunity, particularly those associated with the inducible pathways and the RNA interference pathway, have been identified and characterized through the process of inference, utilizing knowledge about drosophila immunity. A representative example is the case of *Dicer2*, a key component of the RNAi pathway. Initially characterized in *Drosophila* [290, 291], in which its function in defense against RNA viruses was demonstrated *in vivo*, *Dicer2*'s influence on arbovirus in mosquitoes was later investigated in mosquito cells, using a *Dicer2*-knockout line [111], then using RNAi-mediated silencing *in vivo* [113, 114], sometimes in a tissue-specific manner [292], before successful generation of *Dicer2*-knockout mosquito lines [112, 117], which allowed to define more robustly the significance of *Dicer2* in mosquito vector competence for arboviruses.

II.B.1.c) Functional homology-based candidate identification

Another type of candidate-based approach relies on the assumption that response mechanisms are conserved between mammalian and arthropod hosts and aims to screen host dependency or restriction factors which have already been validated in humans. This hypothesis of functional homology has been successfully employed to characterize **mosquito orthologs of human antiviral factors** as restriction factors in the vector. [158, 293]. For instance, *ATCAY* and *FKBP1* genes are conserved in both human and mosquito cells, and display anti-DENV activity in both hosts, potentially associated with their ability to manipulate apoptosis [293]. The inverse strategy, which implies the identification of human orthologs of previously validated mosquito factors, has also been demonstrated to be a valuable approach in practice [181].

II.B.2) Casting the net wide: high-throughput screens

II.B.2.a) RNAi screens

The study of the modulation of the genetic landscape by flaviviruses during mosquito infection, using transcriptomic profiling, has identified hundreds of potential pro- or antiviral factors which

can subsequently be used as targets for functional characterization. **RNAi screen**-based studies have allowed to identify host dependency factors, either first screened in *Drosophila* cells and later confirmed in mosquito cells with a candidate-based method [181, 294], or directly carried out on mosquito cells [130, 151]. For example, a broad RNAi screen focusing on RNA-binding proteins paved the way for the identification of the proviral factor *Dhx15* and further mechanistic characterization of its proviral activity mediated by glycolysis regulation [130].

Nevertheless, RNAi approaches *in vivo* can be challenging, due to tissue-dependent, time-dependent and target-dependent variability in silencing efficiency, as well as administration methods and lack of reproducibility [276].

II.B.2.b) CRISPR screens

CRISPR/Cas9-mediated gene editing has been developed in mosquito cells, then *in vivo*, but never at the genome scale. Some proof-of-concept studies have demonstrated the feasibility of versatile plasmid-based CRISPR/Cas9 gene edition in mosquito cell lines [295] and developed tools optimized for genome-scale screening in vector species [296]. Such tools hold great potential for genome wide-scale investigation of mosquito-virus molecular interactions, as they did for mammalian host studies [297, 298].

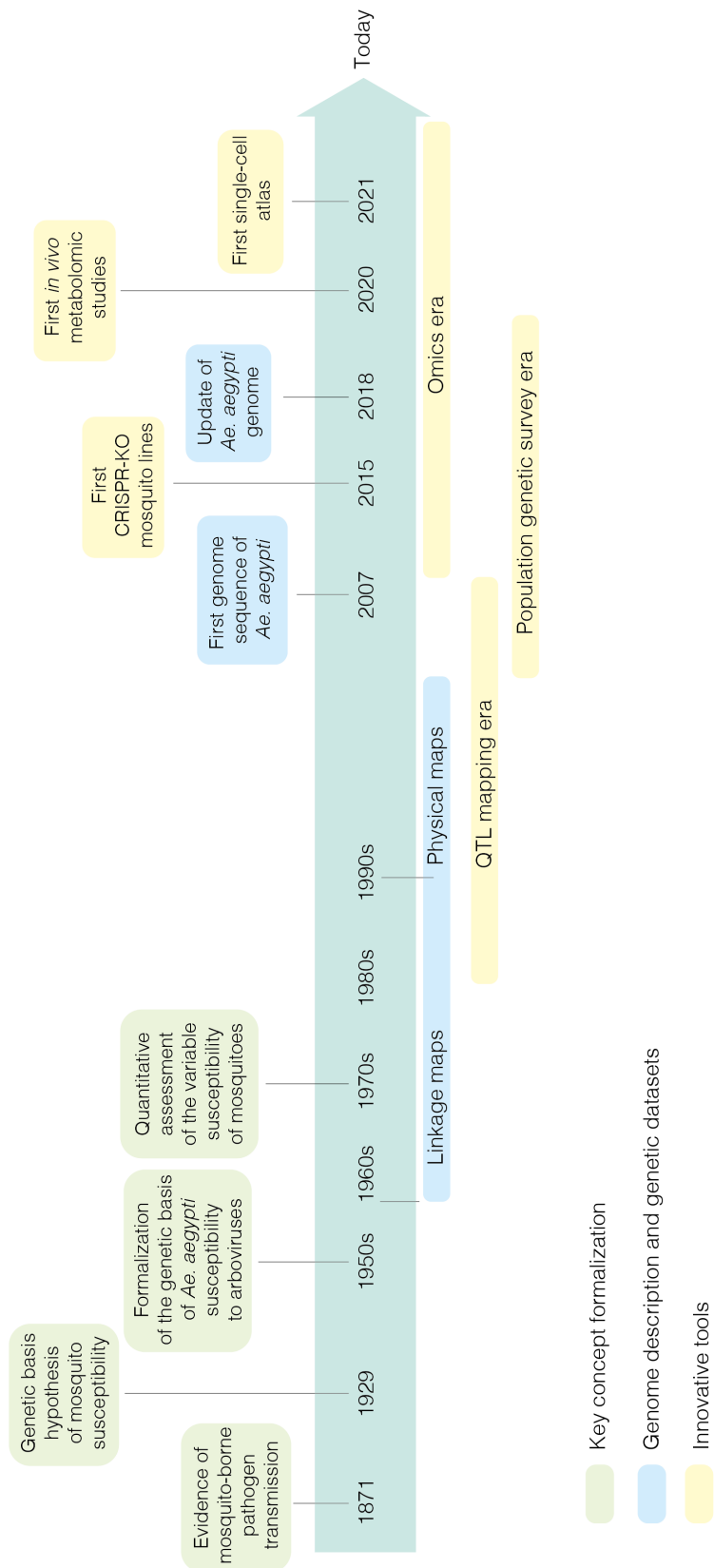


Figure 7. Historical timeline of approaches and technologies used for the discovery of *Ae. aegypti* genetic determinants of vector competence towards arboviruses.

CONCLUSION

This review of the methodologies employed to describe mosquito-virus relationships, and more specifically, identify mosquito molecular determinants of vector competence, highlights the complexity of this research field.

The intricate nature of vector-virus associations and the vast array of genetic factors influencing vector competence render this endeavor particularly challenging. Indeed, this research field faces several limitations. Genetic resources available for mosquito studies are overall much more limited than for the insect model *Drosophila melanogaster*, as evidenced by the lack of mutant panels and of relevant reference strains of *Ae. aegypti*. The genome of *Ae. aegypti* is notably large and highly repetitive [186]. This contributes to an average gene length and intergenic region size that is approximately five times larger than that of *D. melanogaster* [234]. Hence, annotation efforts and genetic manipulation attempts are inherently more complex. Additionally, their longer life cycle and more complex rearing environments have slowed down experimental progress. Finally, the remarkable genetic diversity observed in wild mosquito populations mitigates the relevance of laboratory-established mosquito colonies and calls for the use of field-derived mosquito populations. Consequently, it is essential that fundamental research on mosquito immunity be conducted in close collaboration with field studies.

Nevertheless, technological advances have enabled the development of high-throughput techniques that facilitate exploration of the mosquito's intrinsic factors at the genome scale. Additionally, the expansion of omics approaches, such as metabolomics, epigenomics or single-cell approaches, offers promising new avenues for investigation.

Eventually, the acquisition of such fundamental knowledge will assist the development of vector control strategies aiming at rendering mosquitoes incapable of transmitting arboviruses. The complex nature of the mosquito-virus interface renders the identification of an ideal universal target a challenging prospect. Conversely, it represents an opportunity for selective targeting of factors involved in specific mosquito-virus interactions, thereby reducing the potential for adverse effects on mosquito fitness and ecology.

In essence, elucidating the mosquito's arsenal and orienting vector control strategies towards the hijacking of the mosquito's natural weapons is critical to tackle the growing global arboviral threat.

-GENERAL INTRODUCTION-

In this context, the following thesis work describes three distinct *in vivo* approaches aimed at investigating mosquito molecular factors which modulate, either positively or negatively, the infection, dissemination and/or transmission of flaviviruses in *Ae. aegypti*.

The **first chapter** is dedicated to the functional investigation of a *Vago*-like gene in *Ae. aegypti* in the context of DENV infection *in vivo*. The current state of knowledge regarding this immune-related factor in *Ae. aegypti* mosquitoes is notably limited, with the majority of existing studies deriving from research conducted in related insect species and *in vitro*.

The **second chapter** is dedicated to the discovery of a novel non-canonical antiviral factor, cytochrome P450 4g15, associated with a natural DENV resistance phenotype identified in a field-derived population of *Ae. aegypti*.

The **third chapter** reports on the *in vivo* characterization of candidate DENV receptors in *Ae. aegypti*, with a specific emphasis on the putative receptor *prohibitin-2*.

REFERENCES

1. Franz, A.W., et al., *Tissue Barriers to Arbovirus Infection in Mosquitoes*. *Viruses*, 2015. **7**(7): p. 3741-67.
2. Karabatsos, N., *Supplement to International Catalogue of Arboviruses including certain other viruses of vertebrates*. *Am J Trop Med Hyg*, 1978. **27**(2 Pt 2 Suppl): p. 372-440.
3. Weaver, S.C. and W.K. Reisen, *Present and future arboviral threats*. *Antiviral Res*, 2010. **85**(2): p. 328-45.
4. Simmonds, P., et al., *ICTV Virus Taxonomy Profile: Flaviviridae*. *J Gen Virol*, 2017. **98**(1): p. 2-3.
5. Lefkowitz, E.J., et al., *Virus taxonomy: the database of the International Committee on Taxonomy of Viruses (ICTV)*. *Nucleic Acids Res*, 2018. **46**(D1): p. D708-D717.
6. Girard, M., et al., *Arboviruses: A global public health threat*. *Vaccine*, 2020. **38**(24): p. 3989-3994.
7. Gubler, D.J., *The global emergence/resurgence of arboviral diseases as public health problems*. *Arch Med Res*, 2002. **33**(4): p. 330-42.
8. Wilder-Smith, A., et al., *Epidemic arboviral diseases: priorities for research and public health*. *Lancet Infect Dis*, 2017. **17**(3): p. e101-e106.
9. Pierson, T.C. and M.S. Diamond, *The continued threat of emerging flaviviruses*. *Nat Microbiol*, 2020. **5**(6): p. 796-812.
10. Bhatt, S., et al., *The global distribution and burden of dengue*. *Nature*, 2013. **496**(7446): p. 504-7.
11. Messina, J.P., et al., *The current and future global distribution and population at risk of dengue*. *Nat Microbiol*, 2019. **4**(9): p. 1508-1515.
12. in *Dengue: Guidelines for Diagnosis, Treatment, Prevention and Control: New Edition*. 2009: Geneva.
13. Vasilakis, N., et al., *Fever from the forest: prospects for the continued emergence of sylvatic dengue virus and its impact on public health*. *Nat Rev Microbiol*, 2011. **9**(7): p. 532-41.
14. Guzman, M.G., et al., *Dengue: a continuing global threat*. *Nat Rev Microbiol*, 2010. **8**(12 Suppl): p. S7-16.
15. Katzelnick, L.C., et al., *Dengue viruses cluster antigenically but not as discrete serotypes*. *Science*, 2015. **349**(6254): p. 1338-43.
16. Pierson, T.C. and M.S. Diamond, *The emergence of Zika virus and its new clinical syndromes*. *Nature*, 2018. **560**(7720): p. 573-581.
17. Gubler, D.J., N. Vasilakis, and D. Musso, *History and Emergence of Zika Virus*. *J Infect Dis*, 2017. **216**(suppl_10): p. S860-S867.
18. Prevention, E.C.f.D. and Control, *Rapid risk assessment: Zika virus epidemic in the Americas: potential association with microcephaly and Guillain-Barré syndrome*. European Centre for Disease Prevention and Control, 2015.
19. Rasmussen, S.A., et al., *Zika Virus and Birth Defects--Reviewing the Evidence for Causality*. *N Engl J Med*, 2016. **374**(20): p. 1981-7.
20. Heymann, D.L., et al., *Zika virus and microcephaly: why is this situation a PHEIC?* *Lancet*, 2016. **387**(10020): p. 719-21.
21. Pintado Silva, J. and A. Fernandez-Sesma, *Challenges on the development of a dengue vaccine: a comprehensive review of the state of the art*. *J Gen Virol*, 2023. **104**(3).

22. Wang, Y., et al., *Current Advances in Zika Vaccine Development*. Vaccines (Basel), 2022. **10**(11).
23. Viglietta, M., et al., *Vector Specificity of Arbovirus Transmission*. Front Microbiol, 2021. **12**: p. 773211.
24. Wu, P., et al., *Arbovirus lifecycle in mosquito: acquisition, propagation and transmission*. Expert Rev Mol Med, 2019. **21**: p. e1.
25. Gutierrez-Bugallo, G., et al., *Vector-borne transmission and evolution of Zika virus*. Nat Ecol Evol, 2019. **3**(4): p. 561-569.
26. Gratz, N.G., *Critical review of the vector status of Aedes albopictus*. Med Vet Entomol, 2004. **18**(3): p. 215-27.
27. Kraemer, M.U., et al., *The global distribution of the arbovirus vectors Aedes aegypti and Ae. albopictus*. Elife, 2015. **4**: p. e08347.
28. Kraemer, M.U., et al., *The global compendium of Aedes aegypti and Ae. albopictus occurrence*. Sci Data, 2015. **2**: p. 150035.
29. Souza-Neto, J.A., J.R. Powell, and M. Bonizzoni, *Aedes aegypti vector competence studies: A review*. Infect Genet Evol, 2019. **67**: p. 191-209.
30. Christophers, S.R., *Aedes aegypti: the yellow fever mosquito*. 1960: CUP Archive.
31. Clemens, A., *The Biology of Mosquitoes, Development, Nutrition, and Reproduction*. 1992, Chapman & Hall, London.
32. Clemens, A., *The Biology of Mosquitoes Vol 2: Sensory Reception and Behaviour*. 1999, CABI, University Press, Cambridge.
33. Fikrig, K., et al., *Aedes albopictus host odor preference does not drive observed variation in feeding patterns across field populations*. Sci Rep, 2023. **13**(1): p. 130.
34. Egid, B.R., et al., *Review of the ecology and behaviour of Aedes aegypti and Aedes albopictus in Western Africa and implications for vector control*. Curr Res Parasitol Vector Borne Dis, 2022. **2**: p. 100074.
35. Powell, J.R., A. Gloria-Soria, and P. Kotsakiozi, *Recent History of Aedes aegypti: Vector Genomics and Epidemiology Records*. Bioscience, 2018. **68**(11): p. 854-860.
36. McBride, C.S., et al., *Evolution of mosquito preference for humans linked to an odorant receptor*. Nature, 2014. **515**(7526): p. 222-7.
37. Lounibos, L.P., *Habitat segregation among African treehole mosquitoes*. Ecological Entomology, 1981. **6**.
38. Ding, F., et al., *Mapping the spatial distribution of Aedes aegypti and Aedes albopictus*. Acta Trop, 2018. **178**: p. 155-162.
39. Laporta, G.Z., et al., *Global Distribution of Aedes aegypti and Aedes albopictus in a Climate Change Scenario of Regional Rivalry*. Insects, 2023. **14**(1).
40. Wilson, A.L., et al., *The importance of vector control for the control and elimination of vector-borne diseases*. PLoS Negl Trop Dis, 2020. **14**(1): p. e0007831.
41. Moyes, C.L., et al., *Contemporary status of insecticide resistance in the major Aedes vectors of arboviruses infecting humans*. PLoS Negl Trop Dis, 2017. **11**(7): p. e0005625.
42. Shaw, W.R. and F. Catteruccia, *Vector biology meets disease control: using basic research to fight vector-borne diseases*. Nat Microbiol, 2019. **4**(1): p. 20-34.
43. Flores, H.A. and S.L. O'Neill, *Controlling vector-borne diseases by releasing modified mosquitoes*. Nat Rev Microbiol, 2018. **16**(8): p. 508-518.

44. Kean, J., et al., *Fighting Arbovirus Transmission: Natural and Engineered Control of Vector Competence in Aedes Mosquitoes*. *Insects*, 2015. **6**(1): p. 236-78.
45. Salazar, M.I., et al., *Dengue virus type 2: replication and tropisms in orally infected Aedes aegypti mosquitoes*. *BMC Microbiol*, 2007. **7**: p. 9.
46. Gubler, D.J., et al., *Variation in susceptibility to oral infection with dengue viruses among geographic strains of Aedes aegypti*. *Am J Trop Med Hyg*, 1979. **28**(6): p. 1045-52.
47. Hall, D.R., et al., *Mosquito immune cells enhance dengue and Zika virus dissemination in Aedes aegypti*. *bioRxiv*, 2024.
48. Leite, T., et al., *Distinct Roles of Hemocytes at Different Stages of Infection by Dengue and Zika Viruses in Aedes aegypti Mosquitoes*. *Front Immunol*, 2021. **12**: p. 660873.
49. Raquin, V. and L. Lambrechts, *Dengue virus replicates and accumulates in Aedes aegypti salivary glands*. *Virology*, 2017. **507**: p. 75-81.
50. Wichit, S., et al., *The effects of mosquito saliva on dengue virus infectivity in humans*. *Curr Opin Virol*, 2016. **21**: p. 139-145.
51. Guerrero, D., T. Cantaert, and D. Misse, *Aedes Mosquito Salivary Components and Their Effect on the Immune Response to Arboviruses*. *Front Cell Infect Microbiol*, 2020. **10**: p. 407.
52. Macdonald, G., *Epidemiologic models in studies of vectorborne diseases*. *Public Health Rep (1896)*, 1961. **76**(9): p. 753-64.
53. Ross, R., *Some Quantitative Studies in Epidemiology*. *Nature*, 1911. **87**(2188): p. 466-467.
54. Hardy, J.L., et al., *Intrinsic factors affecting vector competence of mosquitoes for arboviruses*. *Annu Rev Entomol*, 1983. **28**: p. 229-62.
55. Beerntsen, B.T., A.A. James, and B.M. Christensen, *Genetics of mosquito vector competence*. *Microbiol Mol Biol Rev*, 2000. **64**(1): p. 115-37.
56. Lewis, J., et al., *Intrinsic factors driving mosquito vector competence and viral evolution: a review*. *Front Cell Infect Microbiol*, 2023. **13**: p. 1330600.
57. Wu, V.Y., et al., *A minimum data standard for vector competence experiments*. *Sci Data*, 2022. **9**(1): p. 634.
58. Black, W. and C. Moore, *Biology of disease vectors*. 2005, Marquardt WC: Burlington, MA: Elsevier Academic Press.
59. Smith, D.L., et al., *Ross, macdonald, and a theory for the dynamics and control of mosquito-transmitted pathogens*. *PLoS Pathog*, 2012. **8**(4): p. e1002588.
60. Kramer, L.D. and A.T. Ciota, *Dissecting vectorial capacity for mosquito-borne viruses*. *Curr Opin Virol*, 2015. **15**: p. 112-8.
61. Rosendo Machado, S., T. van der Most, and P. Miesen, *Genetic determinants of antiviral immunity in dipteran insects - Compiling the experimental evidence*. *Dev Comp Immunol*, 2021. **119**: p. 104010.
62. Alonso-Palomares, L.A., et al., *Molecular Basis for Arbovirus Transmission by Aedes aegypti Mosquitoes*. *Intervirology*, 2018. **61**(6): p. 255-264.
63. Bosio, C.F., B.J. Beaty, and W.C.t. Black, *Quantitative genetics of vector competence for dengue-2 virus in Aedes aegypti*. *Am J Trop Med Hyg*, 1998. **59**(6): p. 965-70.
64. Carrington, L.B., et al., *Fluctuations at a low mean temperature accelerate dengue virus transmission by Aedes aegypti*. *PLoS Negl Trop Dis*, 2013. **7**(4): p. e2190.

65. Vaidyanathan, R., et al., *Nutritional stress affects mosquito survival and vector competence for West Nile virus*. Vector Borne Zoonotic Dis, 2008. **8**(6): p. 727-32.
66. Yan, J., et al., *Nutritional stress compromises mosquito fitness and antiviral immunity, while enhancing dengue virus infection susceptibility*. Commun Biol, 2023. **6**(1): p. 1123.
67. Hillyer, J.F. and M.R. Strand, *Mosquito hemocyte-mediated immune responses*. Curr Opin Insect Sci, 2014. **3**: p. 14-21.
68. Hillyer, J.F., *Insect immunology and hematopoiesis*. Dev Comp Immunol, 2016. **58**: p. 102-18.
69. Cardoso-Jaime, V., et al., *The Role of Mosquito Hemocytes in Viral Infections*. Viruses, 2022. **14**(10).
70. Costa, A., et al., *The Imd pathway is involved in antiviral immune responses in Drosophila*. PLoS One, 2009. **4**(10): p. e7436.
71. Nainu, F., et al., *Protection of Insects against Viral Infection by Apoptosis-Dependent Phagocytosis*. J Immunol, 2015. **195**(12): p. 5696-706.
72. Lamiable, O., et al., *Analysis of the Contribution of Hemocytes and Autophagy to Drosophila Antiviral Immunity*. J Virol, 2016. **90**(11): p. 5415-5426.
73. Parikh, G.R., J.D. Oliver, and L.C. Bartholomay, *A haemocyte tropism for an arbovirus*. J Gen Virol, 2009. **90**(Pt 2): p. 292-296.
74. Cheng, L., et al., *Prohemocytes are the main cells infected by dengue virus in Aedes aegypti and Aedes albopictus*. Parasit Vectors, 2022. **15**(1): p. 137.
75. Choi, Y.J., et al., *Tissue-enriched expression profiles in Aedes aegypti identify hemocyte-specific transcriptome responses to infection*. Insect Biochem Mol Biol, 2012. **42**(10): p. 729-38.
76. Wang, X., et al., *The diversity of pattern recognition receptors (PRRs) involved with insect defense against pathogens*. Current opinion in insect science, 2019. **33**: p. 105-110.
77. Weng, S.C., et al., *A Thioester-Containing Protein Controls Dengue Virus Infection in Aedes aegypti Through Modulating Immune Response*. Front Immunol, 2021. **12**: p. 670122.
78. Cheng, G., et al., *An in vivo transfection approach elucidates a role for Aedes aegypti thioester-containing proteins in flaviviral infection*. PLoS One, 2011. **6**(7): p. e22786.
79. Price, D.P., et al., *The fat body transcriptomes of the yellow fever mosquito Aedes aegypti, pre- and post- blood meal*. PLoS One, 2011. **6**(7): p. e22573.
80. Hun, L.V., et al., *Increased insulin signaling in the Anopheles stephensi fat body regulates metabolism and enhances the host response to both bacterial challenge and Plasmodium falciparum infection*. Insect Biochem Mol Biol, 2021. **139**: p. 103669.
81. Zou, Z., et al., *Transcriptome analysis of Aedes aegypti transgenic mosquitoes with altered immunity*. PLoS Pathog, 2011. **7**(11): p. e1002394.
82. Jupatanakul, N., et al., *Engineered Aedes aegypti JAK/STAT Pathway-Mediated Immunity to Dengue Virus*. PLoS Negl Trop Dis, 2017. **11**(1): p. e0005187.
83. Pan, X., et al., *Wolbachia induces reactive oxygen species (ROS)-dependent activation of the Toll pathway to control dengue virus in the mosquito Aedes aegypti*. Proc Natl Acad Sci U S A, 2012. **109**(1): p. E23-31.

84. Ramirez, J.L. and G. Dimopoulos, *The Toll immune signaling pathway control conserved anti-dengue defenses across diverse Ae. aegypti strains and against multiple dengue virus serotypes*. Dev Comp Immunol, 2010. **34**(6): p. 625-9.
85. Xiao, X., et al., *Complement-related proteins control the flavivirus infection of Aedes aegypti by inducing antimicrobial peptides*. PLoS Pathog, 2014. **10**(4): p. e1004027.
86. Rodriguez-Andres, J., et al., *Phenoloxidase activity acts as a mosquito innate immune response against infection with Semliki Forest virus*. PLoS Pathog, 2012. **8**(11): p. e1002977.
87. Ramesh Kumar, J., et al., *Use of Clodronate Liposomes to Deplete Phagocytic Immune Cells in Drosophila melanogaster and Aedes aegypti*. Front Cell Dev Biol, 2021. **9**: p. 627976.
88. Dong, S., et al., *Infection pattern and transmission potential of chikungunya virus in two New World laboratory-adapted Aedes aegypti strains*. Sci Rep, 2016. **6**: p. 24729.
89. O'Neill, K., et al., *Rapid selection against arbovirus-induced apoptosis during infection of a mosquito vector*. Proc Natl Acad Sci U S A, 2015. **112**(10): p. E1152-61.
90. Eng, M.W., M.N. van Zuylen, and D.W. Severson, *Apoptosis-related genes control autophagy and influence DENV-2 infection in the mosquito vector, Aedes aegypti*. Insect Biochem Mol Biol, 2016. **76**: p. 70-83.
91. Brackney, D.E., M.A. Correa, and D.W. Cozens, *The impact of autophagy on arbovirus infection of mosquito cells*. PLoS Negl Trop Dis, 2020. **14**(5): p. e0007754.
92. Chen, T.Y. and C.T. Smartt, *Activation of the autophagy pathway decreases dengue virus infection in Aedes aegypti cells*. Parasit Vectors, 2021. **14**(1): p. 551.
93. Darnell Jr, J.E., I.M. Kerr, and G.R. Stark, *Jak-STAT pathways and transcriptional activation in response to IFNs and other extracellular signaling proteins*. Science, 1994. **264**(5164): p. 1415-1421.
94. Souza-Neto, J.A., S. Sim, and G. Dimopoulos, *An evolutionary conserved function of the JAK-STAT pathway in anti-dengue defense*. Proc Natl Acad Sci U S A, 2009. **106**(42): p. 17841-6.
95. Sim, S., et al., *Transcriptomic profiling of diverse Aedes aegypti strains reveals increased basal-level immune activation in dengue virus-refractory populations and identifies novel virus-vector molecular interactions*. PLoS Negl Trop Dis, 2013. **7**(7): p. e2295.
96. Anglero-Rodriguez, Y.I., et al., *Aedes aegypti Toll pathway is induced through dsRNA sensing in endosomes*. Dev Comp Immunol, 2021. **122**: p. 104138.
97. Paradkar, P.N., et al., *Secreted Vago restricts West Nile virus infection in Culex mosquito cells by activating the Jak-STAT pathway*. Proc Natl Acad Sci U S A, 2012. **109**(46): p. 18915-20.
98. Paradkar, P.N., et al., *Dicer-2-dependent activation of Culex Vago occurs via the TRAF-Rel2 signaling pathway*. PLoS Negl Trop Dis, 2014. **8**(4): p. e2823.
99. Deddouche, S., et al., *The DExD/H-box helicase Dicer-2 mediates the induction of antiviral activity in drosophila*. Nat Immunol, 2008. **9**(12): p. 1425-32.
100. Xi, Z., J.L. Ramirez, and G. Dimopoulos, *The Aedes aegypti toll pathway controls dengue virus infection*. PLoS Pathog, 2008. **4**(7): p. e1000098.

101. McFarlane, M., et al., *Characterization of Aedes aegypti innate-immune pathways that limit Chikungunya virus replication*. PLoS Negl Trop Dis, 2014. **8**(7): p. e2994.
102. Rai, P., et al., *Insulin reduces the transmission potential of chikungunya virus and activates the toll pathway in Aedes aegypti mosquitoes*. Insect Mol Biol, 2023. **32**(6): p. 648-657.
103. Chowdhury, A., et al., *JNK pathway restricts DENV2, ZIKV and CHIKV infection by activating complement and apoptosis in mosquito salivary glands*. PLoS Pathog, 2020. **16**(8): p. e1008754.
104. Waldock, J., K.E. Olson, and G.K. Christophides, *Anopheles gambiae antiviral immune response to systemic O'nyong-nyong infection*. PLoS Negl Trop Dis, 2012. **6**(3): p. e1565.
105. Carissimo, G., et al., *Antiviral immunity of Anopheles gambiae is highly compartmentalized, with distinct roles for RNA interference and gut microbiota*. Proc Natl Acad Sci U S A, 2015. **112**(2): p. E176-85.
106. Luplertlop, N., et al., *Induction of a peptide with activity against a broad spectrum of pathogens in the Aedes aegypti salivary gland, following Infection with Dengue Virus*. PLoS Pathog, 2011. **7**(1): p. e1001252.
107. Pompon, J., et al., *Dengue subgenomic flaviviral RNA disrupts immunity in mosquito salivary glands to increase virus transmission*. PLoS Pathog, 2017. **13**(7): p. e1006535.
108. Méndez, Y., C. Pacheco, and F. Herrera, *Inhibition of defensin A and cecropin A responses to dengue virus 1 infection in Aedes aegypti*. Biomedica, 2021. **41**(1): p. 161-167.
109. Cheung, Y.P., et al., *The antiviral role of NF- κ B-mediated immune responses and their antagonism by viruses in insects*. J Gen Virol, 2022. **103**(5).
110. Sim, S. and G. Dimopoulos, *Dengue virus inhibits immune responses in Aedes aegypti cells*. PLoS One, 2010. **5**(5): p. e10678.
111. Varjak, M., et al., *Aedes aegypti Piwi4 Is a Noncanonical PIWI Protein Involved in Antiviral Responses*. mSphere, 2017. **2**.
112. Samuel, G.H., et al., *RNA interference is essential to modulating the pathogenesis of mosquito-borne viruses in the yellow fever mosquito Aedes aegypti*. Proc Natl Acad Sci U S A, 2023. **120**(11): p. e2213701120.
113. Campbell, C.L., et al., *Aedes aegypti uses RNA interference in defense against Sindbis virus infection*. BMC Microbiol, 2008. **8**: p. 47.
114. Sanchez-Vargas, I., et al., *Dengue virus type 2 infections of Aedes aegypti are modulated by the mosquito's RNA interference pathway*. PLoS Pathog, 2009. **5**(2): p. e1000299.
115. Dong, Y., et al., *The Aedes aegypti siRNA pathway mediates broad-spectrum defense against human pathogenic viruses and modulates antibacterial and antifungal defenses*. PLoS Biol, 2022. **20**(6): p. e3001668.
116. Olmo, R.P., et al., *Control of dengue virus in the midgut of Aedes aegypti by ectopic expression of the dsRNA-binding protein Loqs2*. Nat Microbiol, 2018. **3**(12): p. 1385-1393.
117. Merklings, S.H., et al., *Multifaceted contributions of Dicer2 to arbovirus transmission by Aedes aegypti*. Cell Rep, 2023. **42**(8): p. 112977.
118. Dong, S. and G. Dimopoulos, *Aedes aegypti Argonaute 2 controls arbovirus infection and host mortality*. Nat Commun, 2023. **14**(1): p. 5773.

119. Serrato-Salas, J., et al., *De Novo DNA Synthesis in Aedes aegypti Midgut Cells as a Complementary Strategy to Limit Dengue Viral Replication*. *Front Microbiol*, 2018. **9**: p. 801.
120. Xu, J., et al., *Transcriptional pausing controls a rapid antiviral innate immune response in Drosophila*. *Cell Host Microbe*, 2012. **12**(4): p. 531-43.
121. Nakamoto, M., et al., *Virus recognition by Toll-7 activates antiviral autophagy in Drosophila*. *Immunity*, 2012. **36**(4): p. 658-67.
122. Shelly, S., et al., *Autophagy is an essential component of Drosophila immunity against vesicular stomatitis virus*. *Immunity*, 2009. **30**(4): p. 588-98.
123. Liu, Y. and S. Cherry, *Zika virus infection activates sting-dependent antiviral autophagy in the Drosophila brain*. *Autophagy*, 2019. **15**(1): p. 174-175.
124. Ahlers, L.R.H., et al., *Insulin Potentiates JAK/STAT Signaling to Broadly Inhibit Flavivirus Replication in Insect Vectors*. *Cell Rep*, 2019. **29**(7): p. 1946-1960 e5.
125. Xu, J., et al., *ERK signaling couples nutrient status to antiviral defense in the insect gut*. *Proc Natl Acad Sci U S A*, 2013. **110**(37): p. 15025-30.
126. Ayers, J.B., et al., *Clustered rapid induction of apoptosis limits ZIKV and DENV-2 proliferation in the midguts of Aedes aegypti*. *Commun Biol*, 2021. **4**(1): p. 69.
127. Ocampo, C.B., et al., *Differential expression of apoptosis related genes in selected strains of Aedes aegypti with different susceptibilities to dengue virus*. *PLoS One*, 2013. **8**(4): p. e61187.
128. Wang, H., et al., *Effects of manipulating apoptosis on Sindbis virus infection of Aedes aegypti mosquitoes*. *J Virol*, 2012. **86**(12): p. 6546-54.
129. Chang, Y.C., et al., *Effect of C-type lectin 16 on dengue virus infection in Aedes aegypti salivary glands*. *PNAS Nexus*, 2024. **3**(5): p. pgae188.
130. Rosendo Machado, S., et al., *The DEAD-box RNA helicase Dhx15 controls glycolysis and arbovirus replication in Aedes aegypti mosquito cells*. *PLoS Pathog*, 2022. **18**(11): p. e1010694.
131. Koh, C., et al., *Dengue virus dominates lipid metabolism modulations in Wolbachia-coinfected Aedes aegypti*. *Commun Biol*, 2020. **3**(1): p. 518.
132. Tree, M.O., et al., *Dengue virus reduces expression of low-density lipoprotein receptor-related protein 1 to facilitate replication in Aedes aegypti*. *Sci Rep*, 2019. **9**(1): p. 6352.
133. Troupin, A., et al., *A novel mosquito ubiquitin targets viral envelope protein for degradation and reduces virion production during dengue virus infection*. *Biochim Biophys Acta*, 2016. **1860**(9): p. 1898-909.
134. Waterhouse, R.M., et al., *Evolutionary dynamics of immune-related genes and pathways in disease-vector mosquitoes*. *Science*, 2007. **316**(5832): p. 1738-43.
135. Bartholomay, L.C. and K. Michel, *Mosquito Immunobiology: The Intersection of Vector Health and Vector Competence*. *Annu Rev Entomol*, 2018. **63**: p. 145-167.
136. Bartholomay, L.C., et al., *Pathogenomics of Culex quinquefasciatus and meta-analysis of infection responses to diverse pathogens*. *Science*, 2010. **330**(6000): p. 88-90.
137. Shin, S.W., et al., *REL1, a homologue of Drosophila dorsal, regulates toll antifungal immune pathway in the female mosquito Aedes aegypti*. *J Biol Chem*, 2005. **280**(16): p. 16499-507.

138. Wang, S. and B.T. Beerntsen, *Functional implications of the peptidoglycan recognition proteins in the immunity of the yellow fever mosquito, Aedes aegypti*. *Insect Mol Biol*, 2015. **24**(3): p. 293-310.
139. Antonova, Y., et al., *The role of NF-kappaB factor REL2 in the Aedes aegypti immune response*. *Insect Biochem Mol Biol*, 2009. **39**(4): p. 303-14.
140. Bronkhorst, A.W. and R.P. van Rij, *The long and short of antiviral defense: small RNA-based immunity in insects*. *Curr Opin Virol*, 2014. **7**: p. 19-28.
141. Marques, J.T., et al., *Loqs and R2D2 act sequentially in the siRNA pathway in Drosophila*. *Nat Struct Mol Biol*, 2010. **17**(1): p. 24-30.
142. Payne, S., *Chapter 1 - Introduction to Animal Viruses*, in *Viruses*, S. Payne, Editor. 2017, Academic Press. p. 1-11.
143. Sakoonwatanyoo, P., V. Boonsanay, and D.R. Smith, *Growth and production of the dengue virus in C6/36 cells and identification of a laminin-binding protein as a candidate serotype 3 and 4 receptor protein*. *Intervirology*, 2006. **49**(3): p. 161-72.
144. Chee, H.Y. and S. AbuBakar, *Identification of a 48kDa tubulin or tubulin-like C6/36 mosquito cells protein that binds dengue virus 2 using mass spectrometry*. *Biochem Biophys Res Commun*, 2004. **320**(1): p. 11-7.
145. Paingankar, M.S., M.D. Gokhale, and D.N. Deobagkar, *Dengue-2-virus-interacting polypeptides involved in mosquito cell infection*. *Arch Virol*, 2010. **155**(9): p. 1453-61.
146. Mercado-Curiel, R.F., et al., *The four serotypes of dengue recognize the same putative receptors in Aedes aegypti midgut and Ae. albopictus cells*. *BMC Microbiol*, 2006. **6**: p. 85.
147. Mercado-Curiel, R.F., W.C.t. Black, and L. Munoz Mde, *A dengue receptor as possible genetic marker of vector competence in Aedes aegypti*. *BMC Microbiol*, 2008. **8**: p. 118.
148. Munoz Mde, L., et al., *Proteomic identification of dengue virus binding proteins in Aedes aegypti mosquitoes and Aedes albopictus cells*. *Biomed Res Int*, 2013. **2013**: p. 875958.
149. Kuadkitkan, A., et al., *Identification and characterization of prohibitin as a receptor protein mediating DENV-2 entry into insect cells*. *Virology*, 2010. **406**(1): p. 149-61.
150. Wichit, S., et al., *Dengue virus type 2 recognizes the carbohydrate moiety of neutral glycosphingolipids in mammalian and mosquito cells*. *Microbiol Immunol*, 2011. **55**(2): p. 135-40.
151. Londono-Renteria, B., et al., *Dengue Virus Infection of Aedes aegypti Requires a Putative Cysteine Rich Venom Protein*. *PLoS Pathog*, 2015. **11**(10): p. e1005202.
152. Acosta, E.G., V. Castilla, and E.B. Damonte, *Functional entry of dengue virus into Aedes albopictus mosquito cells is dependent on clathrin-mediated endocytosis*. *J Gen Virol*, 2008. **89**(Pt 2): p. 474-484.
153. Acosta, E.G., et al., *Changes in antiviral susceptibility to entry inhibitors and endocytic uptake of dengue-2 virus serially passaged in Vero or C6/36 cells*. *Virus Res*, 2014. **184**: p. 39-43.
154. Mosso, C., et al., *Endocytic pathway followed by dengue virus to infect the mosquito cell line C6/36 HT*. *Virology*, 2008. **378**(1): p. 193-9.
155. Alcalá, A.C., et al., *Dengue Virus NS1 Uses Scavenger Receptor B1 as a Cell Receptor in Cultured Cells*. *J Virol*, 2022. **96**(5): p. e0166421.

156. Liu, J., et al., *Flavivirus NS1 protein in infected host sera enhances viral acquisition by mosquitoes*. Nat Microbiol, 2016. **1**(9): p. 16087.
157. Colpitts, T.M., et al., *Use of a tandem affinity purification assay to detect interactions between West Nile and dengue viral proteins and proteins of the mosquito vector*. Virology, 2011. **417**(1): p. 179-87.
158. Gestuveo, R.J., et al., *Analysis of Zika virus capsid-Aedes aegypti mosquito interactome reveals pro-viral host factors critical for establishing infection*. Nat Commun, 2021. **12**(1): p. 2766.
159. Junjhon, J., et al., *Ultrastructural characterization and three-dimensional architecture of replication sites in dengue virus-infected mosquito cells*. J Virol, 2014. **88**(9): p. 4687-97.
160. Besson, B., et al., *Arbovirus-vector protein interactomics identifies Loquacious as a co-factor for dengue virus replication in Aedes mosquitoes*. PLoS Pathog, 2022. **18**(9): p. e1010329.
161. Shivaprasad, S., et al., *Loquacious modulates flaviviral RNA replication in mosquito cells*. PLoS Pathog, 2022. **18**(4): p. e1010163.
162. Perera, R., et al., *Dengue virus infection perturbs lipid homeostasis in infected mosquito cells*. PLoS Pathog, 2012. **8**(3): p. e1002584.
163. Barletta, A.B., et al., *Emerging role of lipid droplets in Aedes aegypti immune response against bacteria and Dengue virus*. Sci Rep, 2016. **6**: p. 19928.
164. Heaton, N.S. and G. Randall, *Multifaceted roles for lipids in viral infection*. Trends Microbiol, 2011. **19**(7): p. 368-75.
165. Vial, T., et al., *Dengue virus reduces AGPAT1 expression to alter phospholipids and enhance infection in Aedes aegypti*. PLoS Pathog, 2019. **15**(12): p. e1008199.
166. Vial, T., et al., *Mosquito metabolomics reveal that dengue virus replication requires phospholipid reconfiguration via the remodeling cycle*. Proc Natl Acad Sci U S A, 2020. **117**(44): p. 27627-27636.
167. Raquin, V., et al., *Individual co-variation between viral RNA load and gene expression reveals novel host factors during early dengue virus infection of the Aedes aegypti midgut*. PLoS Negl Trop Dis, 2017. **11**(12): p. e0006152.
168. Chotiwan, N., et al., *Dynamic remodeling of lipids coincides with dengue virus replication in the midgut of Aedes aegypti mosquitoes*. PLoS Pathog, 2018. **14**(2): p. e1006853.
169. Rubio-Miranda, J.A., et al., *Septin 2 interacts with dengue virus replication complex proteins and participates in virus replication in mosquito cells*. Virology, 2022. **570**: p. 67-80.
170. Rosales Ramirez, R. and J.E. Ludert, *The Dengue Virus Nonstructural Protein 1 (NS1) Is Secreted from Mosquito Cells in Association with the Intracellular Cholesterol Transporter Chaperone Caveolin Complex*. J Virol, 2019. **93**(4).
171. Mondotte, J.A., et al., *Essential role of dengue virus envelope protein N glycosylation at asparagine-67 during viral propagation*. J Virol, 2007. **81**(13): p. 7136-48.
172. Bryant, J.E., et al., *Glycosylation of the dengue 2 virus E protein at N67 is critical for virus growth in vitro but not for growth in intrathoracically inoculated Aedes aegypti mosquitoes*. Virology, 2007. **366**(2): p. 415-23.

173. Crabtree, M.B., R.M. Kinney, and B.R. Miller, *Deglycosylation of the NS1 protein of dengue 2 virus, strain 16681: construction and characterization of mutant viruses*. Arch Virol, 2005. **150**(4): p. 771-86.
174. Jupatanakul, N., S. Sim, and G. Dimopoulos, *Aedes aegypti ML and Niemann-Pick type C family members are agonists of dengue virus infection*. Dev Comp Immunol, 2014. **43**(1): p. 1-9.
175. Amarante, A.M., et al., *Zika virus infection drives epigenetic modulation of immunity by the histone acetyltransferase CBP of Aedes aegypti*. PLoS Negl Trop Dis, 2022. **16**(6): p. e0010559.
176. Talyuli, O.A.C., et al., *The Aedes aegypti peritrophic matrix controls arbovirus vector competence through HPx1, a heme-induced peroxidase*. PLoS Pathog, 2023. **19**(2): p. e1011149.
177. Oliveira, J.H.M., et al., *Catalase protects Aedes aegypti from oxidative stress and increases midgut infection prevalence of Dengue but not Zika*. PLoS Negl Trop Dis, 2017. **11**(4): p. e0005525.
178. Merklung, S.H., et al., *Tudor-SN Promotes Early Replication of Dengue Virus in the Aedes aegypti Midgut*. iScience, 2020. **23**(2): p. 100870.
179. Olmo, R.P., et al., *Mosquito vector competence for dengue is modulated by insect-specific viruses*. Nat Microbiol, 2023. **8**(1): p. 135-149.
180. Sri-In, C., et al., *A salivary protein of Aedes aegypti promotes dengue-2 virus replication and transmission*. Insect Biochem Mol Biol, 2019. **111**: p. 103181.
181. Sessions, O.M., et al., *Discovery of insect and human dengue virus host factors*. Nature, 2009. **458**(7241): p. 1047-50.
182. Holmes, E.C. and S.S. Twiddy, *The origin, emergence and evolutionary genetics of dengue virus*. Infect Genet Evol, 2003. **3**(1): p. 19-28.
183. Zanotto, P.d., et al., *Population dynamics of flaviviruses revealed by molecular phylogenies*. Proceedings of the National Academy of Sciences, 1996. **93**(2): p. 548-553.
184. Hill, V., et al., *A new lineage nomenclature to aid genomic surveillance of dengue virus*. medRxiv, 2024.
185. Rico-Hesse, R., et al., *Origins of dengue type 2 viruses associated with increased pathogenicity in the Americas*. Virology, 1997. **230**(2): p. 244-51.
186. Matthews, B.J., et al., *Improved reference genome of Aedes aegypti informs arbovirus vector control*. Nature, 2018. **563**(7732): p. 501-507.
187. Gloria-Soria, A., et al., *Global genetic diversity of Aedes aegypti*. Mol Ecol, 2016. **25**(21): p. 5377-5395.
188. Bennett, K.E., et al., *Variation in vector competence for dengue 2 virus among 24 collections of Aedes aegypti from Mexico and the United States*. Am J Trop Med Hyg, 2002. **67**(1): p. 85-92.
189. Vazeille-Falcoz, M., et al., *Variation in oral susceptibility to dengue type 2 virus of populations of Aedes aegypti from the islands of Tahiti and Moorea, French Polynesia*. The American journal of tropical medicine and hygiene, 1999. **60**(2): p. 292-299.
190. Armstrong, P.M. and R. Rico-Hesse, *Differential susceptibility of Aedes aegypti to infection by the American and Southeast Asian genotypes of dengue type 2 virus*. Vector Borne Zoonotic Dis, 2001. **1**(2): p. 159-68.

191. Fansiri, T., et al., *Genetic Mapping of Specific Interactions between Aedes aegypti Mosquitoes and Dengue Viruses*. PLoS Genet, 2013. **9**(8): p. e1003621.
192. Gaye, A., et al., *Oral susceptibility of Aedes aegypti (Diptera: Culicidae) from Senegal for dengue serotypes 1 and 3 viruses*. Trop Med Int Health, 2014. **19**(11): p. 1355-9.
193. Rosen, L., et al., *Comparative susceptibility of mosquito species and strains to oral and parenteral infection with dengue and Japanese encephalitis viruses*. Am J Trop Med Hyg, 1985. **34**(3): p. 603-15.
194. Lambrechts, L. and T.W. Scott, *Mode of transmission and the evolution of arbovirus virulence in mosquito vectors*. Proc Biol Sci, 2009. **276**(1660): p. 1369-78.
195. Lambrechts, L., et al., *Specificity of resistance to dengue virus isolates is associated with genotypes of the mosquito antiviral gene Dicer-2*. Proc Biol Sci, 2013. **280**(1751): p. 20122437.
196. Flor, H.H., *Current status of the gene-for-gene concept*. Annual review of phytopathology, 1971. **9**(1): p. 275-296.
197. Agrawal, A.F. and C.M. Lively, *Infection genetics: gene-for-gene versus matching-alleles models and all points in between*. Evolutionary Ecology Research, 2002. **4**: p. 79-90.
198. Frank, S.A., *Recognition and polymorphism in host-parasite genetics*. Philos Trans R Soc Lond B Biol Sci, 1994. **346**(1317): p. 283-93.
199. Diallo, M., et al., *Vector competence of Aedes aegypti populations from Senegal for sylvatic and epidemic dengue 2 virus isolated in West Africa*. Trans R Soc Trop Med Hyg, 2008. **102**(5): p. 493-8.
200. Agha, S.B., et al., *Vector competence of populations of Aedes aegypti from three distinct cities in Kenya for chikungunya virus*. PLoS Negl Trop Dis, 2017. **11**(8): p. e0005860.
201. Dickson, L.B., et al., *Vector competence in West African Aedes aegypti is Flavivirus species and genotype dependent*. PLoS Negl Trop Dis, 2014. **8**(10): p. e3153.
202. Chen, B., et al., *Exploring the Mosquito-Arbovirus Network: A Survey of Vector Competence Experiments*. Am J Trop Med Hyg, 2023. **108**(5): p. 987-994.
203. Black, W.C.t., et al., *Flavivirus susceptibility in Aedes aegypti*. Arch Med Res, 2002. **33**(4): p. 379-88.
204. Miller, B.R. and C.J. Mitchell, *Genetic selection of a flavivirus-refractory strain of the yellow fever mosquito Aedes aegypti*. Am J Trop Med Hyg, 1991. **45**(4): p. 399-407.
205. Wallis, G.P., et al., *Selection for susceptibility and refractoriness of Aedes aegypti to oral infection with yellow fever virus*. Am J Trop Med Hyg, 1985. **34**(6): p. 1225-31.
206. Bennett, K.E., et al., *Quantitative trait loci that control dengue-2 virus dissemination in the mosquito Aedes aegypti*. Genetics, 2005. **170**(1): p. 185-94.
207. Bosio, C.F., et al., *Quantitative trait loci that control vector competence for dengue-2 virus in the mosquito Aedes aegypti*. Genetics, 2000. **156**(2): p. 687-98.
208. Gomez-Machorro, C., et al., *Quantitative trait loci affecting dengue midgut infection barriers in an advanced intercross line of Aedes aegypti*. Insect Mol Biol, 2004. **13**(6): p. 637-48.
209. Wilfert, L. and P. Schmid-Hempel, *The genetic architecture of susceptibility to parasites*. BMC Evol Biol, 2008. **8**: p. 187.

210. Huff, C.G., *The Effects of Selection Upon Susceptibility to Bird Malaria in Culex Pipiens Linn.* Annals of Tropical Medicine and Parasitology, 1929. **23**: p. 427-442.
211. Mattingly, P.F., *Genetical aspects of the Aedes aegypti problem. I. Taxonom: and bionomics.* Ann Trop Med Parasitol, 1957. **51**(4): p. 392-408.
212. Craig, G.B., Jr., R.C. Vandehey, and W.A. Hickey, *Genetic variability in populations of Aedes aegypti.* Bull World Health Organ, 1961. **24**(4-5): p. 527-39.
213. Bruce-Chwatt, L.J., *Recent studies on insect vectors of yellow fever and malaria in British West Africa.* J Trop Med Hyg, 1950. **53**(4): p. 71-9.
214. Kilama, W. and G. Craig Jr, *Monofactorial inheritance of susceptibility to Plasmodium gallinaceum in Aedes aegypti.* Annals of Tropical Medicine & Parasitology, 1969. **63**(4): p. 419-432.
215. Macdonald, W.W., *The Genetic Basis of Susceptibility to Infection with Semi-Periodic Brugia malayi in Aedes aegypti.* Annals of Tropical Medicine and Parasitology, 1962. **56**: p. 373-382.
216. Christensen, B.M. and D.W. Severson, *Biochemical and molecular basis of mosquito susceptibility to Plasmodium and filarioid nematodes,* in *Parasites and pathogens of insects.* 1993, Elsevier. p. 245-266.
217. Aitken, T.H.G., R.E. Shope, and W.G. Downs, *Aedes aegypti strain fitness for yellow fever virus transmission.* The American journal of tropical medicine and hygiene, 1977. **26 5 Pt 1**: p. 985-9.
218. Beaty, B.J. and T.H.G. Aitken. *In vitro transmission of yellow fever virus by geographic strains of Aedes aegypti.* 1979.
219. Severson, D.W., et al., *Linkage map for Aedes aegypti using restriction fragment length polymorphisms.* J Hered, 1993. **84**(4): p. 241-7.
220. Antolin, M.F., et al., *Intensive linkage mapping in a wasp (Bracon hebetor) and a mosquito (Aedes aegypti) with single-strand conformation polymorphism analysis of random amplified polymorphic DNA markers.* Genetics, 1996. **143**(4): p. 1727-38.
221. Munstermann, L.E. and G.B. Craig, *Genetics of Aedes aegypti Updating the linkage map.* Journal of Heredity, 1979. **70**: p. 291-296.
222. Craig, G.B., Jr. and W.A. Hickey, *Current status of the formal genetics of Aedes aegypti.* Bull World Health Organ, 1967. **36**(4): p. 559-62.
223. McClelland, G.A.H., *A preliminary study of the genetics of abdominal colour variations in Aedes aegypti (L.) (Diptera, Culicidae).* Annals of Tropical Medicine and Parasitology, 1960. **54**: p. 305-320.
224. Craig, C.B. and R.C. Vandehey, *Genetic Variability in Aedes aegypti (Diptera: Culicidae) I. Mutations Affecting Color Pattern.* Annals of The Entomological Society of America, 1962. **55**: p. 47-58.
225. Brown, S.E., et al., *Toward a physical map of Aedes aegypti.* Insect Mol Biol, 1995. **4**(3): p. 161-7.
226. Brown, S.E. and D.L. Knudson, *FISH landmarks for Aedes aegypti chromosomes.* Insect Mol Biol, 1997. **6**(2): p. 197-202.
227. Severson, D.W., et al., *Linkage map organization of expressed sequence tags and sequence tagged sites in the mosquito, Aedes aegypti.* Insect Mol Biol, 2002. **11**(4): p. 371-8.
228. Black, W.C. and N.M. DuTeau, *RAPD-PCR and SSCP analysis for insect population genetic studies,* in *The Molecular Biology of Insect Disease Vectors: A Methods*

- Manual*, J.M. Crampton, C.B. Beard, and C. Louis, Editors. 1997, Springer Netherlands: Dordrecht. p. 361-373.
229. Bosio, C.F., et al., *Genetic structure of Aedes aegypti populations in Thailand using mitochondrial DNA*. The American journal of tropical medicine and hygiene, 2005. **72** 4: p. 434-42.
230. Molina-Cruz, A., et al., *Effect of mosquito midgut trypsin activity on dengue-2 virus infection and dissemination in Aedes aegypti*. Am J Trop Med Hyg, 2005. **72**(5): p. 631-7.
231. Gorrochotegui-Escalante, N., et al., *Association mapping of segregating sites in the early trypsin gene and susceptibility to dengue-2 virus in the mosquito Aedes aegypti*. Insect Biochem Mol Biol, 2005. **35**(7): p. 771-88.
232. Brown, J.E., et al., *Worldwide patterns of genetic differentiation imply multiple 'domestications' of Aedes aegypti, a major vector of human diseases*. Proc Biol Sci, 2011. **278**(1717): p. 2446-54.
233. Chen, C., et al., *Marker-assisted mapping enables forward genetic analysis in Aedes aegypti, an arboviral vector with vast recombination deserts*. Genetics, 2022. **222**(3).
234. Nene, V., et al., *Genome sequence of Aedes aegypti, a major arbovirus vector*. Science, 2007. **316**(5832): p. 1718-23.
235. Lawson, D., et al., *VectorBase: a home for invertebrate vectors of human pathogens*. Nucleic Acids Res, 2007. **35**(Database issue): p. D503-5.
236. Lawson, D., et al., *VectorBase: a data resource for invertebrate vector genomics*. Nucleic Acids Res, 2009. **37**(Database issue): p. D583-7.
237. Hixson, B., et al., *A transcriptomic atlas of Aedes aegypti reveals detailed functional organization of major body parts and gut regional specializations in sugar-fed and blood-fed adult females*. Elife, 2022. **11**.
238. Dickson, L.B., et al., *Exome-wide association study reveals largely distinct gene sets underlying specific resistance to dengue virus types 1 and 3 in Aedes aegypti*. PLoS Genet, 2020. **16**(5): p. e1008794.
239. Cosme, L.V., et al., *Genome-wide Association Study Reveals New Loci Associated With Pyrethroid Resistance in Aedes aegypti*. Front Genet, 2022. **13**: p. 867231.
240. Hancock, P.A., E. Ochomo, and L.A. Messenger, *Genetic surveillance of insecticide resistance in African Anopheles populations to inform malaria vector control*. Trends Parasitol, 2024.
241. Behura, S.K., et al., *High-throughput cis-regulatory element discovery in the vector mosquito Aedes aegypti*. BMC Genomics, 2016. **17**: p. 341.
242. Kuno, G., *Early history of laboratory breeding of Aedes aegypti (Diptera: Culicidae) focusing on the origins and use of selected strains*. J Med Entomol, 2010. **47**(6): p. 957-71.
243. Macdonald, W., *The selection of a strain of Aedes aegypti susceptible to infection with semi-periodic Brugia malayi*. Annals of Tropical Medicine & Parasitology, 1962. **56**(3): p. 368-372.
244. Gloria-Soria, A., et al., *Genetic diversity of laboratory strains and implications for research: The case of Aedes aegypti*. PLoS Negl Trop Dis, 2019. **13**(12): p. e0007930.

245. Colpitts, T.M., et al., *Alterations in the Aedes aegypti transcriptome during infection with West Nile, dengue and yellow fever viruses*. PLoS Pathog, 2011. **7**(9): p. e1002189.
246. Bonizzoni, M., et al., *Complex modulation of the Aedes aegypti transcriptome in response to dengue virus infection*. PLoS One, 2012. **7**(11): p. e50512.
247. Etebari, K., et al., *Global Transcriptome Analysis of Aedes aegypti Mosquitoes in Response to Zika Virus Infection*. mSphere, 2017. **2**(6).
248. Angleró-Rodríguez, Y.I., et al., *An Aedes aegypti-associated fungus increases susceptibility to dengue virus by modulating gut trypsin activity*. Elife, 2017. **6**: p. e28844.
249. Zhao, L., et al., *Transcriptomic Analysis of Aedes aegypti Innate Immune System in Response to Ingestion of Chikungunya Virus*. Int J Mol Sci, 2019. **20**(13).
250. Vedururu, R.K., et al., *RNASeq Analysis of Aedes albopictus Mosquito Midguts after Chikungunya Virus Infection*. Viruses, 2019. **11**(6).
251. Severo, M.S., et al., *Unbiased classification of mosquito blood cells by single-cell genomics and high-content imaging*. Proc Natl Acad Sci U S A, 2018. **115**(32): p. E7568-E7577.
252. Raddi, G., et al., *Mosquito cellular immunity at single-cell resolution*. Science, 2020. **369**(6507): p. 1128-1132.
253. Sim, S., J.L. Ramirez, and G. Dimopoulos, *Dengue virus infection of the Aedes aegypti salivary gland and chemosensory apparatus induces genes that modulate infection and blood-feeding behavior*. PLoS Pathog, 2012. **8**(3): p. e1002631.
254. Ribeiro, J.M., et al., *An annotated catalogue of salivary gland transcripts in the adult female mosquito, Aedes aegypti*. BMC Genomics, 2007. **8**: p. 6.
255. Kwon, H., et al., *Single-cell analysis of mosquito hemocytes identifies signatures of immune cell subtypes and cell differentiation*. Elife, 2021. **10**.
256. Cui, Y., S.K. Behura, and A.W.E. Franz, *Cellular diversity and gene expression profiles in the male and female brain of Aedes aegypti*. BMC Genomics, 2022. **23**(1): p. 119.
257. Wang, S., et al., *A cell atlas of the adult female Aedes aegypti midgut revealed by single-cell RNA sequencing*. Sci Data, 2024. **11**(1): p. 587.
258. Yin, C., T. Morita, and J.Z. Parrish, *A cell atlas of the larval Aedes aegypti ventral nerve cord*. Neural Dev, 2024. **19**(1): p. 2.
259. Herre, M., et al., *Non-canonical odor coding in the mosquito*. Cell, 2022. **185**(17): p. 3104-3123.e28.
260. Behura, S.K. and D.W. Severson, *Intrinsic features of Aedes aegypti genes affect transcriptional responsiveness of mosquito genes to dengue virus infection*. Infect Genet Evol, 2012. **12**(7): p. 1413-8.
261. Behura, S.K., et al., *Global cross-talk of genes of the mosquito Aedes aegypti in response to dengue virus infection*. PLoS Negl Trop Dis, 2011. **5**(11): p. e1385.
262. Salas-Benito, J., et al., *Evidence that the 45-kD glycoprotein, part of a putative dengue virus receptor complex in the mosquito cell line C6/36, is a heat-shock related protein*. Am J Trop Med Hyg, 2007. **77**(2): p. 283-90.
263. Munoz, M.L., et al., *Putative dengue virus receptors from mosquito cells*. FEMS Microbiol Lett, 1998. **168**(2): p. 251-8.

264. Reyes-del Valle, J. and R.M. del Angel, *Isolation of putative dengue virus receptor molecules by affinity chromatography using a recombinant E protein ligand*. J Virol Methods, 2004. **116**(1): p. 95-102.
265. Caraballo, G.I., et al., *The Dengue Virus Nonstructural Protein 1 (NS1) Interacts with the Putative Epigenetic Regulator DIDO1 to Promote Flavivirus Replication in Mosquito Cells*. J Virol, 2022. **96**(12): p. e0070422.
266. Mairiang, D., et al., *Identification of new protein interactions between dengue fever virus and its hosts, human and mosquito*. PLoS One, 2013. **8**(1): p. e53535.
267. Tham, H.W., et al., *Protein-protein interactions between A. aegypti midgut and dengue virus 2: two-hybrid screens using the midgut cDNA library*. J Infect Dev Ctries, 2015. **9**(12): p. 1338-49.
268. Horvath, T.D., S. Dagan, and P.Y. Scaraffia, *Unraveling mosquito metabolism with mass spectrometry-based metabolomics*. Trends Parasitol, 2021. **37**(8): p. 747-761.
269. Manokaran, G., et al., *Modulation of acyl-carnitines, the broad mechanism behind Wolbachia-mediated inhibition of medically important flaviviruses in Aedes aegypti*. Proc Natl Acad Sci U S A, 2020. **117**(39): p. 24475-24483.
270. Duchemin, J.B. and P.N. Paradkar, *Iron availability affects West Nile virus infection in its mosquito vector*. Virol J, 2017. **14**(1): p. 103.
271. Sasao, F., A. Igarashi, and K. Fukai, *Amino acid requirements for the growth of Aedes albopictus clone C6/36 cells and for the production of dengue and Chikungunya viruses in the infected cells*. Microbiol Immunol, 1980. **24**(10): p. 915-24.
272. Weng, S.C., P.N. Tsao, and S.H. Shiao, *Blood glucose promotes dengue virus infection in the mosquito Aedes aegypti*. Parasit Vectors, 2021. **14**(1): p. 376.
273. Zhu, Y., et al., *Host serum iron modulates dengue virus acquisition by mosquitoes*. Nat Microbiol, 2019. **4**(12): p. 2405-2415.
274. Dey, L. and A. Mukhopadhyay, *DenvInt: A database of protein-protein interactions between dengue virus and its hosts*. PLoS Negl Trop Dis, 2017. **11**(10): p. e0005879.
275. Doolittle, J.M. and S.M. Gomez, *Mapping protein interactions between Dengue virus and its human and insect hosts*. PLoS Negl Trop Dis, 2011. **5**(2): p. e954.
276. Figueiredo Prates, L.H., et al., *Challenges of Robust RNAi-Mediated Gene Silencing in Aedes Mosquitoes*. Int J Mol Sci, 2024. **25**(10).
277. Munawar, K., A.M. Alahmed, and S.M.S. Khalil, *Delivery Methods for RNAi in Mosquito Larvae*. J Insect Sci, 2020. **20**(4).
278. Singh, A.D., et al., *Oral delivery of double-stranded RNA in larvae of the yellow fever mosquito, Aedes aegypti: implications for pest mosquito control*. J Insect Sci, 2013. **13**: p. 69.
279. Das, S., et al., *Chitosan, Carbon Quantum Dot, and Silica Nanoparticle Mediated dsRNA Delivery for Gene Silencing in Aedes aegypti: A Comparative Analysis*. ACS Appl Mater Interfaces, 2015. **7**(35): p. 19530-5.
280. Romoli, O., et al., *Limitations in harnessing oral RNA interference as an antiviral strategy in Aedes aegypti*. iScience, 2024. **27**(3): p. 109261.
281. Blitzer, E.J., I. Vyazunova, and Q. Lan, *Functional analysis of AeSCP-2 using gene expression knockdown in the yellow fever mosquito, Aedes aegypti*. Insect Mol Biol, 2005. **14**(3): p. 301-7.

282. Lopez, S.B.G., et al., *RNAi-based bioinsecticide for Aedes mosquito control*. Sci Rep, 2019. **9**(1): p. 4038.
283. Mehlhorn, S., et al., *Establishing RNAi for basic research and pest control and identification of the most efficient target genes for pest control: a brief guide*. Frontiers in Zoology, 2021. **18**: p. 1-16.
284. Kistler, K.E., L.B. Vosshall, and B.J. Matthews, *Genome engineering with CRISPR-Cas9 in the mosquito Aedes aegypti*. Cell Rep, 2015. **11**(1): p. 51-60.
285. Aryan, A., et al., *TALEN-based gene disruption in the dengue vector Aedes aegypti*. PLoS One, 2013. **8**(3): p. e60082.
286. DeGennaro, M., et al., *orco mutant mosquitoes lose strong preference for humans and are not repelled by volatile DEET*. Nature, 2013. **498**(7455): p. 487-91.
287. Liesch, J., L.L. Bellani, and L.B. Vosshall, *Functional and genetic characterization of neuropeptide Y-like receptors in Aedes aegypti*. PLoS Negl Trop Dis, 2013. **7**(10): p. e2486.
288. McMeniman, C.J., et al., *Multimodal integration of carbon dioxide and other sensory cues drives mosquito attraction to humans*. Cell, 2014. **156**(5): p. 1060-71.
289. Aryan, A., K.M. Myles, and Z.N. Adelman, *Targeted genome editing in Aedes aegypti using TALENs*. Methods, 2014. **69**(1): p. 38-45.
290. Lee, Y.S., et al., *Distinct roles for Drosophila Dicer-1 and Dicer-2 in the siRNA/miRNA silencing pathways*. Cell, 2004. **117**(1): p. 69-81.
291. Galiana-Arnoux, D., et al., *Essential function in vivo for Dicer-2 in host defense against RNA viruses in drosophila*. Nat Immunol, 2006. **7**(6): p. 590-7.
292. Khoo, C.C., et al., *Transgene-mediated suppression of the RNA interference pathway in Aedes aegypti interferes with gene silencing and enhances Sindbis virus and dengue virus type 2 replication*. Insect Mol Biol, 2013. **22**(1): p. 104-14.
293. Kang, S., et al., *Homologs of Human Dengue-Resistance Genes, FKBP1B and ATCAY, Confer Antiviral Resistance in Aedes aegypti Mosquitoes*. Insects, 2019. **10**(2).
294. Yasunaga, A., et al., *Genome-wide RNAi screen identifies broadly-acting host factors that inhibit arbovirus infection*. PLoS Pathog, 2014. **10**(2): p. e1003914.
295. Rozen-Gagnon, K., et al., *A selectable, plasmid-based system to generate CRISPR/Cas9 gene edited and knock-in mosquito cell lines*. Sci Rep, 2021. **11**(1): p. 736.
296. Viswanatha, R., et al., *Bioinformatic and cell-based tools for pooled CRISPR knockout screening in mosquitos*. Nat Commun, 2021. **12**(1): p. 6825.
297. Marceau, C.D., et al., *Genetic dissection of Flaviviridae host factors through genome-scale CRISPR screens*. Nature, 2016. **535**(7610): p. 159-63.
298. Zhang, R., et al., *A CRISPR screen defines a signal peptide processing pathway required by flaviviruses*. Nature, 2016. **535**(7610): p. 164-8.

-CHAPTER 1-

**A *Vago*-like gene enhances dengue and Zika virus dissemination in
*Aedes aegypti***

Elodie Couderc, Anna B. Crist, Josquin Daron, Hugo Varet, Femke A. H. van Hout, Pascal Miesen, Umberto Palatini, Stéphanie Dabo, Thomas Vial, Louis Lambrechts[‡], Sarah H. Merklings[‡]

Preprint available at: <https://doi.org/10.1101/2024.07.01.601473>

CHAPTER 1: A *Vago*-like gene enhances dengue and Zika virus dissemination in *Aedes aegypti*

Elodie Couderc^{1,2}, Anna B. Crist¹, Josquin Daron¹, Hugo Varet³, Femke A. H. van Hout⁴, Pascal Miesen⁴, Umberto Palatini^{1,5}, Stéphanie Dabo¹, Thomas Vial¹, Louis Lambrechts^{1,‡,*}, Sarah H. Merklings^{1,‡,*}

¹Institut Pasteur, Université Paris Cité, CNRS UMR2000, Insect-Virus Interactions Unit, 75015 Paris, France

²Sorbonne Université, Collège Doctoral, 75005 Paris, France

³Institut Pasteur, Université Paris Cité, Bioinformatics and Biostatistics Hub, 75015 Paris, France

⁴Department of Medical Microbiology, Radboud University Medical Center, P.O. box 9101 6500 HB Nijmegen, The Netherlands

⁵Laboratory of Neurogenetics and Behavior, The Rockefeller University, New York, NY 10065, USA

‡These authors contributed equally

*Correspondence to: Louis Lambrechts (louis.lambrechts@pasteur.fr) and Sarah Merklings (sarah.merkling@pasteur.fr)

ABSTRACT

Arthropod-borne viruses (arboviruses) such as dengue virus (DENV) and Zika virus (ZIKV) pose a significant threat to global health. Novel approaches to control the spread of arboviruses focus on harnessing the antiviral immune system of their primary vector, the *Aedes aegypti* mosquito. In arthropods, genes of the *Vago* family are often presented as analogs of mammalian cytokines with potential antiviral functions, but the role of *Vago* genes upon virus infection in *Ae. aegypti* is largely unknown. We conducted a phylogenetic analysis of the *Vago* gene family in Diptera, which led us to focus on a *Vago*-like gene that we named *VLG-1*. Using CRISPR/Cas9-mediated gene editing, we generated a *VLG-1* mutant line of *Ae. aegypti* that revealed a proviral effect of this gene upon DENV and ZIKV infection. In the absence of *VLG-1*, virus dissemination throughout the mosquito's body was impaired, albeit not altering virus transmission rates. A tissue-specific transcriptome analysis revealed that the loss of *VLG-1* impacted numerous biological processes potentially linked to viral replication, such as the oxidative stress response. Our results challenge the conventional understanding of *Vago*-like genes as antiviral factors and underscore the need for further research to elucidate the molecular mechanisms underlying mosquito-arbovirus interactions.

INTRODUCTION

Arthropod-borne viruses (arboviruses) pose a significant threat to global health, causing numerous human diseases with substantial morbidity and mortality. Among the most medically significant arboviruses are the mosquito-borne flaviviruses [1]. For instance, dengue virus (DENV) infects approximately 400 million people each year and is responsible for about 100 million symptomatic cases [2-4]. In addition, Zika virus (ZIKV) emerged in more than 87 countries and territories in the last 15 years, causing severe neuropathologies and birth defects [5]. DENV and ZIKV are primarily transmitted by *Aedes aegypti* (*Ae. aegypti*), a mosquito species found throughout the tropics and subtropics whose range is expected to further expand with global change [6, 7]. To date, there are no globally approved vaccines or specific antivirals for these diseases. Traditional vector control methods are limited in efficacy because of the emergence of insecticide-resistant mosquitoes. Thus, the release of lab-modified mosquitoes that are incapable of transmitting viruses is an alternative strategy for reducing the incidence of human arboviral diseases [8, 9]. The development of such novel interventions is conditioned by the identification of optimal target genes that mediate interactions between mosquitoes and viruses [9, 10].

Female mosquitoes acquire arboviruses by biting and blood feeding on viremic vertebrate hosts. The bloodmeal is digested in the midgut, where viral particles infect epithelial cells [11, 12]. The virus then disseminates through the mosquito body, likely via circulating immune cells called hemocytes [13-15], until it reaches the salivary glands, where it replicates before being released in the saliva [16]. The mosquito can then transmit the virus to the next host during a subsequent blood-feeding event [13]. Within mosquitoes, virus infection and dissemination are hindered by physical tissue barriers [13] and innate immune pathways, including RNA interference (RNAi) [17-19], Janus kinase/signal transducers and activators of transcription (JAK-STAT), Toll, and immune deficiency (IMD) pathways, which are activated upon viral detection and trigger the production of effector molecules that can inhibit viral replication [20-22]. Most of our knowledge about antiviral immunity in mosquitoes is derived from pioneering work in the model organism *Drosophila melanogaster*. However, fruit flies are neither arbovirus vectors, nor hematophagous insects, leaving our understanding of mosquito antiviral responses incomplete [10, 20, 23].

For instance, only a few studies have investigated the role of immunoregulatory genes with cytokine-like functions, such as *Vago* genes, in mosquito immunity. The first *Vago* gene was identified in *D. melanogaster* [24] and encodes a secreted antiviral protein induced upon infection by *Drosophila C virus* (DCV) [25]. In *D. melanogaster*, *Vago* induction in response to

DCV infection requires the RNAi gene *Dicer2* [25]. In mosquitoes, a *Vago* gene called *CxVago*, was shown to limit viral replication in *Culex* mosquitoes infected with the flavivirus West Nile virus (WNV) [26]. In addition, WNV infection was found to induce the expression of *CxVago* in a *Dicer2*-dependent manner in a *Culex*-derived cell line, leading to secretion of the protein and activation of the JAK-STAT pathway via an unknown non-canonical receptor [26]. *Rel2* and *TRAF* genes were also involved in *CxVago* induction, suggesting a link between *CxVago* induction and NF- κ B pathways [27]. However, the antiviral function of *Vago* genes in *Culex* mosquitoes was not investigated *in vivo*. Finally, another study using an *Aedes*-derived cell line reported an antiviral role for a *Vago* gene called *AaeVago1*, in the context of DENV and *Wolbachia* co-infection [28].

The *Vago* protein family is often referred to as “arthropod cytokines” because they are functionally analogous to mammalian cytokines [26, 29-31]. In dipteran insects (flies and mosquitoes), *Vago* proteins consist of 100-200 amino acids with a secretion signal peptide and a single domain von Willebrand factor type C (SVWC) functional domain. SVWC proteins, characterized by a repetitive pattern of eight cysteines, represent a broadly conserved protein family in arthropods, associated with responses to environmental challenges, including nutritional stress and microbial infections [29]. Despite their characteristic structural features, the functions of *Vago* proteins in insects remain elusive, particularly *in vivo*.

Here, we investigated the role of *Vago* genes in *Ae. aegypti* mosquitoes *in vivo* in the context of flavivirus infection. We generated and characterized a mosquito mutant line for the gene that had hitherto been called *AaeVago1* and determined its impact on infection, systemic dissemination, and transmission of DENV and ZIKV. Unexpectedly, we found a proviral effect of this gene, challenging the hypothesis that genes belonging to the *Vago* family exert exclusively antiviral functions in arthropods.

RESULTS

VLG-1 is a *Vago*-like gene exclusively found in the Culicinae

To investigate the role of *Vago* genes in *Ae. aegypti*, we first reconstituted their evolutionary history (Figure 1A). We identified the homologs of AAEL000200 and AAEL000165, two genes that were previously described as *AaeVago1* and *AaeVago2*, in a panel of Diptera species from the Culicidae family (mosquitoes) and from the *Drosophila* genus, and we determined their phylogenetic relationships at the protein level (Supplementary Figure S1). First, we discovered that the first *Vago* gene characterized in *Drosophila melanogaster* (*DmVago*, CG2081) [25] is not the most likely homolog of AAEL000200 and AAEL000165. These two *Ae.*

aegypti genes encode proteins that are ~40-50 amino acid shorter and only share 27% and 24% identity with *DmVago*, respectively (Figure 1B). Reciprocally, *DmVago* does not have a homolog in the Culicidae sharing at least 30% protein sequence identity. We found that the most likely homolog of *AAEL000200* and *AAEL000165* in the *D. melanogaster* genome is an uncharacterized gene (*CG14132*), which we named “*D. melanogaster Vago-like gene*” (*DmVLG*). *DmVLG* shares 36% and 31% protein identity with *AAEL000200* and *AAEL000165*, respectively (Figure 1B). Thus, we renamed *AAEL000200* “*Ae. aegypti Vago-like gene 1*” (*AaeVLG-1*, referred to later in this study as *VLG-1*) and *AAEL000165* “*Ae. aegypti Vago-like gene 2*” (*AaeVLG-2*, referred to later in this study as *VLG-2*). A summary of our proposed updated designation of *Vago* and *Vago-like* genes is provided in Supplementary Table 1.

The overall topology of the phylogenetic tree of *Vago-like* gene homologs revealed two distinct sister clades among the Culicidae (Supplementary Figure S1). One clade encompasses members of both the Culicinae and Anophelinae subfamilies, including *AaeVLG-2*. The other clade exclusively consists of Culicinae members, including *AaeVLG-1*. The *VLG* clade that includes *AaeVLG-2* likely represents the orthologous group of *DmVLG*, whereas the clade that includes *AaeVLG-1* likely corresponds to *Vago-like* paralogs that arose by duplication of the ancestral *VLG*. This scenario is further supported by the nested and inverted position of the *AaeVLG-1* locus within an intron of *AaeVLG-2*. Our analysis suggests that the duplication occurred prior to the divergence of Anophelinae and Culicinae and was followed by a loss of the duplicated copy in Anophelinae prior to their diversification (Figure 1A and Supplementary Figure S1). Together, our analysis identified *AaeVLG-2* (previously named *AaeVago2* [28]) as the direct ortholog of *DmVLG* in *Ae. aegypti*, and *AaeVLG-1* (previously named *AaeVago1* [28]) as the duplicated copy. Accordingly, we also propose to rename the *Culex quinquefasciatus* gene *CQUJHB003889*, previously known as *CxVago* [26, 27], as *CxVLG-1* because it belongs to the *VLG-1* clade (Supplementary Figure S1 and Supplementary Table 1).

To determine whether the two *Vago-like* copies in the Culicidae family evolved under a different selection regime after the duplication event, we estimated the evolutionary rates of *AaeVLG-1* and *AaeVLG-2*. We computed the ratio of non-synonymous to synonymous substitutions (ω) for all *VLG* homologs of our panel of Culicidae and *Drosophila* species. The ω ratio, also known as dN/dS, indicates the mode and strength of natural selection, where $\omega=0$ means that the gene is under purifying selection, $\omega=1$ indicates neutral selection, and $\omega>1$ indicates diversifying selection. We used a branch model that evaluates the variation of ω within the tree and tests for differences in selection regimes between lineages. According to this model, both *VLG-1* and Culicinae *VLG* are under purifying selection ($\omega=0.18$ and $\omega=0.15$ respectively), but slightly weaker purifying selection than Anophelinae *VLG* ($\omega=0.1$) and *Drosophila VLG*

($\omega=0.09$) (Supplementary Figure S1 and Supplementary Table 3). This analysis suggests that the *VLG* duplication in the Culicinae was followed by relaxed selective pressure on both copies.

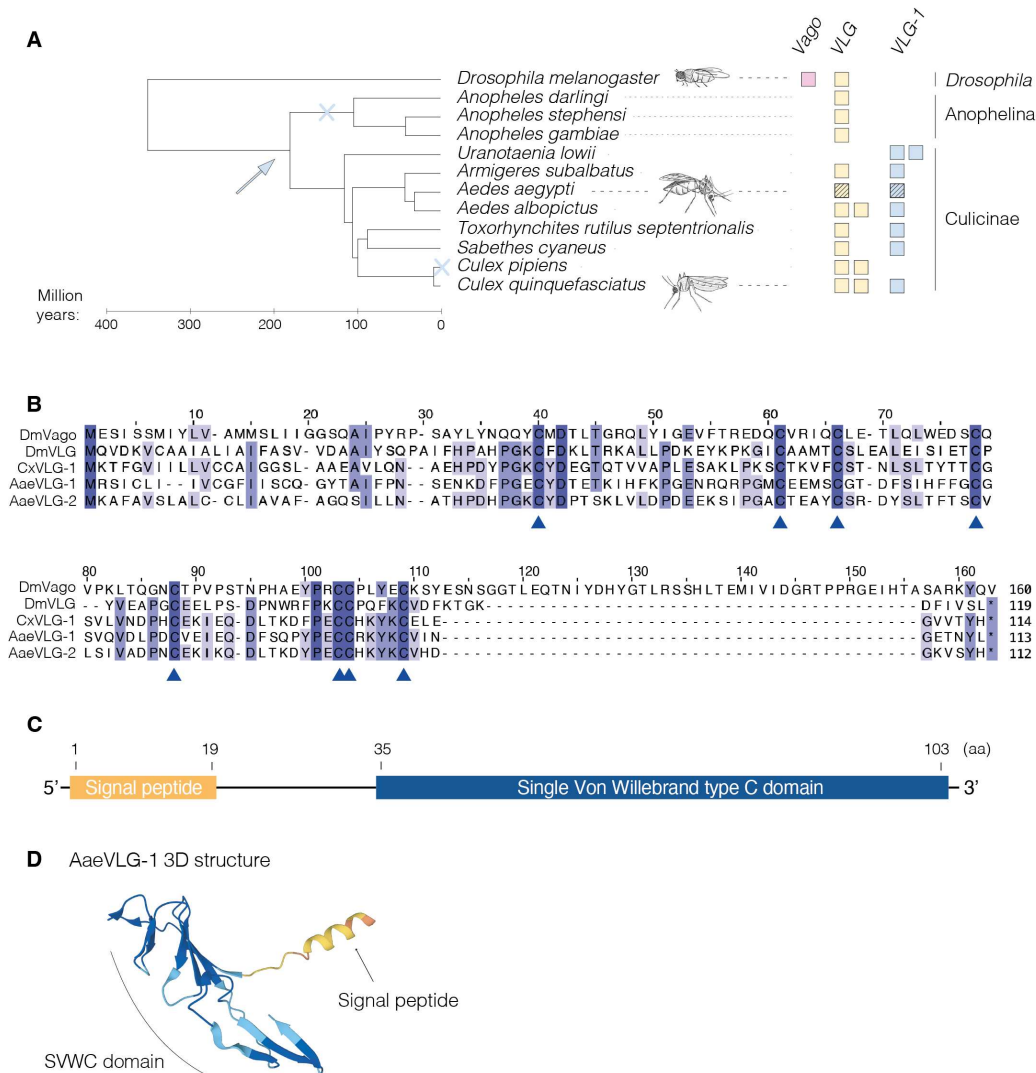


Figure 1. *VLG-1* is a *Vago*-like gene specific to the Culicinae subfamily. (A) Schematic cladogram of the evolutionary history of *Vago*-like gene homologs in Culicidae and *Drosophila* species. The putative origin of duplication of *VLG-1* from the ancestral *VLG*, inferred from the phylogenetic analysis of *Vago*-like gene homologs (Supplementary Figure S1), is indicated with a blue arrow, whereas putative losses of *VLG-1* are indicated with blue crosses. *AaeVLG-2* and *AaeVLG-1* are represented with black-striped yellow and blue squares, respectively. (B) Amino-acid sequence alignment of *Ae. aegypti* VLG-1 (AaeVLG-1, XP 001658930.1) and VLG-2 (isoform RB, XP 001658929.1) proteins with *D. melanogaster* Vago (DmVago, NP_001285106.1), *D. melanogaster* VLG (DmVLG, NP_001097586) and *Culex quinquefasciatus* VLG-1 (XP_001842264). The percentage of identity shared between all sequences for each amino-acid position is represented by shades of colors, ranging from light purple (when 3 out of 5 sequences are identical) to dark purple (when all 5 sequences are identical). The conserved cysteine residues typical of SWWC domains are indicated by blue arrows. (C) Functional domains of AaeVLG-1 with amino-acid (aa) positions. (D) Predicted 3D structure of AaeVLG-1 protein obtained with Alphafold (<https://alphafold.ebi.ac.uk/entry/Q17PX2>) [50, 51].

At the amino-acid level, *AaeVLG-1* shares 57% identity with *CxVLG-1*, whereas *AaeVLG-2* shares 38% identity with *CxVLG-1* (Figure 1B). *AaeVLG-1* is transcribed into a 451-bp mRNA transcript encoding a protein of 113 amino acids, including a signal peptide, theoretically responsible for addressing the protein to the membrane prior to its secretion, and an SVWC domain with the characteristic eight-cysteine repeat (Figure 1B-D).

VLG-1* is persistently induced by bloodmeal ingestion in *Ae. aegypti

In arthropods, *Vago* genes have been described as factors induced by biotic or abiotic stress [25-29, 32-35]. To test whether *VLG-1* and *VLG-2* are induced upon viral infection in *Ae. aegypti*, we exposed mosquitoes to a bloodmeal containing DENV serotype 1 (DENV-1) or a control mock bloodmeal. We quantified the expression of *VLG-1* and *VLG-2* by quantitative RT-PCR (RT-qPCR) in individual midguts, heads, and carcasses (*i.e.*, bodies without midgut and head) on several timepoints post bloodmeal, from day 0 to day 9 (Figure 2). As reported previously [36], we found that in *Ae. aegypti*, overall transcript abundance is ~2- to 10-fold higher for *VLG-1* than for *VLG-2* across tissues (Figure 2C and 2F). A mock bloodmeal triggered a persistent up-regulation of *VLG-1* transcription lasting up to 9 days post bloodmeal in carcasses and heads (Figure 2B and 2C). DENV exposure triggered an additional increase in *VLG-1* expression in heads on day 2 post bloodmeal (Figure 2C). No differences in *VLG-2* expression kinetics were detected between the mock and the infectious bloodmeals. Therefore, we chose to focus our study on the role of *AaeVLG-1* upon virus infection.

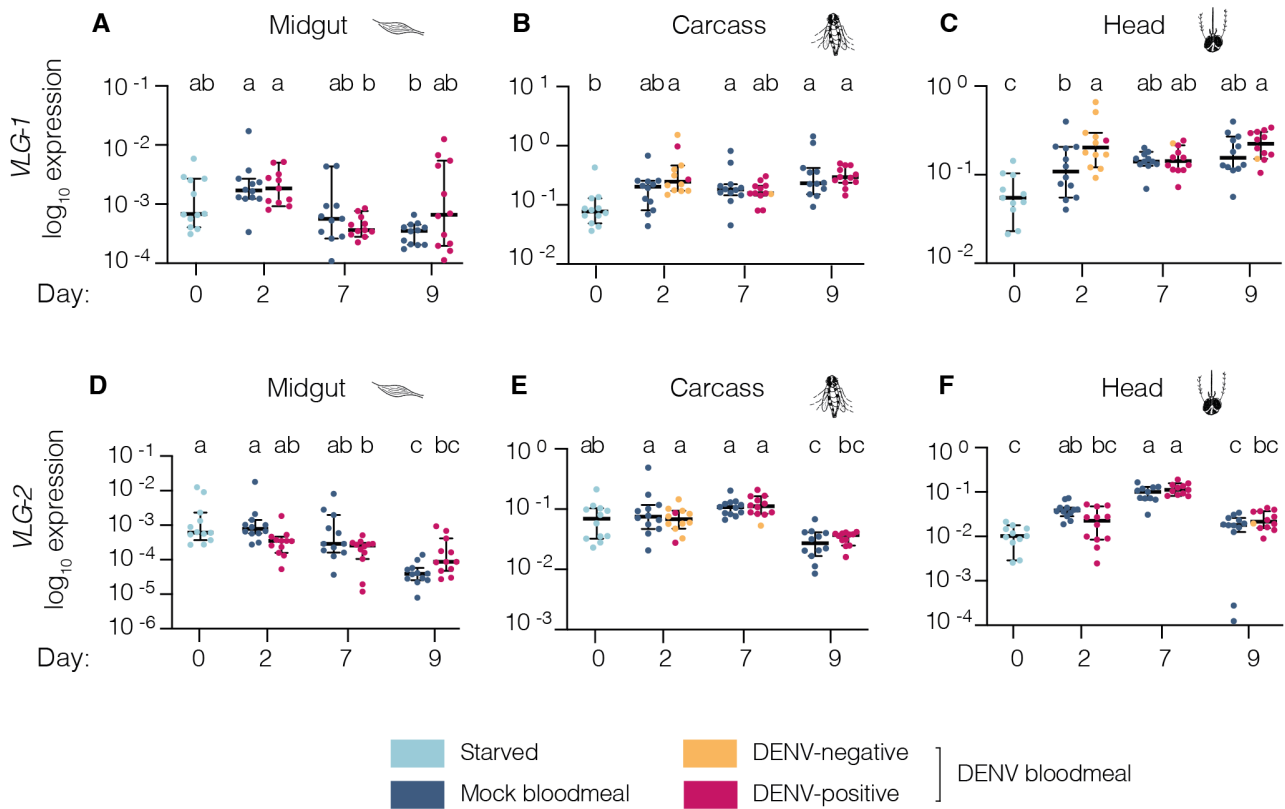


Figure 2. *VLG-1* is persistently induced by bloodmeal ingestion and DENV exposure in non-midgut tissues of *Ae. aegypti*. Expression levels of *AaeVLG-1* (A-C) and *AaeVLG-2* (D-F) were quantified by RT-qPCR in midguts (A,D), carcasses (B,E), and heads (C,F) on 0, 2, 7, and 9 days after ingestion of a mock or DENV-1 infectious bloodmeal, in mosquitoes of the wild-type control line. Gene expression levels are normalized to the *ribosomal protein S 17* housekeeping gene (*RPS17*), and expressed as 2^{-dCt} , where $dCt = Ct_{Gene} - Ct_{RPS17}$. Each dot represents an individual tissue. Horizontal bars represent medians and vertical bars represent 95% confidence intervals. Statistical significance was determined by a one-way ANOVA after \log_{10} -transformation of the 2^{-dCt} values, followed by Tukey-Kramer's HSD test. Statistical significance is represented above the graph using letters; groups that do not share a letter are significantly different.

***Ae. aegypti* VLG-1^Δ mutant mosquitoes do not exhibit major fitness defects**

To further investigate the role of *VLG-1* in *Ae. aegypti*, we generated a mutant line by CRISPR/Cas9-mediated gene editing. Shortly, mosquito embryos were microinjected with Cas9 coupled to 3 single-guide RNAs (sgRNAs) targeting 3 *VLG-1* exons together with a repair template (Figure 3A). We isolated one generation zero (G₀) female carrying a 212-bp (55 amino acids) deletion in the *VLG-1* locus, resulting from a combined 246-bp deletion and a 34-bp insertion from the repair template. This G₀ female was crossed to wild-type males and G₁ males carrying the deletion were crossed to wild-type females for three more generations. G₄ adults carrying the *VLG-1* mutation at the homozygous state were used to establish a *VLG-1* mutant line that we called *VLG-1^Δ*. Within the same crossing scheme, we generated a control “sister” line carrying the wild-type version of *VLG-1*. The *VLG-1^Δ* line encodes a *VLG-1* protein with only 58 of the 113 original amino acids left and 81% of the SVWC functional domain truncated, suggesting a *VLG-1* loss of function. We found a strong decrease of *VLG-1* transcript abundance in the mutant line relative to the control line, by RT-qPCR and by RNA sequencing (RNA-seq) (Supplementary Figure S2A-B), which is a hallmark of nonsense-mediated decay of the aberrant mRNA [37]. We also confirmed the absence of detectable *VLG-1* protein in the mutant line by Western blot using a previously developed anti-*VLG-1* antibody [26] (Supplementary Figure S2C). No off-target effect on *AaeVLG-2* expression was detected by RT-qPCR or RNA-seq in the *VLG-1^Δ* mutant line (Supplementary Figure S2D-E). Together, these results strongly suggest that we generated a *bona fide* knock-out *VLG-1* mutant line.

To assess the impact of *VLG-1* absence on mosquito fitness, we monitored adult survival rates in standard insectary conditions. Mortality rates were slightly higher in the *VLG-1^Δ* mutant line compared to controls, particularly for males (Figure 3C-D). We also measured fecundity (*i.e.*, the number of eggs laid per blood-fed female; Figure 3E) and fertility (*i.e.*, the number of viable larvae hatched over total number of eggs laid; Figure 3F) and found no differences between the *VLG-1^Δ* mutant and the control lines. In sum, *VLG-1^Δ* mutants are viable and display no major fitness defects.

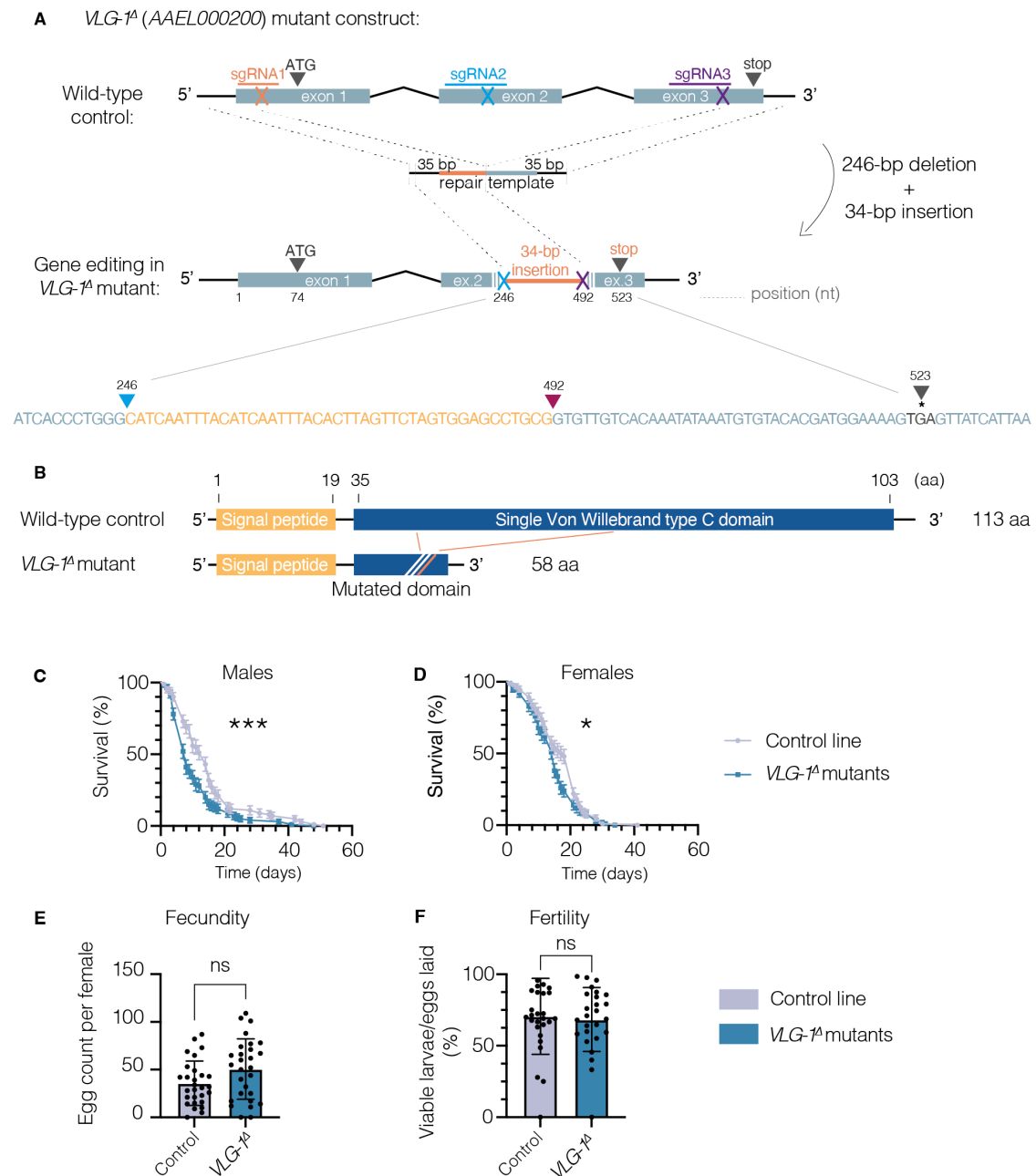


Figure 3. *VLG-1^A* mutants are viable and fertile without major fitness defects. (A) Structure of the *VLG-1* locus in the wild-type control and the *VLG-1^A* mutant lines. Exons are displayed as light blue boxes, connected by black segments representing introns. The positions and cut-sites of single-guide RNAs are depicted on each exon. (B) Structure of the *VLG-1* protein in the wild-type control line and the *VLG-1^A* mutant line. (C-D) Survival curves of adult males (C) and females (D) from the wild-type control (grey) and *VLG-1^A* mutant (blue) lines in standard insectary conditions. Data represent mean and standard deviation of 4 replicates performed with 25 mosquitoes for each condition. * $p < 0.05$; *** $p < 0.001$ (Gehan-Breslow-Wilcoxon test). (E) Fecundity (number of eggs laid per individual blood-fed female for 7 days after a bloodmeal) in the *VLG-1^A* mutant and control lines. Data represents mean and standard deviation of 28 mosquitoes. * $p < 0.05$; ** $p < 0.01$; *** $p < 0.001$ (Mann-Whitney's test). (F) Fertility (number of viable hatched larvae over the total number of eggs laid) in the *VLG-1^A* mutant and control lines. Data represent mean and standard errors of 26 mosquitoes. * $p < 0.05$; ** $p < 0.01$; *** $p < 0.001$ (chi-squared test).

VLG-1* promotes systemic dissemination of DENV and ZIKV in *Ae. aegypti

To investigate the role of *VLG-1* upon virus infection in *Ae. aegypti* mosquitoes, we performed experimental DENV-1 or ZIKV infections and analyzed infection prevalence (proportion of virus-positive tissues) and viral load (abundance of viral RNA) by RT-qPCR in individual tissues (midguts, carcasses, and heads). We selected timepoints representing key steps in the infection cycle: early midgut infection (day 2), systemic viral dissemination from the midgut to secondary organs (day 5), and head infection (day 9) (Figure 4 and Figure 5). Midgut infection prevalence is defined as the proportion of virus-positive midguts over the total number of blood-fed mosquitoes. Carcass infection prevalence is the proportion of virus-positive carcasses over the number of virus-positive midguts. Head infection prevalence is the number of virus-positive heads over the number of virus-positive carcasses. On days 7, 10, and 14 post bloodmeal, we measured viral titers in saliva samples collected from individual mosquitoes to assess virus transmission levels. Transmission efficiency was calculated as the proportion of virus-exposed mosquitoes with virus-positive saliva.

Upon DENV-1 infection, we found that virus dissemination was reduced in *VLG-1^A* mutant mosquitoes (Figure 4). In a first experimental replicate, we found that infection prevalence in the midgut (day 2), carcass (day 5) and head (day 9) was lower in *VLG-1^A* mutant mosquitoes (Figure 4A-C). We also detected decreased viral loads in the *VLG-1^A* mutant midguts on day 5, and in heads on days 5 and 9 in the second experimental replicate (Figure 4D-F). Small phenotypic differences between replicates presumably reflect minor uncontrolled variation in the bloodmeal titers that result in slightly different infection dynamics. Finally, we found no difference in DENV transmission efficiency between wild-type and *VLG-1^A* mutant mosquitoes (Figure 4G).

Next, we performed a similar set of experiments with ZIKV and confirmed *VLG-1*'s proviral role in virus dissemination (Figure 5). Two days after the bloodmeal, we found a strong decrease in infection prevalence in the carcass, where only 12% of the *VLG-1^A* mosquitoes harbored ZIKV RNA compared to 70% of the control mosquitoes (Figure 5A-C). In midguts, we consistently found a decrease in viral loads (~10-fold) in *VLG-1^A* mutants at all three timepoints (Figure 5D). In carcasses and heads, viral loads were 5- to 10-fold lower in *VLG-1^A* mutants 9 days post bloodmeal (Figure 5E-F). Similar to DENV, we found no detectable difference in virus transmission efficiency between wild-type and *VLG-1^A* mutant mosquitoes (Figure 5G).

Of note, we estimated virus transmission efficiency with standard salivation assays that potentially underestimate vector competence compared to live-host transmission assays [38],

which might have limited our ability to detect differences in transmission efficiency between the *VLG-1^A* mutant and control lines. Together, these results reveal a proviral activity of *VLG-1* upon flavivirus infection in *Ae. aegypti*. Our data demonstrate that *VLG-1* promotes flavivirus dissemination across the mosquito's body but does not seem to significantly impact virus transmission.

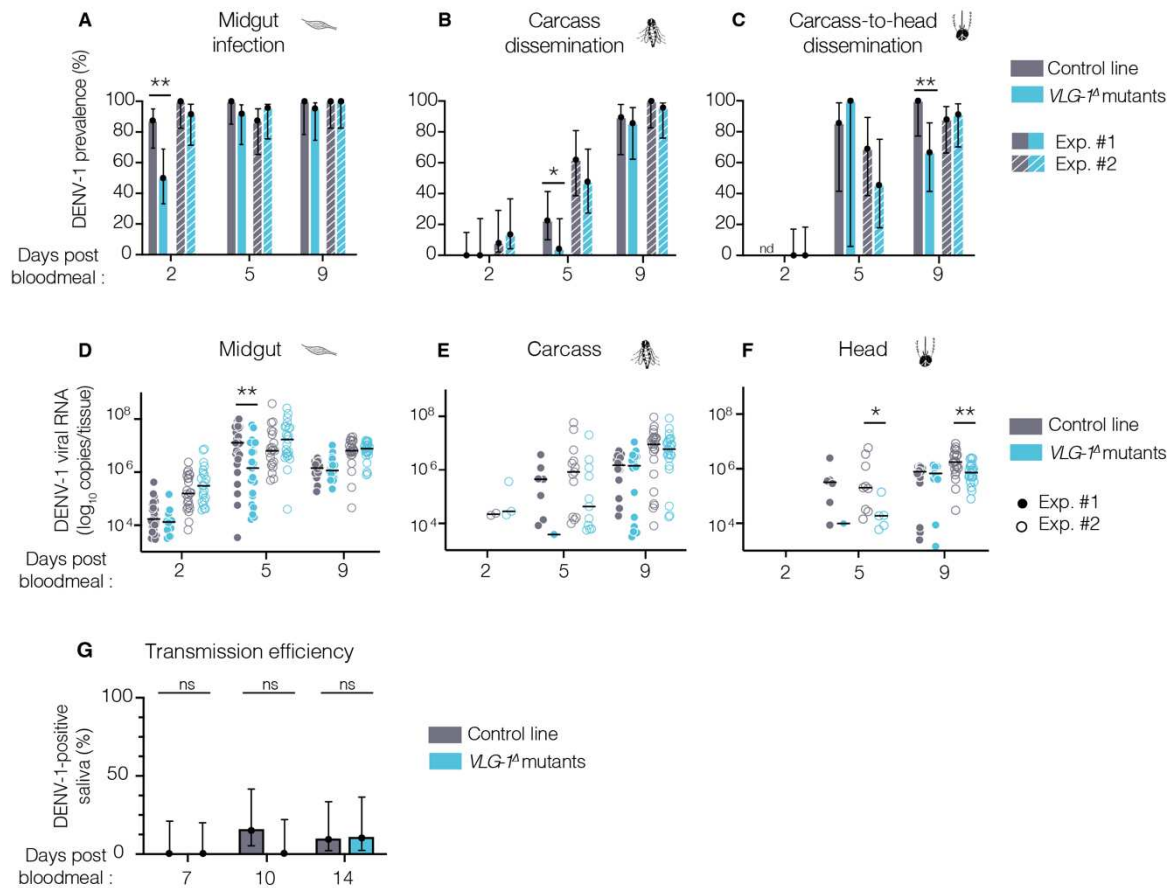


Figure 4. *VLG-1* promotes systemic DENV dissemination in *Ae. aegypti*. (A-F) Female mosquitoes from the control (grey) and *VLG-1^A* mutant (blue) lines were offered an infectious bloodmeal containing 5×10^6 FFU/mL of DENV-1. DENV-1 infection prevalence (A-C) and non-zero viral loads (D-F) were measured by RT-qPCR in the midgut, carcass, and head of individual mosquitoes on days 2, 5, and 9 post bloodmeal. (A-C) Midgut infection prevalence was calculated as the number of virus-positive midguts over the total number of virus-exposed mosquitoes. Carcass dissemination prevalence was calculated as the number of virus-positive carcasses over the number of virus-positive midguts. Carcass-to-head dissemination prevalence was calculated as the number of virus-positive heads over the number of virus-positive carcasses. (D-F) Each dot represents an individual tissue. The horizontal black lines represent the median values. * $p < 0.05$; ** $p < 0.01$; *** $p < 0.001$ (Mann-Whitney's test). (G) Saliva samples from virus-exposed mosquitoes were collected on days 7, 10, and 14 after exposure and infectious virus particles in the saliva were detected by focus-forming assay. In (A-C) and (G), vertical error bars represent the 95% confidence intervals of the proportions. * $p < 0.05$; ** $p < 0.01$; *** $p < 0.001$ (chi-squared test). In (A-F), data from two experimental replicates, analyzed and displayed separately because a significant experiment effect was detected, are plotted using two shades of the same color.

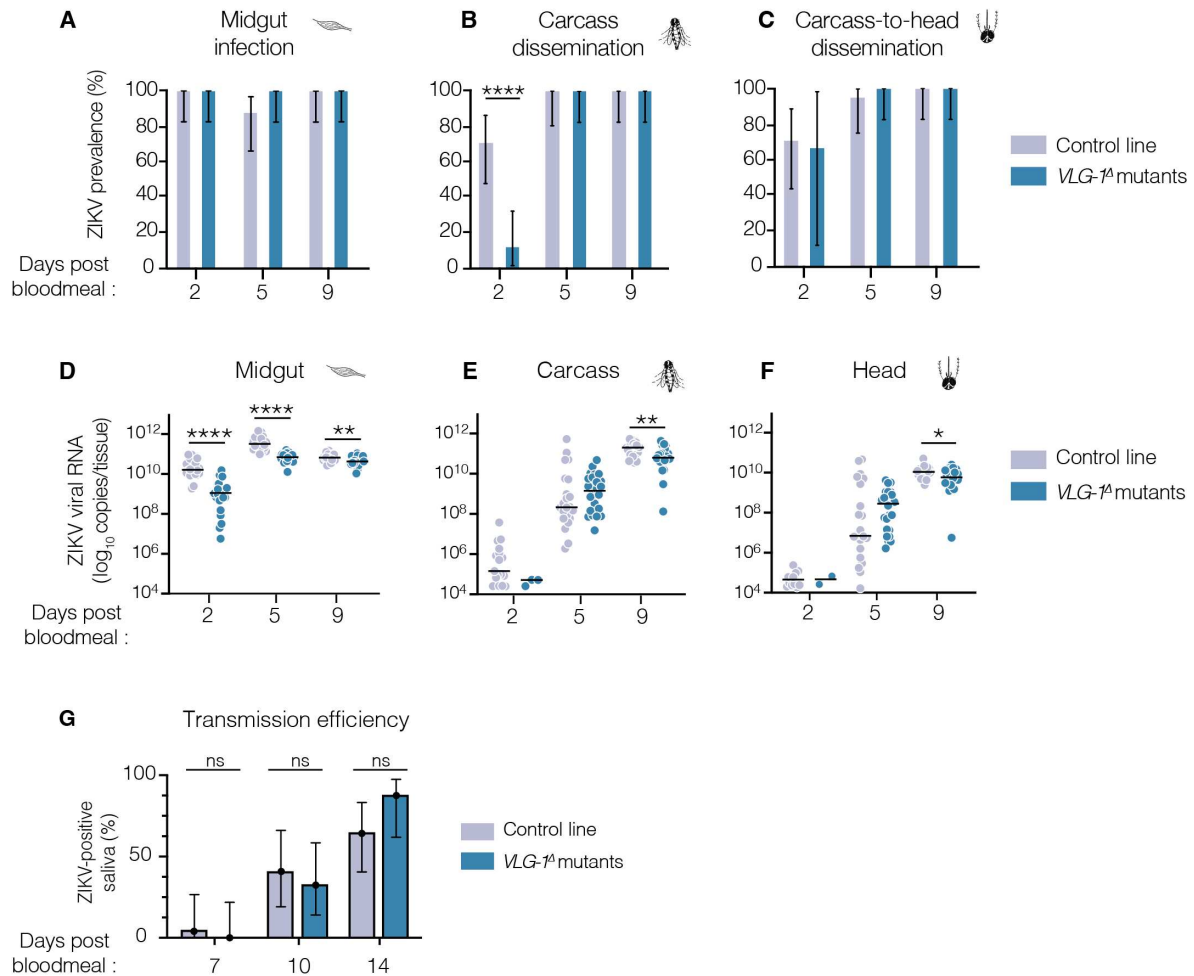


Figure 5. *VLG-1* promotes systemic ZIKV dissemination in *Ae. aegypti*. (A-F) Female mosquitoes from the control (grey) and *VLG-1* mutant (blue) lines were offered an infectious bloodmeal containing 5×10^5 PFU/mL of ZIKV. ZIKV infection prevalence (A-C) and non-zero viral loads (D-F) were measured by RT-qPCR in the midgut, carcass, and head of individual mosquitoes on days 2, 5, and 9 post bloodmeal. (A-C) Midgut infection prevalence was calculated as the number of virus-positive midguts over the total number of virus-exposed mosquitoes. Carcass dissemination prevalence was calculated as the number of virus-positive carcasses over the number of virus-positive midguts. Carcass-to-head dissemination prevalence was calculated as the number of virus-positive heads over the number of virus-positive carcasses. (D-F) Each dot represents an individual tissue. The horizontal black lines represent the median values. * $p < 0.05$; ** $p < 0.01$; *** $p < 0.001$ (Mann-Whitney's test). (G) Saliva samples from virus-exposed mosquitoes were collected on days 7, 10, and 14 after exposure and infectious virus particles in the saliva were detected by focus-forming assay. In (A-C) and (G), vertical error bars represent the 95% confidence intervals of the proportions. * $p < 0.05$; ** $p < 0.01$; *** $p < 0.001$ (chi-squared test).

VLG-1 and VLG-2 have non-additive proviral effects on DENV in *Ae. aegypti*

The finding of *VLG-1*'s proviral effect prompted us to test whether its paralog *VLG-2* could share similar properties in *Ae. aegypti*. Using RNAi-mediated knockdown, we depleted *VLG-2* transcripts in adult *VLG-1^A* mutants or control mosquitoes. Two days after injection of double-stranded RNA (dsRNA) targeting *VLG-2* or *Luciferase* (as a control), mosquitoes were exposed to a DENV-1 infectious bloodmeal and their heads collected 7 days later. Consistent to previous results, we found that infection prevalence in heads was lower for *VLG-1^A* mutants than for wild types upon control dsRNA injection (Supplementary Figure S3A). Head infection prevalence was also lower in wild-type mosquitoes depleted in *VLG-2* transcripts, revealing a proviral role for *VLG-2*. Finally, head infection prevalence was not further reduced in mosquitoes that were depleted for both *VLG-1* and *VLG-2* transcripts (Supplementary Figure S3A). Additionally, we did not detect differences in viral loads between any of the experimental treatments (Supplementary Figure S2B). On the day of the bloodmeal, we tested *VLG-2* gene knockdown efficiency and found a strong reduction in transcript abundance for both isoforms (*VLG-2-RA* and *-RB*) in all conditions (Supplementary Figure S3C-D). Together, these results indicate that *VLG-1* and *VLG-2* exert non-additive proviral effects on DENV infection in *Ae. aegypti*.

The transcriptional landscape of *VLG-1* mutants is broadly altered

To investigate the overall impact of *VLG-1* loss and its link with virus infection in *Ae. aegypti*, we analyzed the midgut and body (carcass + head) transcriptomes of *VLG-1^A* mutant and control lines on days 2, 5, and 9 after a DENV-1 or mock bloodmeal. We detected transcripts from a total of ~15,000 unique genes in midguts and ~16,800 unique genes in bodies, representing 75% to 85% of all annotated genes depending on the samples and conditions.

In midguts, several hundreds of genes (ranging from 236 to 681) were significantly differentially expressed, defined by a fold change ≥ 2 and a p-value ≤ 0.05 between *VLG-1^A* mutants and controls (Figure 6A-B and Supplementary Figure S5). The highest number of differentially expressed genes (DEGs) was observed on day 2 after DENV exposure, with 380 up-regulated and 301 down-regulated genes. Overall, up to 4.5% of all detected genes were differentially expressed between *VLG-1^A* mutants and controls in midguts. In the bodies, fewer DEGs were detected, but the highest number of DEGs was still detected 2 days after DENV exposure. These results suggest that *VLG-1* has a wide impact on biological processes, most prominently 2 days after a bloodmeal and especially in the presence of DENV.

VLG-1-dependent changes in gene expression occurred in the midgut and the rest of the body, but the overlap between DEGs in midguts and bodies was minimal (Figure 6C-D and

Supplementary Figure S4). Only 18 and 34 up- or down-regulated transcripts (out of 684 and 592) were shared between both compartments, suggesting tissue-specific functions for *VLG-1*. Conversely, a noteworthy overlap of DEGs was detected between the mock and DENV bloodmeal conditions in both compartments, suggesting that *VLG-1*-dependent gene expression is only partially affected by virus infection.

To explore the biological functions of DEGs in *VLG-1^A* mutants, we examined their gene ontology (GO) annotations at the level of biological processes. We found that enriched GO terms in both midguts and bodies included mainly response to oxidative stress, translation regulation, and molecule transport (Figure 6E). Midgut-specific DEGs were mostly associated with RNA processing and broad metabolic processes, whereas most body-specific DEGs belonged to protein phosphorylation, protein modification, and ion transport categories. We did not specifically identify immune genes or pathways that are differentially expressed in *VLG-1^A* mutants. None of the genes previously reported to be involved in the activation or function of *CxVLG-1* (*Rel2*, *TRAF*, *Dicer2*, and *vir-1*) [26, 27] were DEGs in our dataset. This observation suggests that *Ae. aegypti VLG-1* and its *Culex* ortholog participate in different signaling pathways despite their close phylogenetic relatedness. However, several DEGs were related to protein phosphorylation, particularly in DENV-exposed mosquitoes. These genes include several activators of immune pathways, such as *Pelle* and *Tube* in the Toll pathway, *Hop* in the JAK-STAT pathway, and *Tak* in the IMD pathway. Similarly, some DEGs identified in infected midguts and related to proteolysis are often associated with the Toll or IMD pathways, such as *CLIP* or *DREDD* genes. Thus, we cannot exclude a link between *Ae. aegypti VLG-1* and the canonical inducible immune pathways, although it would be distinct from previous observations in *Culex* mosquitoes. We also found an enrichment of DEGs involved in oxidoreduction and oxidative stress response across tissues, timepoints and bloodmeal types. The anti-oxidative response is predominantly reduced in the bodies of the *VLG-1^A* mutants relative to the controls, suggesting that *VLG-1* limits cellular oxidation, possibly contributing to its proviral effect. Finally, we observed large number of enriched GO terms related to translation regulation, which might explain the broad impact of *VLG-1* across diverse biological processes.

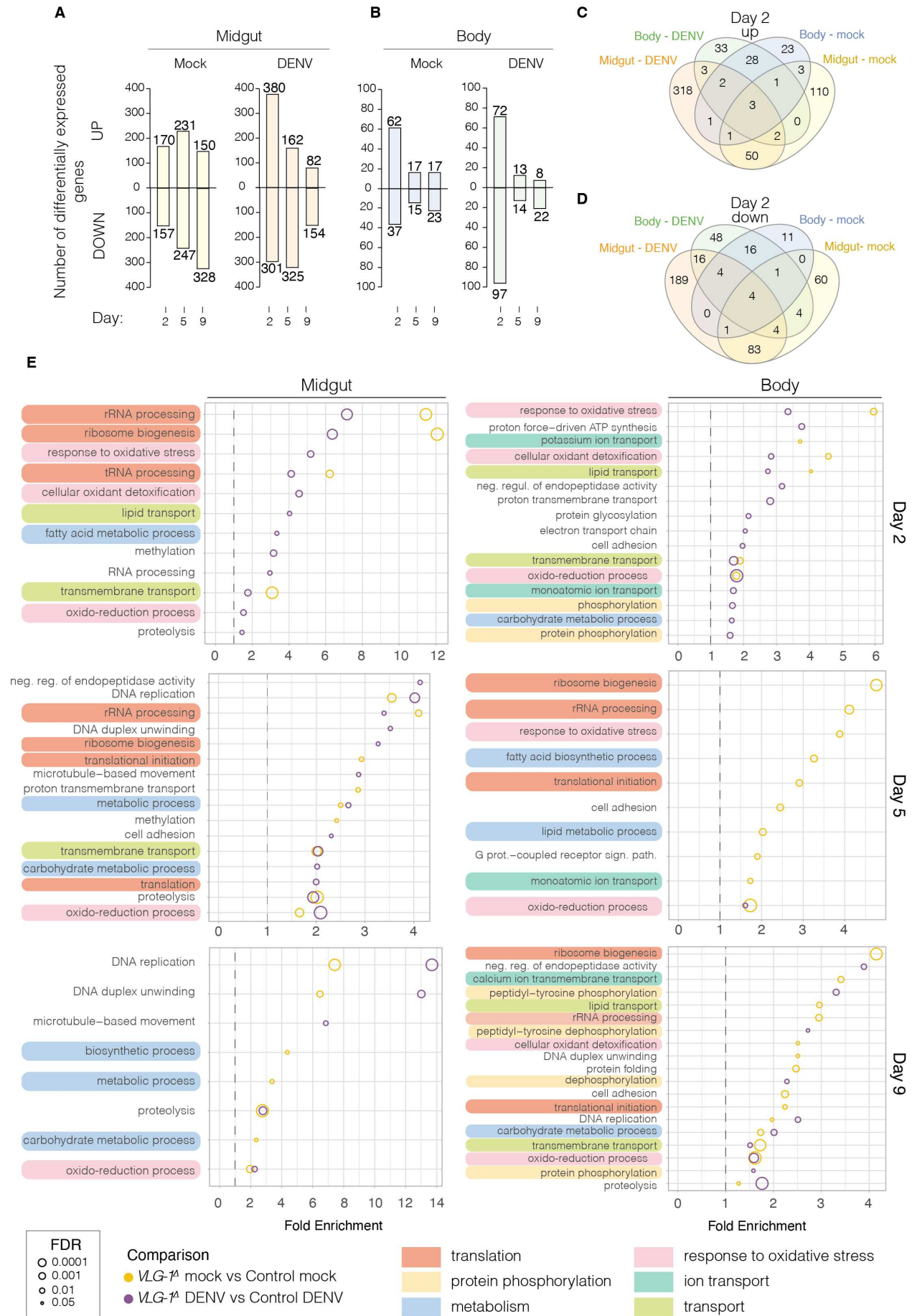


Figure 6. The transcriptome of *VLG-1^A* mutants is broadly altered. Female mosquitoes of the control and *VLG-1^A* mutant lines were offered a mock or infectious bloodmeal containing 5×10^6 FFU/mL of DENV-1. On days 2, 5, and 9 post bloodmeal, 3 pools of 10 tissues (midguts or bodies) were collected and analyzed by RNA-seq. (A-B) Number of differentially expressed genes (DEGs) in *VLG-1^A* mutants compared to wild-type controls in midguts (A) and bodies (B) for both directions of change (up- or down-regulated). A gene was considered DEG when the absolute fold change was ≥ 2 and the adjusted p-value was ≤ 0.05 . (C-D) Venn diagrams showing the overlap of up-regulated (C) and down-regulated (D) genes in *VLG-1^A* mutants compared to controls between all combinations of midguts, bodies, and bloodmeal type, on day 2 post bloodmeal. (E) Gene ontology (GO) enrichment of DEGs in *VLG-1^A* mutants compared to controls for both bloodmeal types, in midguts and bodies. Fold enrichment of each GO term is represented by a circle whose size is inversely proportional to the false discovery rate (FDR) of the enrichment score. GO terms with a similar biological function are identified with a color code and assigned a higher-order functional annotation. Correspondence between GO term names and IDs are listed in Supplementary Table 4.

DISCUSSION

In this study, we identified the *Ae. aegypti* gene *AAEL000200* as a Culicinae-specific *Vago*-like gene that we renamed *AaeVLG-1*. We generated a *VLG-1* mutant line of *Ae. aegypti* that displayed a slight reduction in lifespan but remained fully viable and fertile. Upon DENV and ZIKV infection, we found that *VLG-1* exerted a proviral role by enhancing virus dissemination, but not virus transmission. Finally, we provided a tissue-specific description of the transcriptomic landscape of *VLG-1^Δ* mutants following a mock or DENV-containing bloodmeal. This newly discovered proviral effect of *VLG-1* in *Ae. aegypti* challenges the universal nature of the antiviral function of *Vago*-like genes in arthropods.

Our transcriptomic analysis revealed that the loss of *VLG-1* interferes with a wide range of biological pathways. Notably, canonical immune pathways were not significantly impacted by *VLG-1* loss of function. Amongst the most altered processes in *VLG-1^Δ* mutants was the response to oxidative stress. Pro-oxidative processes were up-regulated and anti-oxidative processes were down-regulated in the *VLG-1^Δ* mutants, suggesting that *VLG-1* confers protection against oxidative stress. Hijacking of oxidative stress by viruses has been reported to facilitate their genome replication [39-42]. Additionally, oxidative stress can also contribute to the cellular antiviral response [43-45]. Thus, modulation of the oxidative stress response by *VLG-1* could contribute to its proviral effect and explain the shorter lifespan of *VLG-1^Δ* mutants.

The induction mechanism of *VLG-1* remains to be elucidated. In *Culex* mosquitoes, *CxVLG-1* induction depends on a NF- κ B Rel-binding site [27]. We ran a promoter analysis to identify binding motifs of transcription factors (TF) in the promoter sequence of *VLG-1* (Supplementary Figure S6 and Supplementary Table 6). Importantly, we did not identify classical immune TF binding motifs, such as NF- κ B motifs. In contrast, we identified TF binding motifs specific to signaling pathways involved in cell cycle regulation, apoptosis and redox stress response. This observation is consistent with the hypothesis that *VLG-1*'s proviral activity in *Ae. aegypti* is not associated with canonical immune pathways but rather with stress response processes.

Mechanistic insights into *VLG-1*'s mode of action in *Ae. aegypti* remain to be investigated. *CxVLG-1* is secreted extracellularly in *Culex*-derived cells [26], and *Vago*-like proteins are presumed to be secreted in several other insect species [25, 32]. The *AaeVLG-1* protein sequence contains a secretion signal peptide, but experimental evidence of extracellular localization is lacking. Technical limitations such as minute protein amounts in the mosquito hemolymph, low sensitivity of detection, and lack of adequate controls prevented us from assessing the extracellular presence of *VLG-1 in vivo* by immunoblotting. Mass spectrometry

analysis of the hemolymph protein content may be required to confirm VLG-1 secretion in the extracellular environment.

Our evolutionary analyses of *Vago*-like gene homologs in dipteran insects showed that both *VLG* paralogs have been retained and maintained under slightly relaxed selective pressure since the Culicinae diversification 150 million years ago. This indicates that they did not undergo pseudogenization (*i.e.*, accumulation of deleterious mutations resulting in a non-functional gene sharing high sequence identity with the ancestral form). Our knockdown experiments also revealed a proviral effect of *AaeVLG-2*, but this remains to be more comprehensively investigated. The evolutionary analysis does not support the hypothesis of neofunctionalization of *VLG-1* following its duplication from *VLG-2*. We found that purifying selection remained the predominant mode of evolution for both paralogs after the duplication in the Culicinae. Neofunctionalization is typically associated with relaxed purifying selection, including sites evolving under positive selection and diversification [46], as well as asymmetry in ω following the duplication event [47]. Our results are more consistent with subfunctionalization, whereby each paralog retains a subset of its original ancestral function. Under a subfunctionalization scenario, higher ω is expected in the daughter lineages compared to the parental lineage [47]. Moreover, *VLG-2* knockdown in *VLG-1^Δ* mutants resulted in a similar phenotype to *VLG-2* knockdown in wild-type controls and control knockdown in *VLG-1^Δ* mutants, suggesting a functional co-dependency of *VLG-2* and *VLG-1*, where both paralogs would provide their proviral activity jointly in *Ae. aegypti*. Subfunctionalization can also occur via specialization, a process in which paralogs divide into various areas of specialty, such as tissue-specificity, rather than function [48]. Additional evidence is needed to support a subfunctionalization scenario for *Vago*-like genes in *Ae. aegypti*.

In conclusion, our study unveils an unexpected proviral activity of the *Vago*-like gene *VLG-1* during flavivirus infection in *Ae. aegypti*. Although the proviral effect of *VLG-1* does not seem to significantly influence vector competence, our findings challenge the notion that genes of the *Vago* family are conserved antiviral factors in arthropods and question their designation as antiviral cytokines. We anticipate that our newly generated *VLG-1^Δ* mosquito mutant line will serve as a valuable tool to investigate the function of *VLG-1* in *Ae. aegypti*. This work underscores the importance of *in vivo* research for identifying and characterizing the biological roles of pro- and antiviral factors that govern the ability of *Ae. aegypti* mosquitoes to transmit arboviruses. This fundamental understanding of mosquito-arbovirus interactions will be critical to the development of new strategies aiming to reduce the burden of arboviral diseases [49].

ACKNOWLEDGEMENTS

We thank Catherine Lallemand for assistance with mosquito rearing, Artem Baidaliuk for preliminary bioinformatic analysis of *Vago*-like gene homology, and Prasad Paradkar for kindly sharing the CxVLG-1 antibody. RNA-seq library preparation was performed by Elodie Turc and Laure Lemée from the Biomix platform (C2RT, Institut Pasteur, Paris, France) supported by France Génomique (ANR-10-INBS-09) and IBISA. This work was supported by the French Government's Investissement d'Avenir program, Laboratoire d'Excellence Integrative Biology of Emerging Infectious Diseases (grant ANR-10-LABX-62-IBEID to L.L. and E.C.), Agence Nationale de la Recherche (grant ANR-18-CE35-0003-01 to L.L.), a PhD grant from Ecole Normale Supérieure de Lyon (to E.C.) and a junior seed grant from Institut Pasteur (to E.C.). The funders had no role in study design, data collection and analysis, decision to publish, or preparation of the manuscript.

AUTHOR CONTRIBUTIONS

Conceptualization: E.C., J.D., P.M., T.V., S.H.M., L.L.

Investigation: E.C., A.B.C., J.D., A.B., F.A.H.v.H., U.P., T.V., S.D.

Data curation: H.V.

Formal analysis: E.C., H.V., J.D., F.A.H.v.H., A.B., U.P., L.L.

Visualization: E.C., F.A.H.v.H., H.V.

Writing – original draft: E.C., S.H.M., L.L.

Writing – review and editing: E.C., P.M., S.H.M., L.L.

Funding acquisition: E.C., S.H.M., L.L.

METHODS

Virus strains

DENV-1 strain KDH0026A was originally isolated in 2010 from the serum of a patient in Kamphaeng Phet, Thailand [52]. ZIKV strain Kedougou2011 was originally isolated in 2011 from a mosquito pool in Kedougou, Senegal [53]. Viral stocks were prepared in C6/36 *Aedes albopictus* cells as previously described [54].

Mosquitoes

Experiments were conducted with a previously described isofemale line of *Ae. aegypti* called Jane [19, 55]. Mosquitoes were reared in controlled conditions (28°C, 12-hour light/12-hour dark cycle and 70% relative humidity). For experiments, eggs were hatched synchronously in a SpeedVac vacuum device (Thermo Fisher Scientific) for 45 minutes. Larvae were reared in plastic trays containing 1.5 L of dechlorinated tap water and fed a standard diet of Tetramin (Tetra) fish food at a density of 200 larvae per tray. After emergence, adults were kept in BugDorm-1 insect cages (BugDorm) with permanent access to 10% sucrose solution.

CRISPR/Cas9-mediated gene editing

sgRNA design and synthesis. A *VLG-1* mutant line and wild-type “sister” line were derived from the 26th generation of the Jane isofemale line. Gene editing was performed using CRISPR/Cas9 technology as previously described [56]. The single-guide RNAs (sgRNAs) were designed using CRISPOR [57] by searching for 20-bp sgRNAs with the NGG protospacer-adjacent-motif (PAM). To reduce chances of off-target mutations, only sgRNAs with off-target sites with at least four mismatches were selected. Three sgRNAs were selected with cut sites respectively located upstream of the start codon, in the middle of the *VLG-1* gene within the second exon, and upstream of the stop codon. Since the *VLG-1* locus is only 471-bp (including introns), a single-stranded oligodeoxynucleotide (ssODN) repair template was provided to delete the entire gene. The ssODN repair template included two 35-bp homology arms matching the sequence upstream from the cut site of the first sgRNA (x1_30rev) and downstream from the cut site of the third sgRNA (x3_67rev) to facilitate excision of the *VLG-1* gene. The ssODN repair template was synthesized and PAGE-purified commercially (Sigma-Aldrich). Single-guide RNAs were synthesized with the MEGAscript T7 *in vitro* transcription kit (Ambion) and purified with the MEGAclear kit (Invitrogen).

Embryonic microinjections. *Ae. aegypti* embryos were injected with a microinjection mix containing 402.5 ng/μL SpCas9 protein (New England Biolabs), 40 ng/μL of each of three sgRNAs (x1_30rev, x2_6rev, x3_67rev), and 125 ng/μL of the ssODN repair template suspended in molecular grade water. The microinjection of *Ae. aegypti* embryos was

performed using standard protocols [58]. *Ae. aegypti* adult females were bloodfed with commercial rabbit blood (BCL) via an artificial membrane feeding system (Hemotek). Three days post bloodmeal, females were transferred to egg-laying vials and oviposition was induced by placing mosquitoes into dark conditions for 15 min. Embryos were injected 30-60 min post oviposition. Embryos were hatched in water 3 days post injection and individual pupae placed into vials containing a small amount of water to isolate and screen adults for mutations before mating could occur.

Mutation isolation and line creation. Individual virgin adult G_0 mosquitoes were screened for mutations by PCR to amplify the *VLG-1* gene from DNA extracted from a single leg (see Genotyping below). The amplified region was 793 bp and deletions were screened for on a 2% agarose gel. If large deletions were detected, the corresponding mosquito was mated with wild-type mosquitoes of the opposite sex and progeny screened for inheritance of the mutation. Sanger sequencing was then performed to characterize the edit. A large deletion of ~200 bp was identified in a G_0 female that was subsequently placed in a cage with 3 wild-type males for mating, blood feeding, and egg laying. The G_1 eggs were hatched in water 5 days post laying and individual pupae isolated into vials containing a small amount of water to isolate and screen adults for mutations before mating could occur. G_1 progeny was screened for the deletion by PCR to confirm heritability of the mutation. Four G_1 males (heterozygous for the mutation) were then crossed with 50 wild-type females. Next, 11 G_2 male heterozygotes were crossed with 23 wild-type females. Finally, 14 G_3 males and 33 G_3 females heterozygous at the mutation site were crossed with each other. G_4 adults were sorted into homozygous mutants (establishing the *VLG-1^A* mutant line) and homozygous wild types (establishing the control “sister” line). The *VLG-1^A* mutant line was established with 9 G_4 males and 24 G_4 females, while the control line was established with 19 males and 29 females. Sequencing of *VLG-1^A* individuals using Sequencing primer F (Supplementary Table 5) revealed that the deletion spanned 246 bp of the wild-type *VLG-1* sequence starting at the cut site of the sgRNA in the middle of the gene (x2_6rev), 170 bp downstream of the still intact start codon, and ending at the cut site of the third sgRNA (x3_67rev), 49 bp upstream of the stop codon. However, the mutation also contained a 34-bp insertion of the upstream 35-bp homology arm of the repair template in-between the sgRNA cut sites, resulting in a PCR product 212-bp shorter than the wild-type PCR product, matching what was visualized on gels during screening.

Genotyping. Genomic DNA was extracted from single legs of individual mosquitoes using DNAzol DIRECT (DN131, Molecular Research Center, Inc.). To obtain legs from live mosquitoes, pupae were placed in vials containing a small volume of water and sealed with a cotton plug (Flugs, Genesee). After adult emergence, the water was drained and vials placed on ice for anesthesia. Single legs were collected using forceps and placed in a 2-mL screw-top plastic tube containing ~20 1-mm glass beads (BioSpec) and 200 μ L of DNAzol DIRECT.

Mosquitoes were then placed back into the vials to remain isolated and unmated until genotyping via PCR. The legs were homogenized for 30 sec at 6,000 revolutions per minute (rpm) in a Precellys 24 tissue homogenizer (Bertin Technologies), briefly centrifuged, and then placed at room temperature (20-25°C) for immediate use. PCR was performed using DreamTaq DNA Polymerase (EP0701, Thermo-Fisher Scientific) based on manufacturer's instructions, using Genotyping primers (Supplementary Table 5). Approximately 0.6 µL of the DNAzol DNA extract from leg tissue was used in 19 µL of DreamTaq PCR master mix. The PCR conditions were as follows: initial denaturation at 95°C for 3 min, 40 cycles of amplification (denaturation at 95°C for 30 sec, annealing at 59°C for 15 sec, and extension at 72°C for 30 sec), and a final extension step at 72°C for 5 min. Amplicons were purified (MinElute PCR purification kit, Qiagen) and subsequently sequenced (Eurofins).

Evolutionary analyses

Gene phylogeny. Using the protein sequence of *AaeVLG-1* (AAEL000200; RefSeq accession number XP_001658930.1) and *AaeVLG-2* (AAEL000165; RefSeq accession number XP_001658929.1) as queries, we performed a BLASTP against the NCBI non-redundant protein database to extract homologous genes present in the *Drosophila* genus and Culicidae family. Only genes present in the reference sequence (RefSeq) were considered in the final dataset of 62 homologous genes (Supplementary Table 2). Then, input coding sequences were aligned with respect to their codon structure using MACSE v2.06 [59] and the protein alignment was used as input for IQ-tree2 [60] to infer the phylogenetic relationships of the *Vago*-like gene homologs. The substitution model WAG+I+G4 was the best fit model based on the Bayesian Information Criterion (BIC) and the maximum-likelihood phylogenetic tree was generated with 1,000 ultra-fast bootstrap iterations. The phylogenetic tree of *Vago*-like genes was rooted using *Drosophila* sequences and visualized using iTOL [61].

Evolutionary rate. To investigate the evolutionary rates of *Vago*-like gene coding sequences, the CODEML tool from the PAML package [62] was used to detect variations of the ratio of non-synonymous to synonymous substitutions (ω) as a proxy for the variation in selective pressure, following the guide for user good practices [63]. CODEML was configured to use the branch model, which assumes different ω parameters for different branches in the phylogeny [64, 65]. Three tests were conducted by designating different branches as the foreground: (i) *VLG-1* branch, (ii) both *VLG* and *VLG-1* branches, (iii) *VLG-1*, Anophelinae *VLG* and Culicinae *VLG* branches. Comparison of the branch model to the null model was performed through a likelihood-ratio test (Supplementary Table 3).

Mosquito fitness assays

Survival. Five to seven days after adult emergence, males and females were sorted and transferred in 1-pint carton boxes with permanent access to 10% sucrose solution at 28°C and 70% relative humidity. Mortality was scored daily. Four replicate boxes containing 25 mosquitoes each were used for each experiment.

Fecundity. Five- to seven-day-old females were blood fed and transferred to individual vials containing a humid blotting paper for egg laying with access to 10% sucrose solution. After 7 days, eggs deposited on the blotting paper were counted under a binocular magnifier. Fecundity was defined as the number of eggs laid per blood-fed female.

Fertility. The aforementioned blotting papers air dried for a week. Eggs were then hatched synchronously in a SpeedVac vacuum device (Thermo Fischer Scientific) for 45 min. Larvae were transferred to individual vials containing tap water and with Tetramin fish food, and viable larvae were enumerated three days later. Fertility was defined as the number of viable larvae over the total number of laid eggs per blood-fed female.

Mosquito infectious bloodmeals

Experimental infections of mosquitoes were performed in a biosafety level-3 containment facility, as previously described [54]. Shortly, 5- to 7-day-old female mosquitoes were deprived of 10% sucrose solution 20 hours prior to being exposed to an artificial infectious bloodmeal containing 5×10^6 FFU/mL of DENV-1 or 5×10^5 PFU/mL of ZIKV. The infectious bloodmeal consisted of a 2:1 mix of washed rabbit erythrocytes (BCL) supplemented with 10 mM adenosine triphosphate (Sigma) and viral suspension supplemented with Leibovitz's L-15 medium (Gibco; described below). Mosquitoes were exposed to the infectious bloodmeal for 15 min through a desalted pig-intestine membrane using an artificial feeder (Hemotek Ltd) set at 37°C. Fully blood-fed females were sorted on ice and incubated at 28°C, 70% relative humidity and under a 12-hour light-dark cycle with permanent access to 10% sucrose solution.

Gene expression and viral load quantification

Mosquito tissues were dissected in $1 \times$ phosphate-buffered saline (PBS), and immediately transferred to a tube containing 400 μ L of RA1 lysis buffer from the Nucleospin 96 RNA core kit (Macherey-Nagel) and ~ 20 1-mm glass beads (BioSpec). Samples were homogenized for 30 sec at 6,000 rpm in a Precellys 24 grinder (Bertin Technologies). RNA was extracted and treated with DNase I following the manufacturer's instructions. Viral RNA was reverse transcribed and quantified using a TaqMan-based qPCR assay, using virus-specific primers and 6-FAM/BHQ-1 double-labelled probe (Supplementary Table 5). Reactions were performed with the GoTaq Probe 1-Step RT-qPCR System (Promega) following the manufacturer's instructions. Viral RNA levels were determined by absolute quantification using a standard

curve. The limit of detection was of 40 copies of viral RNA per microliter. Transcript RNA levels were normalized to the housekeeping gene encoding ribosomal protein S 17 (*RPS17*), and expressed as 2^{-dCt} , where $dCt = Ct_{Gene} - Ct_{RPS17}$.

Virus titration

Focus-forming assay (FFA). DENV infectious titers were measured by standard FFA in C6/36 cells. Cells were seeded at a density of 5×10^4 cells/well in a 96-well plate 24 hours before inoculation. Serial sample dilutions were prepared in Leibovitz's L-15 medium (Gibco) supplemented with 0.1% penicillin/streptomycin (pen/strep; Gibco ThermoFisher Scientific), 2% tryptose phosphate broth (TPB; Gibco Thermo Fischer Scientific), $1 \times$ non-essential amino acids (NEAA; Life Technologies) and 2% fetal bovine serum (FBS; Life Technologies). Cells were inoculated with 40 μ L of sample. After 1 hour of incubation at 28°C, the inoculum was replaced with 150 μ L of overlay medium (1:1 mix of Leibovitz's L-15 medium supplemented with 0.1% pen/strep, 2% TPB, $1 \times$ NEAA, $2 \times$ Antibiotic-Antimycotic [Life Technologies], 10% FBS and 2% carboxyl methylcellulose) and incubated for 5 days at 28°C. Cells were fixed for 30 min in 3.6% paraformaldehyde (PFA; Sigma-Aldrich). Cells were then washed three times with PBS $1 \times$, and permeabilized for 30 min with 50 μ L of PBS $1 \times$; 0.3% Triton X-100 (Sigma-Aldrich) at room temperature (20-25°C). The cells were washed three times in PBS $1 \times$ and incubated for 1 hour at 37°C with 40 μ L of mouse anti-DENV complex monoclonal antibody MAB8705 (Merck Millipore) diluted 1:200 in PBS $1 \times$; 1% bovine serum albumin (BSA) (Interchim). After another three washes in PBS, cells were incubated at 37°C for 30 min with 40 μ L of an Alexa Fluor 488-conjugated goat anti-mouse antibody (Life Technologies) diluted 1:500 in PBS $1 \times$; 1% BSA. After three washes in PBS $1 \times$ and a final wash in water, infectious foci were counted under a fluorescent microscope (Evos) and converted into focus-forming units/mL (FFU/mL).

Plaque assay. ZIKV infectious titers were measured by plaque assay in Vero E6 cells. Cells were seeded in 24-well plates at a density of 150,000 cells/well 24 hours before inoculation. Ten-fold sample dilutions were prepared in Dulbecco's Modified Eagle Medium (DMEM) with 2% FBS, 1% pen/strep, $4 \times$ Antibiotic-Antimycotic and cells were incubated with 200 μ L of inoculum. After 1 hour at 37°C, the inoculum was replaced with DMEM supplemented with 2% FBS, 1% pen/strep, $4 \times$ Antibiotic-Antimycotic and 0.8% agarose. Cells were fixed with 3.6% PFA after 6 days and plaques were counted manually after staining with 0.1% crystal violet (Sigma).

Salivation assay

Mosquitoes were anesthetized with triethylamine ($\geq 99\%$, Sigma-Aldrich) for 10 min and their legs were removed. The proboscis of each female was inserted into a 20- μ L pipet tip containing

10 µL of FBS for 30 min at room temperature (20-25°C). Saliva-containing FBS was expelled into 90 µL of Leibovitz's L-15 medium supplemented with 0.1% pen/strep, 2% TPB, 1× NEAA and 4× Antibiotic-Antimycotic. Virus presence in saliva samples was determined by virus titration after 5 days of amplification in C6/36 cells. Transmission potential was assessed qualitatively based on the presence or absence of infectious virus.

Transcriptome analysis

Library preparation and mRNA sequencing

Total RNA extracts from pools of 10 tissues were isolated with TRIzol (Invitrogen) as previously described [66] and treated with DNA-free kit (Invitrogen, AM1906) following the manufacturer's instructions. The quality of the samples was assessed using a BioAnalyzer RNA Nano kit (Agilent Technologies). RNA libraries were built using an Illumina Stranded mRNA library Preparation Kit (Illumina) following the manufacturer's protocol depending on the insert size required. Of note, to obtain 300-bp inserts, all the samples were eluted for 2 minutes at 80°C after polyA capture, instead of the 8-min fragmentation at 94°C recommended by the supplier. Sequencing was performed on two lanes 10B300 of NovaSeqX (Illumina) by Novogene.

Bioinformatics

Raw RNA-seq reads were cleaned of adapter sequences and low-quality sequences using cutadapt version 2.10 [67] with options "-m 25 -q 30 -O 6 --trim-n --max-n 1". Gene expression quantification was performed using salmon version 1.9.0 [68]. First, the *Ae. aegypti* reference transcriptome (downloaded from VectorBase (release 66) at https://vectorbase.org/common/downloads/release-66/AaegyptiLVP_AGWG/fasta/data/) was indexed along with its corresponding genome using the "--decoys" option. Transcript expression was then quantified for each sample using the "-l A" option and summarized at the gene level using the "--geneMap" parameter [69, 70]. Gene expression data was imported into R version 4.3.2 [71] using the tximport package [72]. The normalization and dispersion estimation were performed with DESeq2 [73] using the default parameters and statistical tests for differential expression were performed applying the independent filtering algorithm. For each tissue (bodies and midguts) at each time point (days 2, 5, and 9), a generalized linear model was set to test for the mutation effect on gene expression, separately for infected and non-infected mosquitoes. For each pairwise comparison, raw p-values were adjusted for multiple testing according to the Benjamini and Hochberg procedure [74] and genes with an adjusted p-value lower than 0.05 and an absolute fold-change higher than 2 were considered differentially expressed.

Gene set enrichment analysis

Gene set enrichment analysis was performed using Fisher's statistical test for the over-representation in differentially expressed genes. *Ae. aegypti* gene ontology (GO) annotations [75] were retrieved from the VectorBase website (version 66). Only gene sets with a false discovery rate (FDR) lower than 0.05 were considered significantly enriched in differentially expressed genes.

Gene knockdown assay

Double-stranded RNA (dsRNA) targeting *AaeVLG-2* (*AAEL000165*) was *in vitro* transcribed from T7 promoter-flanked PCR products using the MEGAscript RNAi kit (Life Technologies). To obtain the PCR products, a first PCR was performed on genomic DNA extracted from wild-type mosquitoes using the previously described Pat-Roman DNA extraction protocol [76]. The T7 sequence was then introduced during a second PCR using T7 universal primers that hybridize to short GC-rich tags introduced to the PCR products in the first PCR (Supplementary Table 5). dsRNA targeting *Luciferase* (as a negative control) was synthesized using T7 promoter-flanked PCR products generated by amplifying a *Luciferase*-containing plasmid with T7-flanked PCR primers with the MEGAscript RNAi kit (Life Technologies) (Supplementary Table 5). dsRNA was resuspended in RNase-free water to reach a final concentration of 10 mg/mL. Five- to seven-day-old females were anesthetized on ice and injected intrathoracically with 1 μ g (in a volume of 100 nL) dsRNA suspension using a Nanoject III apparatus (Drummond). After injection, mosquitoes were incubated for 2 days at 28°C before the infectious bloodmeal. The knockdown efficiency was estimated by RT-qPCR on the day of the bloodmeal as $(1 - ddCt) * 100$, where $ddCt = (\text{mean}(2^{-dCt} \text{ in dsVLG-2 condition})) / (\text{mean}(2^{-dCt} \text{ in dsLuciferase condition}))$, and $dCt = Ct_{VLG-2} - Ct_{RPS17}$.

Western blotting

Five female mosquitoes were collected in 250 μ L of 2 \times RIPA buffer complemented with protease inhibitor (Complete 1 \times , Roche) in tubes containing ~20 1-mm glass beads (BioSpec). Samples were homogenized for 30 sec at 6,000 rpm in a Precellys 24 grinder (Bertin Technologies). Lysates were clarified by centrifugation at 14,000 rpm for 5 min at 4°C and kept on ice. Fifty microliters of lysate were heated at 95°C with 50 μ L of Laemmli buffer for 5 min. Twenty microliters of denatured samples were loaded on a PROTEAN TGX 4-20% stain-free precast gel (Biorad) in 1 \times Tris-Glycine-SDS running buffer (Alfa Aesar). Transfer on a nitrocellulose membrane was done using a Trans-Blot Turbo transfer pack (Biorad) for 30 min at 25 V. The membrane was then incubated in PBS 1 \times -Tween 0.1%-powdered milk (Régilait) 5% (PBST-milk) for 1 hour. Incubation with the primary antibody (rabbit anti-CxVVG-1 (GenScript) generated in [26], 1:2,000 in PBST-milk) was done for 1 hour at room temperature

(20-25°C) before washing three times for 5 min in PBST. The anti-CxV_{LG-1} antibody targets the C-terminal sequence CEKIKQDLTKDY_{PE} which is located within the deleted region in the *V_{LG-1}^A* mutant sequence. The membrane was then incubated in the secondary antibody (donkey anti-rabbit, ab216779, 1:20,000 in PBST-milk) for 1 hour at room temperature. After three washes of 5 min in PBST, the membrane was imaged on an Odyssey LICOR imager.

Promoter analysis

To analyze the presence of transcription factor (TF) binding motifs in the promoter of *V_{LG-1}*, we used MoLoTool (<https://molotool.autosome.org/>), which contains 1443 verified position weight matrices from the HOCOMOCO H12CORE collection [77]. Motifs were searched for within the 500 bp upstream and 50 bp downstream regions of the *V_{LG-1}* transcription start site. Matched motifs were considered as hits after multiple testing correction using the Bonferroni method. Before visualization of the motifs on the *V_{LG-1}* promoter, redundancy was addressed by merging hits from the same TF family overlapping more than 50% in position, as well as merging similar TF families into categories.

Statistics

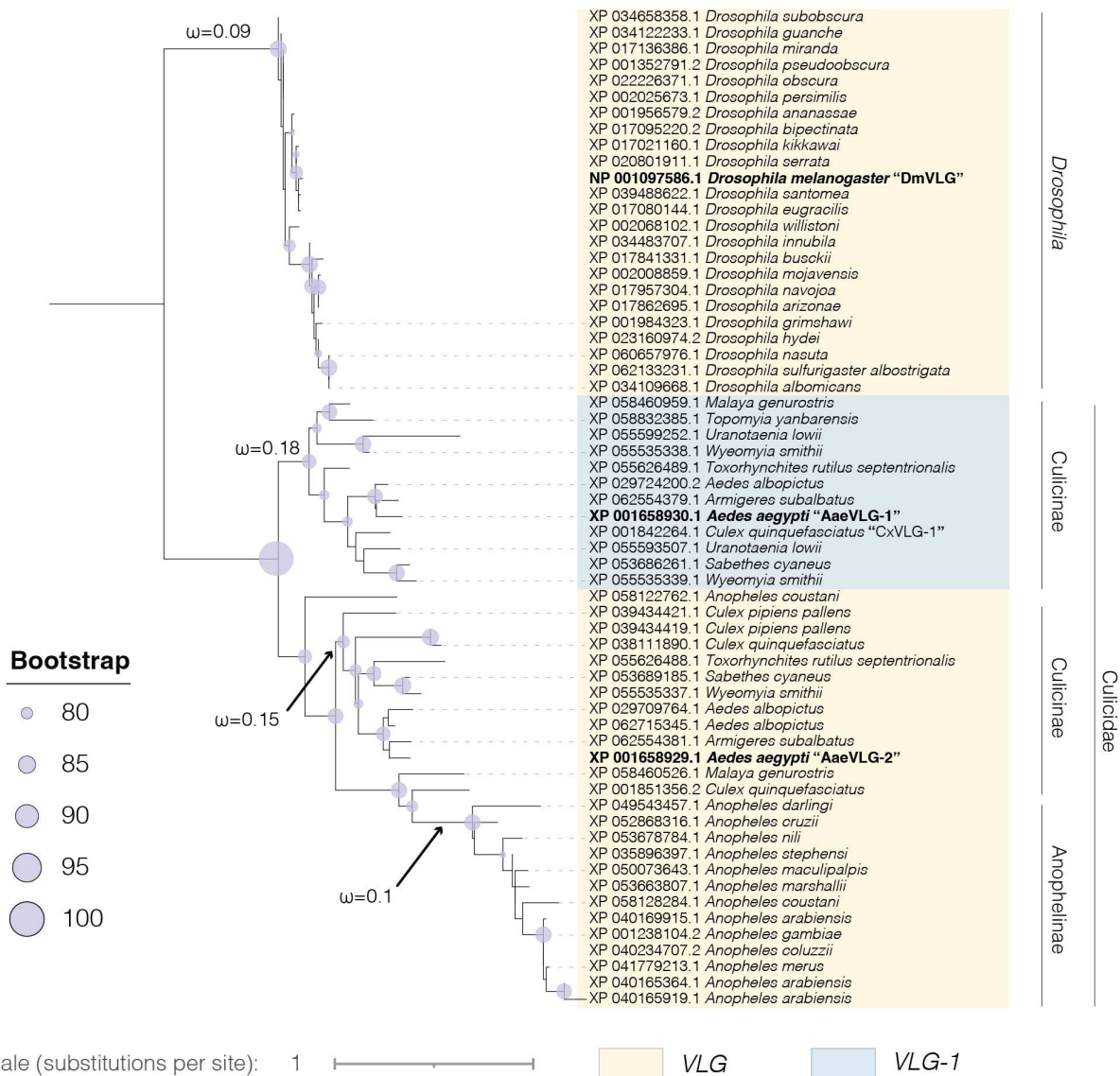
Gene expression data were analyzed by one-way analysis of variance (ANOVA) after log₁₀-transformation of the 2^{-dCt} values, followed by Tukey-Kramer's Honest Significant Difference (HSD) test. Viral loads, knockdown efficiency, and fecundity estimates were compared pairwise with a Mann-Whitney's non-parametric test. Proportions (midgut prevalence, carcass prevalence, carcass-to-head dissemination prevalence, transmission efficiency, fertility) were analyzed using a chi-squared non-parametric test. Survival assays were analyzed with a Gehan-Breslow-Wilcoxon test. Gene set enrichment analysis in the transcriptomic dataset was performed with Fisher's statistical test. Only genes with FDR < 0.05 were considered significantly enriched. Statistical analyses were performed in Prism v.10.1.0 (www.graphpad.com), JMP v.14.0.0 (www.jmp.com), and R v.4.3.2 (www.r-project.org).

Data availability

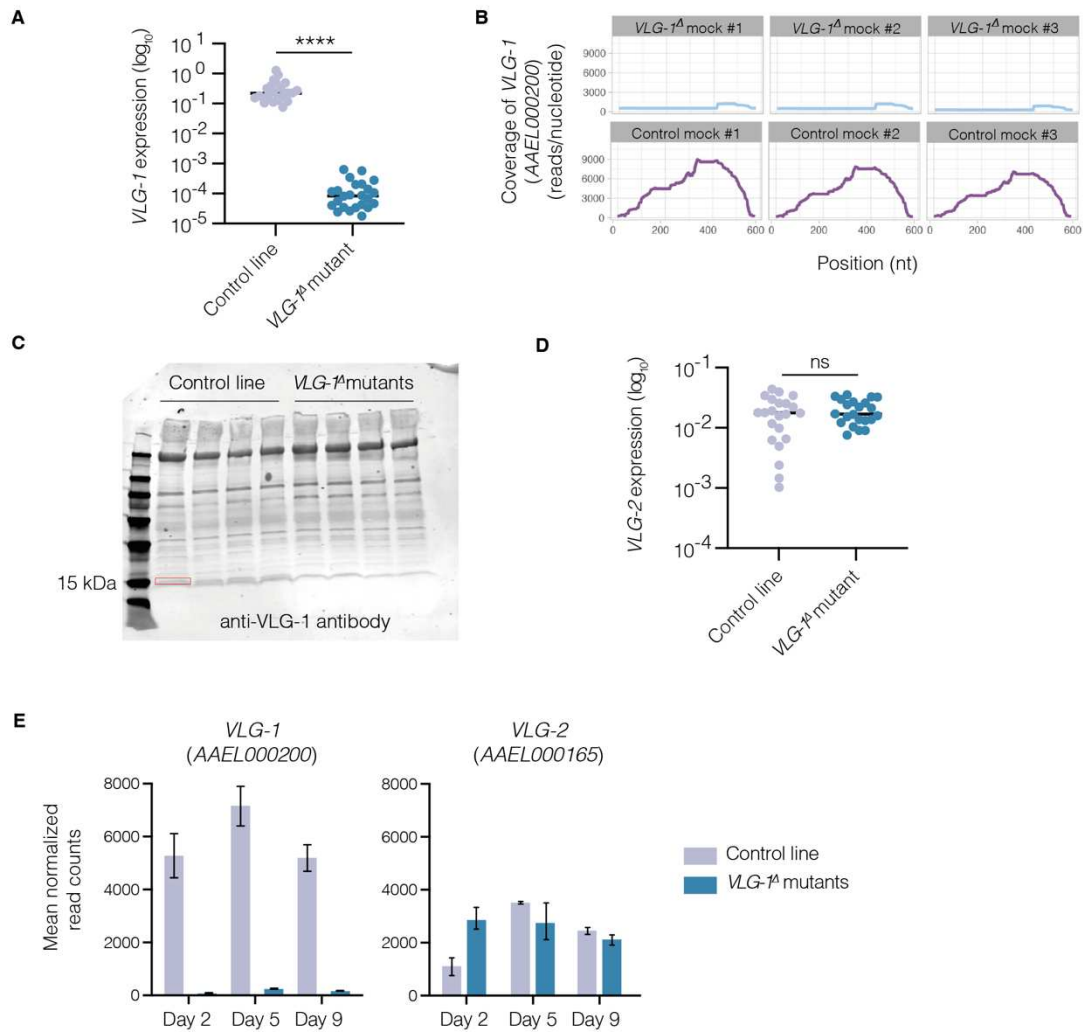
The data discussed in this publication have been deposited in NCBI's Gene Expression Omnibus [78] and are accessible through GEO Series accession number GSE269945.

SUPPLEMENTARY FIGURES

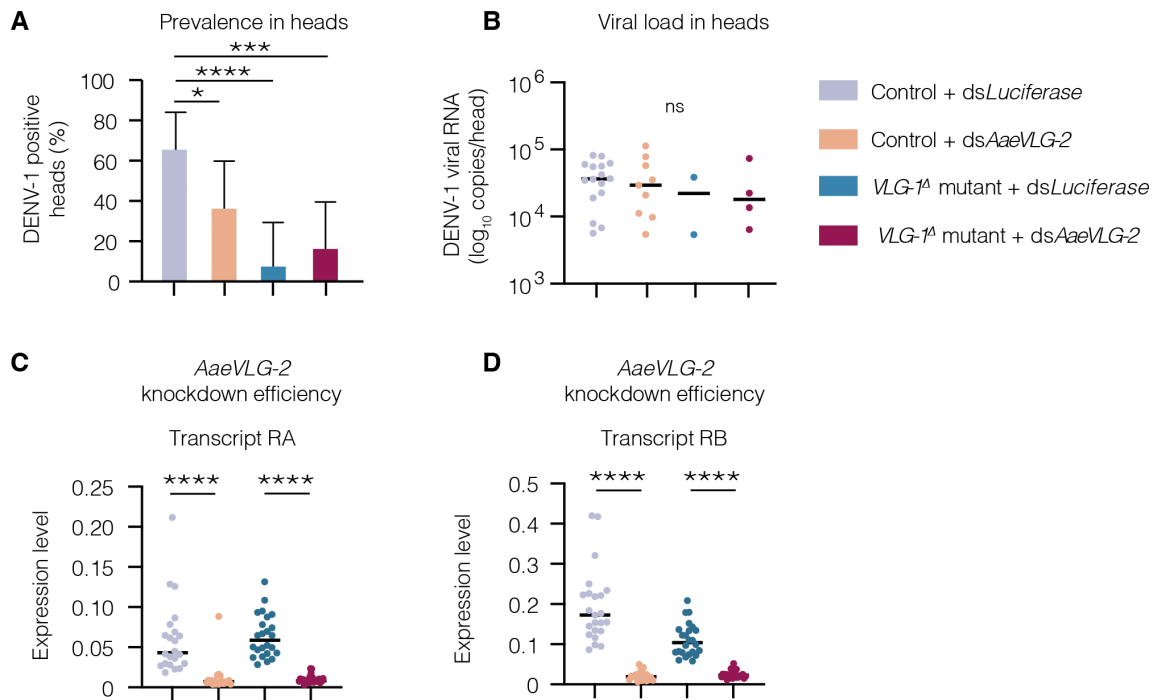
A Phylogeny of *Vago*-like genes in Diptera



Supplementary Figure S1. Phylogenetic tree of *Vago*-like gene homologs among Culicidae and *Drosophila* species. The tree was constructed with a maximum-likelihood analysis of amino-acid sequences with at least 30% identity with *D. melanogaster* VLG (DmVLG, *CG14132*). Accession number (RefSeq) of the homolog protein and name of the species are indicated at the tip of each branch. VLG and VLG-1 clades are colored in yellow and blue, respectively. The size of blue dots represents the bootstrap support of each node. The dN/dS (ω) estimates are indicated for the main branches.

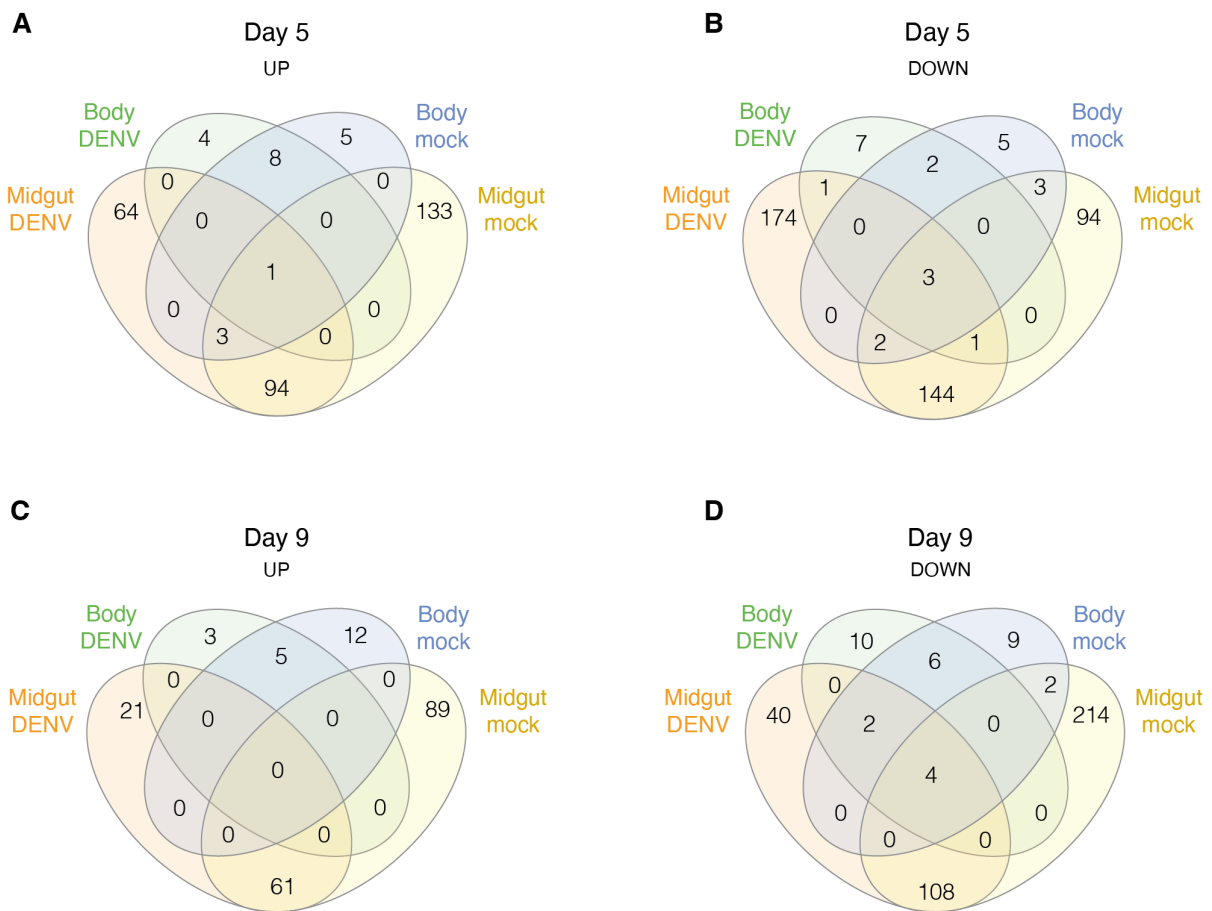


Supplementary Figure S2. Evidence for *VLG-1* loss of function in mutant *Ae. aegypti*. (A) *AaeVLG-1* transcript expression levels detected by RT-qPCR in the control and *VLG-1⁻* mutant lines. **** $p < 0.0001$ (Mann-Whitney's test) (B) Coverage (number of reads per nucleotide position) of *AaeVLG-1* transcripts by RNA-seq in *VLG-1⁻* mutants (top panels) and controls (bottom panels) in three pools of 10 bodies for each line. (C) Western blotting of *VLG-1* protein using an anti-Cx*VLG-1* antibody in controls and *VLG-1⁻* mutants, in four pools of five females for each line. The band corresponding to *VLG-1* theoretical size (15 kiloDaltons (kDa)) is highlighted in red and is detected in the controls but not in the *VLG-1⁻* mutants. (D) *AaeVLG-2* transcript expression levels detected by RT-qPCR in the control and *VLG-1⁻* mutant lines. (E) Number of reads of *AaeVLG-1* and *AaeVLG-2* transcripts detected by RNA-seq in bodies of controls and *VLG-1⁻* mutants on days 2, 5, and 9 after a mock bloodmeal. Mean normalized counts (obtained with DESeq2 [73]) from three pools of 10 bodies for each line are depicted. Vertical bars represent standard deviations. In (A) and (D), gene expression levels are normalized to the transcript abundance of the housekeeping gene encoding ribosomal protein S 17 (*RPS17*), and expressed as 2^{-dCt} , where $dCt = Ct_{Gene} - Ct_{RPS17}$.

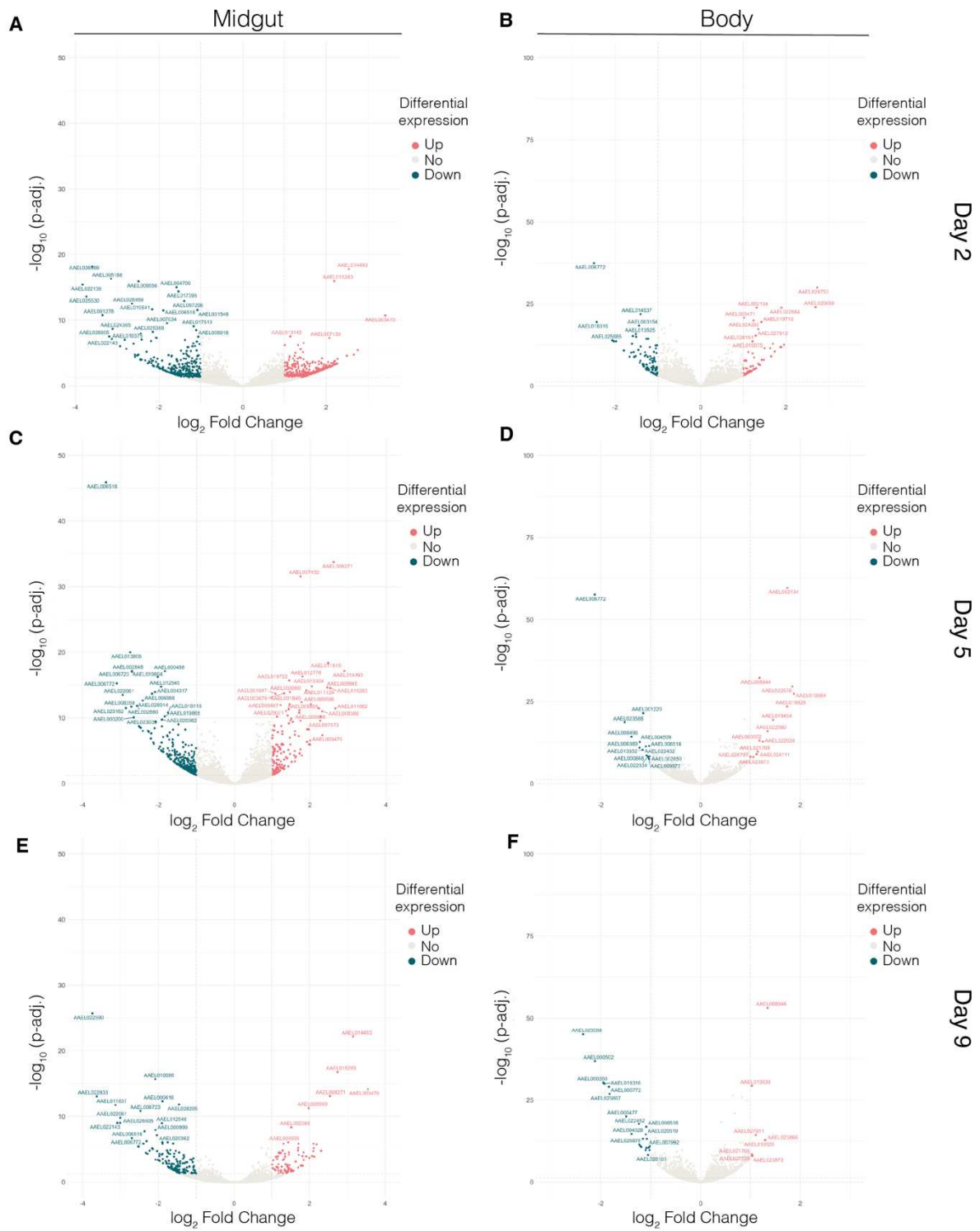


Supplementary Figure S3. *AaeVLG-2* knockdown reduces the proportion of DENV-positive heads.

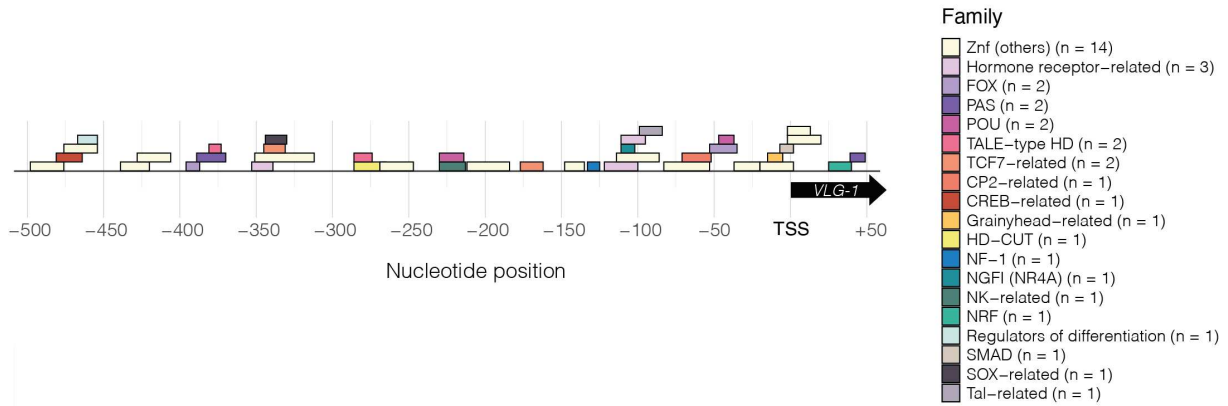
Female *Ae. aegypti* from both the *VLG-1^A* mutant line and the control line were injected with either dsRNA targeting *AaeVLG-2* or a dsRNA targeting the *Luciferase* gene as a negative control. Forty-eight hours after injection (on the day of the infectious bloodmeal), mosquitoes were offered an infectious bloodmeal containing 5×10^6 FFU/mL of DENV-1. Heads were collected on day 7 after the bloodmeal and processed for viral RNA quantification to evaluate infection prevalence (A) and viral loads (B). In parallel, whole unfed mosquitoes were collected on the day of the bloodmeal to quantify *AaeVLG-2* transcript RA (C) and transcript RB (D) abundance by RT-qPCR. Gene expression levels are normalized to the transcript abundance of the housekeeping gene encoding ribosomal protein S 17 (*RPS17*), and expressed as 2^{-dCt} , where $dCt = Ct_{Gene} - Ct_{RPS17}$. * $p < 0.05$; ** $p < 0.01$; *** $p < 0.001$ (Mann-Whitney's test for gene knockdown efficiency and viral loads, chi-squared test for prevalence).



Supplementary Figure S4. Overlap of differentially expressed genes in *VLG-1^A* mutants compared to wild-type controls on days 5 and 9 post bloodmeal. Venn diagrams show the number of up-regulated (A, C) and down-regulated (B, D) differentially expressed genes shared between experimental conditions on day 5 (A-B) and day 9 (C-D) post bloodmeal.






Supplementary Figure S5. Volcano plots of differentially expressed genes in *VLG-1 Δ* mutants compared to wild-type controls in the DENV-exposed condition. Statistical significance of the difference in gene expression between mutants and controls (adjusted for multiple testing) is shown as a function of the \log_2 -transformed fold change in expression. Genes that are significantly up-regulated and down-regulated are shown in red and blue, respectively. Comparisons were performed separately by tissue ((A, C, E): midgut; (B, D, F): body) and timepoint ((A-B): day 2; (C-D): day 5; (E-F): day 9 post bloodmeal). When detected, *AAEL000200* was removed from the plot to avoid graphical distortion due to its extremely low expression in *VLG-1 Δ* mutants.



Supplementary Figure S6. Transcription factor binding motifs found in the *Ae. aegypti* *VLG-1* promoter sequence. Motif hits identified and classified per transcription factor family in the promoter region (500 bp upstream and 50 bp downstream of the *VLG-1* transcription start site (TSS) (TSS coordinates: chr3:215,597,712). Nucleotide position is indicated relative to the TSS. The Znf (others) category includes the “Other with up to three adjacent zinc fingers”, “More than 3 adjacent zinc fingers” and “Multiple dispersed zinc fingers” transcription factor families. The “Hormone-receptor related” category includes the “Steroid hormone receptors”, “Thyroid hormone receptor-related” and “RXR-related receptors” families. The number of identified motifs is indicated for each motif category.

SUPPLEMENTARY TABLES

Supplementary Table 1. Proposed updated designation of *Vago* and *Vago*-like genes.

Species	Previous designation	New proposed designation	Refs
 <i>Drosophila melanogaster</i>	<i>DmVago</i> (CG2081)	<i>DmVago</i> (CG2081)	[25]
	CG14132	<i>DmVLG</i> (CG14132)	-
 <i>Culex quinquefasciatus</i>	<i>CxVago1</i> (CQUJHB003889)	<i>CxVLG-1</i> (CQUJHB003889)	[26,27]
 <i>Aedes aegypti</i>	<i>AaeVago1</i> (AAEL000200)	<i>AaeVLG-1</i> (AAEL000200)	[28]
	<i>AaeVago2</i> (AAEL000165)	<i>AaeVLG-2</i> (AAEL000165)	[28]

Supplementary Table 2. Vago-like gene homologs used in the gene phylogeny.

Locus ID	Species	Taxa id	Genomic_nucleotide_accession.version	Sequence ID	Family	SubFamily	group
LOC5570039	<i>Aedes aegypti</i>	7159	NC_035109.1	NC_035109.1_cds_XP_001658929.1_4926	Culicidae	Culicinae	B
LOC5570040	<i>Aedes aegypti</i>	7159	NC_035109.1	NC_035109.1_cds_XP_001658930.1_4928	Culicidae	Culicinae	A
LOC109400458	<i>Aedes albopictus</i>	7160	NC_085138.1	NC_085138.1_cds_XP_029709764.1_5850	Culicidae	Culicinae	B
LOC115253693	<i>Aedes albopictus</i>	7160	NC_085138.1	NC_085138.1_cds_XP_062715345.1_5797	Culicidae	Culicinae	B
LOC115264547	<i>Aedes albopictus</i>	7160	NC_085138.1	NC_085138.1_cds_XP_029724200.2_5800	Culicidae	Culicinae	A
LOC120901461	<i>Anopheles arabiensis</i>	7173	NC_053518.1	NC_053518.1_cds_XP_040165364.1_4462	Culicidae	Anophelinae	B
LOC120901758	<i>Anopheles arabiensis</i>	7173	NC_053518.1	NC_053518.1_cds_XP_040165919.1_4461	Culicidae	Anophelinae	B
LOC120904171	<i>Anopheles arabiensis</i>	7173	NC_053518.1	NC_053518.1_cds_XP_040169915.1_4463	Culicidae	Anophelinae	B
LOC120959656	<i>Anopheles coluzzii</i>	1518534	NC_064671.1	NC_064671.1_cds_XP_040234707.2_4268	Culicidae	Anophelinae	B
LOC131264480	<i>Anopheles coustani</i>	139045	NC_071289.1	NC_071289.1_cds_XP_058122762.1_3080	Culicidae	Anophelinae	B
LOC131269784	<i>Anopheles coustani</i>	139045	NC_071289.1	NC_071289.1_cds_XP_058128284.1_136	Culicidae	Anophelinae	B
LOC128274233	<i>Anopheles cruzii</i>	68878	NC_069143.1	NC_069143.1_cds_XP_052868316.1_116	Culicidae	Anophelinae	B
LOC125956039	<i>Anopheles darlingi</i>	43151	NC_064873.1	NC_064873.1_cds_XP_049543457.1_501	Culicidae	Anophelinae	B
LOC4578297	<i>Anopheles gambiae</i>	7165	NC_064602.1	NC_064602.1_cds_XP_001238104.2_5216	Culicidae	Anophelinae	B
LOC126561500	<i>Anopheles maculipalpis</i>	1496333	NC_064870.1	NC_064870.1_cds_XP_050073643.1_391	Culicidae	Anophelinae	B
LOC128712963	<i>Anopheles marshallii</i>	1521116	NC_071325.1	NC_071325.1_cds_XP_053663807.1_1003	Culicidae	Anophelinae	B
LOC121597485	<i>Anopheles merus</i>	30066	NC_054084.1	NC_054084.1_cds_XP_041779213.1_4853	Culicidae	Anophelinae	B
LOC128729155	<i>Anopheles niti</i>	185578	NC_071293.1	NC_071293.1_cds_XP_053678784.1_673	Culicidae	Anophelinae	B
LOC118505143	<i>Anopheles stephensi</i>	30069	NC_050201.1	NC_050201.1_cds_XP_035896397.1_769	Culicidae	Anophelinae	B
LOC134219609	<i>Armigeres subulbatus</i>	124917	NC_085141.1	NC_085141.1_cds_XP_062554379.1_5609	Culicidae	Culicinae	A
LOC134219610	<i>Armigeres subulbatus</i>	124917	NC_085141.1	NC_085141.1_cds_XP_062554381.1_5607	Culicidae	Culicinae	B
LOC120416670	<i>Culex pipiens pallens</i>	42434	NC_068938.1	NC_068938.1_cds_XP_039434419.1_5341	Culicidae	Culicinae	B
LOC120416672	<i>Culex pipiens pallens</i>	42434	NC_068938.1	NC_068938.1_cds_XP_039434421.1_5342	Culicidae	Culicinae	B
LOC119767415	<i>Culex quinquefasciatus</i>	7176	NC_051862.1	NC_051862.1_cds_XP_038111890.1_4281	Culicidae	Culicinae	B
LOC6031460	<i>Culex quinquefasciatus</i>	7176	NC_051862.1	NC_051862.1_cds_XP_001842264.1_4279	Culicidae	Culicinae	A
LOC6042215	<i>Culex quinquefasciatus</i>	7176	NC_051863.1	NC_051863.1_cds_XP_001851356.2_1354	Culicidae	Culicinae	B
LOC117571568	<i>Drosophila albomicans</i>	7291	NC_047629.2	NC_047629.2_cds_XP_034109668.1_6313	Drosophilidae	Drosophilinae	C
LOC6507152	<i>Drosophila ananassae</i>	7217	NC_057928.1	NC_057928.1_cds_XP_001956579.2_3507	Drosophilidae	Drosophilinae	C
LOC108613639	<i>Drosophila arizonae</i>	7263	NW_017127684.1	NW_017127684.1_cds_XP_017862695.1_2490	Drosophilidae	Drosophilinae	C
LOC108124169	<i>Drosophila bipunctinata</i>	42026	NW_025063860.1	NW_025063860.1_cds_XP_017095220.2_1735	Drosophilidae	Drosophilinae	C
LOC108599062	<i>Drosophila busckii</i>	30019	NC_046606.1	NC_046606.1_cds_XP_017841331.1_246	Drosophilidae	Drosophilinae	C
LOC108113944	<i>Drosophila eugracilis</i>	29029	NW_024573038.1	NW_024573038.1_cds_XP_017080144.1_1410	Drosophilidae	Drosophilinae	C
LOC6558867	<i>Drosophila grimshawi</i>	7222	NW_025063240.1	NW_025063240.1_cds_XP_001984323.1_1790	Drosophilidae	Drosophilinae	C
LOC117580089	<i>Drosophila guanche</i>	7266	NW_022995744.1	NW_022995744.1_cds_XP_034122233.1_1073	Drosophilidae	Drosophilinae	C
LOC111592799	<i>Drosophila hydei</i>	7224	NW_022045643.1	NW_022045643.1_cds_XP_023160974.2_1719	Drosophilidae	Drosophilinae	C
LOC117788884	<i>Drosophila innubila</i>	198719	NW_022995376.1	NW_022995376.1_cds_XP_034483707.1_2069	Drosophilidae	Drosophilinae	C
LOC108073886	<i>Drosophila kikkawai</i>	30033	NW_024571631.1	NW_024571631.1_cds_XP_017021160.1_246	Drosophilidae	Drosophilinae	C
LOC108151958	<i>Drosophila miranda</i>	7229	NC_046674.1	NC_046674.1_cds_XP_017136386.1_158	Drosophilidae	Drosophilinae	C
50290	<i>Drosophila melanogaster</i>	7227	NM_001104116	NM_001104116.3_cds_NP_001097586.1_1	Drosophilidae	Drosophilinae	C
LOC6583183	<i>Drosophila mojavensis</i>	7230	NW_025318899.1	NW_025318899.1_cds_XP_002008859.1_3620	Drosophilidae	Drosophilinae	C
LOC132792566	<i>Drosophila nasuta</i>	42062	NC_083457.1	NC_083457.1_cds_XP_060657976.1_5750	Drosophilidae	Drosophilinae	C
LOC108651886	<i>Drosophila navojoa</i>	7232	NW_022045982.1	NW_022045982.1_cds_XP_017957304.1_13	Drosophilidae	Drosophilinae	C
LOC111076754	<i>Drosophila obscura</i>	7282	NW_024542769.1	NW_024542769.1_cds_XP_022226371.1_179	Drosophilidae	Drosophilinae	C
LOC6600482	<i>Drosophila persimilis</i>	7234	NW_020825336.1	NW_020825336.1_cds_XP_002025673.1_156	Drosophilidae	Drosophilinae	C
LOC4812122	<i>Drosophila pseudoobscura</i>	7237	NC_046683.1	NC_046683.1_cds_XP_001352791.2_9098	Drosophilidae	Drosophilinae	C
LOC120449979	<i>Drosophila santomea</i>	129105	NC_053018.2	NC_053018.2_cds_XP_039488622.1_2487	Drosophilidae	Drosophilinae	C
LOC110178951	<i>Drosophila serrata</i>	7274	NW_018366417.1	NW_018366417.1_cds_XP_020801911.1_214	Drosophilidae	Drosophilinae	C
LOC117895078	<i>Drosophila subobscura</i>	7241	NC_048532.1	NC_048532.1_cds_XP_034658358.1_1098	Drosophilidae	Drosophilinae	C
LOC133843618	<i>Drosophila sulfurigaster albostrigata</i>	89887	NC_084883.1	NC_084883.1_cds_XP_062133231.1_5928	Drosophilidae	Drosophilinae	C
LOC6645467	<i>Drosophila willistoni</i>	7260	NW_025814056.1	NW_025814056.1_cds_XP_002068102.1_551	Drosophilidae	Drosophilinae	C
LOC131436079	<i>Malaya genurostris</i>	325434	NC_080572.1	NC_080572.1_cds_XP_058460526.1_4332	Culicidae	Culicinae	B
LOC131436314	<i>Malaya genurostris</i>	325434	NC_080572.1	NC_080572.1_cds_XP_058460959.1_4330	Culicidae	Culicinae	A
LOC128735801	<i>Sabethes cyaneus</i>	53552	NC_071354.1	NC_071354.1_cds_XP_053686261.1_2994	Culicidae	Culicinae	A
LOC128738226	<i>Sabethes cyaneus</i>	53552	NC_071354.1	NC_071354.1_cds_XP_053689185.1_2993	Culicidae	Culicinae	B
LOC131690538	<i>Topomyia yanbarensis</i>	2498891	NC_080672.1	NC_080672.1_cds_XP_058832385.1_5074	Culicidae	Culicinae	A
LOC129768709	<i>Toxorhynchites rutilus septentrionalis</i>	329112	NC_073745.1	NC_073745.1_cds_XP_055626488.1_5181	Culicidae	Culicinae	B
LOC129768710	<i>Toxorhynchites rutilus septentrionalis</i>	329112	NC_073745.1	NC_073745.1_cds_XP_055626489.1_5180	Culicidae	Culicinae	A
LOC129744816	<i>Uranotaenia lowii</i>	190385	NC_073692.1	NC_073692.1_cds_XP_055593507.1_6878	Culicidae	Culicinae	A
LOC129748614	<i>Uranotaenia lowii</i>	190385	NC_073692.1	NC_073692.1_cds_XP_055599252.1_9407	Culicidae	Culicinae	A
LOC129724442	<i>Wyeomyia smithii</i>	174621	NC_073695.1	NC_073695.1_cds_XP_055535337.1_6339	Culicidae	Culicinae	B
LOC129724443	<i>Wyeomyia smithii</i>	174621	NC_073695.1	NC_073695.1_cds_XP_055535338.1_6336	Culicidae	Culicinae	A
LOC129724444	<i>Wyeomyia smithii</i>	174621	NC_073695.1	NC_073695.1_cds_XP_055535339.1_6337	Culicidae	Culicinae	A

Supplementary Table 3. Results of dN/dS analysis in CODEML

model	likelihood	outgroup ω0	Vago1 ω1	Vago (Culicinae) ω2	Vago (Anophelinae) ω3	2Δℓ	pvalue	df	model description
M0	-7009,86928	0.12623							M0: null model assumes the same ω for all branches.
M1	-7004,40804	0.106562	0.174765			10,922466	0.0009500506	1	M1: foreground group is only Vago1
M2	-7002,76217	0.0853288	0.17507	0.120153		14,214216	0.0008192609	2	M2: 2 foreground groups Vago1 and Vago Culicinae and Anophelinae
M3	-7001,25308	0.0878059	0.175461	0.149161	0.0972423	17,232404	0.0006330647	3	M3: 3 foreground groups (Vago1, Vago Culicinae and Vago Anophelinae)
# alpha critical value = 3.841459									

Supplementary Table 4. GO terms

GO term	GO ID	Functional annotation
biosynthetic process	GO:0009058	metabolism
calcium ion transmembrane transport	GO:0070588	ion transport
carbohydrate metabolic process	GO:0005975	metabolism
cell adhesion	GO:0007155	
cellular oxidant detoxification	GO:0098869	response to oxidative stress
cytoskeleton organization	GO:0007010	
dephosphorylation	GO:0016311	protein phosphorylation
DNA duplex unwinding	GO:0032508	
DNA replication	GO:0006260	
electron transport chain	GO:0022900	
fatty acid biosynthetic process	GO:0006633	metabolism
fatty acid metabolic process	GO:0006631	metabolism
G protein-coupled receptor signaling pathway	GO:0007186	
GO:0055114 NONAME - redox processes	GO:0055114 NONAME	response to oxidative stress
lipid metabolic process	GO:0006629	metabolism
lipid transport	GO:0006869	transport
metabolic process	GO:0008152	metabolism
methylation	GO:0032259	
microtubule-based movement	GO:0007018	
monoatomic ion transport	GO:0006811	ion transport
negative regulation of endopeptidase activity	GO:0010951	
peptidyl-tyrosine dephosphorylation	GO:0035335	protein phosphorylation
peptidyl-tyrosine phosphorylation	GO:0018108	protein phosphorylation
phosphorylation	GO:0016310	protein phosphorylation
potassium ion transport	GO:0006813	ion transport
protein folding	GO:0006457	

protein glycosylation	GO:0006486	
protein phosphorylation	GO:0006468	protein phosphorylation
protein transport	GO:0015031	transport
proteolysis	GO:0006508	
proton motive force-driven ATP synthesis	GO:0015986	
proton transmembrane transport	GO:1902600	
response to oxidative stress	GO:0006979	response to oxidative stress
ribosome biogenesis	GO:0042254	translation
RNA processing	GO:0006396	translation
rRNA processing	GO:0006364	translation
translation	GO:0006412	translation
translational initiation	GO:0006413	translation
transmembrane transport	GO:0055085	transport
tRNA processing	GO:0008033	translation

Supplementary Table 5. Oligonucleotide sequences.

Oligo name	Target gene	Application	Sequence (5'-3')
VAGOs _g _x 1_30rev_F	AAEL000200	sgRNA	GAAATTAATACGACTCACTATAGGTCGCGTCGTGA CTTTCGCGCGTTTTAGAGCTAGAAAT
VAGOs _g _x 3_67rev_F	AAEL000200	sgRNA	GAAATTAATACGACTCACTATAGGTATATTTGTGAC AACACTCCGTTTTAGAGCTAGAAATAGC
VAGOs _g _x 2_6rev_F	AAEL000200	sgRNA	GAAATTAATACGACTCACTATAGGTTGGATCGTAG CACTTCCCAGTTTTAGAGCTAGAAATAGC
Sequencing primer F	AAEL000200	sequencing	AGTCGGCCATCTTAGG
VAGO_35H A_RT		repair template for gene editing	GCATCAATTTACACTTAGTTCTAGTGGAGCCTGCC GTGTTGTCACAAATATAAATGTGTACACGATGGAA
Genotyping primer F	AAEL000200	PCR	TCCGGTATTATTGGCTTTGTGC
Genotyping primer R	AAEL000200	PCR	ACTCACTTTTCCATCGTGTACAC
NS5F-VR- D1Thai	NS5 DENV1 KDH0026A	qPCR	GGAAGGAGAAGGACTCCACA
NS5R-VR- D1Thai	NS5 DENV1 KDH0026A	qPCR	ATCCTTGTATCCCATCCGGCT

DSQ1-VR	DENV1 KDH0026A	qPCR probe	5'-FAM-CTCAGAGACATATCAAAGATTCCAGGG- BHQ1-3'
ZIKV-Af-for	NS1 ZIKV African strain	qPCR	GTCGCTGTCCAACACAAG
ZIKV-Af-for	NS1 ZIKV African strain	qPCR	CACCAGTGTTCTCTTGACAGACAT
ZIKV-Af- probe	NS1 ZIKV African strain	qpCR probe	6FAM/AGCCTACCT/ZEN/TGACAAGCAATCAGACA CTCAA/ 3'IABkFQ
gBlock Zika	ZIKV African strain	Standards for qPCR	GAGGCATCAATATCGGACATGGCTTCGGACAGTC GCTGTCCAACACAAGGTGAAGCCTACCTTGACAA GCAATCAGACACTCAATATGTCTGCAAGAGAACA CTGGTGGATAGAGGTTGGGGAAATGGGTGTGGA CT
RPS17- EC1- qPCRfor	AAEL004175	qPCR	AAGAAGTGGCCATCATTCCA
RPS17- EC1- qPCRrev	AAEL004175	qPCR	GGTCTCCGGGTCGACTTC
Vago1- EC1- qPCRfor	AAEL000200	qPCR	AAATCCATTCTGGTGCTTG
Vago1- EC1- qPCRrev	AAEL000200	qPCR	AACACTCCGGGTAATCCTTG
T7-VAGO2- EC-for	AAEL000165	dsRNA synthesis	GCCCGACGCgatcaagccggcaatATGAG
T7-VAGO2- EC-rev	AAEL000165	dsRNA synthesis	CGCCTCGGCTGGATTGAGAAATCCGTTCC
Vago2- EC2-for	AAEL000165	qPCR	gatcaagccggcaatATGAG
Vago2- EC2-rev	AAEL000165	qPCR	AGCATTACCCGGGAAAATC
T7-tag for		dsRNA synthesis	taatacgactcactatagggGCCCGACGC
T7-tag rev		dsRNA synthesis	taatacgactcactatagggCGCCTCGGC

Supplementary Table 6: Hits for transcription factor DNA binding motifs from HOCOMOCO H12CORE in the promoter of *VLG-1*. Start and end positions of motifs are indicated relative to *VLG-1* transcription start site.

TF	Start	End	Strand	TF Family	p-value	Corrected p-value
ZBTB49	-498	-476	-	More than 3 adjacent zinc fingers	3.311e-5	0.04778
CREM	-481	-464	+	CREB-related	1.312e-5	0.01893
ZNF766	-476	-454	-	More than 3 adjacent zinc fingers	1.718e-5	0.02479
MEF2B	-467	-454	+	Regulators of differentiation	1.841e-5	0.02657
ZNF615	-439	-420	-	More than 3 adjacent zinc fingers	1.510e-5	0.02179
ZNF26	-428	-406	-	More than 3 adjacent zinc fingers	2.999e-5	0.04328
FOXP3	-396	-387	-	FOX	2.624e-5	0.03786
NPAS2	-389	-370	+	PAS	2.636e-5	0.03804
IRX1	-381	-373	-	TALE-type HD	2.089e-5	0.03014
CLOCK	-380	-370	-	PAS	2.489e-5	0.03592
NPAS2	-380	-370	+	PAS	2.636e-5	0.03804
PGR	-353	-339	+	Steroid hormone receptors	2.037e-5	0.02939
ZIK1	-351	-329	-	More than 3 adjacent zinc fingers	3.155e-5	0.04553
ZNF613	-350	-326	+	More than 3 adjacent zinc fingers	2.812e-6	0.00406
ZNF570	-348	-330	-	More than 3 adjacent zinc fingers	1.268e-6	0.00183
ZNF362	-348	-326	-	More than 3 adjacent zinc fingers	1.589e-5	0.02293
LEF1	-345	-331	+	TCF7-related	1.274e-5	0.01838
ZNF791	-345	-323	+	More than 3 adjacent zinc fingers	2.317e-5	0.03343
SOX17	-344	-330	+	SOX-related	5.754e-6	0.00830
ZNF362	-343	-321	-	More than 3 adjacent zinc fingers	1.995e-5	0.02879
ZNF585A	-343	-321	-	More than 3 adjacent zinc fingers	2.291e-5	0.03306
ZNF716	-342	-318	-	More than 3 adjacent zinc fingers	2.612e-5	0.03769
ZNF354A	-334	-312	+	More than 3 adjacent zinc fingers	1.352e-5	0.01951
ONECUT2	-286	-265	-	HD-CUT	2.163e-5	0.03121
MEIS1	-286	-274	-	TALE-type HD	2.410e-5	0.03478
ZNF432	-269	-247	+	More than 3 adjacent zinc fingers	3.013e-6	0.00435
POU2F2	-230	-218	-	POU	9.311e-7	0.00134
POU5F1B	-230	-214	+	POU	2.084e-6	0.00301
VENTX	-230	-213	-	NK-related	2.118e-5	0.03056
ZNF768	-212	-190	+	More than 3 adjacent zinc fingers	4.853e-6	0.00700
ZNF490	-206	-184	-	More than 3 adjacent zinc fingers	2.443e-6	0.00353
LEF1	-177	-163	+	TCF7-related	5.689e-6	0.00821
TCF7L2	-176	-165	+	TCF7-related	1.161e-6	0.00168
TCF7	-176	-162	-	TCF7-related	1.945e-6	0.00281
TCF7L1	-176	-165	+	TCF7-related	2.296e-6	0.00331
LEF1	-176	-165	+	TCF7-related	2.158e-5	0.03114
YY2	-148	-135	-	More than 3 adjacent zinc fingers	4.667e-6	0.00673
YY1	-147	-136	-	More than 3 adjacent zinc fingers	2.094e-5	0.03022
NFIB	-133	-125	+	NF-1	3.027e-5	0.04368
THRB	-122	-101	+	Thyroid hormone receptor-related	2.203e-5	0.03179

-CHAPTER 1-

ZNF558	-114	-90	+	More than 3 adjacent zinc fingers	2.692e-5	0.03885
NR2C2	-111	-100	+	RXR-related receptors	1.786e-5	0.02577
NR4A2	-111	-102	+	NGFI (NR4A)	2.051e-5	0.02960
NR2F2	-111	-100	+	RXR-related receptors	2.767e-5	0.03993
NR2F6	-110	-95	+	RXR-related receptors	1.368e-5	0.01974
NR2C1	-110	-95	+	RXR-related receptors	1.452e-5	0.02095
RARA	-110	-100	+	Thyroid hormone receptor-related	2.729e-5	0.03938
NR2C1	-110	-99	+	RXR-related receptors	3.342e-5	0.04823
TWIST1	-99	-84	-	Tal-related	5.000e-6	0.00722
MSC	-98	-87	-	Tal-related	2.312e-5	0.03336
TWIST2	-96	-87	+	Tal-related	5.224e-6	0.00754
ZBTB18	-96	-86	+	More than 3 adjacent zinc fingers	3.334e-5	0.04811
ZNF534	-83	-53	-	More than 3 adjacent zinc fingers	6.887e-6	0.00994
ZNF534	-82	-65	-	More than 3 adjacent zinc fingers	1.368e-5	0.01974
TFCP2L1	-71	-52	+	CP2-related	2.716e-5	0.03919
TFCP2L1	-60	-52	-	CP2-related	2.472e-5	0.03567
FOXB1	-53	-35	+	FOX	9.661e-6	0.01394
FOXC1	-53	-35	+	FOX	1.466e-5	0.02115
FOXA1	-50	-35	+	FOX	1.589e-5	0.02293
FOXA3	-49	-38	+	FOX	2.032e-5	0.02932
FOXA2	-47	-36	+	FOX	1.449e-5	0.02091
POU2F1	-47	-37	-	POU	1.538e-5	0.02219
POU5F1	-47	-37	-	POU	1.563e-5	0.02255
FOXA1	-47	-37	+	FOX	1.849e-5	0.02668
POU2F2	-47	-37	-	POU	2.228e-5	0.03215
FOXM1	-47	-36	+	FOX	2.710e-5	0.03911
ZSCAN1	-37	-20	-	Other with up to three adjacent zinc fingers	3.281e-5	0.04734
ZNF490	-20	2	-	More than 3 adjacent zinc fingers	8.147e-6	0.01176
GRHL2	-15	-5	-	Grainyhead-related	9.661e-6	0.01394
SMAD2	-7	2	+	SMAD	2.432e-5	0.03509
SMAD3	-6	2	-	SMAD	2.858e-5	0.04124
ZNF787	-2	13	+	Multiple dispersed zinc fingers	2.056e-5	0.02967
ZNF354A	-2	20	+	More than 3 adjacent zinc fingers	2.228e-5	0.03215
NRF1	25	40	-	NRF	1.466e-5	0.02115
NPAS4	39	49	-	PAS	1.067e-6	0.00154

REFERENCES

1. Pierson, T.C. and M.S. Diamond, *The continued threat of emerging flaviviruses*. Nat Microbiol, 2020. **5**(6): p. 796-812.
2. World Health Organization. *Dengue: Guidelines for Diagnosis, Treatment, Prevention and Control: New Edition* (2009).
3. Brady, O.J., et al., *Refining the global spatial limits of dengue virus transmission by evidence-based consensus*. PLoS Negl Trop Dis, 2012. **6**(8): p. e1760.
4. Bhatt, S., et al., *The global distribution and burden of dengue*. Nature, 2013. **496**(7446): p. 504-7.
5. Musso, D., A.I. Ko, and D. Baud, *Zika Virus Infection - After the Pandemic*. N Engl J Med, 2019. **381**(15): p. 1444-1457.
6. Kraemer, M.U., et al., *The global distribution of the arbovirus vectors Aedes aegypti and Ae. albopictus*. Elife, 2015. **4**: p. e08347.
7. Kraemer, M.U.G., et al., *Past and future spread of the arbovirus vectors Aedes aegypti and Aedes albopictus*. Nat Microbiol, 2019. **4**(5): p. 854-863.
8. Flores, H.A. and S.L. O'Neill, *Controlling vector-borne diseases by releasing modified mosquitoes*. Nat Rev Microbiol, 2018. **16**(8): p. 508-518.
9. Kean, J., et al., *Fighting Arbovirus Transmission: Natural and Engineered Control of Vector Competence in Aedes Mosquitoes*. Insects, 2015. **6**(1): p. 236-78.
10. Sigle, L.T. and E.A. McGraw, *Expanding the canon: Non-classical mosquito genes at the interface of arboviral infection*. Insect Biochem Mol Biol, 2019. **109**: p. 72-80.
11. Gubler, D.J., et al., *Variation in susceptibility to oral infection with dengue viruses among geographic strains of Aedes aegypti*. Am J Trop Med Hyg, 1979. **28**(6): p. 1045-52.
12. Salazar, M.I., et al., *Dengue virus type 2: replication and tropisms in orally infected Aedes aegypti mosquitoes*. BMC Microbiol, 2007. **7**: p. 9.
13. Franz, A.W., et al., *Tissue Barriers to Arbovirus Infection in Mosquitoes*. Viruses, 2015. **7**(7): p. 3741-67.
14. Hall, D.R., et al., *Mosquito immune cells enhance dengue and Zika virus dissemination in Aedes aegypti*. bioRxiv, 2024.
15. Leite, T., et al., *Distinct Roles of Hemocytes at Different Stages of Infection by Dengue and Zika Viruses in Aedes aegypti Mosquitoes*. Front Immunol, 2021. **12**: p. 660873.
16. Raquin, V. and L. Lambrechts, *Dengue virus replicates and accumulates in Aedes aegypti salivary glands*. Virology, 2017. **507**: p. 75-81.
17. Bronkhorst, A.W. and R.P. van Rij, *The long and short of antiviral defense: small RNA-based immunity in insects*. Curr Opin Virol, 2014. **7**: p. 19-28.
18. Mongelli, V. and M.C. Saleh, *Bugs Are Not to Be Silenced: Small RNA Pathways and Antiviral Responses in Insects*. Annu Rev Virol, 2016. **3**(1): p. 573-589.
19. Suzuki, Y., et al., *Non-retroviral Endogenous Viral Element Limits Cognate Virus Replication in Aedes aegypti Ovaries*. Curr Biol, 2020. **30**(18): p. 3495-3506 e6.
20. Rosendo Machado, S., T. van der Most, and P. Miesen, *Genetic determinants of antiviral immunity in dipteran insects - Compiling the experimental evidence*. Dev Comp Immunol, 2021. **119**: p. 104010.

21. Merklings, S.H. and R.P. van Rij, *Beyond RNAi: antiviral defense strategies in Drosophila and mosquito*. J Insect Physiol, 2013. **59**(2): p. 159-70.
22. Sim, S., N. Jupatanakul, and G. Dimopoulos, *Mosquito immunity against arboviruses*. Viruses, 2014. **6**(11): p. 4479-504.
23. Alonso-Palomares, L.A., et al., *Molecular Basis for Arbovirus Transmission by Aedes aegypti Mosquitoes*. Intervirology, 2018. **61**(6): p. 255-264.
24. Dostert, C., et al., *The Jak-STAT signaling pathway is required but not sufficient for the antiviral response of drosophila*. Nat Immunol, 2005. **6**(9): p. 946-53.
25. Deddouche, S., et al., *The DExD/H-box helicase Dicer-2 mediates the induction of antiviral activity in drosophila*. Nat Immunol, 2008. **9**(12): p. 1425-32.
26. Paradkar, P.N., et al., *Secreted Vago restricts West Nile virus infection in Culex mosquito cells by activating the Jak-STAT pathway*. Proc Natl Acad Sci U S A, 2012. **109**(46): p. 18915-20.
27. Paradkar, P.N., et al., *Dicer-2-dependent activation of Culex Vago occurs via the TRAF-Rel2 signaling pathway*. PLoS Negl Trop Dis, 2014. **8**(4): p. e2823.
28. Asad, S., R. Parry, and S. Asgari, *Upregulation of Aedes aegypti Vago1 by Wolbachia and its effect on dengue virus replication*. Insect Biochem Mol Biol, 2018. **92**: p. 45-52.
29. Labropoulou, V., et al., *Single domain von Willebrand factor type C "cytokines" and the regulation of the stress/immune response in insects*. Arch Insect Biochem Physiol, 2024. **115**(1): p. e22071.
30. Ruckert, C., et al., *Antiviral responses of arthropod vectors: an update on recent advances*. Virusdisease, 2014. **25**(3): p. 249-60.
31. Wang, H., G. Smagghe, and I. Meeus, *The Single von Willebrand factor C-domain protein (SVC) coding gene is not involved in the hymenoptaecin upregulation after Israeli acute paralysis virus (IAPV) injection in the bumblebee Bombus terrestris*. Dev Comp Immunol, 2018. **81**: p. 152-155.
32. Niu, J., I. Meeus, and G. Smagghe, *Differential expression pattern of Vago in bumblebee (Bombus terrestris), induced by virulent and avirulent virus infections*. Sci Rep, 2016. **6**: p. 34200.
33. Wang, H., G. Smagghe, and I. Meeus, *The role of a single gene encoding the Single von Willebrand factor C-domain protein (SVC) in bumblebee immunity extends beyond antiviral defense*. Insect Biochem Mol Biol, 2017. **91**: p. 10-20.
34. Gao, J., et al., *Interferon functional analog activates antiviral Jak/Stat signaling through integrin in an arthropod*. Cell Rep, 2021. **36**(13): p. 109761.
35. Li, C., et al., *Activation of Vago by interferon regulatory factor (IRF) suggests an interferon system-like antiviral mechanism in shrimp*. Sci Rep, 2015. **5**: p. 15078.
36. Hixson, B., et al., *A transcriptomic atlas of Aedes aegypti reveals detailed functional organization of major body parts and gut regional specializations in sugar-fed and blood-fed adult females*. Elife, 2022. **11**.
37. Lykke-Andersen, S. and T.H. Jensen, *Nonsense-mediated mRNA decay: an intricate machinery that shapes transcriptomes*. Nat Rev Mol Cell Biol, 2015. **16**(11): p. 665-77.
38. Gloria-Soria, A., D.E. Brackney, and P.M. Armstrong, *Saliva collection via capillary method may underestimate arboviral transmission by mosquitoes*. Parasit Vectors, 2022. **15**(1): p. 103.

39. Foo, J., et al., *Mitochondria-mediated oxidative stress during viral infection*. Trends Microbiol, 2022. **30**(7): p. 679-692.
40. Zhang, Z., L. Rong, and Y.P. Li, *Flaviviridae Viruses and Oxidative Stress: Implications for Viral Pathogenesis*. Oxid Med Cell Longev, 2019. **2019**: p. 1409582.
41. Gullberg, R.C., et al., *Oxidative stress influences positive strand RNA virus genome synthesis and capping*. Virology, 2015. **475**: p. 219-29.
42. Camini, F.C., et al., *Implications of oxidative stress on viral pathogenesis*. Arch Virol, 2017. **162**(4): p. 907-917.
43. Olagnier, D., et al., *Cellular oxidative stress response controls the antiviral and apoptotic programs in dengue virus-infected dendritic cells*. PLoS Pathog, 2014. **10**(12): p. e1004566.
44. Oliveira, J.H.M., et al., *Catalase protects Aedes aegypti from oxidative stress and increases midgut infection prevalence of Dengue but not Zika*. PLoS Negl Trop Dis, 2017. **11**(4): p. e0005525.
45. Talyuli, O.A.C., et al., *The Aedes aegypti peritrophic matrix controls arbovirus vector competence through HPx1, a heme-induced peroxidase*. PLoS Pathog, 2023. **19**(2): p. e1011149.
46. Estevez-Castro, C.F., et al., *Neofunctionalization driven by positive selection led to the retention of the loqs2 gene encoding an Aedes specific dsRNA binding protein*. BMC Biol, 2024. **22**(1): p. 14.
47. David, K.T., J.R. Oaks, and K.M. Halanych, *Patterns of gene evolution following duplications and speciations in vertebrates*. PeerJ, 2020. **8**: p. e8813.
48. Birchler, J.A. and H. Yang, *The multiple fates of gene duplications: Deletion, hypofunctionalization, subfunctionalization, neofunctionalization, dosage balance constraints, and neutral variation*. Plant Cell, 2022. **34**(7): p. 2466-2474.
49. Shaw, W.R. and F. Catteruccia, *Vector biology meets disease control: using basic research to fight vector-borne diseases*. Nat Microbiol, 2019. **4**(1): p. 20-34.
50. Jumper, J., et al., *Highly accurate protein structure prediction with AlphaFold*. Nature, 2021. **596**(7873): p. 583-589.
51. Varadi, M., et al., *AlphaFold Protein Structure Database: massively expanding the structural coverage of protein-sequence space with high-accuracy models*. Nucleic Acids Res, 2022. **50**(D1): p. D439-D444.
52. Fansiri, T., et al., *Genetic mapping of specific interactions between Aedes aegypti mosquitoes and dengue viruses*. PLoS Genet, 2013. **9**(8): p. e1003621.
53. Aubry, F., et al., *Recent African strains of Zika virus display higher transmissibility and fetal pathogenicity than Asian strains*. Nat Commun, 2021. **12**(1): p. 916.
54. Fontaine, A., et al., *Excretion of dengue virus RNA by Aedes aegypti allows non-destructive monitoring of viral dissemination in individual mosquitoes*. Sci Rep, 2016. **6**: p. 24885.
55. Lequime, S., et al., *Genetic Drift, Purifying Selection and Vector Genotype Shape Dengue Virus Intra-host Genetic Diversity in Mosquitoes*. PLoS Genet, 2016. **12**(6): p. e1006111.
56. Kistler, K.E., L.B. Vosshall, and B.J. Matthews, *Genome engineering with CRISPR-Cas9 in the mosquito Aedes aegypti*. Cell Rep, 2015. **11**(1): p. 51-60.
57. Concordet, J.P. and M. Haeussler, *CRISPOR: intuitive guide selection for CRISPR/Cas9 genome editing experiments and screens*. Nucleic Acids Res, 2018. **46**(W1): p. W242-W245.

58. Jasinskiene, N., J. Juhn, and A.A. James, *Microinjection of A. aegypti embryos to obtain transgenic mosquitoes*. J Vis Exp, 2007(5): p. 219.
59. Ranwez, V., et al., *MACSE v2: Toolkit for the Alignment of Coding Sequences Accounting for Frameshifts and Stop Codons*. Mol Biol Evol, 2018. **35**(10): p. 2582-2584.
60. Minh, B.Q., et al., *IQ-TREE 2: New Models and Efficient Methods for Phylogenetic Inference in the Genomic Era*. Mol Biol Evol, 2020. **37**(5): p. 1530-1534.
61. Letunic, I. and P. Bork, *Interactive Tree Of Life (iTOL) v5: an online tool for phylogenetic tree display and annotation*. Nucleic Acids Res, 2021. **49**(W1): p. W293-W296.
62. Yang, Z., *PAML 4: phylogenetic analysis by maximum likelihood*. Mol Biol Evol, 2007. **24**(8): p. 1586-91.
63. Alvarez-Carretero, S., P. Kapli, and Z. Yang, *Beginner's Guide on the Use of PAML to Detect Positive Selection*. Mol Biol Evol, 2023. **40**(4).
64. Yang, Z. and R. Nielsen, *Synonymous and nonsynonymous rate variation in nuclear genes of mammals*. J Mol Evol, 1998. **46**(4): p. 409-18.
65. Yang, Z., *On the best evolutionary rate for phylogenetic analysis*. Syst Biol, 1998. **47**(1): p. 125-33.
66. Raquin, V., et al., *Individual co-variation between viral RNA load and gene expression reveals novel host factors during early dengue virus infection of the Aedes aegypti midgut*. PLoS Negl Trop Dis, 2017. **11**(12): p. e0006152.
67. Martin, M., *Cutadapt removes adapter sequences from high-throughput sequencing reads*. 2011, 2011. **17**(1): p. 3.
68. Patro, R., et al., *Salmon provides fast and bias-aware quantification of transcript expression*. Nat Methods, 2017. **14**(4): p. 417-419.
69. Dobin, A., et al., *STAR: ultrafast universal RNA-seq aligner*. Bioinformatics, 2013. **29**(1): p. 15-21.
70. Liao, Y., G.K. Smyth, and W. Shi, *featureCounts: an efficient general purpose program for assigning sequence reads to genomic features*. Bioinformatics, 2013. **30**(7): p. 923-930.
71. Team, R.C., *R: A language and environment for statistical computing*. MSOR connections, 2014. **1**.
72. Sonesson, C., M.I. Love, and M.D. Robinson, *Differential analyses for RNA-seq: transcript-level estimates improve gene-level inferences*. F1000Research, 2015. **4**.
73. Love, M.I., W. Huber, and S. Anders, *Moderated estimation of fold change and dispersion for RNA-seq data with DESeq2*. Genome Biol, 2014. **15**(12): p. 550.
74. Benjamini, Y. and Y. Hochberg, *Controlling the False Discovery Rate: A Practical and Powerful Approach to Multiple Testing*. Journal of the Royal Statistical Society: Series B (Methodological), 2018. **57**(1): p. 289-300.
75. Gene Ontology, C., et al., *The Gene Ontology knowledgebase in 2023*. Genetics, 2023. **224**(1).
76. Dickson, L.B., et al., *Exome-wide association study reveals largely distinct gene sets underlying specific resistance to dengue virus types 1 and 3 in Aedes aegypti*. PLoS Genet, 2020. **16**(5): p. e1008794.

-CHAPTER 1-

77. Vorontsov, I.E., et al., *HOCOMOCO in 2024: a rebuild of the curated collection of binding models for human and mouse transcription factors*. *Nucleic Acids Res*, 2024. **52**(D1): p. D154-D163.
78. Barrett, T., et al., *NCBI GEO: archive for functional genomics data sets--update*. *Nucleic Acids Res*, 2013. **41**(Database issue): p. D991-5.

-CHAPTER 2-

Cytochrome *P450 4g15* polymorphism mediates dengue virus susceptibility in a field-derived *Aedes aegypti* population

Sarah H. Merklings, **Elodie Couderc**, Anna Crist, Natapong Jupatanakul, Morgane Lavina, David Hardy, Myriam Burckbuchler, Isabelle Moltini-Conclois, Albin Fontaine, Odile Sismeiro, Rachel Legendre, Hugo Varet, Davy Jiolle, Christophe Paupy, Eric Marois, Louis Lambrechts

CHAPTER 2: Cytochrome *P450 4g15* polymorphism mediates dengue virus susceptibility in a field-derived *Aedes aegypti* population

Sarah H. Merklings¹, **Elodie Couderc**^{1,2}, Anna B. Crist¹, Natapong Jupatanakul^{1,3}, Morgane Lavina¹, David Hardy⁴, Myriam Burckbuchler⁵, Isabelle Moltini-Conclois^{1,9}, Albin Fontaine^{1,6}, Odile Sismeiro^{7,8}, Rachel Legendre⁸, Hugo Varet⁸, Davy Jiolle^{1,9}, Christophe Paupy⁹, Eric Marois⁵, Louis Lambrechts¹

¹Institut Pasteur, Université Paris Cité, CNRS UMR2000, Insect-Virus Interactions Unit, 75015 Paris, France

²Sorbonne Université, Collège Doctoral, 75005 Paris, France

³National Center for Genetic Engineering and Biotechnology (BIOTEC), Pathum Thani, 12120, Thailand

⁴Institut Pasteur, Université Paris Cité, Histopathology Platform, Paris, France

⁵CNRS UPR9022, INSERM U1257, Université de Strasbourg, France

⁶Unité Parasitologie et Entomologie, Département Microbiologie et Maladies Infectieuses, Institut de Recherche Biomédicale des Armées (IRBA), Marseille, France

⁷Institut Pasteur, Université Paris Cité, Biology of Gram-positive Pathogens Unit, 75015 Paris, France

⁸Institut Pasteur, Université Paris Cité, Bioinformatics and Biostatistics Hub, 75015 Paris, France

⁹MIVEGEC, IRD, CNRS, Université de Montpellier, Montpellier, France

This chapter is part of a larger study, “Polymorphisms in the cytochrome P450 4g15 mediate dengue virus susceptibility in a Aedes aegypti field-derived population”, Merklings et al. (manuscript in preparation). The approaches and data described here, to the exception of Figure 1 data, reflect E.C.'s involvement in the project.

ABSTRACT

This study explores the natural resistance phenotype of an *Aedes aegypti* mosquito population from Bakoumba, Gabon, against dengue virus serotype 1 (DENV-1), which led to the discovery of cytochrome *P450 4g15* as a novel antiviral factor. We showed that *P450 4g15* expression is transiently induced in the midgut in response to bloodmeal ingestion, and its subcellular protein localization in midgut cells is affected upon DENV exposure. Using RNA-FISH imaging in midgut tissues as well as midgut-specific overexpression lines, we demonstrated the correlation between *P450 4g15* expression levels and DENV infection success. Finally, we showed that *P450 4g15* expression level is determined by genetic variation in its promoter

sequence. Overall, our study identifies genetic polymorphisms in the promoter of a newly identified non-canonical antiviral factor that drive resistance to DENV during early steps of midgut infection. This work demonstrates how the remarkable genetic diversity of wild mosquito populations can be leveraged to elucidate the molecular mechanisms underlying vector competence.

INTRODUCTION

I- Natural resistance phenotype leads to identification of a novel antiviral factor

Aedes aegypti (*Ae. aegypti*) mosquitoes are major vectors of several arthropod-borne viruses (arboviruses) such as dengue virus (DENV) [1]. The past five decades have witnessed a considerable emergence of arboviral diseases, including about 100 million symptomatic DENV infections reported in the human population every year [2]. DENV consists of four serotypes (DENV-1, -2, -3 and -4) that belong to the *Flavivirus* genus [3].

Mosquito infection occurs when a female mosquito feeds on a viremic human and is followed by systemic infection of the arthropod and virus transmission to another human host during a subsequent bloodmeal. Infection of the midgut is the primary critical step of DENV infection of mosquitoes. At the level of individual mosquitoes, infection outcome is binary (infection either takes hold or fails), viral dose-dependent, and determined within the first 48 hours after the infectious bloodmeal [4-8].

Although the biology of arboviruses is characterized by a triangular network of interactions between the virus, its vertebrate hosts and its arthropod vectors, research in arbovirology until now has been mostly focused on viral infection in mammalian hosts. More specifically, the molecular mechanisms underlying vector susceptibility or resistance are largely unknown and represent a major knowledge gap in arbovirus biology.

Major innate immune pathways have been identified in mosquitoes, but our knowledge of their antiviral responses remains incomplete. The transcriptomic landscape of arbovirus-infected mosquito cells has revealed that a wide variety of pathways responds to viral infections [9-12]. Among these dysregulated genes are hundreds of potential non-canonical pro- and antiviral factors.

Mosquito populations vary in their susceptibility to arboviruses even within a competent species [5]. In addition, DENV susceptibility in *Ae. aegypti* is virus strain-specific [13-15]. For example, a field-derived *Ae. aegypti* population from Bakoumba, Gabon was significantly more resistant to infection with a DENV-1 strain than with a DENV-3 strain [15]. Furthermore, the

outcome of infection generally depends on the specific pairing of the mosquito and the virus strains [13-15]. Since both *Ae. aegypti* and DENV are genetically diverse [3, 16], such genetic specificity makes it difficult to predict the outcome of the interaction but provides great opportunities to discover novel facets of the mosquito response to viral infections.

Given the lack of an effective vaccine and the limitations of insecticide-based vector control strategies, novel approaches based on engineering mosquitoes that cannot transmit viruses are being investigated. These approaches require identification of optimal target genes for modification and natural resistance factors are promising candidates. However, it is important to distinguish virus strain-specific from universal resistance factors. The previous study on DENV strain-specific resistance in the *Ae. aegypti* population from Bakoumba found that among the top candidate genes associated with either DENV-1 or DENV-3 resistance, only about one third were shared [15].

The natural DENV-1 resistance phenotype observed in the Bakoumba population [15] was manifested by a DENV-1 infection prevalence of only 50% while the same infectious dose resulted in 100% infection with DENV-3. A mere difference of infectivity between the DENV-1 and DENV-3 strains was ruled out with another *Ae. aegypti* population from Cairns, Australia that was 100% infected with both virus strains (Figure 1A).

The establishment of the DENV-1-specific resistance phenotype was observed within 48 hours after the bloodmeal, suggesting that the underlying mechanism occurred in the midgut, prior to systemic viral dissemination in the mosquito body (Figure 1B-C).

To dissect this resistance phenotype, a midgut-specific transcriptome analysis was performed by RNA-sequencing on individual midguts. Female mosquitoes were offered an infectious DENV-1-containing bloodmeal, and 24 and 48 hours later, we dissected midguts and sorted virus-positive (*i.e.*, susceptible) and virus-negative (*i.e.*, resistant) midguts. Comparison of the transcriptome of resistant and susceptible midguts led to the identification of a few differentially expressed genes (Figure 1D), including cytochrome *P450 4g15* (*AAEL006824*, *LOC5568416*).

Top hits identified in the single-midgut transcriptomic dataset were selected for functional validation. *In vivo* gene knockdown of these candidates was performed and the impact of the silencing on DENV-1 infection *via* an infectious bloodmeal was assessed by RT-qPCR of the viral genome. Silencing of *P450 4g15* induced an increase of 35% in viral prevalence (Figure 1E). This assay provided direct evidence of the antiviral function of *P450 4g15* during DENV-1 infection of *Ae. aegypti*.

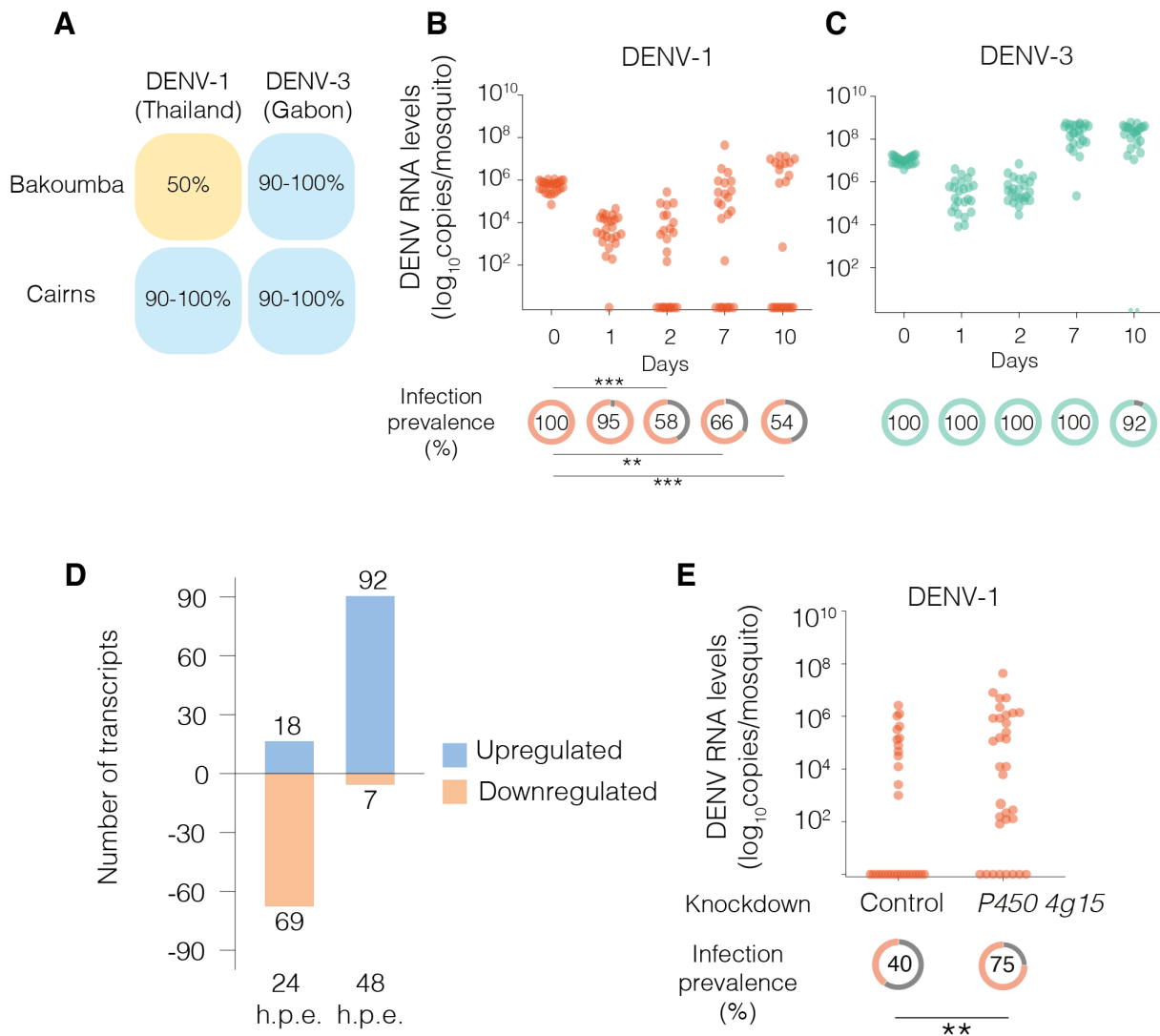


Figure 1. *P450 4g15* is an antiviral factor associated with natural DENV resistance in the midgut. (A) Virus strain-specific resistance phenotype observed in the Bakoumba mosquito population. Percentages indicate the infection prevalence obtained in experimental infections of mosquito populations from Bakoumba (Gabon) or Cairns (Australia), with DENV-1 and DENV-3 strains, 14 days after a bloodmeal containing 5×10^6 FFU/mL of virus. (B-C) DENV viral loads and prevalence in midguts of mosquitoes exposed to an infectious bloodmeal containing 5×10^6 FFU/mL of DENV-1 (B) or DENV-3 (C) on days 0, 1, 2, 7 and 10 after virus exposure. Each datapoint represents an individual midgut. $**p < 0.01$; $***p < 0.001$ (chi-squared test) (D) Number of differentially expressed genes in resistant or susceptible midguts in a single-midgut RNA sequencing analysis performed on Bakoumba mosquitoes exposed to a DENV-1-containing bloodmeal (5×10^6 FFU/mL). A gene was considered differentially expressed when the fold change was ≥ 2 and the adjusted p-value was ≤ 0.05 . (E) Impact of *in vivo* *P450 4g15* gene silencing on

DENV-1 viral loads and prevalence. Female *Ae. aegypti* from the Bakoumba population were injected with dsRNA targeting *P450 4g15* or *Luciferase* as a negative control. Two days later mosquitoes were exposed to an infectious bloodmeal containing 5×10^6 FFU/mL of DENV-1. Whole bodies were collected on day 5 after the bloodmeal and processed for viral RNA quantification to evaluate infection prevalence and viral loads.

II- Known functions of cytochromes P450

P450 4g15 is a member of the superfamily of cytochromes, which are broadly conserved among almost all organisms. Cytochromes P450 were initially characterized as monooxygenases, but their enzymatic functions have since been further investigated in mammals and can be associated with a range of chemical reactions involved in foreign compound detoxification and developmental processes [17-19]. Some P450 members are also modulated by cytokines during injury-, diet-, cancer- or infection-associated inflammation in mammals [20].

Despite extensive characterization of cytochromes P450 in plants and mammals, the functions of their insect homologs are less characterized. Only a few examples of insect cytochrome functions have been reported, including synthesis of insect hormones (such as ecdysone and juvenile hormone), insecticide resistance, development of sensory bristles or even behavioral phenotypes such as aggressive behavior or mating [21-27]. In flies, many *P450s* have been detected in the gut with various expression patterns, in different regions of the gut and in different larval stages [28]. To our knowledge, there is no evidence of insect cytochromes P450 involved in antiviral immune responses.

Thus, the molecular processes underlying *P450 4g15* antiviral activity during the early steps of DENV-1 infection in *Ae. aegypti* remain undetermined. Hence, the aim of this study was to functionally characterize *P450 4g15*'s antiviral activity in the mosquito midgut.

RESULTS

I- *P450 4g15* is a midgut antiviral response factor during early DENV infection

A) *P450 4g15* is transiently induced in midguts in response to a bloodmeal

To refine the association of the Bakoumba population's infection phenotype with the expression of the newly identified antiviral factor *P450 4g15*, we performed experimental infection assays of Bakoumba female mosquitoes by exposing them to a bloodmeal containing either DENV-1 or DENV-3, or a mock control. Then, we collected midguts to quantify viral replication and *P450 4g15* expression levels by RT-qPCR (Figure 2).

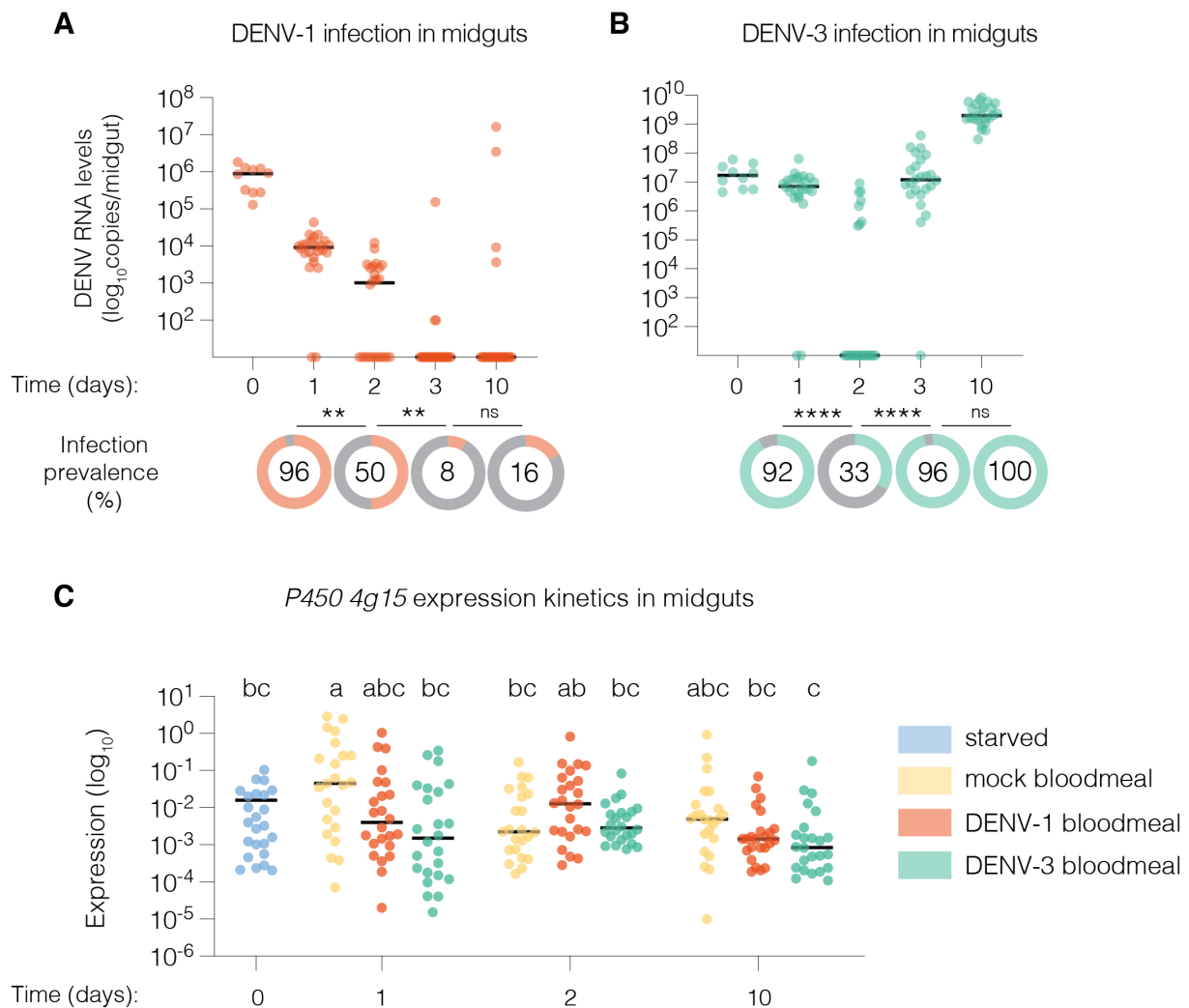


Figure 2. *P450 4g15* is transiently induced in midguts within the first 24 hours after bloodmeal ingestion. (A-B) Viral RNA loads and prevalence in midguts of mosquitoes exposed to an infectious bloodmeal containing 2.5×10^7 FFU/mL of DENV-1 (A) or 8.8×10^7 of DENV-3 (C) on days 0, 1, 2, 7 and 10 after virus exposure. $**p < 0.01$; $****p < 0.0001$ (chi-squared test) (C) Expression levels of *P450 4g15* in mosquito midguts were quantified by RT-qPCR and normalized to the expression levels of the housekeeping gene *RP49* and expressed as $2^{-dCt} = 2^{-(CtP450\ 4g15 - CtRP49)}$. Statistical significance was determined using one-way ANOVA after \log_{10} -transformation of the 2^{-dCt} values, followed by Tukey-Kramer's HSD test. Statistical significance is represented above the graph using connecting letters, whereby groups that do not share a letter are significantly different. In (A-C), each datapoint represents an individual midgut.

In midguts of Bakoumba mosquitoes exposed to DENV-1, both the viral RNA load and the proportion of individuals which tested positive for DENV RNA declined from the time of virus exposure until day 2 post exposure (p.e.). Three days p.e., the distinction between susceptible and resistant individuals was clearly visible. From this timepoint, viral loads detected in susceptible individuals increased till day 10 p.e.. At the latest timepoints, only 16% of individuals had virus-positive midguts, confirming the previously described resistance phenotype (Figure 2A). Of note, the viral prevalence obtained was much lower than in the

previous experiment (Figure 1B) despite a higher infectious titer in the bloodmeal and could be attributed to a genetic drift of the Bakoumba population which became increasingly resistant over generations.

For mosquitoes exposed to DENV-3, 100% of individuals had virus-positive midguts by the end of the time course. DENV-3 RNA loads in virus-positive individuals were comparable between days 0, 1, 2 and 3, whereas DENV-1 RNA loads were plummeting at the same timepoints (Figure 2B).

This experiment confirmed the DENV-1-specific resistance phenotype of the Bakoumba population. We also validated that the resistance to infection was established within the first two to three days following midgut exposure to DENV-1.

Secondly, as we had previously identified *P450 4g15* as an antiviral factor in this mosquito population, we questioned whether expression of this factor correlated with the kinetics of establishment of the resistance phenotype. We assessed variations in gene expression along virus infection kinetics by RT-qPCR (Figure 2C).

Exposure of the Bakoumba females to a mock bloodmeal triggered a significant ~10-fold upregulation of *P450 4g15* expression within 24 hours. Then, transcript levels returned to their basal level two days p.e.. This observation justifies the qualification of *P450 4g15* as a response factor. In presence of DENV-1 or DENV-3 in the bloodmeal, we did not observe an upregulation of the gene in midguts (Figure 2C). In carcasses, *P450 4g15* expression was not impacted by bloodmeal ingestion or virus infection (Supplementary figure S1).

These data suggest that *P450 4g15*'s antiviral activity during DENV early steps of replication is indeed associated with the midgut response to bloodmeal ingestion.

B) *P450 4g15* protein subcellular localization is impacted by DENV exposure

Next, we aimed to assess *P450 4g15* expression in response to a bloodmeal at the protein level. To get an indication of *P450 4g15*'s subcellular localization in parallel, we used an immunostaining approach on midgut tissues. We exposed female mosquitoes from the Bakoumba population to a bloodmeal, either mock or containing DENV-3. We chose DENV-3 because the DENV-1-specific resistance phenotype prevented us from getting a sufficient sample size of infected individuals. Later, we collected midgut tissues one, two or five days p.e. and we evaluated DENV E protein and *P450 4g15* protein expression and localization

(Figure 3). For P450 4g15 staining, custom antibodies were generated and we assessed their specificity in C6/36 mosquito cells (Supplementary Figure S2).

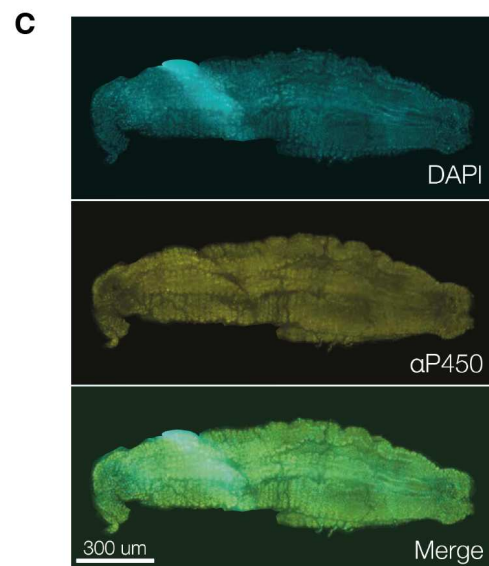
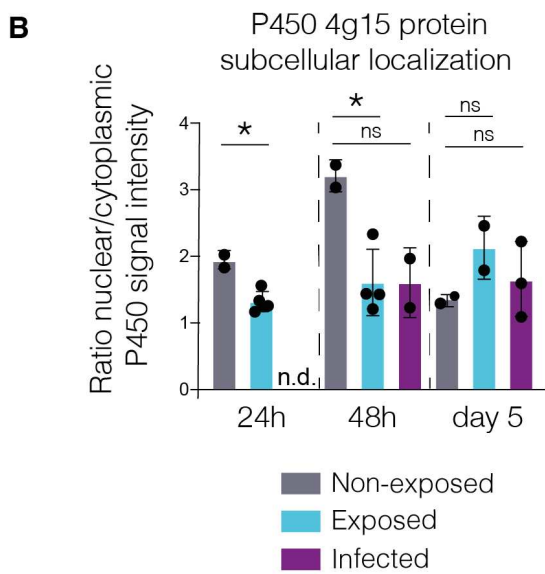
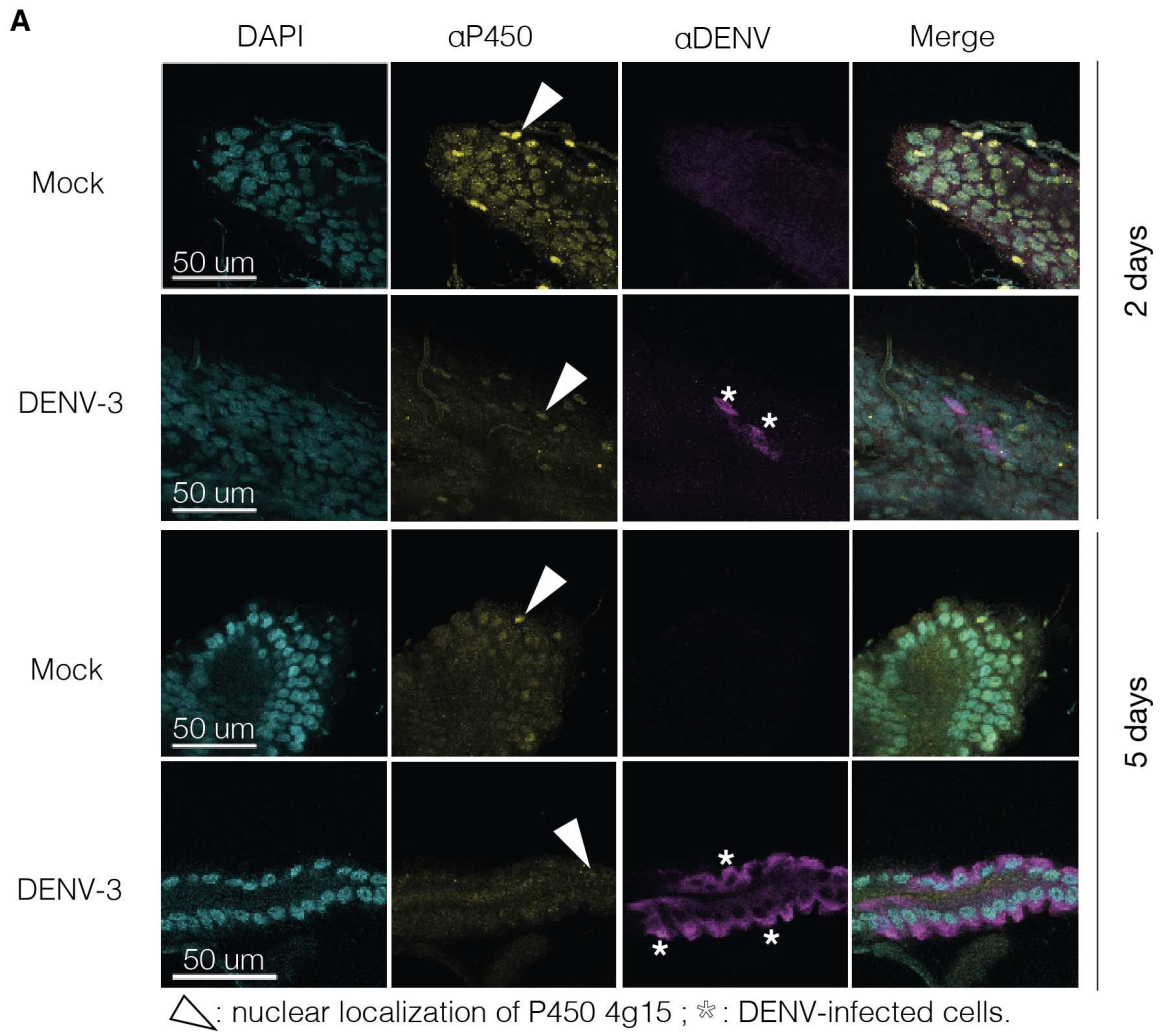


Figure 3. Midgut exposure to blood and DENV affects P450 4g15 subcellular localization. (A-C) Immunostaining of mosquito midguts exposed to a mock or DENV-3-containing bloodmeal, 2 and 5 days after exposure. Tissues were stained with DAPI (nuclei), antibodies against P450 4g15 and DENV E protein and imaged with a confocal microscope (Zeiss LSM780). Maximum intensity projection of z-stacks is represented. White arrows indicate nuclear localization of P450 4g15, stars indicate DENV-positive cells. (B) Quantitative analysis of P450 4g15 subcellular localization. The ratio of nuclear over cytoplasmic signal intensity for P450 4g15 staining is represented for mock-exposed (*non-exposed*) tissues, DENV-exposed but DENV-negative tissues (*exposed uninfected*) and DENV-positive tissues (*exposed infected*). Statistical significance of the pairwise differences was analyzed with Student's t-test. (* $p < 0.05$; ** $p < 0.01$; *** $p < 0.001$). (C) P450 4g15 immunostaining in a whole sugar-fed mosquito midgut. Image was cropped around the tissue to remove background noise and artefacts.

Firstly, we did not detect any signal of DENV E protein within the first day p.e.. This was expected as the sensitivity of the immunostaining method on *ex vivo* tissues is limited, and the amount of viral protein at such an early timepoint is very low. From two days p.e., we managed to clearly detect early infection foci (Figure 3A).

Secondly, we detected P450 4g15 protein in all conditions (Figure 3A) and in the entire midgut tissue (Figure 3C). We observed two distinct patterns of subcellular localization: either an intense signal which overlapped with DAPI staining of the nuclei, or a more diffuse signal in the cytoplasm (Figure 3A). We were not able to compare P450 4g15 protein signal intensity between conditions because of the strong background noise in most images. As a result, we could not confirm the upregulation of the factor in response to a bloodmeal at the protein level. Yet, we could analyze the protein's subcellular localization in a quantitative manner, by comparing P450 4g15's nuclear signal intensity with its cytoplasmic signal intensity (Figure 3B).

These quantifications led to several observations. Exposure to a mock bloodmeal led to an increase in the ratio of the nuclear over cytoplasmic signal intensity between one and two days post exposure. This suggests that blood ingestion induces some spatial rearrangements of P450 4g15 protein within midgut cells. The ratio variation could be either explained by an increased amount of the nuclear form, a decreased amount in the cytoplasmic form, or a re-addressing of the protein from the cytoplasm to the nucleus. In virus-exposed or -infected cells, we detected as much nuclear presence than cytoplasmic presence of P450 4g15, with no significant variation between conditions and timepoints. Therefore, we concluded that compared to a mock bloodmeal ingestion, the localization of P450 4g15 is biased towards cytoplasmic localization upon DENV exposure.

C) *P450 4g15* transcript levels correlate with DENV infection *in situ*

The lack of sensitivity of the immunostaining method did not allow to detect differences in protein levels between cells and thus establish a correlation between *P450 4g15* expression levels and the infection status of midgut cells.

To address this limitation, we developed a protocol of RNA-FISH (RNA-Fluorescent *In Situ* Hybridization) on midgut tissues. We opted for the multiplex RNAscope method [29], which allows for simultaneous *in situ* detection of low abundance transcripts at a single-cell level in tissues. Hence, the sensitivity of this method allowed to detect the replicative (*i.e.*, negative) RNA strand of DENV during very early steps of replication and to estimate *P450 4g15* transcript levels at the cell level using imaging. We exposed female mosquitoes from the Bakoumba population to a bloodmeal, either mock or containing DENV-3, and collected tissues one and two days after exposure. Then, we stained midgut tissue cryosections with probes targeting *P450 4g15* transcripts and DENV negative strand and imaged the samples with a confocal microscope (Figure 4 and Supplementary figure S2).

We were able to detect viral RNA in midgut cells as early as 24 hours after ingestion of an infectious bloodmeal (Figure 4A). Imaging also revealed that early infection foci are distributed over the entire length of the midgut tissue, with no detectable preference for a specific midgut region. These observations match the previous descriptions of the early infection pattern of midguts upon exposure to arboviruses [30, 31].

P450 4g15 transcripts were detected as RNA dots (Figure 4A). We estimated transcript expression levels by the number of *P450 4g15* RNA dots normalized per surface unit of the cell layer. Then we compared *P450 4g15* transcript levels in midgut cells respectively exposed to a mock bloodmeal, virus-exposed but uninfected, and infected. One day after bloodmeal ingestion, we observed that virus-positive midgut cells showed higher *P450 4g15* transcript levels (~2-fold), compared to mock or exposed cells. After two days, all conditions were associated with similar *P450 4g15* transcript levels, as expression levels in non-exposed and exposed cells had caught up with those in infected cells (Figure 4B).

Two hypotheses can be drawn from these observations: either DENV infection in midgut cells triggers an upregulation of the antiviral factor *P450 4g15*, as part of an immune response process, or DENV infection is biased towards target cells that express higher levels of *P450 4g15*. The first hypothesis is more consistent with the previously observed kinetics of expression of *P450 4g15* in midgut tissues.

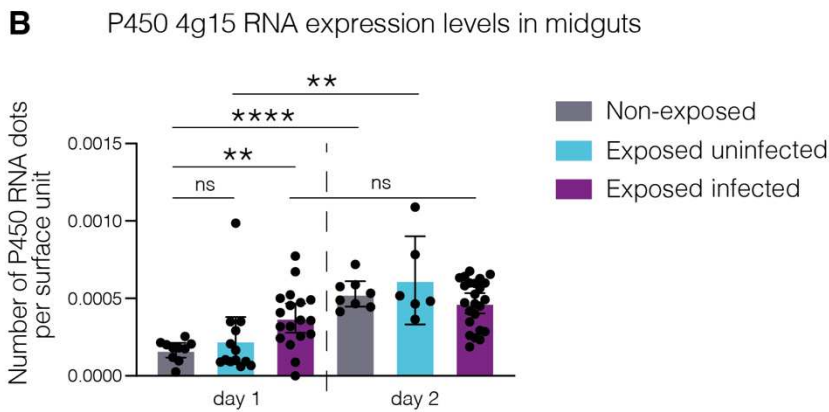
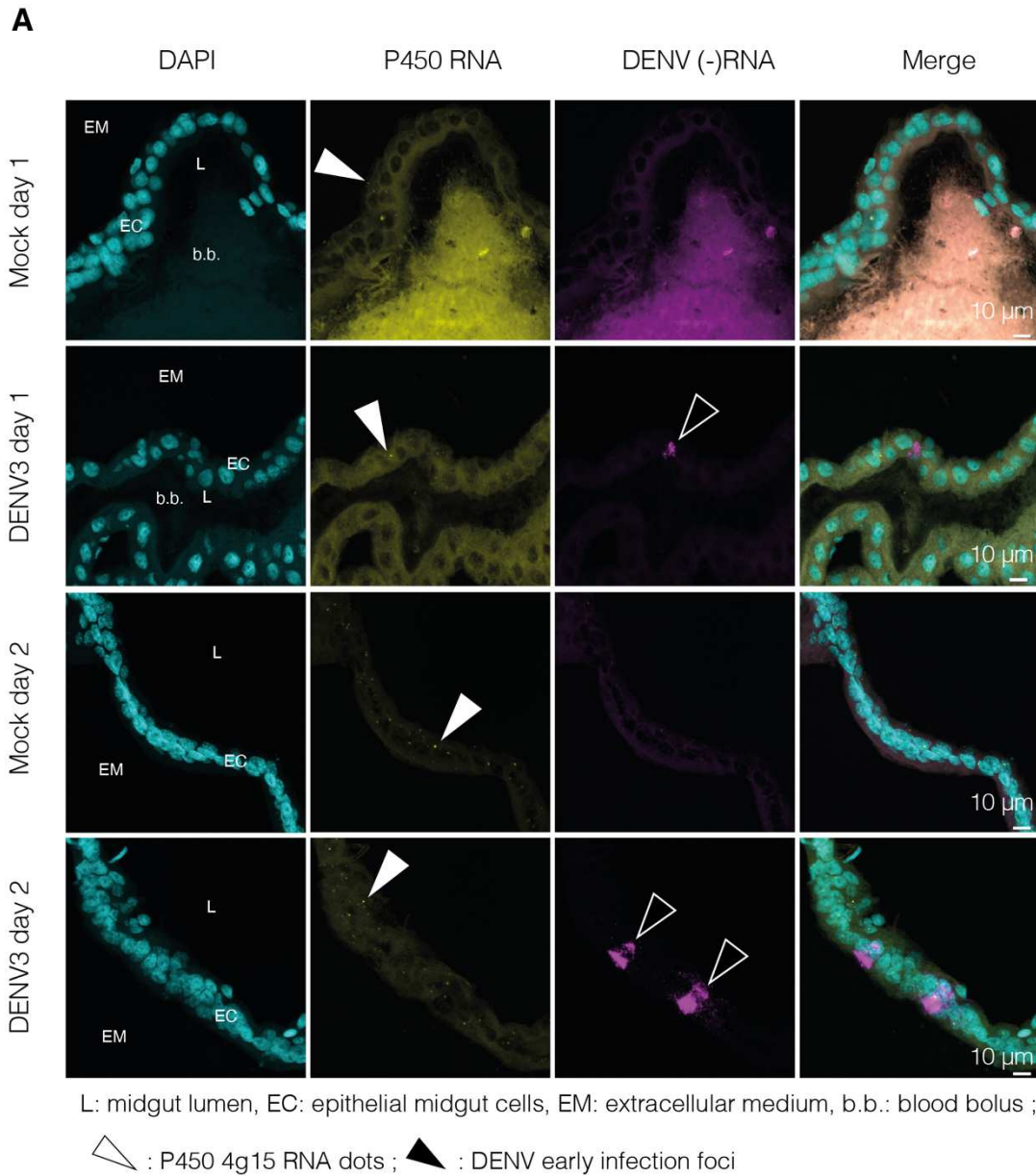


Figure 4. Early DENV infection of midgut cells is associated with higher levels of *P450 4g15* expression *in situ*. (A-B) Multiplex RNA-FISH on midgut tissue cryosections of Bakoumba mosquitoes

exposed to a mock or DENV-3-containing bloodmeal, 1 and 2 days after exposure. (A) Ten μm -thick tissue slices were stained using DAPI (nuclei) and probes targeting *P450 4g15* RNA and DENV RNA (negative strand) and imaged using a confocal microscope (Zeiss LSM780). Maximum intensity projection of z-stacks is represented. White arrows indicate *P450 4g15* RNA clusters, and black arrows indicate DENV infection foci. (B) Quantification of *P450 4g15* transcripts levels was assessed based on the number of RNA dots per surface unit of the cell layer. Quantification was done in mock-exposed (*non-exposed*) tissues, DENV-exposed but DENV-negative tissue areas (*exposed uninfected*) and DENV-positive tissues areas (infection foci, *exposed infected*). Statistical significance of the pairwise differences was analyzed with Student's t-test (* $p < 0.05$; ** $p < 0.01$; *** $p < 0.001$).

D) *P450 4g15* expression levels in midguts determine DENV systemic infection success

Our previous kinetics data revealed that the establishment of resistance occurs within the first 48 hours after ingestion of infectious blood (Figures 1B-C & 2A-B). We also confirmed that *P450 4g15* expression in midgut cells positively correlates with DENV infection of these cells (Figure 4B). Therefore, we hypothesized that the induction of *P450 4g15*, specifically in the midgut, is a determinant of the resistance phenotype during DENV-1 infection.

To test this hypothesis, we generated a midgut-specific *P450 4g15*-overexpression mosquito line (Figure 5A). In this “*Cp-P450*” line, overexpression of *P450 4g15* is controlled by a carboxypeptidase (Cp) promoter, which is activated by ingestion of a bloodmeal in a transient and midgut-specific manner [32-34]. Hence, this mosquito line overexpresses *P450 4g15* only in the midgut for a few hours following ingestion of a bloodmeal and offers the opportunity to test whether midgut-specific expression of *P450 4g15* is determining specifically during the early steps of mosquito infection. In parallel, we generated a control line from the same genetic background. We exposed female mosquitoes from both the *Cp-P450* overexpression line and the control line to a DENV-1-containing bloodmeal and performed RT-qPCR of the viral genome on day 2 and day 5 after exposure to evaluate viral loads and prevalence in whole mosquito bodies.

Two days after virus exposure, DENV-1 loads in *Cp-P450* overexpressing individuals were significantly lower than in the controls (Figure 5B). Five days after exposure, viral loads in infected individuals were similar in both conditions, but viral prevalence was almost 30% lower in the *Cp-P450* line than in the controls.

This experiment demonstrates that transient overexpression of *P450 4g15* in the midgut is sufficient to change the outcome of infection and to induce a resistance phenotype at later stages of infection.

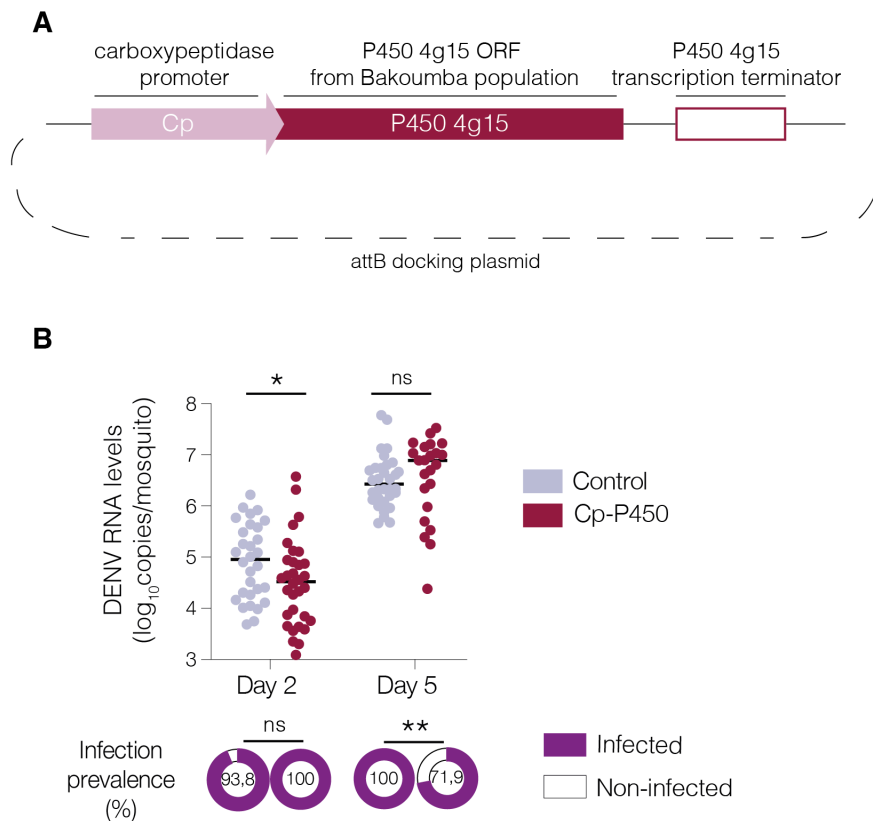


Figure 5. Midgut-specific ectopic expression of *P450 4g15* hampers DENV infection in mosquitoes. (A) Plasmid construct for midgut-specific ectopic expression of *P450 4g15* in the transgenic *Cp-P450* line. The *P450 4g15* open reading frame from the Bakoumba sequence is controlled by the bloodmeal-inducible midgut-specific carboxypeptidase promoter, followed by the native *P450 4g15* transcription terminator, in an attB docking plasmid used for cloning. (B) Viral RNA loads and prevalence in whole mosquito bodies of the *Cp-P450* transgenic line and a control line, 2 and 5 days after exposure to an DENV-1 infectious bloodmeal (5×10^6 FFU/mL). Statistical significance of the differences was assessed with Mann-Whitney's test for the viral loads and a chi-squared test for the prevalence (* $p < 0.05$; ** $p < 0.01$; *** $p < 0.001$).

II- Correlation between *P450 4g15* promoter haplotypes and expression levels

Previously, an exome-wide association study (EWAS) was carried out to investigate DENV strain-specific resistance of Bakoumba mosquitoes [15]. Briefly, Bakoumba females were exposed to low and high infectious doses of DENV-1. Infection status was determined from RT-PCR on body samples, and heads were used for exome sequencing. The analysis compared pools of individuals that were uninfected at the high dose (*i.e.*, “resistant”) versus individuals infected at the low dose (*i.e.*, “susceptible”), for each DENV strain separately.

P450 4g15 promoter sequence diversity consists of three major haplotypes, that we designate HAP-1, HAP-2, and HAP-3. HAP-1 and HAP-3 sequences mostly differ by an 18-base pair (bp) sequence that is absent in HAP-3. HAP-2 sequence displays a 1-bp deletion, absent in both

HAP-1 and HAP-3 sequences. Using the EWAS samples, we found a statistical association between DENV-1 infection status and *P450 4g15* promoter genotype (Figure 6A). HAP-1 homozygotes are predominantly resistant whereas HAP-3 homozygotes are predominantly susceptible. HAP-2 homozygotes are a mixture of resistant and susceptible individuals.

We had previously shown a correlation between *P450 4g15* expression levels and infection status, and the EWAS indicated an association between promoter haplotypes and infection status. Therefore, we sought to confirm the missing link, that is, the correlation between *P450 4g15* promoter haplotypes and expression levels.

A) Expression levels of *P450 4g15* correlate with promoter haplotypes

As a first approach, we exposed female mosquitoes of the Bakoumba colony to a mock bloodmeal and quantified the *P450 4g15* expression levels in their bodies one day after by RT-qPCR. We chose this specific timepoint based on the gene expression kinetics which indicated that the strongest induction of *P450 4g15* was obtained one day after blood ingestion (Figure 2C). In parallel, we also genotyped the promoter sequence of each individual by Sanger sequencing, to evaluate the association between *P450 4g15* promoter haplotype and expression level in response to a bloodmeal (Figure 6B).

We confirmed that individuals with a homozygous HAP-1 promoter displayed high *P450 4g15* expression in response to a bloodmeal, whereas HAP-3 homozygotes showed low expression (~5-fold lower than HAP-1). Heterozygous individuals and HAP-2 homozygotes showed intermediate *P450 4g15* expression levels (Figure 6B).

This first approach supports our hypothesis of a correlation between *P450 4g15* promoter haplotypes and expression levels of this antiviral factor.

B) *P450 4g15* promoter haplotypes determine the gene's expression level

To assess a direct relationship of promoter haplotypes and expression levels, we generated haplotype-reporter mosquito lines. In the HAP-reporter lines, a reporter GFP sequence is controlled by either HAP-1 or HAP-3 promoter sequence (Figure 6C-G).

GFP signal was observed in both reporter lines, in pupal and adult stages (Figure 6D, 6F). We observed a very clear GFP signal in the abdomens, in the form of dots longitudinally aligned on each side of the abdomen.

We imaged pupae from both the HAP-1-GFP and HAP-3-GFP reporter lines and quantified GFP signal intensity in both lines. Mean GFP intensity was measured in the GFP signal-positive patches along the pupae's abdomens using an image analysis software. This quantification showed that GFP intensity under the control of HAP-3 promoter sequence was ~30% lower than under the control of HAP-1 (Figure 6D-E).

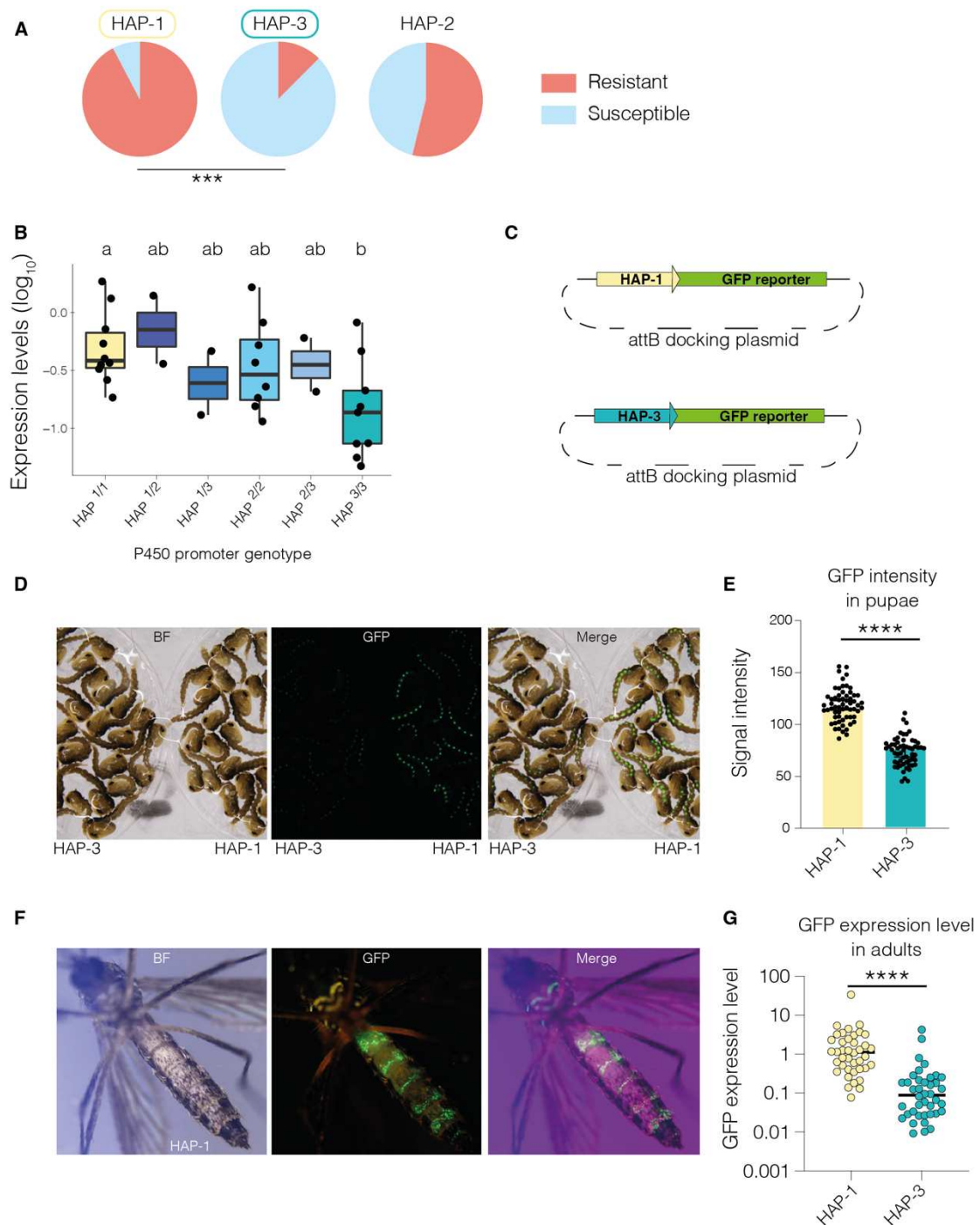


Figure 6. *P450 4g15* promoter haplotypes determine its expression level. (A) Association detected between three major haplotypes (HAP-1, HAP-2, and HAP-3) in the promoter sequence of *P450 4g15* and DENV-1 infection status in the EWAS. Resistant individuals were uninfected after exposure to a high

virus dose whereas susceptible individuals were infected after exposure to a low virus dose. Statistical significance of pairwise differences was assessed with a chi-squared test. *** $p < 0.001$ (B) *P450 4g15* transcript levels determined by RT-qPCR, normalized by housekeeping gene *RPS17* levels, in mosquitoes with different *P450 4g15* promoter genotypes. Promoter genotypes are indicated on the x-axis (HAP^{1/1}, HAP^{2/2} and HAP^{3/3}: homozygous HAP-1, HAP-2, and HAP-3 respectively; HAP^{1/2}, HAP^{1/3} and HAP^{2/3}: heterozygous combinations of HAP-1, HAP-2 and HAP-3). Statistical significance of the differences was determined using one-way ANOVA after log₁₀-transformation of the 2^{-dCt} values, followed by Tukey-Kramer's HSD test. (C) Transgenesis plasmid constructs for HAP-1- and HAP-3-GFP reporter lines. The eGFP reporter gene is under the control of either the HAP-1 or HAP-3 haplotype of *P450 4g15* promoter region. (D) Images of brightfield (BF) and eGFP (GFP) signals in pupae from the HAP-3- (left) and HAP-1- (right) GFP reporter lines. (E) Image quantification of eGFP signal intensity in pupae from the HAP-1- and HAP-3-GFP reporter lines. (F) Images of brightfield (BF) and eGFP (GFP) signals in an adult female of the HAP-1-GFP reporter line. Imaging was done using an epifluorescence microscope. (G) Quantification of eGFP transcript levels by RT-qPCR in adult females from the HAP-1- and HAP-3-GFP reporter lines. Statistical significance of the differences in (F, G) was assessed with Mann-Whitney's test.

In adults, the thickness of the cuticle prevented us from imaging and quantifying accurately GFP intensity levels. Instead, we quantified GFP expression by RT-qPCR on whole bodies (Figure 6F-G). This method confirmed that in adults, the HAP-3 promoter's activity is ~10 times lower than HAP-1's.

Thus, both approaches validate that the polymorphisms in the *P450 4g15* promoter determine differential expression levels and demonstrate that the activity of the HAP-1 promoter is much stronger than the HAP-3 promoter.

DISCUSSION

Using a natural DENV resistance phenotype in a field-derived colony of *Ae. aegypti*, we identified a novel antiviral factor, cytochrome *P450 4g15*, expressed in the midgut of mosquitoes. We demonstrated that this factor is induced in the midgut upon bloodmeal ingestion, where its expression hampers DENV infection in the mosquito. Additionally, we showed that polymorphisms in the promoter sequence of *P450 4g15* determine its expression level. Finally, we proved that differential *P450 4g15* expression levels translate to differential susceptibility to DENV infection. Overall, our study identifies genetic polymorphisms in the promoter sequence of a non-canonical antiviral factor that drives resistance to DENV.

The kinetics of infection in Bakoumba individuals suggested that the antiviral activity of *P450 4g15* occurs during the early stages of the mosquito infection. Since midgut cells expressing *P450 4g15* can be infected, this suggests that expression of this antiviral factor does not imply cell refractoriness. The higher *P450 4g15* transcript levels in infected cells rather indicate that its expression is associated with a more efficient antiviral response which consequently prevents further viral replication. Further investigation is needed to determine whether viral infection in resistant Bakoumba individuals is inhibited prior to systemic dissemination or not, and thus whether *P450 4g15* is a determinant of the midgut escape barrier. Targeting factors which modulate early infection steps would hamper the viral transmission cycle in the mosquito even before systemic dissemination and would therefore represent a safer approach. Integrating this knowledge into vector control strategies might enhance their efficacy and contribute to their long-term success.

Immunostaining of midgut tissues revealed that subcellular localization of *P450 4g15* is enriched in the nucleus upon bloodmeal ingestion and in the cytoplasm upon virus exposure. Cytochromes *P450* have been described in association with membranes of diverse cellular organelles, including the nuclear membrane. Yet, to our knowledge, there is no evidence of an intranuclear function of any cytochrome *P450*. Mitochondrial cytochrome *c* nuclear translocation is associated with remodeling of the nucleolus conformation, which drives further release of activator proteins [35]. *P450 4g15* might indirectly modulate antiviral processes by relocating from intranuclear regions to the cytoplasm and controlling gene accessibility and expression, or release of activator proteins from (or in) the nucleus.

The HAP-reporter lines allowed to correlate polymorphisms in the promoter sequence with the gene's expression levels. Interestingly, the specific expression pattern in the reporter lines was reminiscent of the typical pattern of oenocyte localization under the mosquito cuticle. Among

other functions, oenocytes produce cuticular components involved in desiccation resistance [36]. Notably, oenocyte-specific knockdown of certain insect-specific cytochromes *P450* induced significant reduction in desiccation tolerance [37]. This is consistent with the lethal desiccation phenotype that we observed in our attempts to generate *P450 4g15*-knockout mutants (data not shown). The tissue-specificity of the HAP-reporters therefore correlates with a potential oenocyte-associated function of *P450 4g15*. Yet, whether *P450 4g15* expression in such cells is linked to its antiviral activity remains to be determined.

We showed that HAP-1 and HAP-3 promoter haplotypes are responsible for differential expression levels of the gene they control. These two haplotype sequences mostly differ by an 18-bp region which is absent in HAP-3, the low-expression-associated haplotype. Therefore, this 18-bp region might facilitate the recruitment of an expression enhancer, resulting in increased *P450 4g15* expression levels in HAP-1 individuals. Moreover, the link between promoter haplotypes and DENV susceptibility had hitherto only been inferred from a statistical association in the EWAS samples. To more directly establish this link, we also generated haplotype-pure lines derived from the Bakoumba population. Infection assays of these haplotype-pure lines confirmed that resistance to DENV correlates with *P450 4g15* promoter sequence (data not shown).

On the whole, we provide here the first report of polymorphism in the promoter of a gene which drives phenotypic variation in vector competence. This study illustrates how the broad genetic diversity of wild mosquito populations can be exploited to discover molecular factors underlying vector competence.

METHODS

Ethics

Mosquito artificial infectious blood meals were prepared with human blood (to the exception of Figure 5 data). Blood samples were supplied by healthy adult volunteers at the ICAReB biobanking platform (BB-0033-00062/ICAReB platform/Institut Pasteur, Paris/BBMRI AO203/[BIORESOURCE]) of the Institut Pasteur in the CoSIImmGen and Diagmicoll protocols, which had been approved by the French Ethical Committee Ile-de-France I. The Diagmicoll protocol was declared to the French Research Ministry under reference 343 DC 2008-68 COL 1. All adult subjects provided written informed consent. Genetic modification of *Ae. aegypti* was performed under authorization number #7614, #3243 and #3912 from the French Ministry of Higher Education, Research, and Innovation. At the IBMC in Strasbourg, mosquito line maintenance involved bloodmeals on mice and was evaluated by the CREMEAS Ethics committee and authorized by MESRI under reference APAFIS #20562-2019050313288887v3.

Cells and virus isolates

C6/36 cells (derived from *Ae. albopictus*) were cultured in Leibovitz's L-15 medium (Life Technologies) supplemented with 10% fetal bovine serum (FBS, Life Technologies), 1% non-essential amino acids (Life Technologies), 2% tryptose phosphate broth (Gibco ThermoFisher Scientific), 10 U/ml of penicillin (Gibco Thermo Fisher Scientific) and 10 µg/ml of streptomycin (Gibco ThermoFisher Scientific) at 28°C. DENV-1 isolate KDH0026A was originally obtained in 2010 from the serum of a dengue patient in Kamphaeng Phet, Thailand [13]. DENV-3 isolate GA28-7 was originally derived in 2010 from the serum of a dengue patient in Moanda, Gabon [38]. Informed consent of the patient was not necessary because viruses isolated in laboratory cell culture are no longer considered human samples. Virus stock was prepared using C6/36 cells, and viral infectious titers were measured on C6/36 cells using a standard focus-forming assay (FFA) as previously described [39].

Mosquito rearing and infectious bloodmeals

Ae. aegypti from the Bangkok genetic background obtained from MR4-BEI were used for genetic engineering. An *Ae. aegypti* mosquito colony derived from a wild population sampled in Bakoumba, Gabon in 2014 was used for infectious assays. Mosquitoes were reared and exposed to DENV as described previously [39]. In short, mosquitoes were reared in standard insectary conditions (28°C ± 1°C, 75 ± 5% relative humidity, 12:12 hour light-dark cycle) on a diet of fish food for larvae (Tetramin), and a 10% sucrose solution for adults. Five- to seven-day-old female mosquitoes were deprived of sucrose solution 20 hours before exposure to the infectious bloodmeal. Fresh human blood (collected on Heparin) (or rabbit blood (BCL) for

Figure 5 data) was centrifuged for 15 min at 1500 rpm to separate the erythrocytes from the plasma. The erythrocytes were washed 3 times with Phosphate Buffer Saline (PBS) 1× and centrifuged for 5 min at 3000 rpm, before being resuspended in PBS 1× and supplemented with ATP at a final concentration of 10 mM to stimulate blood uptake by mosquitoes. The infectious bloodmeal consisted of a 2:1 mix of washed erythrocytes and viral suspension supplemented with 10 mM adenosine triphosphate (ATP) (Sigma). Bloodmeal aliquots were collected prior to feeding, and viral titers subsequently determined by Focus-Forming Assay. Mosquitoes were exposed to an infectious bloodmeal for 15 min through a desalted pig-intestine membrane using an artificial feeder (Hemotek Ltd) set at 37°C. Fully engorged females were sorted on ice and incubated at 28°C, 70% relative humidity and under a 12-hour light-dark cycle with permanent access to 10% sucrose solution.

RNA extraction

Mosquito body parts and organs were dissected in 1× phosphate-buffered saline (PBS), and immediately transferred to a tube containing 400 µL of RA1 lysis buffer from Nucleospin 96 RNA core kit (Macherey-Nagel) and ~20 1-mm glass beads (BioSpec). Samples were homogenized for 30 sec at 6,000 rpm in a Precellys 24 grinder (Bertin Technologies). RNA was extracted and treated with DNase using Nucleospin 96 RNA core kit (Macherey-Nagel) following the manufacturer's instructions and stored at -20°C until further use.

Gene expression measurement

Gene expression levels were measured using a BRYT-Green based RT-qPCR assay (GoTaq® 1-Step RT-qPCR System; Promega) following the manufacturer's instructions and using gene-specific primers (sequences provided in Supplementary Table 1). Relative expression was calculated as 2^{-dCt} , where $dCt = Ct_{Gene} - Ct_{RP49}$, using the *Ae. aegypti* ribosomal protein-coding gene *RP49* (AAEL003396) for normalization. Detection of *P450 4g15* (AAEL006824) expression was performed with several primer sets: for the expression kinetics in midguts and carcasses (Figure 2C and Supplementary Figure 1), primers "KD-38/2-qPCR-fwd" and "KD-38/2-qPCR-rev" were used; for the expression in whole bodies of genotyped individuals (Figure 6B), primers "P450-qPCR-wobble-FOR" and "P450-qPCR-wobble-REV" were used.

DENV RNA quantification

Viral RNA was reverse transcribed and quantified using a TaqMan based qPCR assay, using NS5-specific primers and 6-FAM/BHQ-1 double-labeled probe (sequences provided in Supplementary Table 1). Reactions were performed with the GoTaq® Probe 1-Step RT-qPCR kit (Promega) following the manufacturer's instructions. Standard curves of *in vitro* synthesized

RNA dilutions were used to determine the absolute number of RNA copies per sample. The limit of detection of the assay was 200 copies of viral RNA per tissue.

DENV virus titration by focus-forming assay

DENV infectious titers were measured by standard FFA in C6/36 cells as previously described [39]. Briefly, the cells were seeded in a 96-well plate 24 hours before inoculation. Serial dilutions of the samples were prepared in Leibovitz's L-15 medium (Gibco) supplemented with 0.1% penicillin/streptomycin (pen/strep), 2% tryptose phosphate broth (Thermo Fischer Scientific), 1× non-essential amino acids (NEAA) and 2% fetal bovine serum (FBS). The cell-culture medium was removed, and the cells were inoculated with 40 µL of sample per well. After 1 hour of incubation at 28°C, the inoculum was removed and cells were overlaid with 150 µL/well of a 1:1 mix of overlay medium (Leibovitz's L-15 medium, 0.1% pen/strep, 2% tryptose phosphate broth [Thermo Fischer Scientific], 1× NEAA, 2× Antibiotic-Antimycotic [Life Technologies] and 10% FBS) and 2% carboxyl methylcellulose solution and incubated for 5 days at 28°C. Cells were fixed for 30 min in 3.6% paraformaldehyde (PFA) (Sigma). The overlay and fixative were removed, and the cells were washed three times with PBS, followed by 30 min of permeabilization with 50 µL/well of 0.3% Triton X-100 (Sigma-Aldrich) in PBS at room temperature (20-25°C). The cells were washed again three times in PBS and incubated for 1 hour at 37°C with 40 µL/well of mouse anti-DENV complex monoclonal antibody MAB8705 (Merck Millipore) diluted 1:200 in PBS + 1% bovine serum albumin (BSA) (Interchim). After another three washes in PBS, cells were incubated at 37°C for 30 min with 40 µL/well of an Alexa Fluor 488-conjugated goat anti-mouse antibody (Life Technologies) diluted 1:500 in PBS + 1% BSA. After three more washes in PBS and a final wash in water, infectious foci were counted under an epifluorescence microscope (Evos) and converted into focus-forming units/mL (FFU/mL).

Custom P450 4g15 antibody synthesis

Custom antibodies directed against P450 4g15 were produced by a commercial partner (Eurogentec). Two synthetic peptides of the following sequences were produced: NH₂-C+LKRTDGFRIQLEPRV -COOH and NH₂- C+AMGSQRTSESKEGFD-CONH₂. The immunization protocol entitled « AS-DOUB-LXP » consisted of 4 injections of both peptides at 0, 14, 28 and 56 days to 2 separate rabbits. A final bleed was performed 87 days after the first immunization. Antibodies were purified by the manufacturer and called "P450-89" and "P450-90".

Immunofluorescence assay on mosquito midguts

Midguts from female mosquitoes were dissected in 1× PBS and transferred on a μ -well slide (81826 ibiTreat 18 well – Flat) for fixation in 3,6% paraformaldehyde for 1 hour in a humid chamber, at room temperature. Midguts were rinsed five times in 1× PBS before permeabilization and saturation in PBS 1× with 0,1% Triton X-100 and 1% BSA (PBT) for 2 hours, at room temperature. Incubation with primary antibodies (anti-P450 4g15-89 1:50, anti-DENV complex (Merck-Millipore, MAB8705) 1:200, diluted in PBT) was done overnight at 4°C, followed by five washes in PBT and incubation with secondary antibodies (chicken anti-mouse 594 (Invitrogen A21201) 1:1000, donkey anti-rabbit 488 (Invitrogen R37118) diluted according to the manufacturers' instructions) for two hours at room temperature. Midguts were then washed in 1× PBS, stained with DAPI (100 nM in PBS), and mounted in anti-fading medium Fluoromount-G (Invitrogen, 00495802). All incubation and wash steps were done on rotation (300 rpm) in a humid chamber. Samples were imaged using a confocal microscope (LSM 780 inverted confocal microscope, Zeiss).

Antibody specificity assay

C6/36 cells were seeded on glass slides treated with poly-L-lysine in 24-well plates (5×10^5 cells/well in 500 μ L of complete L15 culture medium) and transfected the following day with either a P450-mCherry plasmid construct or a mCherry empty vector as a control, using Lipofectamine LTX Plus (Invitrogen) according to the manufacturer's instructions. Cells were fixed 48 hours post-transfection in 3,6% paraformaldehyde for 30 min and permeabilized in 1× PBS, 0.1% Triton X-100 for 15 min. Incubation with primary antibody (anti-P450 4g15 "89" 1:50 or anti-P450 4g15 "90" 1:100 diluted in antibody dilution buffer (1× PBS, 0.1% Triton X-100, 0.03% Normal Goat Serum)) was done overnight at 4°C in humid chamber, before three washes in 1× PBS, Triton 0.1%. Incubation with secondary antibody (donkey anti-rabbit 488 (Invitrogen R37118) diluted in antibody dilution buffer according to manufacturers' instructions) was done for 1 hour at room temperature. Slides were then washed 3 times in 1× PBS, Triton 0.1%, stained with DAPI (100nM in 1× PBS) for 1 min, rinsed in 1× PBS and mounted in anti-fading medium Fluoromount-G (Invitrogen, 00495802). Samples were imaged using a confocal microscope (LSM 780 inverted confocal microscope, Zeiss).

RNAscope

In Situ Hybridization. Mosquito midguts were dissected on ice in PBS 1×, fixed in 3.6% paraformaldehyde at room temperature for 20 min, and washed 3 times for 5 min in PBS 1×. Midguts were embedded with OCT (Shandon cryochrome blue, ThermoScientific). Frozen tissue blocks were kept on dry ice or stored at -80°C. Cryosections of 10 μ M were collected on

Manzel-Gläser SuperFrost microscope slides (ThermoScientific) and stored at -80°C before further use. RNAscope probe *Dengue V sense-pool-C1* (#528011) were designed by the manufacturer (ACD, Inc.) to target the negative strand of all 4 serotypes of DENV viruses. A custom probe targeting *P450 4g15* RNA was also synthesized by the manufacturer and called *LOC5568416-C2* (#820101-C2). *In situ* hybridization was performed using the RNAscope Multiplex Fluorescent Reagent Kit V2 according to manufacturer's instructions [40]. Hydrogen peroxide was applied for 10 min at RT and Protease III was applied for 30 min at 40°C. Detection of the probes was done with Opal540 (FP1494001KT) and Opal620 (FP1495001KT) reagents (diluted at 1:1000 and 1:750 in TSA buffer provided with the kit; Akoya Biosciences). Slides were incubated with DAPI for 30 min at RT and mounted with Prolong Gold Antifade reagent (Thermo Fisher Scientific) overnight at RT. Slides were imaged within 2 weeks on a LSM780 confocal microscope (Zeiss).

Image analysis. Maximum projection images of z-stacks were analyzed using Icy software (version 2.4.2.0) [41]. Regions of interest (ROI), respectively infection foci, virus-exposed but non-infected regions and non-exposed regions, were manually delimited based on DENV-positive signal. *P450 4g15* RNA dots were automatically counted in all ROIs using Icy's *Spot detector* function. ROIs smaller than 3700 pixels were excluded from the analysis to avoid null counts of RNA dots. The number of *P450 4g15* RNA dots per surface unit was used as a proxy of RNA levels and means were compared using a Mann-Whitney's test.

Mosquito genetic modification

Plasmids for transgenesis were assembled by Golden Gate Cloning [42, 43]. For this, each module to be included in the final assemblies (promoters, open reading frames, transcription terminators, fluorescence marker cassettes) was initially cloned with appropriate flanking *Bsal* restriction sites in ampicillin resistant vector pKSB- (Addgene #62540). In a second step, relevant modules were assembled in the desired order into a final kanamycin resistant transgenesis plasmid (piggyBac or attB docking plasmid) in a single *Bsal* restriction-ligation reaction [42, 43]. The HAP-1 haplotype of the promoter region of the *P450* gene was amplified by PCR from *Aedes aegypti* strain Bakoumba mosquito genomic DNA with primers EM2063 and EM2064. An equivalent region from the HAP-3 haplotype promoter was ordered as a synthetic DNA gBlock fragment (IDT DNA, Belgium). The carboxypeptidase promoter was amplified from *Ae. aegypti* Bangkok strain with primers EM1031 and EM1032, the Polyubiquitin promoter with EM758 and EM759. The *P450* open reading frame was amplified from Bakoumba with EM1552 and EM1553; the *P450* transcription terminator region with EM1554 and EM1555. The Golden Gate Cloning-compatible destination vectors used were either the attB docking plasmids pDSAT and pDSAR ([43]; Addgene #62290 and 62292) for the HAP1 promoter-GFP and HAP3 promoter-GFP reporter genes or a new attB docking plasmid,

pENTR-R4-ATCCLacZGCTT-attB (available on request), for the Carboxipeptidase-P450 construct. For transgenesis, freshly laid *Aedes aegypti* eggs of wild-type strain Bangkok, or of docking line X18A5 carrying an attP site (see below, strain available on request), were aligned along a wet nitrocellulose membrane as described for *Anopheles*[43] and injected with 400 ng/μl DNA in 0.5X PBS in the posterior pole, using quartz capillaries: 300 ng/μl transgenesis plasmid and 100 ng/μl helper plasmid encoding either piggyBac transposase ([44], available on request) or PhiC31 integrase (Addgene #183966). Survivor injected mosquito adults were crossed to an excess of wild-type mosquitoes; transgenic larvae were identified in the progeny by screening for fluorescence markers[44]. The *Ae. aegypti* docking line X18A5 was created by excising the *Cp-Loqs2* transgene from a previously described transgenic line [45] via embryo microinjection of a Cre recombinase-expressing helper plasmid, leaving in the genome only a piggyBac insertion carrying an attP docking site, which we made homozygous.

***In situ* GFP quantification**

Pupae were imaged with a Nikon SMZ-18 fluorescence microscope. Every image was taken at the same magnification and exposure time. Images obtained were analyzed using Icy software [41] (version 2.4.2.0). GFP-positive patches were manually delimited, and mean GFP signal intensity was automatically computed using Icy's ROI analysis tool. Mean signal intensities were compared using a Mann-Whitney's test.

Promoter genotyping

Five- to seven-day-old female mosquitoes were submitted to a mock bloodmeal as described above. 24 hours after blood feeding, individual legs were collected in DNAzol DIRECT (DN131, Molecular Research Center, Inc.) for genotyping. The leg tissue was homogenized using a Precellys® tissue homogenizer (6000 x 30 s), briefly centrifuged, and then placed at room temperature for immediate use in PCR.

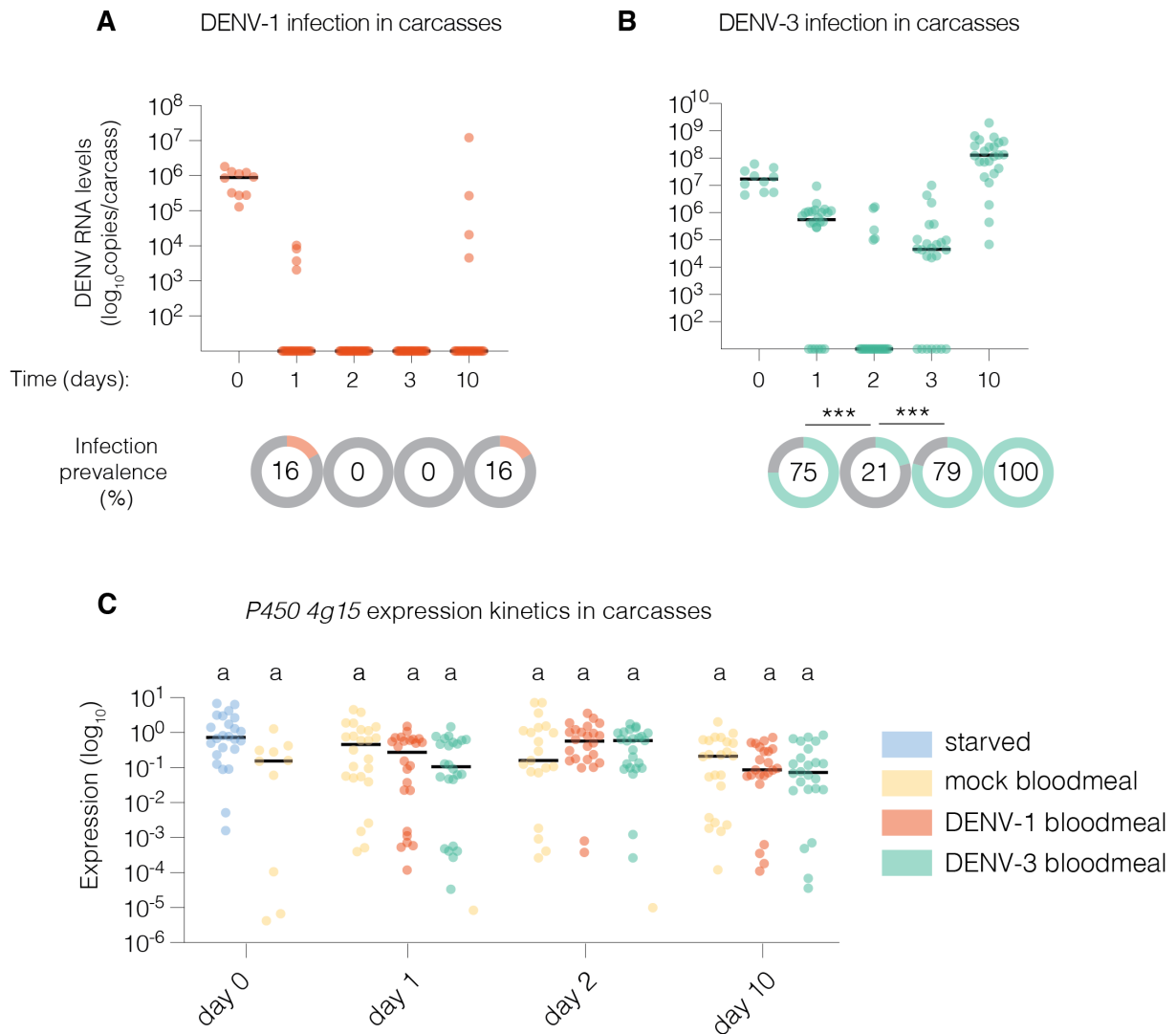
PCRs were performed using DreamTaq DNA Polymerase (EP0701, ThermoFisher Scientific) based on manufacturer's instructions, using "P450 GT F" and "P450 GT rev I" primers*. Approximately 0.6ul of the DNAzol DNA extract from leg tissue was used in 19ul of DreamTaq PCR master mix. The PCR cycle consisted of 3 min of initial denaturation at 95°C, 38 cycles of denaturation (98°C for 1 min, annealing (62°C for 18 sec), extension (72°C for 45 sec), and a final extension step of 5 min at 72°C. Amplicons (~1200 bp) were purified and subsequently Sanger sequenced (Eurofins) with "P450 x1 seq 420R" primer *. Promoter haplotypes were determined based on the obtained sequencing chromatograms.

*See Supplementary Table 1 for oligonucleotide sequences.

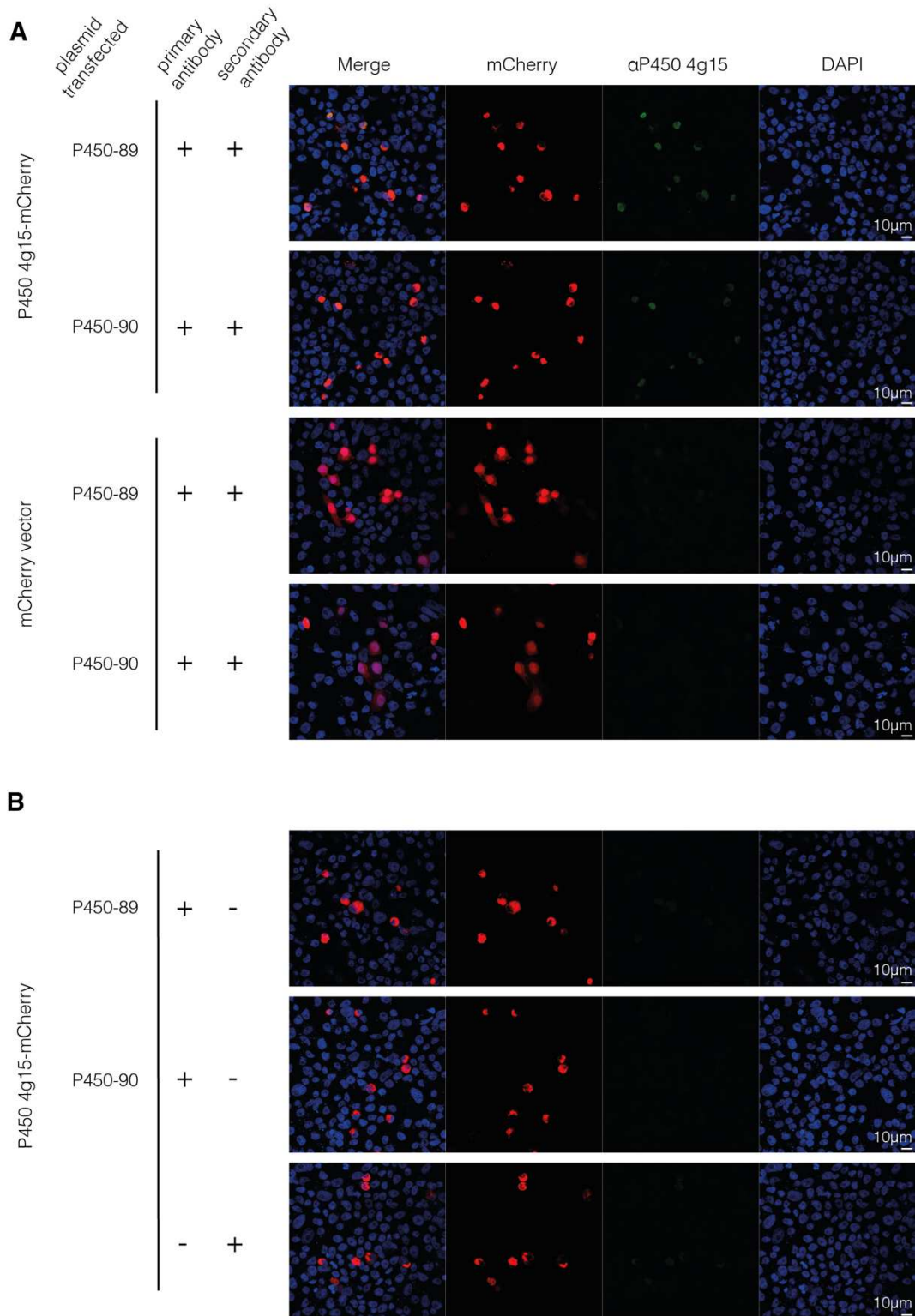
Statistical analysis

Gene expression data were analyzed by one-way analysis of variance (ANOVA) after \log_{10} -transformation of the 2^{-dCt} values, followed by Tukey-Kramer's HSD test. Non-zero viral loads, mean signal intensities and GFP transcript levels were compared pairwise with Mann-Whitney's non-parametric tests because their distribution did not satisfy the assumptions of ANOVA. Differences in intensity ratios and dot counts were compared using Student's t-tests. Viral prevalence was analyzed using chi-squared non-parametric test. Statistical analyses were performed in GraphPad Prism v.10.1.0 (www.graphpad.com) and JMP v.14.0.0 (www.jmp.com).

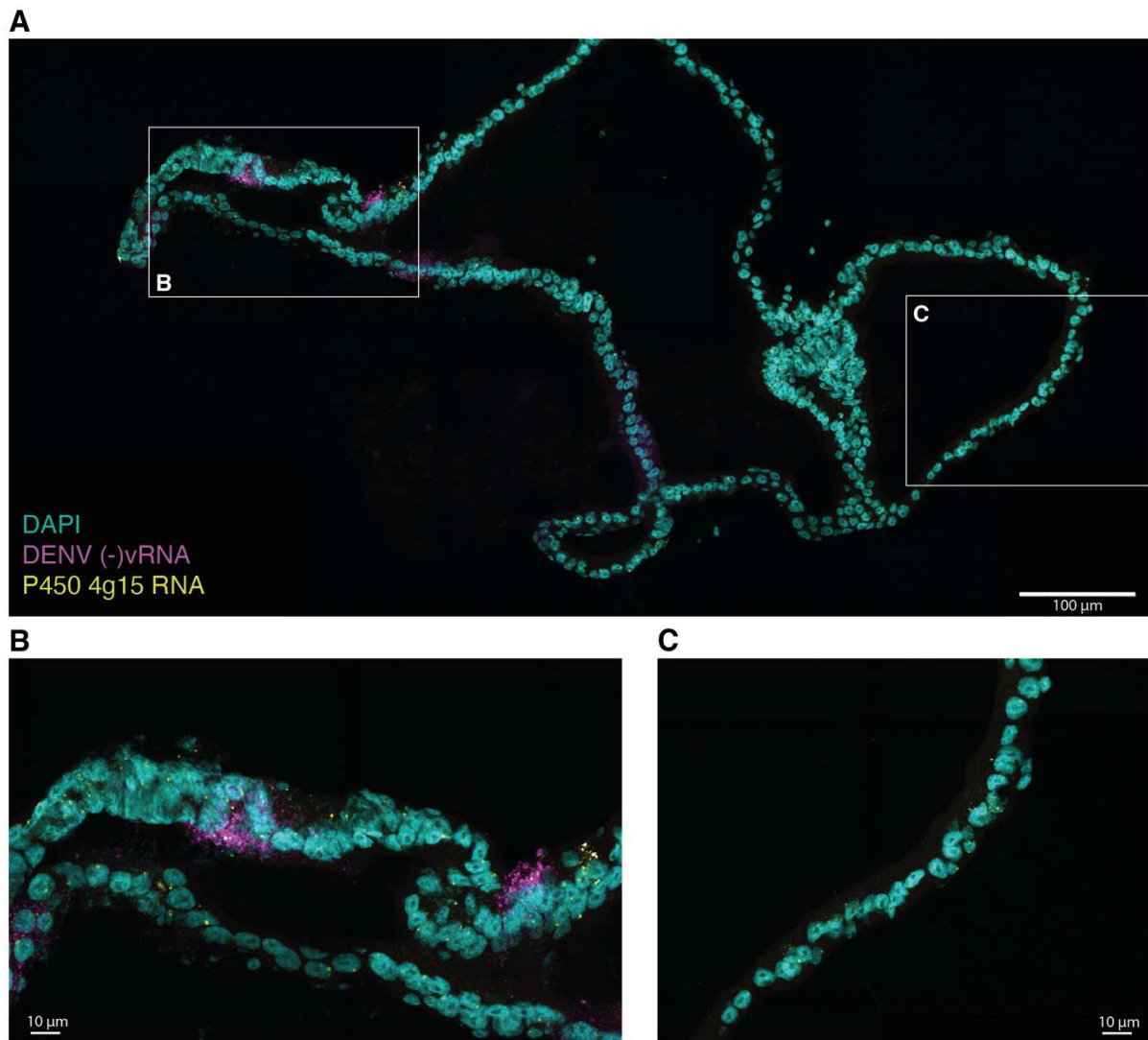
SUPPLEMENTARY FIGURES



Supplementary Figure S1. *P450 4g15* is not induced in carcasses after bloodmeal ingestion. (A-B) Viral RNA loads and prevalence in carcasses (bodies without midgut) of mosquitoes exposed to an infectious bloodmeal containing 2.5×10^7 FFU/mL of DENV-1 (A) or 8.8×10^7 of DENV-3 (C) on days 0, 1, 2, 7 and 10 after virus exposure. (C) Corresponding expression levels of *P450 4g15* in mosquito midguts quantified by RT-qPCR, in DENV-1- and DENV-3-exposed conditions as well as a mock bloodmeal condition. Expression levels are normalized with the expression levels of the housekeeping gene *RP49* and expressed as $2^{-dCt} = 2^{-(Ct_{P450\ 4g15} - Ct_{RP49})}$. Statistical significance was determined using one-way ANOVA after \log_{10} -transformation of the 2^{-dCt} values, followed by Tukey-Kramer's HSD test. Statistical significance is represented above the graph using connecting letters, whereby groups that do not share a letter are significantly different. In (A-C), each datapoint represents an individual midgut.



Supplementary Figure S2. P450 4g15 antibody specificity assay. (A-B) P450 4g15 immunostaining of C6/36 cells transfected with either a control mCherry plasmid (empty vector) or a P450 4g15-mCherry construct. (A) Cells were stained with custom-made rabbit antibodies targeting P450 4g15, respectively designated “-89” and “-90” and a secondary anti-rabbit antibody, as well as DAPI. mCherry signal correspond to the 594 nm signal, α P450 4g15 signal correspond to the 488 nm signal from the secondary antibody. (B) Staining controls with (+) or without (-) primary or secondary antibodies respectively.



Supplementary Figure S3. RNAscope imaging for *in situ* quantification of *P450 4g15* RNA levels in midguts. Multiplex RNA-FISH of a whole midgut slice of a Bakoumba mosquito 48 hours after a DENV-3-containing bloodmeal. Sample was stained with DAPI and probes targeting *P450 4g15* RNA and DENV RNA (negative strand) and imaged using a confocal microscope. (B-C) are magnified images of white-delimited regions in (A). (B) Early infection foci. (C) Uninfected region. Maximum intensity projection of z-stacks is represented. Scale bars: 100 μm in (A), 10 μm in (B-C).

SUPPLEMENTARY TABLES

Supplementary Table 1. Oligonucleotide sequences

Primer name	Application	Sequence (5'-3')
KD-38/2-qPCR-fwd	<i>P450 4g15</i> qPCR	AGGGATTCTGACTATGCGATG
KD-38/2-qPCR-rev	<i>P450 4g15</i> qPCR	GGTGAAGTTGAAGACGGAGTC
NS5F-VR-D1Thai	DENV-1 qPCR	GGAAGGAGAAGGACTCCACA
NS5R-VR-D1Thai	DENV-1 qPCR	ATCCTTGTATCCCATCCGGCT
DSQ1-VR	probe for DENV-1 qPCR	5'-FAM-CTCAGAGACATATCAAAGATTCCAGGG-BHQ1-3'
NS5F-D3GabThai-DJ	DENV-3 qPCR	AGAAGGAGAAGGACTGCACA
NS5R-D3GabThai-DJ	DENV-3 qPCR	ATTCTTGTGTCCCAACCGGCT
D3T-NS5-FamProb	probe for DENV-3 qPCR	5'-FAM-ACATCTCTAAGATACCCGGAGGAG-BHQ1-3'
P450-qPCR-wobble-FOR	<i>P450 4g15</i> qPCR	AGGGATTYGAYTATGCGATG
P450-qPCR-wobble-REV	<i>P450 4g15</i> qPCR	GGTGAAGTTGAAGACRGAGTC
RP49 for	<i>RP49</i> qPCR	ACAAGCTTGCCCCCAACT
RP49 rev	<i>RP49</i> qPCR	GTAACCGATGTTTGGC

ACKNOWLEDGEMENTS

We thank Catherine Lallemand for assistance with mosquito rearing, Natalia Zmarlak for kindly sharing the protocol for mosquito midgut immunostaining, and the Van Rij lab for providing the mCherry plasmid and advice on the antibody specificity assay. We also thank the Photonic BioImaging Hub (C2RT, Institut Pasteur, France) and the Image Analysis Hub (Institut Pasteur, France) for assistance with *in situ* imaging and image analysis.

REFERENCES

1. Kraemer, M.U., et al., *The global distribution of the arbovirus vectors Aedes aegypti and Ae. albopictus*. Elife, 2015. **4**: p. e08347.
2. Brady, O.J. and S.I. Hay, *The Global Expansion of Dengue: How Aedes aegypti Mosquitoes Enabled the First Pandemic Arbovirus*. Annu Rev Entomol, 2020. **65**: p. 191-208.
3. Katzelnick, L.C., et al., *Dengue viruses cluster antigenically but not as discrete serotypes*. Science, 2015. **349**(6254): p. 1338-43.
4. Gubler, D.J. and L. Rosen, *A simple technique for demonstrating transmission of dengue virus by mosquitoes without the use of vertebrate hosts*. Am J Trop Med Hyg, 1976. **25**(1): p. 146-50.
5. Gubler, D.J., et al., *Variation in susceptibility to oral infection with dengue viruses among geographic strains of Aedes aegypti*. Am J Trop Med Hyg, 1979. **28**(6): p. 1045-52.
6. Salazar, M.I., et al., *Dengue virus type 2: replication and tropisms in orally infected Aedes aegypti mosquitoes*. BMC Microbiol, 2007. **7**: p. 9.
7. Conway, M.J., T.M. Colpitts, and E. Fikrig, *Role of the Vector in Arbovirus Transmission*. Annu Rev Virol, 2014. **1**(1): p. 71-88.
8. Johnson, R.M., et al., *Investigating the dose-dependency of the midgut escape barrier using a mechanistic model of within-mosquito dengue virus population dynamics*. PLoS Pathog, 2024. **20**(4): p. e1011975.
9. Sigle, L.T. and E.A. McGraw, *Expanding the canon: Non-classical mosquito genes at the interface of arboviral infection*. Insect Biochem Mol Biol, 2019. **109**: p. 72-80.
10. Martins, N., J.L. Imler, and C. Meignin, *Discovery of novel targets for antivirals: learning from flies*. Curr Opin Virol, 2016. **20**: p. 64-70.
11. Bonizzoni, M., et al., *Complex modulation of the Aedes aegypti transcriptome in response to dengue virus infection*. PLoS One, 2012. **7**(11): p. e50512.
12. Colpitts, T.M., et al., *Alterations in the Aedes aegypti transcriptome during infection with West Nile, dengue and yellow fever viruses*. PLoS Pathog, 2011. **7**(9): p. e1002189.
13. Fansiri, T., et al., *Genetic mapping of specific interactions between Aedes aegypti mosquitoes and dengue viruses*. PLoS Genet, 2013. **9**(8): p. e1003621.
14. Dabo, S., et al., *Extensive variation and strain-specificity in dengue virus susceptibility among African Aedes aegypti populations*. PLoS Negl Trop Dis, 2024. **18**(3): p. e0011862.
15. Dickson, L.B., et al., *Exome-wide association study reveals largely distinct gene sets underlying specific resistance to dengue virus types 1 and 3 in Aedes aegypti*. PLoS Genet, 2020. **16**(5): p. e1008794.
16. Gloria-Soria, A., et al., *Global genetic diversity of Aedes aegypti*. Mol Ecol, 2016. **25**(21): p. 5377-5395.
17. Isin, E.M. and F.P. Guengerich, *Complex reactions catalyzed by cytochrome P450 enzymes*. Biochim Biophys Acta, 2007. **1770**(3): p. 314-29.
18. Hannemann, F., et al., *Cytochrome P450 systems--biological variations of electron transport chains*. Biochim Biophys Acta, 2007. **1770**(3): p. 330-44.
19. Mansuy, D., *The great diversity of reactions catalyzed by cytochromes P450*. Comp Biochem Physiol C Pharmacol Toxicol Endocrinol, 1998. **121**(1-3): p. 5-14.

20. Stavropoulou, E., G.G. Pircalabioru, and E. Bezirtzoglou, *The Role of Cytochromes P450 in Infection*. Front Immunol, 2018. **9**: p. 89.
21. Warren, J.T., et al., *Molecular and biochemical characterization of two P450 enzymes in the ecdysteroidogenic pathway of Drosophila melanogaster*. Proc Natl Acad Sci U S A, 2002. **99**(17): p. 11043-8.
22. Warren, J.T., et al., *Phantom encodes the 25-hydroxylase of Drosophila melanogaster and Bombyx mori: a P450 enzyme critical in ecdysone biosynthesis*. Insect Biochem Mol Biol, 2004. **34**(9): p. 991-1010.
23. Ono, H., et al., *Spook and Spookier code for stage-specific components of the ecdysone biosynthetic pathway in Diptera*. Dev Biol, 2006. **298**(2): p. 555-70.
24. Daborn, P.J., et al., *A single p450 allele associated with insecticide resistance in Drosophila*. Science, 2002. **297**(5590): p. 2253-6.
25. Berge, J.B., R. Feyereisen, and M. Amichot, *Cytochrome P450 monooxygenases and insecticide resistance in insects*. Philos Trans R Soc Lond B Biol Sci, 1998. **353**(1376): p. 1701-5.
26. Dierick, H.A. and R.J. Greenspan, *Molecular analysis of flies selected for aggressive behavior*. Nat Genet, 2006. **38**(9): p. 1023-31.
27. Fujii, S., A. Toyama, and H. Amrein, *A male-specific fatty acid omega-hydroxylase, SXE1, is necessary for efficient male mating in Drosophila melanogaster*. Genetics, 2008. **180**(1): p. 179-90.
28. Chung, H., et al., *Characterization of Drosophila melanogaster cytochrome P450 genes*. Proc Natl Acad Sci U S A, 2009. **106**(14): p. 5731-6.
29. Erben, L. and A. Buonanno, *Detection and Quantification of Multiple RNA Sequences Using Emerging Ultrasensitive Fluorescent In Situ Hybridization Techniques*. Curr Protoc Neurosci, 2019. **87**(1): p. e63.
30. Franz, A.W., et al., *Tissue Barriers to Arbovirus Infection in Mosquitoes*. Viruses, 2015. **7**(7): p. 3741-67.
31. Zhang, M., et al., *Quantitative analysis of replication and tropisms of Dengue virus type 2 in Aedes albopictus*. Am J Trop Med Hyg, 2010. **83**(3): p. 700-7.
32. Zhao, B., et al., *Regulation of the gut-specific carboxypeptidase: a study using the binary Gal4/UAS system in the mosquito Aedes aegypti*. Insect Biochem Mol Biol, 2014. **54**: p. 1-10.
33. Isoe, J., et al., *Molecular genetic analysis of midgut serine proteases in Aedes aegypti mosquitoes*. Insect Biochem Mol Biol, 2009. **39**(12): p. 903-12.
34. Edwards, M.J., et al., *Characterization of a carboxypeptidase A gene from the mosquito, Aedes aegypti*. Insect Mol Biol, 2000. **9**(1): p. 33-8.
35. Gonzalez-Arzola, K., et al., *Nucleus-translocated mitochondrial cytochrome c liberates nucleophosmin-sequestered ARF tumor suppressor by changing nucleolar liquid-liquid phase separation*. Nat Struct Mol Biol, 2022. **29**(10): p. 1024-1036.
36. Makki, R., E. Cinnamon, and A.P. Gould, *The development and functions of oenocytes*. Annu Rev Entomol, 2014. **59**: p. 405-25.
37. Qiu, Y., et al., *An insect-specific P450 oxidative decarbonylase for cuticular hydrocarbon biosynthesis*. Proc Natl Acad Sci U S A, 2012. **109**(37): p. 14858-63.
38. Caron, M., et al., *First evidence of simultaneous circulation of three different dengue virus serotypes in Africa*. PLoS ONE, 2013. **8**(10): p. e78030.

39. Fontaine, A., et al., *Excretion of dengue virus RNA by Aedes aegypti allows non-destructive monitoring of viral dissemination in individual mosquitoes*. Sci Rep, 2016. **6**: p. 24885.
40. Wang, F., et al., *RNAscope: a novel in situ RNA analysis platform for formalin-fixed, paraffin-embedded tissues*. J Mol Diagn, 2012. **14**(1): p. 22-9.
41. de Chaumont, F., et al., *Icy: an open bioimage informatics platform for extended reproducible research*. Nat Methods, 2012. **9**(7): p. 690-6.
42. Engler, C. and S. Marillonnet, *Golden Gate cloning*. Methods Mol Biol, 2014. **1116**: p. 119-31.
43. Volohonsky, G., et al., *Tools for Anopheles gambiae Transgenesis*. G3 (Bethesda), 2015. **5**(6): p. 1151-63.
44. Lutrat, C., et al., *Transgenic expression of Nix converts genetic females into males and allows automated sex sorting in Aedes albopictus*. Commun Biol, 2022. **5**(1): p. 210.
45. Olmo, R.P., et al., *Control of dengue virus in the midgut of Aedes aegypti by ectopic expression of the dsRNA-binding protein Loqs2*. Nat Microbiol, 2018. **3**(12): p. 1385-1393.

-CHAPTER 3-

***In vivo* characterization of a candidate dengue virus receptor,
prohibitin-2, in *Aedes aegypti* mosquito midguts.**

Elodie Couderc, Anna B. Crist, Louis Lambrechts[‡], Sarah H. Merklings[‡]

CHAPTER 3: *In vivo* characterization of a candidate dengue virus receptor, prohibitin-2, in *Aedes aegypti* mosquito midguts

Elodie Couderc^{1,2}, Anna B. Crist¹, Louis Lambrechts^{1,‡}, Sarah H. Merklings^{1,‡}

¹Institut Pasteur, Université Paris Cité, CNRS UMR2000, Insect-Virus Interactions Unit, 75015 Paris, France

²Sorbonne Université, Collège Doctoral, 75005 Paris, France

‡These authors contributed equally

ABSTRACT

The identity of dengue virus (DENV) receptors in the mosquito host remains undetermined. Candidate receptors have been identified *in vitro*, but evidence of their importance for viral entry *in vivo* is lacking. Nevertheless, viral receptors in the vector are very promising targets for strategies aiming at hindering arbovirus infection in mosquitoes and subsequent transmission to humans. Therefore, confirming the relevance of these putative receptors *in vivo* is critical. This chapter presents a candidate-oriented approach based on reverse genetics, where we aimed to characterize the function of putative DENV receptors in the midgut of *Aedes aegypti* mosquitoes, with a particular focus on the candidate receptor *prohibitin-2*. We showed a proviral effect of *prohibitin-2* on DENV replication in mosquitoes' bodies. Yet, despite a variety of experimental approaches, *prohibitin-2* did not demonstrate a significant role in DENV entry in mosquito midgut cells *in vivo*.

INTRODUCTION

Dengue viruses (DENVs) are the etiological agents of the most prevalent mosquito-borne viral disease in humans [1]. DENVs are flaviviruses transmitted to humans by mosquitoes of the *Aedes* genus [2]. Almost half the world's population is estimated at risk for DENV infection, which can trigger pathologies ranging from a self-limiting illness to a severe hemorrhagic fever and fatal dengue shock syndrome responsible for 22,000 deaths each year [3-6].

Elucidating the molecular mechanisms underlying interactions between DENV and their arthropod and mammalian hosts is essential to understanding flavivirus transmission routes and associated pathologies. Host cell susceptibility to virus infection is mediated, at least partially, by the presence and abundance of viral receptors on the cell membrane. Flavivirus receptors are key targets for antiviral drugs [7] and have been the focus of extensive work aimed at characterizing them in mammals [8].

Identifying flavivirus entry receptors in the mosquito could potentially lead to identification of novel therapeutic targets and alternatives for vector control. However, flavivirus receptors in *Aedes* mosquitoes remains poorly known and characterized.

I- Definition of virus receptors

Viral receptors are surface molecules which bind the viral particle and trigger its internalization. Hence, a viral receptor is a cell surface component recognized by the virus as an entry gateway into the cell [9-12]. Proteins are over-represented among viral receptors compared to carbohydrates and lipids, probably because of the higher specificity and stronger affinity they confer to the physical interaction between virus and host [13].

This definition gives rise to certain requirements for a protein to be identified as a candidate receptor. A receptor must be expressed on the surface of susceptible cells and bind to at least one viral protein present at the surface of the virion. Functionally, competition on the binding site of the receptor should hamper viral entry. Additionally, the receptors' identity is linked to the virus' host range and its cellular and tissular tropism [14]. Of note, some receptors form complexes composed of several proteins [14].

Receptors *per se* differ from attachment factors and entry factors. Attachment factors are responsible for the early attachment of the virus to the cell surface via non-specific interactions, often non-protein-protein interactions, which catalyze virus binding to receptors [10, 12]. "Entry factor" is an umbrella term for cellular proteins which facilitate viral entry but are not necessarily capable of binding viral particles and triggering their internalization on their own. Entry factors

are not necessarily expressed on the plasma membrane as they can facilitate virus entry from the cytoplasm [9, 12, 15].

The variety of flavivirus candidate receptors identified from mammalian studies suggests these viruses recognize and bind to several cell surface molecules rather than having a unique specific receptor [8, 14, 16]. Such a panel of interacting molecules might suggest an evolution towards a non-specific interaction with the host which allows to infect a wider diversity of cells, tissues and organs. Yet, some DENV receptors also seem to be serotype-specific [17-20]. In mosquitoes however, the identity of flavivirus receptors remains unclear. Protein binding assays and mass spectrometry analyses identified putative receptors [21-29]. However, a limited number of candidate receptors in the mosquito have been functionally validated. Examples of these candidates include the laminin-binding protein [27], the tubulin-like protein [22], hsc70 [30], enolase [23, 24, 26], prohibitin 1/2 [31, 32], or glycosphingolipid-L3 [33].

Reasons for existing gaps between studies in arthropods and mammals are plural. Biomolecular tools (antibodies, relevant cell models, etc.) are often limited in mosquito studies and bioinformatics databases and genome annotations remain incomplete. Functional annotations, such as Gene Ontology terms or KEGG (Kyoto Encyclopedia of Genes and Genomes) pathway annotations are still scarce. Most studies carried out in mosquitoes led to the identification of virus-interacting proteins based on their molecular weight, without further characterization, which led to uncertainties about the identity and the physiological relevance of these candidate receptors *in vivo*. This observation emphasizes the importance of *in vivo* functional validation of these mosquito candidate receptors.

II- Approaches for discovery of DENV receptors in mosquitoes

A) Relevance of models used for receptor investigation

To this day, studies aiming to identify DENV receptors in mosquitoes relied mostly on *in vitro* work. Classical assays are based on measuring interactions between viral proteins or particles with mosquito protein lysates in denaturing conditions, in which protein tridimensional conformations and accessibility of interaction motifs are altered. Moreover, physiological conditions *in vivo* are associated with a number of parameters that are not taken into account in these *in vitro* studies, such as native receptor conformations, transient interactions within receptor complexes, temperature change between hosts [34], differential pH between tissues [35], etc.

Several mosquito cell lines are available and commonly used, e.g., Aag2 and CCL-125 (*Ae. aegypti*-derived), C6/36 and U4.4 (*Ae. albopictus*-derived). Yet, these cell lines were derived

from mosquito embryonic or larval stages [36-38] and are each composed of an unknown and likely single cell type. It is likely that these cell lines are not physiologically relevant to model the infection cycle like it occurs in the mosquito's organism. Indeed, homogenous cell cultures do not feature the variety of cell populations (and potential receptors) encountered by the virus. In the mosquito, the virus transits from the midgut to intermediate tissues, such as the fat body and hemocytes, to the salivary glands. Additionally, the strong temperature change between the mammalian host (~37°C) and the mosquito (~28°C but variable depending on the environment, as mosquitoes are ectotherms) is likely to impact virion conformation throughout the different stages of mosquito infection [34].

It is hitherto unclear whether the different mosquito tissues share the same viral receptors. The fact that human receptors vary between different organs [8] suggest the existence of a similar panel of receptors in the mosquito tissues. This possibility is consistent with the variety of candidate receptors currently considered. Additionally, primary infection of the mosquito midgut involves viral particles produced in mammalian cells, whereas virions reaching the salivary glands originate from mosquito cells. The differences expected in the surface conformation of the virions (detailed in the next section) could potentially imply different receptors at the cell surface of each tissue. Thus, *in vivo* studies remain most relevant to recapitulate the physiological conditions that characterize the full infectious cycle of viral particles in the mosquito's organism.

B) Conformational variation in virion structure and impact on receptor compatibility

The existence of a range of structurally distinct virions makes the study of arbovirus receptors quite complex.

Indeed, temperature influences the conformation of flaviviral particles [39]. As temperature conditions differ between mammalian and insect organisms (~37°C versus ~28°C), differences in virion morphology in each host must be kept in mind while investigating host-specific viral receptors [34].

Additionally, it was recently demonstrated that envelope (E) protein ubiquitination is important for flavivirus infection in mice but not in mosquitoes [40]. Viral entry in mammalian cells, but not mosquito cells, was facilitated by E protein ubiquitination. In mammals, ubiquitination of the E protein promoted its binding to TIM1, which likely facilitates subsequent virus entry in mammalian cells. Interestingly, virions originating from mosquito cells have reduced ubiquitination levels [40]. However, since viral transmission from mosquitoes to humans occurs

nevertheless *in vivo*, other molecular mechanisms must facilitate the entry into mammalian cells.

Moreover, virions originating from vertebrate and invertebrate cells do not share the same glycosylation patterns presented on their membrane. Mosquito cells produce virions with a high mannose content, whereas mammalian cells produce virions that have a more complex carbohydrate structure [41]. E protein glycosylation was also shown to rather enhance viral entry in human but not mosquito cells, in which it decreased infectivity [42, 43]. Overall, the impact of E protein glycosylation on flaviviral entry in both vertebrate and invertebrate hosts is not consensual and is probably virus- and host-specific.

Therefore, the versatility in structural conformation inherent to viruses adapted to radically different hosts should be taken into consideration when looking for candidate receptors.

C) Technical approaches for receptor identification

It is likely that the mechanism of entry into mammalian and insect cells is, to a certain extent, evolutionarily conserved, considering that flavivirus virions present only one glycoprotein, the envelope protein E, on their surface [15, 44, 45]. The molecular mechanisms underlying flavivirus binding and entry in mammalian cells have been extensively elucidated: the E protein domain III is responsible for the interaction with attachment factors and receptors on the target cell prior to entry [46, 47]. Similarity-based prediction methods of virus-receptors interactions can be used to systematically identify candidate receptors [13, 48]. Knowledge on mammalian DENV receptors could therefore provide a foundation for mosquito receptors identification. Screening mammalian DENV receptor homologs in mosquito genomes could guide the identification of novel mosquito candidate receptors prior to further functional investigation.

Most mosquito candidate receptors were identified by protein interactomic studies. Among the most common techniques in early studies, virus overlay protein binding assays (VOPBA) and envelope protein binding assays, following by protein separation methods and/or mass spectrometry on membrane fractions, identified several putative receptors [21-26]. In a similar way, protein microarrays allow for the detection of protein interactions without the need for an SDS-PAGE separation [49-51]. However, these methods may detect interactions that are not biologically relevant *in vivo*. Nevertheless, novel cross-linking strategies coupled with mass spectrometry now allow for the detection of transient intermolecular interactions within native environments [49, 52].

Genomic approaches, such as loss- or gain-of-function screens, allow to inactivate host factors, introduce exogenous factors or overexpress endogenous genes, to identify candidates promoting viral entry. CRISPR-associated methods have proven useful for the identification of many viral host factors [53, 54], but these techniques have had limited success in identifying viral receptors. The use of RNA interference (RNAi) for gene knockdowns facilitates the implementation of loss-of-function screens, despite a notable lack of reproducibility between studies [49].

D) Functional validation of candidate receptors

Following the identification of candidate receptors, functional validation of the candidates is required to conclude on their biological relevance. The gold standard of receptor identification consists in expressing the identified receptor candidate in a non-permissive cell line to render it susceptible to infection (*i.e.*, gain-of-function confirmation). Additionally, genes whose expression correlates with host susceptibility stand as promising candidates.

However, other functional assays allow to distinguish host factors from receptors [55]. Competition assays, *e.g.*, antibody-mediated inhibition assays, can demonstrate that competing for the accessibility of a membrane protein prevents viral entry, and thus confirm the classification of a factor as a receptor. Binding and entry assays allow to desynchronize viral attachment to the cell membrane, endocytosis, and fusion, using variation in temperature and pH. Thus, combining gene-silencing techniques or molecule-mediated inhibition together with a binding and entry assay can provide strong evidence for the involvement of a candidate protein in one of the early steps of viral infection.

In short, the identity of the viral receptors mediating DENV entry in *Ae. aegypti* mosquito cells remain unclear. Putative receptors have never been functionally validated *in vivo*. Our study aimed to provide *in vivo* functional validation and characterization of candidate receptors of DENV in mosquitoes.

RESULTS

I- Screening of DENV candidate receptors in *Ae. aegypti*

A) Selection of candidate receptors from the literature

To pick the most promising candidate receptors to test *in vivo*, we defined stringent selection criteria as follows: presence at the membrane of mosquito cells, validated interaction with DENV particles and/or proteins, sequence similarity with characterized mammalian DENV receptors, and functional evidence of their role in DENV infection of mosquito cell lines. Based on these selection criteria, we identified three putative DENV receptors: *phb2*, *enolase* and *Hsc70-4*.

Prohibitin-2 (*phb2*, *AAEL013952*) is a mitochondrial protein, but its presence on the plasma membrane was also proven [31]. It was shown to colocalize and co-precipitate with DENV E protein [31]. Its proviral activity was demonstrated by RNAi-mediated knockdown and its involvement in the entry step of DENV serotype 2 (DENV-2) was proven using an antibody-mediated inhibition assay [31]. Moreover, the human orthologs of *phb1* and *phb2* (accession numbers 528281407 and 221307584) were identified as a receptor complex mediating the entry of DENV-3 in human neuroblastoma and microglial cells, which might indicate a functional homology with mosquito *phb2* [56].

The *enolase* gene (*AAEL024228*) is expressed on the mosquito midgut brush border [57]. The enolase protein from C6/36 cells and *Ae. aegypti* midguts was shown to co-precipitate with DENV and West Nile virus E and capsid proteins and was proposed as a marker of vector competence in *Ae. aegypti* [23-26, 58]. Additionally, the human α -enolase is known to be secreted by hepatic cells in response to DENV infection, even though its involvement in entry is unknown [59].

The heat-shock 70 kDa protein cognate 4 (*Hsc70-4*, *AAEL019403*) is found in mosquito midguts and is known to be re-addressed to the cell surface upon DENV infection [29, 30]. The related protein Hsp70 appeared to be upregulated upon blood feeding [60]. A model suggests that Hsc70 might modulate the transition of the E protein from a dimer to a trimer conformation, like the human homolog Hsp70 [29, 30, 61]. Hsp70 is involved in DENV binding to human cells [17].

Thus, we selected these three putative DENV receptors for *in vivo* investigation of their proviral activities.

B) Characterization of DENV candidate receptors by *in vivo* gene knockdown in mosquitoes

To validate the role of these pre-selected candidate receptors during DENV infection of *Ae. aegypti*, *in vivo* silencing of the candidates was performed using RNAi by injection of double-stranded RNA (dsRNA) targeting one of the genes of interest: *phb2*, *enolase* and *hsc70-4* (Figure 1). Control mosquitoes were injected with a dsRNA targeting *Luciferase*. Experiments were performed in an *Ae. aegypti* mosquito colony originating from Kamphaeng Phet province, Thailand. Candidate-depleted mosquitoes were exposed to DENV-1 via an infectious bloodmeal. With gene knockdown efficiency verified by RT-qPCR (Figure 1A-C), viral prevalence and loads in candidate-depleted mosquitoes were assessed five days after infection by RT-qPCR of the viral genome on whole mosquito bodies (Figure 1D-E).

Hsc 70-4 knockdown induced severe mortality after blood feeding which did not allow to conclude on its role upon DENV infection. The results displayed on the graph were obtained from surviving mosquitoes presenting signs of moribundity; hence they should hardly be interpreted (Figure 1C, 1E).

In contrast, we managed to obtain an efficient and viable knockdown of *phb2* and *enolase* (Figure 1A-B). In the first experimental replicate, DENV prevalence was significantly reduced in *phb2*- and *enolase*-silenced mosquitoes (~30% reduction in transcript abundance, $p < 0.01$) compared to the controls (Figure 1D-E). These data indicated a potential proviral activity of both candidate genes in *Ae. aegypti* during DENV infection.

When performing a second experimental replicate to confirm the phenotype observed for *phb2* and *enolase*, we found no statistically significant impact of the knockdown of any of these two candidate genes on DENV prevalence. However, *phb2* knockdown led to reduced DENV RNA levels (up to a 10-fold reduction, $p < 0.0001$) in infected mosquitoes (Figure 1D-E). The impact of *phb2* depletion on viral prevalence and viral load suggested a potential involvement of *phb2* in two distinct mechanisms modulating DENV infection of mosquitoes, *i.e.*, establishment of the infection and subsequent viral replication.

In light of these results, and with *phb2* being the most characterized receptor candidate in mosquito cell lines [31], we decided to focus our efforts on investigating *phb2*'s potential proviral activity upon DENV infection of *Ae. aegypti*.

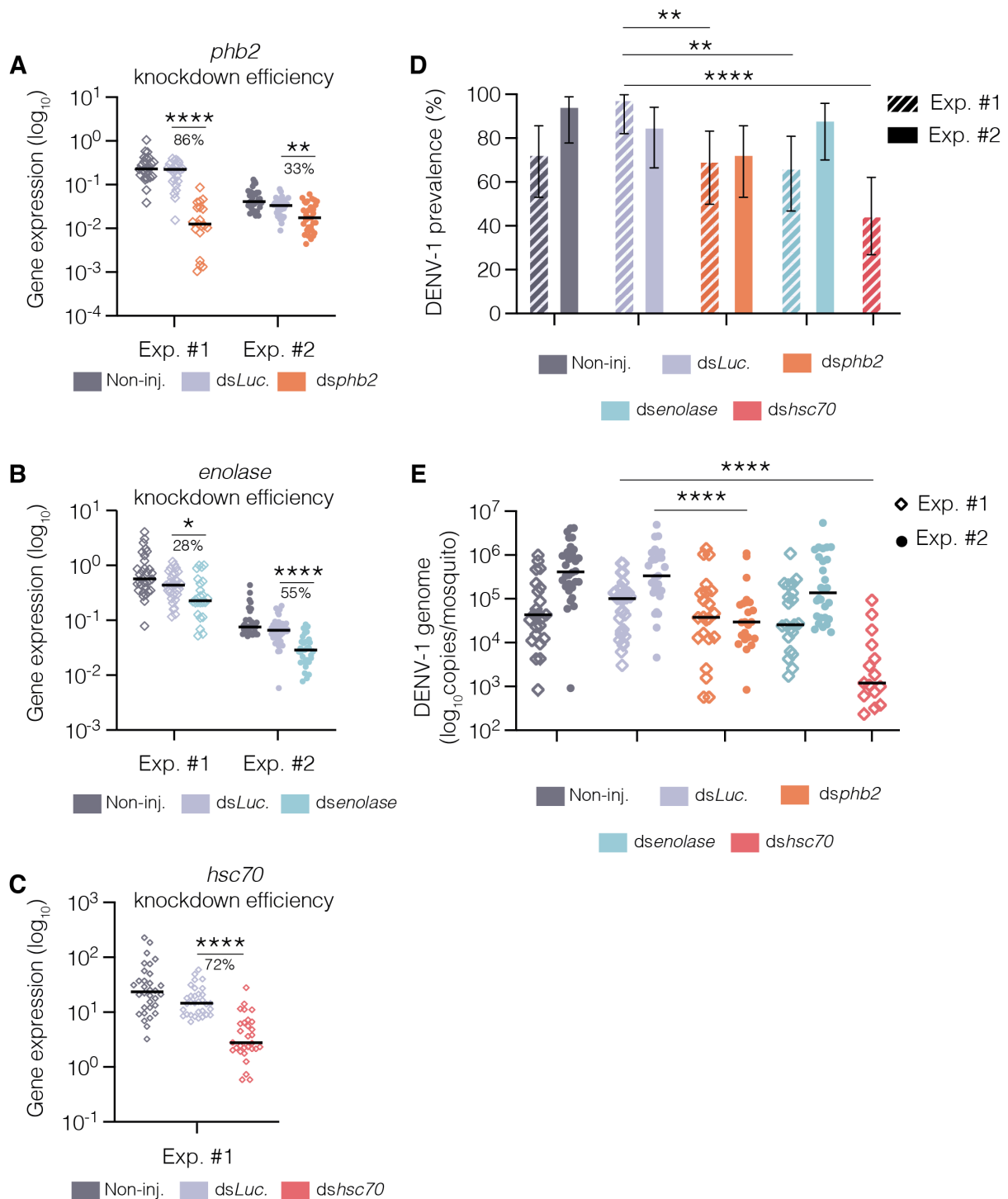


Figure 1. *phb2* has a proviral effect on DENV infection in *Ae. aegypti*. (A-C) Gene knockdown efficiency by RNAi-mediated *in vivo* gene silencing of *phb2* (A), *enolase* (B) and *hsc70* cognate 4 (C). Transcript abundance was quantified by RT-qPCR, normalized by transcript levels of the housekeeping gene *ribosomal protein 49* (*RP49*) and represented as $\log_{10}(2^{-\Delta\Delta Ct})$ with $\Delta\Delta Ct = Ct_{Gene} - Ct_{RP49}$. Knockdown efficiencies are represented for two experimental replicates. Non-injected mosquitoes and mosquitoes injected with a dsRNA targeting *Luciferase* are used as controls. Percentages indicated below significance stars represent the knockdown efficiency (KD%), calculated as $KD\% = (1 - \Delta(\Delta Ct)) * 100$, with $\Delta(\Delta Ct) = 2^{-\Delta\Delta Ct_{SilencedCondition}} / 2^{-\Delta\Delta Ct_{ControlCondition}}$. Statistical significance of pairwise differences were assessed with Mann-Whitney's test (* $p < 0.05$; ** $p < 0.01$; *** $p < 0.001$). (D-E)

DENV prevalence (D) and viral loads (E) of whole mosquito bodies (controls or candidate-depleted) after a DENV-1 infectious bloodmeal (containing 5×10^6 focus-forming units (FFU)/mL) were quantified by RT-qPCR of the viral genome. Experimental replicates are represented using different symbols. Vertical bars in (D) represent 95% confidence intervals. Statistical significance of pairwise differences were assessed with Mann-Whitney's test for the viral loads and a chi-squared test for the viral prevalence (* $p < 0.05$; ** $p < 0.01$; *** $p < 0.001$).

II- Investigation of the proviral activity of the DENV candidate receptor *prohibitin-2*

A) Description of the candidate receptor *phb2*

In mammals, *phb2* is a ubiquitously expressed mitochondrial protein which belongs to the superfamily of stomatin, prohibitin and HflK/C (lipid raft markers). Phb2 proteins can form homodimers or heterodimers with the paralog *phb1*. The designation of "prohibitin" originates from its function as a cell cycle-arrest protein [62]. Prohibitins are often described as coordinator or shuttle proteins, which act as intermediates between cellular compartments and mediate mitochondrial stability, transcriptional suppression, and signal transduction. *Phb2* expression is also correlated with lower levels of reactive oxygen species (ROS) and reduced inflammation processes (reviewed in [63]). Human *phb1* and *phb2* were suggested as receptor complexes for DENV-3 [56], while *phb1* was found downregulated in response to DENV-2 and DENV-4 infection [64].

Ae. aegypti mosquito prohibitins share ~75% amino acid identity with human prohibitins. *Ae. aegypti* *phb2* (AAEL013952) is a 299-amino-acid protein (33 kDa) containing a transmembrane domain required for mitochondrial localization in N-terminal position, a central PHB domain and a coiled-coil domain. In addition to these domains, *phb2* displays an ER-binding domain which contains a putative nuclear import sequence (Figure 2).

phb2 (AAEL013952) protein structure

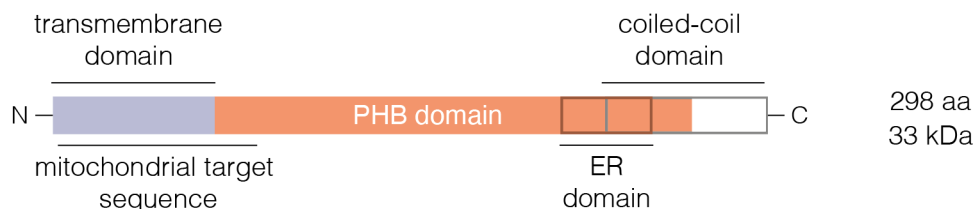


Figure 2. Structure of the *Ae. aegypti* *phb2* protein. Functional domains as annotated in the mammalian version of the *phb2* protein are depicted as colored boxes. The transmembrane domain is depicted in grey, the prohibitin domain in orange, the overlapping ER-interacting domain as an empty brown box and the overlapping coiled-coil domain as an empty grey box. The putative mitochondrial target sequence is also indicated. Size in amino acids (aa) and weight (kDa) are indicated on the right of the structure.

Ae. aegypti phb2 colocalizes with DENV E protein in C6/36 mosquito cells [31]. Phb2 was also identified as a DENV-2-binding protein in the membrane protein fraction of C6/36 and CCL-125 cells, as well as lysates of *Ae. aegypti* bodies (but not *Culex quinquefasciatus*, which are refractory to DENV [65]). Additionally, *in vitro* silencing of *phb2* reduces DENV-2 viral production and binding to the cell surface of C6/36 cells. Moreover, pre-incubation of C6/36 and CCL-125 cells with an anti-phb2 antibody hampers DENV-2 entry [31]. Remarkably, the proviral activity of *phb2* was observed for DENV-2 infection, but not for Japanese encephalitis virus, a flavivirus transmitted by mosquitoes of the *Culex* genus [31]. In contrast, another study proposed phb2 as a refractivity-conferring non-receptor molecule for DENV-2 [32].

Since the midgut is the first organ infected by DENV during the infectious cycle in the mosquito, we assessed the expression of phb2 in midgut tissues (Figure 3, Figure 8E). We performed immunostainings on midguts of female mosquitoes exposed to DENV-1 and observed a strong phb2 signal, in a patchy pattern, mostly in the posterior region of the tissue, indicating that phb2 is expressed in this organ, but with a heterogenous pattern (Figure 3). We also detected *phb2* transcripts by RT-qPCR on dissected mosquito midguts exposed to DENV-1 (Figure 8E). Hence, we confirmed the expression of the candidate receptor phb2 *in vivo*, in the midguts of a susceptible mosquito line exposed to DENV-1.

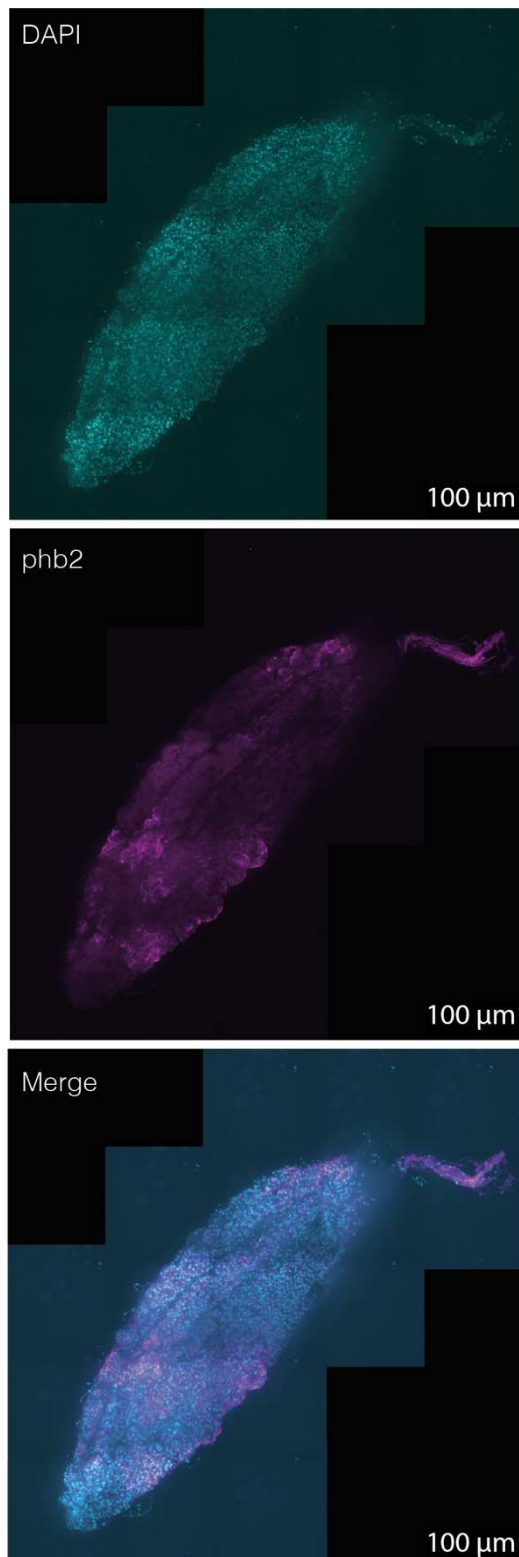


Figure 3. The phb2 protein is expressed in *Ae. aegypti* midguts. Immunostaining of phb2 in a female mosquito midgut exposed to DENV-1. Female mosquitoes were fed on a DENV-1 infectious bloodmeal and midguts were dissected five days after virus exposure. Midgut tissues were stained using an anti-phb2 antibody and nuclei were stained using DAPI. Imaging was performed using a spinning-disk confocal microscope (Cell Voyager CV1000). Maximum projection of z-stacks is represented.

B) *Phb2*'s proviral activity is observed during DENV infection but not CHIKV or ZIKV infection of *Ae. aegypti*

To further investigate the proviral activity of *phb2* in *Ae. aegypti* during DENV infection, we performed similar *phb2* knockdown experiments followed by infection with two other medically relevant viruses: another flavivirus, Zika virus (ZIKV), and an alphavirus, chikungunya virus (CHIKV). We injected female mosquitoes with dsRNA targeting *phb2* or *Luciferase* as a control. We confirmed knockdown efficiency and quantified viral RNA levels by RT-qPCR on whole mosquito bodies, on day 5 for ZIKV, and on day 2 for CHIKV (Figure 4).

Despite significant reduction of *phb2* expression levels (Figure 4A-B), we did not detect differences in ZIKV nor CHIKV prevalence and loads (Figure 4C-D). This assay suggests that the potential proviral effect of *phb2* is virus-specific and does not apply to ZIKV or CHIKV infection.

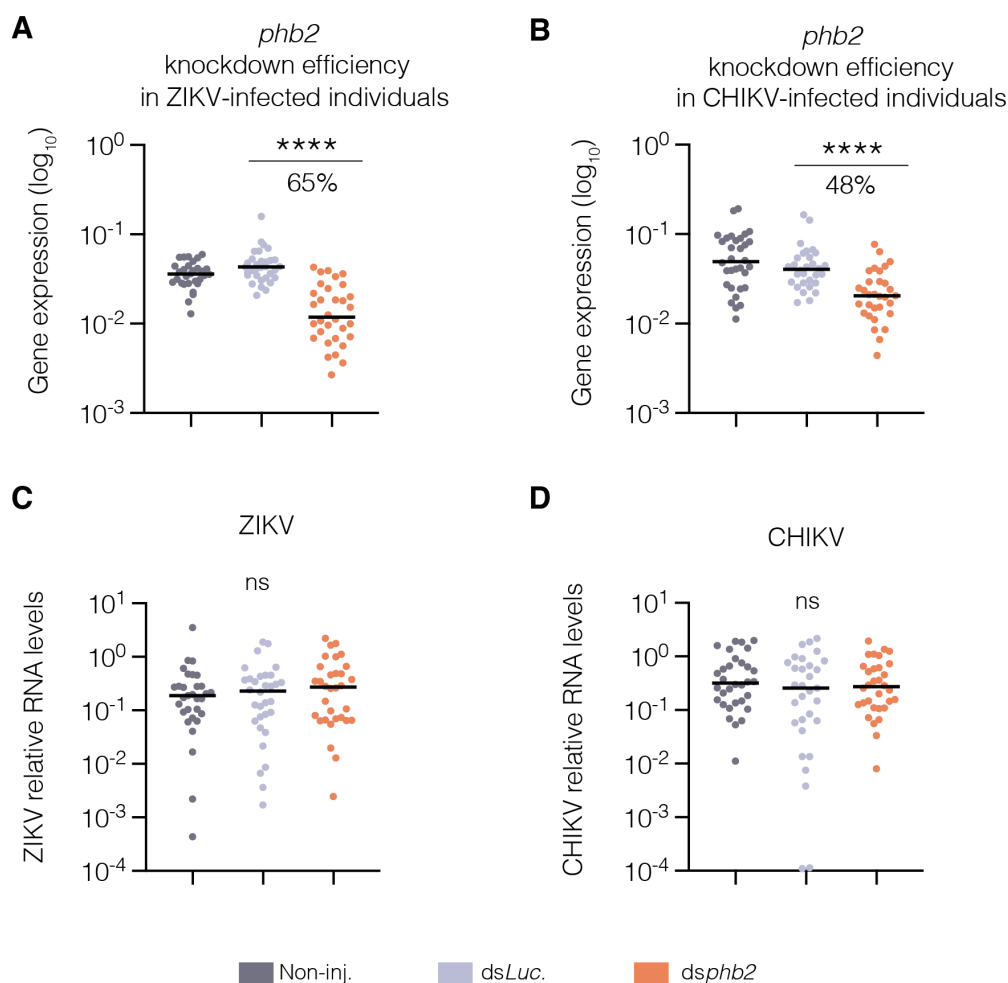


Figure 4. Lack of *phb2* proviral activity in ZIKV- or CHIKV-infected *Ae. aegypti*. (A-B) *phb2* knockdown efficiency by RNAi-mediated *in vivo* gene silencing of *phb2* in ZIKV- (A) or CHIKV- (B) exposed

mosquitoes, five days after ZIKV exposure or two days after CHIKV exposure. Transcript abundance was quantified by RT-qPCR, normalized by transcript levels of the housekeeping gene *ribosomal protein 49* (*RP49*) and represented as $\log_{10}(2^{-\Delta\Delta Ct})$ with $\Delta\Delta Ct = Ct_{Gene} - Ct_{RP49}$. Non-injected mosquitoes and mosquitoes injected with a dsRNA targeting the irrelevant Luciferase gene are used as controls. Percentages indicated below significance stars represent the knockdown efficiency (KD%), calculated as $KD\% = (1 - \Delta(\Delta Ct)) * 100$, with $\Delta(\Delta Ct) = 2^{-\Delta\Delta Ct_{SilencedCondition}} / 2^{-\Delta\Delta Ct_{ControlCondition}}$. Statistical significance of pairwise differences were assessed with Mann-Whitney's test (* $p < 0.05$; ** $p < 0.01$; *** $p < 0.001$). (C-D) ZIKV (C) and CHIKV (D) viral loads of whole mosquito bodies (controls or *phb2*-depleted) were quantified by RT-qPCR of the viral genome five days after ZIKV exposure or two days after CHIKV exposure. Viral RNA levels were quantified by RT-qPCR, normalized by transcript levels of the housekeeping gene *ribosomal protein 49* (*RP49*) and represented as $\log_{10}(2^{-\Delta\Delta Ct})$ with $\Delta\Delta Ct = Ct_{ViralGenome} - Ct_{RP49}$. Statistical significance of pairwise differences were assessed with Mann-Whitney's test for the viral loads and a chi-squared test for the viral prevalence (* $p < 0.05$; ** $p < 0.01$; *** $p < 0.001$).

C) *Phb2* has no proviral activity during DENV infection of Aag2 cells

In vitro models are more easily compatible with biomolecular approaches aiming to provide molecular insights in the characterization of a candidate receptor. Therefore, we performed additional assays *in vitro*, in *Ae. aegypti*-derived Aag2 cells, in order to provide functional insights about *phb2*'s proviral effect (Figure 5).

First, we assessed *phb2* subcellular localization in Aag2 cells using immunostaining (Figure 5A). We observed a mostly cytoplasmic and perinuclear localization of *phb2*, which matches its description as a mitochondrial protein. Remarkably, we also noted the presence of *phb2* signal in membranous extensions, which is compatible with a potential role as a virus entry factor.

Then, we assessed *phb2* expression in Aag2 cells in response to DENV-1 (Figure 5B). We observed an upregulation (3- to 4-fold) of *phb2* expression within two hours following virus exposure, followed by a return to basal levels 48 hours after exposure. These results indicate that *phb2* is transcriptionally induced in response to DENV infection. This induction is consistent with the hypothesis of viral hijacking of signaling pathways to support entry processes, as reported in the context of various viral infections [66].

Finally, we optimized a cell transfection protocol to silence *phb2* expression by transfection of dsRNA targeting *phb2*. We managed to obtain a knockdown efficiency of 90% at 48 hours post transfection, at the time of virus exposure, using a double transfection protocol (Figure 5C). In parallel, control cells were transfected with an irrelevant dsRNA targeting the *Luciferase* gene. We infected *phb2*-silenced and control cells with DENV-1 at a multiplicity of infection (MOI) of

1, and collected them 14, 24 and 48 hours after virus exposure. Then, we quantified DENV-1 replication levels by RT-qPCR quantification of the viral genome. Contrary to the phenotype obtained *in vivo*, we observed no significant differences in DENV replication levels in the *phb2*-silenced cells compared to the control condition, at any timepoint (Figure 5D).

This experiment failed to demonstrate a proviral effect of *phb2* in Aag2 cells and suggests that this gene might not be involved in the infectious cycle of DENV in this cell line.

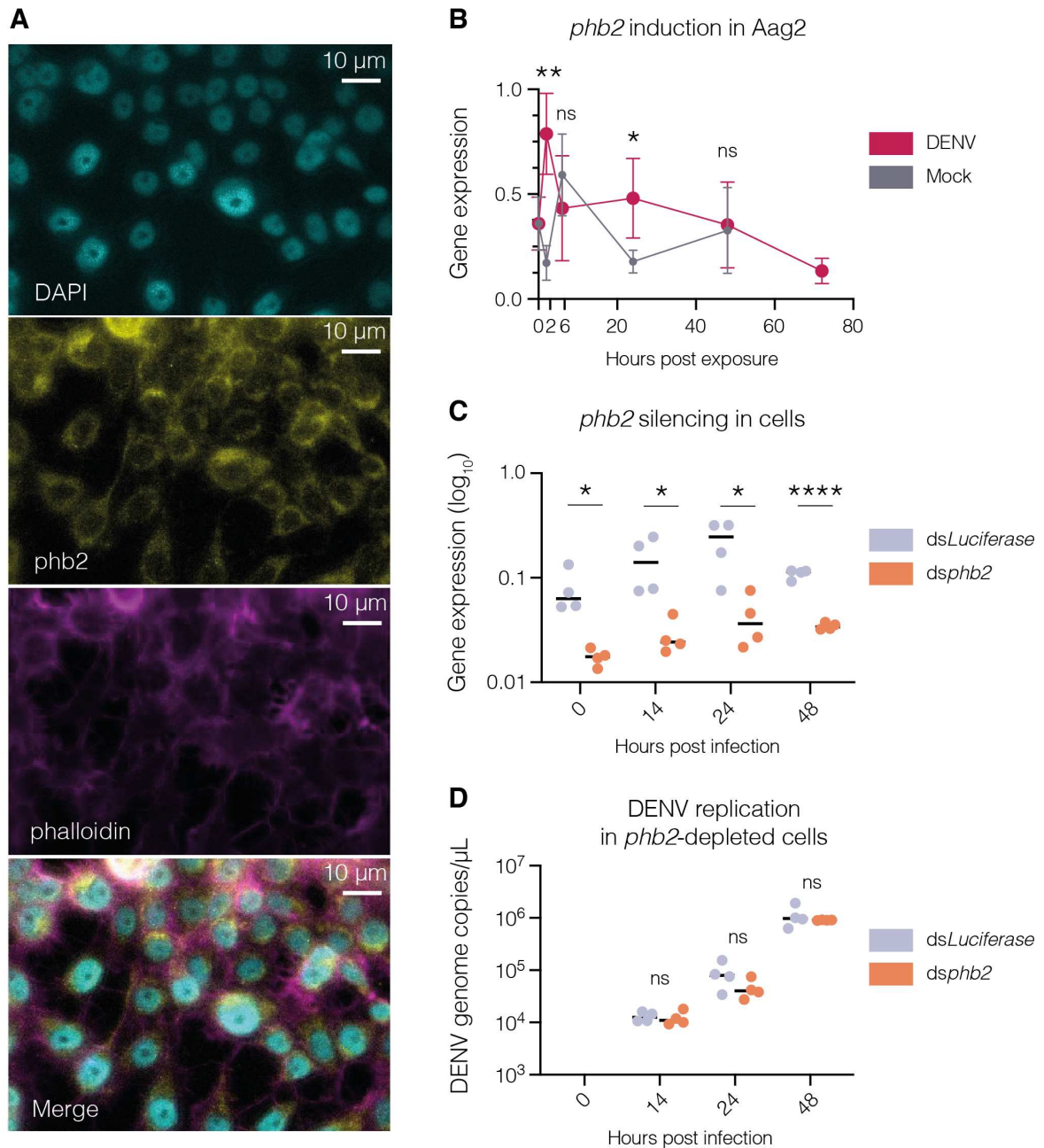


Figure 5. Lack of *phb2* proviral activity in Aag2 cells during DENV infection. (A) Immunostaining of *phb2* protein in Aag2 cells. Nuclei are stained with DAPI and actin filaments with phalloidin-rhodamine. Imaging was done using an epifluorescence microscope. Scale bar: 10 μ m. (B) Expression levels of *phb2*

in DENV-virus exposed or control cells were quantified by RT-qPCR 2, 6, 24, 48 and 72 hours post exposure. Vertical bars represent standard deviations. (C) *phb2* knockdown efficiency by RNAi-mediated gene silencing in DENV-exposed Aag2 cells. Cells were transfected with a dsRNA targeting *phb2* or a control dsRNA targeting the *Luciferase* gene as control. 24 hours after the second transfection, cells were infected with DENV at a MOI of 1. Transcript abundance was quantified by RT-qPCR at 0, as well as 14, 24 and 48 hours after virus exposure, normalized by transcript levels of the housekeeping gene *ribosomal protein 49 (RP49)* and represented as $2^{-\Delta\Delta Ct}$ with $\Delta\Delta Ct = Ct_{Gene} - Ct_{RP49}$. (D) DENV replication levels were quantified by RT-qPCR of the viral genome 14, 24 and 48 hours after virus exposure, in control and *phb2*-depleted cells. Statistical significance of the pairwise differences was assessed with Student's t-test.

D) Generation of a *phb2*-knockout mosquito line by CRISPR/Cas9-mediated gene editing

To investigate the potential proviral activity of *phb2* *in vivo* and exclude the hypothesis of some residual *phb2* expression after incomplete knockdown, we sought to generate a *phb2*-knockout, using CRISPR/Cas9-mediated gene editing (Figure 6). The line was generated from an *Ae. aegypti* isofemale line called “Jane”, previously derived from a wild mosquito population in Kamphaeng Phet province, Thailand [67, 68].

Shortly, we injected mosquito embryos with the Cas9 protein coupled to three single guide RNAs (sgRNAs), one targeting exon 2 and the two others targeting exon 3, together with a repair template. sgRNAs were designed using the CRISPOR tool [69] (<http://crispor.tefor.net/>) to limit the risk of off-targets and displayed at least 3 mismatches with other potential undesired targets in the genome. Sequences of the sgRNAs and the repair template are available in Supplementary Table 1.

We screened generation zero (G_0) individuals for a mutation in the desired locus, and one G_0 individual was obtained, with a ~100 bp deletion. After mating with wild-type individuals, one G_1 male was obtained and crossed with fifteen wild-type females. The heterozygous sequence obtained showed a 102 bp deletion at the end of exon 3 (Figure 6A). G_2 heterozygous individuals were crossed together but did not lead to the production of homozygous progeny. Unfortunately, *phb2*-knockout homozygous mutants were not viable. Crosses of heterozygous mutants never produced viable homozygous individuals. Even among the partially emerged adults or non-eclosed pupae, we never identified any homozygous individual, suggesting the homozygous mutation was lethal at an early stage of development. This observation suggests that *phb2* is an essential gene in *Ae. aegypti*. This correlates with the report that a whole-body knockout of *phb2* was embryonic lethal in several species [70, 71].

Nevertheless, we performed an experimental infection assay on *phb2* heterozygous mutant individuals, which were viable (Figure 6B-C). We exposed female heterozygous mutant mosquitoes to a DENV-1-containing bloodmeal (5×10^6 FFU/mL) and collected whole mosquitoes on day 2 after virus exposure. No significant differences were observed in viral loads or prevalence in the heterozygous mutants compared to the wild-type controls. These data suggest that the single intact copy of *phb2* left in the genome was sufficient to maintain its function, or that *phb2* was not required in the establishment of infection.

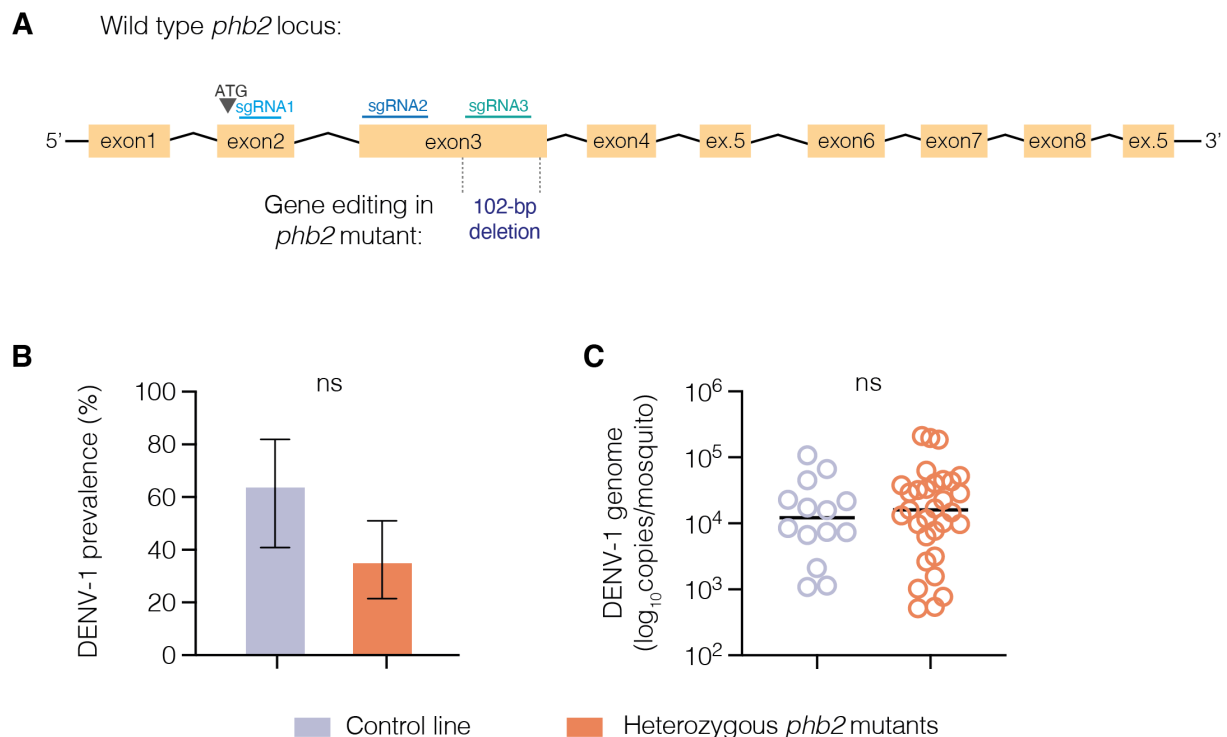


Figure 6. Heterozygous *phb2* mutants show similar levels of DENV replication than wild-type mosquitoes. (A) Sequence of the *phb2* genomic locus and gene edit in *phb2* mutants. Exons are represented as yellow boxes linked with broken segments representing introns. Single guide RNAs (sgRNA) used for CRISPR/Cas9-mediated gene editing are depicted above the sequence: sgRNA1 (x2_78fwd) in light blue, sgRNA2 (x3_41fwd) in dark blue and sgRNA3 (x3_608fwd) in green. DENV prevalence (B) and viral loads (C) in control or heterozygous *phb2* mutants. Viral replication levels were determined by RT-qPCR of the viral genome on whole mosquito bodies. Vertical bars in (C) represent 95% confidence intervals. Statistical significance of pairwise differences were assessed with a Mann Whitney test for the viral loads and a chi-squared test for the viral prevalence (* $p < 0.05$; ** $p < 0.01$; *** $p < 0.001$).

E) Evaluation of *phb2*'s role in DENV entry in midguts

1) *Ex vivo* evaluation of *phb2*'s role in DENV binding to midguts

It is hypothesized that *phb2* may act as a receptor for DENV entry during the early stages of the virus infection cycle in the mosquito. Therefore, the silencing of *phb2* expression in the midgut should impair DENV's ability to infect this tissue.

To test this hypothesis, we silenced *phb2* expression by injection of dsRNA in adult female mosquitoes. Two days later, we dissected midguts from *phb2*-silenced individuals in ice-cold insect cell culture medium and cut them open longitudinally to expose the lumen of the organ. Open midguts were then pooled by pairs and incubated in serial ten-fold dilutions of DENV in insect cell culture medium, for 1 hour at 4°C. This step allows the virus to bind the tissue, while preventing the entry process and protecting the tissue from degradation. After 1 hour incubation, midguts were centrifuged and rinsed thoroughly in ice-cold medium to remove unattached viral particles. Finally, washed midguts were processed for RT-qPCR quantification of the viral genome (Figure 7).

Unfortunately, we were not able to detect viral RNA in any condition using this method. This approach failed to confirm or refute the involvement of *phb2* in DENV entry into midgut cells. Possible explanations for the lack of success of this approach are discussed in the Discussion section of this chapter.

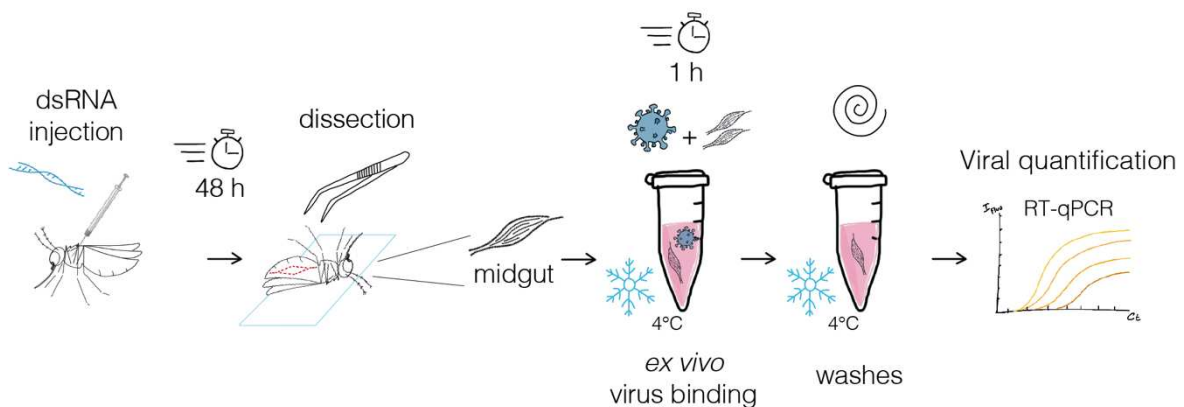


Figure 7. *Ex vivo* virus binding assay on midguts. Experimental design of the *ex vivo* virus binding assay on female mosquito midguts. Female mosquitoes were reared until five-to-seven days after emergence, and *in vivo* *phb2*-silencing induced by dsRNA injection was performed as described in the Methods. 48 hours after dsRNA injection, midguts were dissected in insect cell culture medium and cut open longitudinally, and additional samples were collected in parallel to check *phb2*-knockdown efficiency. Midguts were then incubated for 1 hour on ice in medium containing serial dilutions of DENV-1, to allow virus binding, but not entry, in the tissues. Midguts were finally washed 8 times by centrifugation in ice-cold medium to remove unattached viral particles, before processing for RNA extraction and RT-qPCR of the viral genome.

2) *In vivo* evaluation of *phb2*'s role in DENV entry in midguts by antibody-mediated inhibition assay

Due to the limitations of the *ex vivo* binding assay, we opted for a different strategy based on an *in vivo* antibody-mediated inhibition assay (Figure 8A-B). The principle of this approach is to feed mosquitoes with a mix of blood, virus, and antibodies targeting the candidate receptor. If the candidate protein is expressed on the surface of midgut cells and is involved in binding and entry of the virus, the antibodies would compete with the virus for binding to the receptor, thereby hindering the establishment of infection in the midgut.

We exposed female mosquitoes to an infectious bloodmeal containing DENV-1 and anti-*phb2* antibody. To exclude a potential effect of antibodies' buffers, we purified and resuspended the anti-*phb2* and control anti-His tag antibodies in the same buffer, which did not contain any stabilizing agent. Indeed, stabilizing agents such as sodium azide or gelatin might be toxic or deleterious for the establishment of infection in the mosquito's gut.

Five days after exposure, whole mosquitoes were collected and viral replication levels assessed by RT-qPCR. Viral loads were similar in all conditions and viral prevalence was comparable between the anti-*phb2*-containing conditions and the control antibody-containing condition (Figure 8A-B). Hence, we were not able to detect any impact of the antibody-mediated *phb2* inhibition on viral infection.

These data suggest that interaction with *phb2* proteins expressed in the midgut is not required for DENV binding and entry in the tissue.

3) Evaluation of *phb2*'s impact on DENV replication in midguts

Our previous experimental attempts failed to demonstrate an involvement of the *phb2* protein in DENV binding to midgut cells. We aimed to test whether *phb2* promotes DENV replication in the midgut after viral entry inside midgut cells, during early replication stages, eventually leading to the reduced viral load or prevalence observed in our *in vivo* assays in whole mosquito bodies.

To evaluate the importance of *phb2* in DENV early replication in the midgut, we performed the same *in vivo* gene knockdown as previously described and exposed mosquitoes to a DENV-1-containing bloodmeal. Two days later, we dissected mosquito midguts, measured efficiency of the gene knockdown and quantified DENV viral replication by RT-qPCR (Figure 8C-E).

Despite an efficient knockdown (Figure 8E), viral replication levels and prevalence were not negatively impacted by *phb2* silencing two days after virus exposure (Figure 8C-D). This observation suggests that the potential role of *phb2* regarding DENV infection does not take place in this organ during early stages of infection.

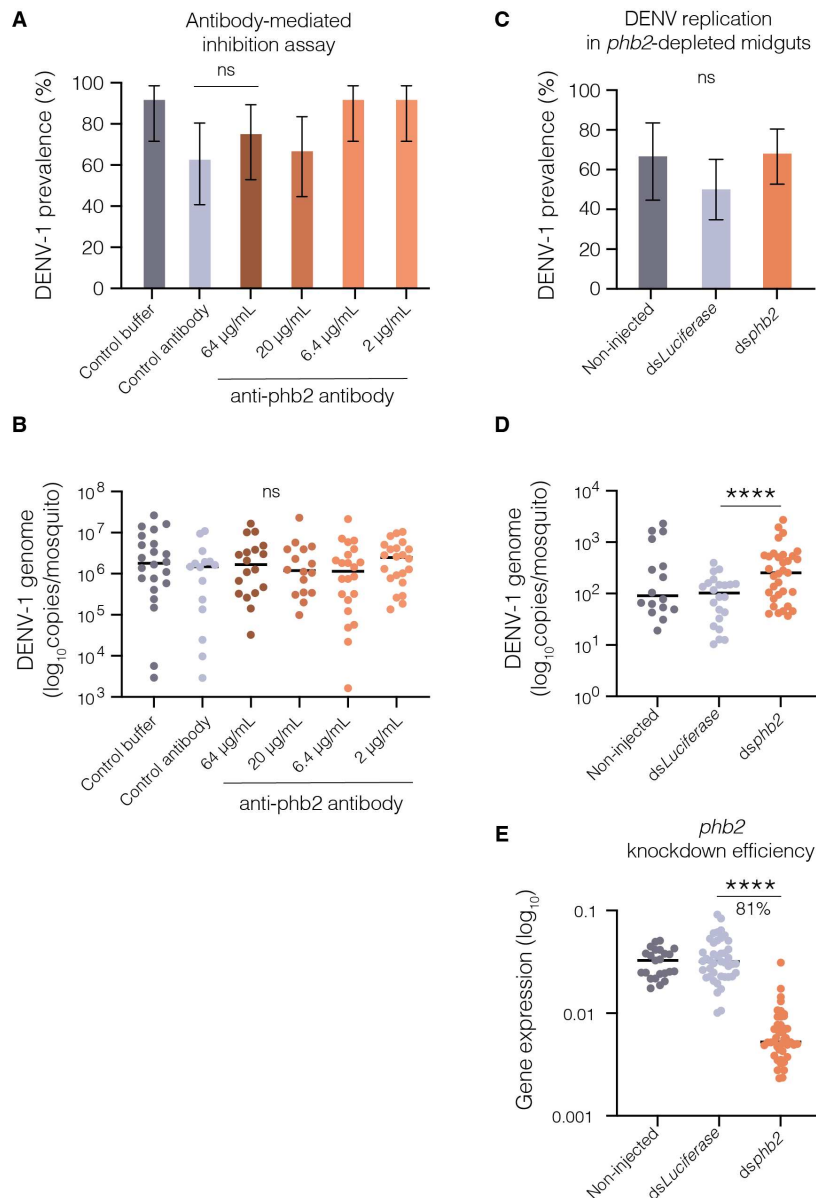


Figure 8. Absence of demonstrated role of *phb2* in DENV early infection steps in *Ae. aegypti* midguts. (A-B) Antibody-mediated inhibition assay. DENV prevalence (A) and viral loads (B) of female mosquito midguts fed with an DENV-1-containing bloodmeal (5×10^6 FFU/mL) supplemented with several concentrations of an antibody targeting *phb2* (ranging from 2 $\mu\text{g/mL}$ to 64 $\mu\text{g/mL}$), or a control antibody (anti-His tag, 64 $\mu\text{g/mL}$) or antibody buffer in a similar volume. (C-E) DENV prevalence (C) and viral loads (D) of female mosquito midguts (controls or *phb2*-depleted by RNAi-mediated *in vivo* gene silencing) were quantified by RT-qPCR of the viral genome. Vertical bars in (C) represent 95% confidence intervals. (E) *phb2* knockdown efficiency. Transcript abundance was quantified by RT-qPCR, normalized by transcript levels of the housekeeping gene *ribosomal protein 49* (*RP49*) and represented as $\log_{10}(2^{-\Delta\Delta\text{Ct}})$ with $\Delta\Delta\text{Ct} = \text{CtPhb2} - \text{CtRP49}$. The percentage indicated below significance stars represents the knockdown efficiency (KD%), calculated as $\text{KD}\% = (1 - \Delta(\Delta\text{Ct})) \times 100$, with $\Delta(\Delta\text{Ct}) = 2^{-\Delta\Delta\text{Ct}}$.

-CHAPTER 3-

$\text{deltaCt}_{inPhb2-SilencedCondition} / 2 - \text{deltaCt}_{inControlCondition}$. Statistical significance of pairwise differences was assessed with Mann-Whitney's test for the viral loads and expression levels, and a chi-squared test for the viral prevalence (* $p < 0.05$; ** $p < 0.01$; *** $p < 0.001$).

DISCUSSION

Our study aimed to confirm the *in vivo* effect of some putative DENV receptors identified in *in vitro* models, in the aim of addressing the limitations of *in vitro* interaction studies.

Using *in vivo* gene knockdown assays, we found a proviral effect of *phb2* gene, a promising candidate proposed as a putative receptor for DENV in *Aedes* mosquitoes' midguts, on DENV replication in mosquitoes' bodies.

Our additional assays on *phb2*-depleted mosquitoes with ZIKV and CHIKV failed to demonstrate a proviral activity of *phb2* towards these viruses. Nevertheless, the viral prevalence obtained in these experiments reached 100% of infected mosquitoes in all conditions. The saturation of infection levels might hamper our ability to detect differences even in the viral load. Additional experiments such as a dose-response assay would be required to conclusively rule out the importance of *phb2* during ZIKV and CHIKV infection of *Ae. aegypti* mosquitoes.

Regarding the exploration of *phb2*'s proviral potential in the midguts, our *ex vivo* binding assay and *in vivo* antibody-mediated inhibition assay could not demonstrate a role of *phb2* in DENV binding and entry processes in midguts. Several hypotheses can explain why the *ex vivo* virus binding conditions did not allow to detect any virus attached to midguts. It is possible that the average amount of DENV particles that bind to a single midgut was too low compared to the sensitivity of the RT-qPCR method. The number of bound particles might also be correlated with the initial concentration of virus in the input solution, however even the condition with pure virus stock, at a concentration of 7.6×10^7 FFU/mL (ten-fold higher than in our experimental infectious bloodmeals), did not result in any virus detection. Additionally, viral stock solutions contain fetal bovine serum, which can impair flavivirus infection to some extent [72]. Also, in natural conditions, the virus is only in contact with the lumen of the midgut, hence it is possible that receptors are only present on one side of the polarized tissue. In this situation, if the tissues' conformation in the medium was coiled, we cannot exclude the possibility of steric hindrance impairing virus access to the receptors. Finally, in this assay, midgut cells were exposed to virus suspension in cell culture medium, rather than blood in natural conditions. Blood-associated factors might be needed to recapitulate the native environmental conditions in which virus attachment can occur optimally. An alternative to these experimental issues would be to perform *in vitro* experiments using an *Ae. aegypti*-derived cell line. This approach would allow to increase the number of cells available for virus binding and to work with a single layer of non-polarized susceptible cells. However, the simplification of the experimental model would exclude some physiologically relevant parameters, such as the diversity of cells in the

target tissue or the cell polarization. Furthermore, as we did not observe any proviral activity of *phb2* in Aag2 cells, other *Ae. aegypti*-derived cell lines should be tested to screen for an adequate cell model prior to implementing this virus binding assay protocol.

Regarding the *in vivo* antibody-mediated inhibition assay, our data suggest that accessibility to *phb2* is not required for DENV infection in midguts. Yet, the antibody's affinity or concentration needed to efficiently block access to all *phb2* proteins is not known. More importantly, we cannot exclude the potential existence of alternative receptors mediating DENV entry in this tissue, since DENV typically uses multiple receptors in mammalian cells.

Nevertheless, we showed that silencing *phb2* in the midguts does not hamper DENV early replication in these tissues. This suggests that the proviral effect of *phb2* observed in the bodies in our initial silencing assay is not the consequence of *phb2*'s function in midguts. These data tend to refute the hypothesis that *phb2* is a credible candidate receptor in the midguts specifically. However, other explanations are possible. The incomplete silencing of *phb2* might allow sufficient expression of the gene to maintain a proviral activity. Alternatively, if this protein is indeed involved in early infection processes such as entry, *phb2* is likely not the only factor involved in processes supporting DENV entry and replication. Alternative host factors could compensate for the silencing of *phb2*. Finally, it is possible that *phb2* still promotes DENV entry into other mosquito tissues and plays a proviral role in the subsequent stages of viral dissemination.

Additionally, the genetic specificity of interactions in host-pathogen relationships is well-known [73-76]. Hence, it is plausible that the physical interaction of *phb2* with DENV E protein relies on host-specific or virus strain-specific interactions. Under this hypothesis, we might not have been able to confirm the phenotype observed in the combination of DENV-2 and *Ae. albopictus*-derived cells ([31]) using another model.

Nevertheless, we confirmed that *phb2* is an essential gene in *Ae. aegypti*'s development, as reported for other species, since the homozygous mutation of *phb2* was lethal at early stages of mosquito development, prior to emergence.

Overall, our study highlights that *in vitro* attempts to identify viral receptors do not necessarily translate into *in vivo* confirmation of the biological role of candidates in viral entry. Thus, *phb2* -at least in the midgut - is an illustration that interaction between viral particles and host factors *in vitro* is not sufficient to indicate physiological relevance of the interaction. Only *in vivo* studies can confirm the biological characterization of a candidate as a viral receptor.

ACKNOWLEDGEMENTS

We thank Catherine Lallemand for assistance with mosquito rearing, Emma Osswald and Julie Delaroche for preliminary data generation, and Pascal Miesen and Nolwenn Jouvenet for their input and suggestions.

METHODS

Virus strains

DENV-1 strain KDH0026A was originally isolated in 2010 from the serum of a patient in Kamphaeng Phet, Thailand [73]. ZIKV strain THA/2014/SV0127-14 was isolated in Thailand in 2014 and obtained from the Armed Forces Research Institute of Medical Sciences [77]. CHIKV isolate M105 was originally isolated in 2014 from the serum of a patient in Martinique [78]. Viral stocks of DENV and ZIKV were prepared as described in [79]. In short, C6/36 *Aedes albopictus* cells were inoculated with DENV or ZIKV with an MOI of 0.1 and cultured for 7 days. Cell culture supernatants were then collected, centrifuged to remove cell debris and concentrated using a Vivaspinn column (100kDa) (Cytiva). Viral stocks titers were quantified by focus-forming assay as described below. Viral stocks of CHIKV were prepared similarly in Vero E6 cells and titers were quantified by plaque assay as described in [80].

Mosquito rearing

Experiments were conducted with *Ae. aegypti* mosquitoes derived from a wild-type colony originally from Kamphaeng Phet province, Thailand [67]. Mosquitoes were reared under controlled conditions (28°C, 12-hour light/12-hour dark cycle and 70% relative humidity). Prior to performing the experiments, their eggs were hatched synchronously with a SpeedVac vacuum device (Thermo Fisher Scientific) for 45 minutes. Larvae were reared in plastic trays containing 1.5 L of tap water and supplemented with Tetramin (Tetra) fish food at a density of 200 larvae per tray. After emergence, adults were kept in BugDorm-1 insect cages (BugDorm) with permanent access to 10% sucrose solution.

Mosquito exposure to infectious bloodmeals

Experimental infections of mosquitoes were performed in a biosafety level-3 containment facility, as previously described [79]. Shortly, 5- to 7-day-old female mosquitoes were deprived of 10% sucrose solution 20 hours before oral exposure to viruses. The infectious blood meal consisted of a 2:1 mix of washed rabbit erythrocytes and viral suspension supplemented with 10 mM ATP (Sigma). The infectious titers used were 5×10^6 FFU/mL for DENV-1 and 5×10^5 PFU/mL for ZIKV. Mosquitoes were offered the infectious blood meal for 15 min through a desalted pig-intestine membrane using an artificial feeder (Hemotek Ltd) set at 37°C. Fully engorged females were sorted and incubated at 28°C, 70% relative humidity and under a 12-hour light-dark cycle with permanent access to 10% sucrose.

Viral RNA quantification

Mosquito body parts and organs were dissected in 1× PBS, and immediately transferred to a tube containing 400 µL of RA1 lysis buffer from Nucleospin 96 RNA core kit (Macherey-Nagel) and ~20 1-mm glass beads (BioSpec). Samples were homogenized for 30 sec at 6,000 rpm in a Precellys 24 grinder (Bertin Technologies). RNA was extracted and treated with DNase using Nucleospin 96 RNA core kit (Macherey-Nagel) following the manufacturer's instructions and stored at -20°C until further use. Viral RNA was reverse transcribed and quantified using a TaqMan-based qPCR assay, using virus-specific primers and 6-FAM/BHQ-1 double-labeled probe (sequences provided in Supplementary Materials Table 1). Reactions were performed with the GoTaq® Probe 1-Step RT-qPCR System (Promega) following the manufacturer's instructions. The limit of detection of the assay was 40 copies of viral RNA per µL.

Virus titrations by focus-forming assay (FFA)

DENV infectious titers were measured by standard focus-forming assay (FFA) in C6/36 cells. C6/36 cells were seeded in a 96-well plate 24 hours before virus inoculation. Serial sample dilutions were prepared in Leibovitz's L-15 medium (Life Technologies) supplemented with 0.1% penicillin/streptomycin (Gibco Thermo Fischer Scientific), 1× non-essential amino acids (Life Technologies) and 2% fetal bovine serum (FBS, Life Technologies). After removal of the culture medium, cells were inoculated with 40 µL of sample. After 1 hour of incubation at 28°C, the inoculum was removed and cells were overlaid with 150 µL of a 1:1 mix of overlay medium (Leibovitz's L-15 medium, 0.1% penicillin/streptomycin, 1× non-essential amino acids, 2× Antibiotic-Antimycotic (Life Technologies) and 10% FBS) and 2% carboxyl methylcellulose (VWR Chemicals, Sigma) solution and incubated for 5 days at 28° C. Cells were fixed for 30 minutes in 3.6% formaldehyde (Sigma-Aldrich). Next, cells were washed three times with 1× PBS, followed by 30 min permeabilization with 0.3% Triton X-100 (Sigma-Aldrich, St Louis, MO, USA) in 1× PBS at room temperature. After 3 washes with 1× PBS, cells were incubated for 1 hour at 37°C with mouse anti-DENV complex monoclonal antibody MAB8705 (Merck Millipore) diluted to 1:200 in 1× PBS + 1% bovine serum albumin (BSA) (Interchim). After 3 washes in 1× PBS, cells were incubated at 37 °C for 30 min with an Alexa Fluor 488-conjugated goat anti-mouse antibody (A11029; Invitrogen) diluted to 1:500 in 1× PBS + 1% BSA. Three final washes in 1× PBS and one wash with distilled water were performed before infectious foci were counted under a fluorescent microscope and converted into focus-forming units/mL (FFU/mL).

Double-stranded RNA synthesis for gene knockdown

Double-stranded RNA for RNAi-mediated gene knockdown was *in vitro* transcribed from T7 promoter-flanked PCR products using the MEGAscript RNAi kit (Life Technologies). To obtain

those PCR products, a first PCR step was performed on genomic DNA extracted from mosquitoes of the control line using the previously described Pat-Roman DNA extraction protocol [74]. The T7 sequence was then introduced during a second PCR step using T7 universal primers that hybridize to short GC-rich tags that were introduced to the PCR products in the first PCR (primer sequences are provided in Supplementary Table 1).

Double-stranded RNA targeting *Luciferase* was synthesized using T7 promoter-flanked PCR products generated by amplifying a *Luciferase*-containing plasmid with T7-flanked PCR primers with the MEGAscript RNAi kit (Life Technologies) (primer sequences are provided in Supplementary Table 1). dsRNA was resuspended in RNase-free water to reach a final concentration of 10 mg/mL.

***In vivo* gene knockdown**

Five- to seven-day-old female mosquitoes were anesthetized on ice and injected intrathoracically with 1 µg (100 nL) of dsRNA suspension using a Nanoject III apparatus (Drummond). After injection, mosquitoes were incubated for 2 days at 28°C before the infectious bloodmeal and gene knockdown quantification.

Gene expression measurement

Gene expression levels were measured using a BRYT-Green based RT-qPCR assay (GoTaq® 1-Step RT-qPCR System; Promega) following the manufacturer's instructions and using gene-specific primers (primer sequences are provided in Supplementary Table 1). Relative expression was calculated as 2^{-dCt} , where $dCt = Ct_{Gene} - Ct_{RP49}$, using the *Ae. aegypti* ribosomal protein-coding gene *RP49* (*AAEL003396*) for normalization.

Immunostaining on mosquito midguts

Midguts from female mosquitoes were dissected in 1× PBS and transferred on a µ-well slide (81826 ibiTreat 18 well – Flat) for fixation in 3.6% paraformaldehyde for 1 hour in a humid chamber at room temperature. Midguts were rinsed five times in 1× PBS before permeabilization and saturation in 1× PBS containing 0.1% Triton X-100 and 1% BSA (PBT) for 2 hours at room temperature (20-25°C). Incubation with primary antibodies (anti-phb2 (sc-133094, Santa Cruz Biotechnology) 1:200, diluted in PBT) was done overnight at 4°C, followed by five washes in PBT and incubation with secondary antibodies (donkey anti-rabbit 488 (Invitrogen R37118) diluted according to the manufacturers' instructions in PBT) for two hours at room temperature. Midguts were then washed in 1× PBS, stained with DAPI (100 nM in 1× PBS) and Rhodamine-Phalloidin (100 nM in 1× PBS, #PHDR1, Cytoskeleton Inc) for 10 minutes, washed in 1× PBS and finally mounted in anti-fading medium Fluoromount-G (Invitrogen, 00495802). All incubation and wash steps were done on a gyro-rocker shaker

(Stuart) (300 rpm) in a humid chamber. Samples were imaged using a confocal microscope (LSM 780 inverted confocal microscope, Zeiss).

Immunostaining on Aag2 cells

Aag2 cells were seeded on sterilized glass slides in 24-well plates at a density of 2.5×10^5 cells/well in 500 μ L of complete L15 (Leibovitz's L-15 medium supplemented with 0.1% penicillin/streptomycin (Gibco Thermo Fischer Scientific), 1 \times non-essential amino acids (Life Technologies), 2% tryptose phosphate broth (Gibco Thermo Fischer Scientific) and 10% FBS (Life Technologies). Twenty-four hours later, cells were fixed in 3.6% paraformaldehyde for 20 minutes and then washed twice with 1 \times PBS. Cells were permeabilized in 1 \times PBS, 0.1% Triton X-100 for 15 minutes at room temperature before staining with primary antibody (anti-phb2 (sc-133094, Santa Cruz Biotechnology) 1:200) diluted in 1 \times PBS, 0.1% Triton X-100 and Normal Goat Serum 0,04% (Invitrogen) for 1 hour at room temperature. After three washes in 1 \times PBS, Triton X-100 0.1%, cells were incubated with the secondary antibody (donkey anti-rabbit 488 (Invitrogen R37118) diluted according to the manufacturers' instructions) for 1 hour at room temperature and washed again three times in 1 \times PBS, Triton X-100 0.1%. Cells were finally stained with DAPI (100 nM in 1 \times PBS) and Rhodamine-Phalloidin (100 nM in 1 \times PBS, #PHDR1, Cytoskeleton Inc) for 10 minutes, washed in 1 \times PBS and mounted in anti-fading medium Fluoromount-G (Invitrogen, 00495802). Slides were imaged using an epifluorescence microscope (Leica).

Ex vivo virus-binding assay on midguts

Five to seven-day-old female mosquitoes were anesthetized on ice and injected intra-thoracically with 1 μ g (100 nL) dsRNA suspension targeting *phb2* or *Luciferase* (as a negative control) using a Nanoject III apparatus (Drummond). After injection, mosquitoes were incubated for 2 days at 28°C with permanent access to 10% sucrose solution. Individual midguts were then dissected in a droplet of cold complete Leibovitz-15 medium with 10% FBS and opened longitudinally using sharp forceps. Pools of two midguts were incubated in 100 μ L of DENV-1 solution, with virus concentrations ranging from 7.6×10^4 FFU/ μ L to 7.6×10^0 FFU/ μ L, at 4°C and on ice to allow virus binding. Midguts were then spun down for 3 minutes at 3500 rpm at 4°C, and supernatants were removed and kept for viral titrations. Midguts were washed 8 times in 1 mL of cold complete Leibovitz-15 medium with 10% FBS to remove unbound viral particles. Finally, midguts were transferred to 400 μ L of RAV1 buffer and processed for viral RNA extraction using Nucleospin 96 Virus core kit (Macherey-Nagel) and DNase I treatment (Invitrogen), according to the manufacturers' instructions. Viral RNA was quantified with GoTaq® Probe 1-Step RT-qPCR System (Promega) as described above.

***In vivo* antibody-mediated inhibition assay**

Five to seven-day-old female mosquitoes were exposed to a DENV-1 infectious bloodmeal following the standard procedure described above. The blood mix, containing DENV (5×10^6 FFU/mL) was supplemented with anti-phb2 antibodies (Santa Cruz Biotechnology, sc133094) at final concentrations ranging from 20 $\mu\text{g/mL}$ to 0.1 $\mu\text{g/mL}$. As controls, conditions with anti-His-tag antibody (20 $\mu\text{g/mL}$) (SAB1305538, Sigma-Aldrich) or antibody buffer (mix of Elution buffer and Neutralization buffer, ratio 13:1, from Protein G HP Spintrap + antibody buffer kit (ref. 28903134) from Cytiva) (equivalent volume) were added. Both antibodies were purified and concentrated using the Protein G HP Spintrap + antibody buffer kit (ref. 28903134) from Cytiva according to the manufacturer's instructions.

dsRNA transfection and DENV infection of Aag2 cells

Aedes aegypti Aag2 cells were seeded at a density of 2.5×10^5 cells/well in 24-well plates in 500 μL of Leibovitz-15 medium with 10% FBS 24 hours prior to the transfection. Cells were then transfected with 500 ng of dsRNA using Lipofectamine LTX Plus (ThermoFisher), according to the manufacturer's instructions. Forty-eight hours later, cells underwent a second transfection. The next day, cells were inoculated with 200 μL DENV-1 (MOI =1) in Leibovitz-15 medium with 2% FBS for 1 hour and then incubated in 500 μL Leibovitz-15 medium with 10% FBS. At the time of collection, the culture medium was removed, and cells were lysed in 400 μL of RAV1 lysis buffer (from Nucleospin 96 Virus core kit (Macherey-Nagel)) and processed for RNA extraction using Nucleospin 96 Virus core kit (Macherey-Nagel) and DNase I treatment (Invitrogen), according to the manufacturers' instructions. Gene expression was then quantified with GoTaq® 1-Step RT-qPCR System (Promega) as described above.

Generation of *phb2*-knockout mutants by CRISPR/Cas9-mediated gene editing

CRISPR/Cas9-mediated gene editing. *Ae. aegypti* from the "Jane" line (previously characterized in [67, 68]) were used for the generation of *phb2*-knockout mutants. Briefly, this isofemale line was derived from wild *Ae. aegypti* specimens collected in Kamphaeng Phet Province, Thailand in 2010. It was initiated with a single male from Mae Na Ree subdistrict and a single female from Nhong Ping Kai subdistrict. The line was subsequently maintained in the laboratory by mass sib-mating and collective oviposition.

Embryos were microinjected with a mix containing 402.5 ng/ μL SpCas9 protein (New England Biolabs), 40 ng/ μL of sgRNAs (x3_41fwd, x3_608fwd, x2_78fwd), and 125 ng/ μL of the ssODN repair template (RT_72nt_rev) suspended in molecular grade water. Microinjection of *Ae. aegypti* embryos was performed according to standard protocols [81]. In short, *Ae. aegypti* adult females were fed with commercial rabbit blood (BCL) via an artificial membrane feeding system (Hemotek). Three days later, females were transferred into egg-laying vials and

oviposition was induced by placing mosquitoes in the dark. Embryos were injected 30-60 min after oviposition. After injection, embryos were desiccated for 3 days and then hatched in water. Individual pupae were collected into small vials (Genesee Scientific) containing a small amount of water in order to isolate and screen adults for mutations before mating.

Individual virgin adult G_0 mosquitoes were screened for CRISPR/Cas9 induced mutations at the *phb2* locus using PCR. DNA was extracted from a single leg of each live mosquito (see Genotyping). The PCR products were analyzed on a 2% agarose gel to detect large deletions. Mosquitoes exhibiting large deletions were released into a cage with wild-type Jane mosquitoes of the opposite sex for mating. Their progeny was then screened for inheritance of the mutation. Additionally, the PCR products were sequenced to confirm the presence of mutations.

A large deletion (~100 bp) was obtained from an injected female mosquito (#43). This G_0 female was placed in a cage with wild-type Jane males for mating, followed by blood-feeding, and egg collection. Eggs were hatched and individual pupae were again placed into small vials (Genesee Scientific) in order to isolate and screen adult mosquitoes. Heritability of the mutation observed in the G_0 was confirmed by PCR. Sequence analysis revealed the presence of a 102-bp deletion at the end of exon 3. One heterozygous G_1 male was then crossed with 15 wild-type females. The subsequent cross between heterozygous G_2 individuals did not generate individual carrying the mutation at a homozygous state. Drowned or non-eclosed females were also genotyped, but no homozygotes were identified. Thus, we concluded that the mutation was lethal at an early developmental stage.

Genotyping. Genomic DNA was extracted from single mosquito legs using DNAzol DIRECT (DN131, Molecular Research Center, Inc.). PCRs were performed using DreamTaq DNA Polymerase (EP0701, Thermo-Fisher Scientific) based on manufacturer's instructions, using primer sets described in Supplementary Table 1. Amplicons were purified (MinElute PCR purification kit, Qiagen) and sequenced using another specific primer set (Supplementary Table 1) (Eurofins).

SUPPLEMENTARY MATERIALS

Supplementary Table 1. Oligonucleotide sequences

Primer name	Target gene	Application	Sequence (5'-3')
T7-GL3-luc-F-F	<i>Luciferase</i>	dsRNA synthesis	TAATACGACTCACTATAGGGCGCCCTGGTT CCTGGAAC
T7-GL3-luc-F-R	<i>Luciferase</i>	dsRNA synthesis	TAATACGACTCACTATAGGGGAGAATCTCACG CAGGCAGTTC
PHB2-T7-for	<i>phb2</i>	dsRNA synthesis	GCCCGACGCGTCACCGTGCAATCATGTTCC
PHB2-T7-rev	<i>phb2</i>		CGCCTCGGCCGTATATTCCTTGCCGAAGC
Enolase-T7-for	<i>enolase</i>	dsRNA synthesis	GCCCGACGCGAAGTTGGACGGTACCGAGA
Enolase-T7-rev	<i>enolase</i>		CGCCTCGGCGATCGTGACTTGCCATCCTT
Hsc70-cognate4-T7-for	<i>Hsc70</i>	dsRNA synthesis	GCCCGACGCATGAACCCAACCAACACCAT
Hsc70-cognate4-T7-rev	<i>Hsc70</i>		CGCCTCGGCTCATCGATGGACAGGATTGA
PHB2-EC2-qPCR-for	<i>phb2</i>	qPCR	CGTCGAAAGCAAACAGGTTG
PHB2-EC3-qPCR-rev	<i>phb2</i>	qPCR	ATATCGTCTGAACTCGGCATCC
Enolase-qPCR-for	<i>enolase</i>	qPCR	TGACGCCAACACTAGCATTC
Enolase-qPCR-rev	<i>enolase</i>	qPCR	TGACCTTCAGCAACAAGCAG
Hsc70-cognate4-qPCR-for	<i>Hsc70</i>	qPCR	CAAGATCACCATCACCAACG
Hsc70-cognate4-qPCR-rev	<i>Hsc70</i>	qPCR	TGGTTTCCTTCTGCTTCTCG
NS5F-VR-D1Thai	<i>DENV</i>	qPCR	GGAAGGAGAAGGACTCCACA
NS5R-VR-D1Thai	<i>DENV</i>	qPCR	ATCCTTGTATCCCATCCGGCT
DSQ1-VR	<i>DENV</i>	probe	5'-FAM- CTCAGAGACATATCAAAGATTCCAGGG- BHQ1-3'
CHIKV-F	<i>CHIKV</i>	qPCR	AAGCTCCGCGTYCTTTACCAAG
CHIKV-R	<i>CHIKV</i>		CAAATTGTCCYGGTCTTCCT
ZIKV-F	<i>ZIKV</i>	qPCR	CCGCTGCCCAACACAAG
ZIKV-R	<i>ZIKV</i>	qPCR	CCACTAACGTTCTTTTGCAGACAT

PHB2_x3_41fwd_F	<i>phb2</i>	gRNA	GAAATTAATACGACTCACTATAGGATCATGT TCAACCGTATCGGGTTTTAGAGCTAGAAATA GC
PHB2_x3_608fwd_F	<i>phb2</i>	gRNA	GAAATTAATACGACTCACTATAGGCTGGCC GTTAGTCAAAATCCGTTTTAGAGCTAGAAAT AGC
PHB2_x2_78fwd_F	<i>phb2</i>	gRNA	GAAATTAATACGACTCACTATAGGTCAGAGT AAGCTGAACGATTGTTTTAGAGCTAGAAATA GC
RT 72nt_rev	<i>phb2</i>	repair template	GCGGCACGGATCTTCCTCAGCTTCAGGTA GCCGGGACTGTAGATATCGTCACCAACACC ACCGATACGGTT
PHB2_x1_GT1_F	<i>phb2</i>	Genotyping and sequencing	TCCATACGTGCTGTTTCTGTGTTCC
PHB2_x2_GT2_R	<i>phb2</i>	genotyping	TGGAATTGTTGATACCGTAGGCAGC
PHB2_x3_GT3_F	<i>phb2</i>	Genotyping	GGGTGGTCACCGTGCAATCATG
PHB2_x4GT5_R	<i>phb2</i>	Sequencing	GACACGGTTCTGCGAGTTTGC
PHB2_x4GT6_R	<i>phb2</i>	Genotyping	ATCAGACTGTTGGCGGAGAG

REFERENCES

1. in *Dengue: Guidelines for Diagnosis, Treatment, Prevention and Control: New Edition*. 2009: Geneva.
2. Kraemer, M.U., et al., *The global distribution of the arbovirus vectors Aedes aegypti and Ae. albopictus*. *Elife*, 2015. **4**: p. e08347.
3. Leta, S., et al., *Global risk mapping for major diseases transmitted by Aedes aegypti and Aedes albopictus*. *Int J Infect Dis*, 2018. **67**: p. 25-35.
4. Brady, O.J., et al., *Refining the global spatial limits of dengue virus transmission by evidence-based consensus*. *PLoS Negl Trop Dis*, 2012. **6**(8): p. e1760.
5. Pierson, T.C. and M.S. Diamond, *The continued threat of emerging flaviviruses*. *Nat Microbiol*, 2020. **5**(6): p. 796-812.
6. Roy, S.K. and S. Bhattacharjee, *Dengue virus: epidemiology, biology, and disease aetiology*. *Can J Microbiol*, 2021. **67**(10): p. 687-702.
7. Perera, R., M. Khaliq, and R.J. Kuhn, *Closing the door on flaviviruses: entry as a target for antiviral drug design*. *Antiviral Res*, 2008. **80**(1): p. 11-22.
8. Cruz-Oliveira, C., et al., *Receptors and routes of dengue virus entry into the host cells*. *FEMS Microbiol Rev*, 2015. **39**(2): p. 155-70.
9. Klasse, P.J., R. Bron, and M. Marsh, *Mechanisms of enveloped virus entry into animal cells*. *Adv Drug Deliv Rev*, 1998. **34**(1): p. 65-91.
10. Dimitrov, D.S., *Virus entry: molecular mechanisms and biomedical applications*. *Nat Rev Microbiol*, 2004. **2**(2): p. 109-22.
11. Baranowski, E., C.M. Ruiz-Jarabo, and E. Domingo, *Evolution of cell recognition by viruses*. *Science*, 2001. **292**(5519): p. 1102-5.
12. Grove, J. and M. Marsh, *The cell biology of receptor-mediated virus entry*. *J Cell Biol*, 2011. **195**(7): p. 1071-82.
13. Zhang, Z., et al., *Cell membrane proteins with high N-glycosylation, high expression and multiple interaction partners are preferred by mammalian viruses as receptors*. *Bioinformatics*, 2019. **35**(5): p. 723-728.
14. Valero-Rello, A., et al., *Cellular receptors for mammalian viruses*. *PLoS Pathog*, 2024. **20**(2): p. e1012021.
15. Maginnis, M.S., *Virus-Receptor Interactions: The Key to Cellular Invasion*. *J Mol Biol*, 2018. **430**(17): p. 2590-2611.
16. Anwar, M.N., et al., *The interactions of flaviviruses with cellular receptors: Implications for virus entry*. *Virology*, 2022. **568**: p. 77-85.
17. Reyes-Del Valle, J., et al., *Heat shock protein 90 and heat shock protein 70 are components of dengue virus receptor complex in human cells*. *J Virol*, 2005. **79**(8): p. 4557-67.
18. Jindadamrongwech, S., C. Thepparit, and D.R. Smith, *Identification of GRP 78 (BiP) as a liver cell expressed receptor element for dengue virus serotype 2*. *Arch Virol*, 2004. **149**(5): p. 915-27.
19. Upanan, S., A. Kuadkitkan, and D.R. Smith, *Identification of dengue virus binding proteins using affinity chromatography*. *J Virol Methods*, 2008. **151**(2): p. 325-328.
20. Cabrera-Hernandez, A., et al., *Dengue virus entry into liver (HepG2) cells is independent of hsp90 and hsp70*. *J Med Virol*, 2007. **79**(4): p. 386-92.
21. Cao-Lormeau, V.M., *Dengue viruses binding proteins from Aedes aegypti and Aedes polynesiensis salivary glands*. *Viol J*, 2009. **6**: p. 35.

22. Chee, H.Y. and S. AbuBakar, *Identification of a 48kDa tubulin or tubulin-like C6/36 mosquito cells protein that binds dengue virus 2 using mass spectrometry*. Biochem Biophys Res Commun, 2004. **320**(1): p. 11-7.
23. Mercado-Curiel, R.F., et al., *The four serotypes of dengue recognize the same putative receptors in Aedes aegypti midgut and Ae. albopictus cells*. BMC Microbiol, 2006. **6**: p. 85.
24. Mercado-Curiel, R.F., W.C.t. Black, and L. Munoz Mde, *A dengue receptor as possible genetic marker of vector competence in Aedes aegypti*. BMC Microbiol, 2008. **8**: p. 118.
25. Munoz, M.L., et al., *Putative dengue virus receptors from mosquito cells*. FEMS Microbiol Lett, 1998. **168**(2): p. 251-8.
26. Munoz Mde, L., et al., *Proteomic identification of dengue virus binding proteins in Aedes aegypti mosquitoes and Aedes albopictus cells*. Biomed Res Int, 2013. **2013**: p. 875958.
27. Sakoonwatanyoo, P., V. Boonsanay, and D.R. Smith, *Growth and production of the dengue virus in C6/36 cells and identification of a laminin-binding protein as a candidate serotype 3 and 4 receptor protein*. Intervirology, 2006. **49**(3): p. 161-72.
28. Salas-Benito, J., et al., *Evidence that the 45-kD glycoprotein, part of a putative dengue virus receptor complex in the mosquito cell line C6/36, is a heat-shock related protein*. Am J Trop Med Hyg, 2007. **77**(2): p. 283-90.
29. Vega-Almeida, T.O., et al., *Surface proteins of C6/36 cells involved in dengue virus 4 binding and entry*. Arch Virol, 2013. **158**(6): p. 1189-207.
30. Paingankar, M.S., M.D. Gokhale, and D.N. Deobagkar, *Dengue-2-virus-interacting polypeptides involved in mosquito cell infection*. Arch Virol, 2010. **155**(9): p. 1453-61.
31. Kuadkitkan, A., et al., *Identification and characterization of prohibitin as a receptor protein mediating DENV-2 entry into insect cells*. Virology, 2010. **406**(1): p. 149-61.
32. Apte-Deshpande, A., et al., *Serratia odorifera a midgut inhabitant of Aedes aegypti mosquito enhances its susceptibility to dengue-2 virus*. PLoS One, 2012. **7**(7): p. e40401.
33. Wichit, S., et al., *Dengue virus type 2 recognizes the carbohydrate moiety of neutral glycosphingolipids in mammalian and mosquito cells*. Microbiol Immunol, 2011. **55**(2): p. 135-40.
34. Zhang, X., et al., *Dengue structure differs at the temperatures of its human and mosquito hosts*. Proc Natl Acad Sci U S A, 2013. **110**(17): p. 6795-9.
35. Nepomuceno, D.B., et al., *pH control in the midgut of Aedes aegypti under different nutritional conditions*. J Exp Biol, 2017. **220**(Pt 18): p. 3355-3362.
36. Grace, T.D., *Establishment of a line of mosquito (Aedes aegypti L.) cells grown in vitro*. Nature, 1966. **211**(5047): p. 366-7.
37. Peleg, J., *Growth of arboviruses in monolayers from subcultured mosquito embryo cells*. Virology, 1968. **35**(4): p. 617-9.
38. Walker, T., et al., *Mosquito cell lines: history, isolation, availability and application to assess the threat of arboviral transmission in the United Kingdom*. Parasit Vectors, 2014. **7**: p. 382.
39. Fibriansah, G., et al., *Structural changes in dengue virus when exposed to a temperature of 37 degrees C*. J Virol, 2013. **87**(13): p. 7585-92.

40. Giraldo, M.I., et al., *Envelope protein ubiquitination drives entry and pathogenesis of Zika virus*. *Nature*, 2020. **585**(7825): p. 414-419.
41. Hsieh, P. and P.W. Robbins, *Regulation of asparagine-linked oligosaccharide processing. Oligosaccharide processing in Aedes albopictus mosquito cells*. *J Biol Chem*, 1984. **259**(4): p. 2375-82.
42. Hanna, S.L., et al., *N-linked glycosylation of west nile virus envelope proteins influences particle assembly and infectivity*. *J Virol*, 2005. **79**(21): p. 13262-74.
43. Mondotte, J.A., et al., *Essential role of dengue virus envelope protein N glycosylation at asparagine-67 during viral propagation*. *J Virol*, 2007. **81**(13): p. 7136-48.
44. Dey, D., et al., *Structural and biochemical insights into flavivirus proteins*. *Virus Res*, 2021. **296**: p. 198343.
45. Hu, T., et al., *The key amino acids of E protein involved in early flavivirus infection: viral entry*. *Virol J*, 2021. **18**(1): p. 136.
46. Hung, J.J., et al., *An external loop region of domain III of dengue virus type 2 envelope protein is involved in serotype-specific binding to mosquito but not mammalian cells*. *J Virol*, 2004. **78**(1): p. 378-88.
47. Chin, J.F., J.J. Chu, and M.L. Ng, *The envelope glycoprotein domain III of dengue virus serotypes 1 and 2 inhibit virus entry*. *Microbes Infect*, 2007. **9**(1): p. 1-6.
48. Yan, C., et al., *ILLIS: predicting virus-receptor interactions based on similarity and semi-supervised learning*. *BMC Bioinformatics*, 2019. **20**(Suppl 23): p. 651.
49. Barrass, S.V. and S.J. Butcher, *Advances in high-throughput methods for the identification of virus receptors*. *Med Microbiol Immunol*, 2020. **209**(3): p. 309-323.
50. Lasswitz, L., et al., *Glycomics and Proteomics Approaches to Investigate Early Adenovirus-Host Cell Interactions*. *J Mol Biol*, 2018. **430**(13): p. 1863-1882.
51. Yu, X., D. Xu, and Q. Cheng, *Label-free detection methods for protein microarrays*. *Proteomics*, 2006. **6**(20): p. 5493-503.
52. Frei, A.P., et al., *Ligand-based receptor identification on living cells and tissues using TRICEPS*. *Nat Protoc*, 2013. **8**(7): p. 1321-36.
53. Ramezannia, Z., A. Shamekh, and H. Bannazadeh Baghi, *CRISPR-Cas system to discover host-virus interactions in Flaviviridae*. *Virol J*, 2023. **20**(1): p. 247.
54. Marceau, C.D., et al., *Genetic dissection of Flaviviridae host factors through genome-scale CRISPR screens*. *Nature*, 2016. **535**(7610): p. 159-63.
55. Zheng, J., et al., *Current approaches on viral infection: proteomics and functional validations*. *Front Microbiol*, 2012. **3**: p. 393.
56. Sharma, A., et al., *Prohibitin 1/2 mediates Dengue-3 entry into human neuroblastoma (SH-SY5Y) and microglia (CHME-3) cells*. *J Biomed Sci*, 2020. **27**(1): p. 55.
57. Popova-Butler, A. and D.H. Dean, *Proteomic analysis of the mosquito Aedes aegypti midgut brush border membrane vesicles*. *J Insect Physiol*, 2009. **55**(3): p. 264-72.
58. Colpitts, T.M., et al., *Use of a tandem affinity purification assay to detect interactions between West Nile and dengue viral proteins and proteins of the mosquito vector*. *Virology*, 2011. **417**(1): p. 179-87.
59. Higa, L.M., et al., *Modulation of alpha-enolase post-translational modifications by dengue virus: increased secretion of the basic isoforms in infected hepatic cells*. *PLoS One*, 2014. **9**(8): p. e88314.

60. Pereira, M.H., et al., *Heat Shock Proteins and Blood-Feeding in Arthropods*, in *Heat Shock Proteins in Veterinary Medicine and Sciences*, A.A.A. Asea and P. Kaur, Editors. 2017, Springer International Publishing: Cham. p. 349-359.
61. Modis, Y., et al., *A ligand-binding pocket in the dengue virus envelope glycoprotein*. Proc Natl Acad Sci U S A, 2003. **100**(12): p. 6986-91.
62. Mishra, S., L.C. Murphy, and L.J. Murphy, *The Prohibitins: emerging roles in diverse functions*. J Cell Mol Med, 2006. **10**(2): p. 353-63.
63. Bavelloni, A., et al., *Prohibitin 2: At a communications crossroads*. IUBMB Life, 2015. **67**(4): p. 239-54.
64. Chumchanchira, C., et al., *A 2D-proteomic analysis identifies proteins differentially regulated by two different dengue virus serotypes*. Sci Rep, 2024. **14**(1): p. 8287.
65. Huang, G., E. Vergne, and D.J. Gubler, *Failure of dengue viruses to replicate in Culex quinquefasciatus (Diptera: Culicidae)*. J Med Entomol, 1992. **29**(6): p. 911-4.
66. Greber, U.F., *Signalling in viral entry*. Cell Mol Life Sci, 2002. **59**(4): p. 608-26.
67. Lequime, S., et al., *Genetic Drift, Purifying Selection and Vector Genotype Shape Dengue Virus Intra-host Genetic Diversity in Mosquitoes*. PLoS Genet, 2016. **12**(6): p. e1006111.
68. Suzuki, Y., et al., *Non-retroviral Endogenous Viral Element Limits Cognate Virus Replication in Aedes aegypti Ovaries*. Curr Biol, 2020. **30**(18): p. 3495-3506 e6.
69. Concordet, J.P. and M. Haeussler, *CRISPOR: intuitive guide selection for CRISPR/Cas9 genome editing experiments and screens*. Nucleic Acids Res, 2018. **46**(W1): p. W242-W245.
70. Artal-Sanz, M., et al., *The mitochondrial prohibitin complex is essential for embryonic viability and germline function in Caenorhabditis elegans*. J Biol Chem, 2003. **278**(34): p. 32091-9.
71. Park, S.E., et al., *Genetic deletion of the repressor of estrogen receptor activity (REA) enhances the response to estrogen in target tissues in vivo*. Mol Cell Biol, 2005. **25**(5): p. 1989-99.
72. Qin, Z.L., et al., *Fetal bovine serum inhibits hepatitis C virus attachment to host cells*. J Virol Methods, 2013. **193**(2): p. 261-9.
73. Fansiri, T., et al., *Genetic mapping of specific interactions between Aedes aegypti mosquitoes and dengue viruses*. PLoS Genet, 2013. **9**(8): p. e1003621.
74. Dickson, L.B., et al., *Exome-wide association study reveals largely distinct gene sets underlying specific resistance to dengue virus types 1 and 3 in Aedes aegypti*. PLoS Genet, 2020. **16**(5): p. e1008794.
75. Gubler, D.J., et al., *Variation in susceptibility to oral infection with dengue viruses among geographic strains of Aedes aegypti*. Am J Trop Med Hyg, 1979. **28**(6): p. 1045-52.
76. Dabo, S., et al., *Extensive variation and strain-specificity in dengue virus susceptibility among African Aedes aegypti populations*. PLoS Negl Trop Dis, 2024. **18**(3): p. e0011862.
77. Aubry, F., et al., *Recent African strains of Zika virus display higher transmissibility and fetal pathogenicity than Asian strains*. Nat Commun, 2021. **12**(1): p. 916.
78. Stapleford, K.A., et al., *Whole-Genome Sequencing Analysis from the Chikungunya Virus Caribbean Outbreak Reveals Novel Evolutionary Genomic Elements*. PLoS Negl Trop Dis, 2016. **10**(1): p. e0004402.

79. Fontaine, A., et al., *Excretion of dengue virus RNA by Aedes aegypti allows non-destructive monitoring of viral dissemination in individual mosquitoes*. Sci Rep, 2016. **6**: p. 24885.
80. Merklings, S.H., et al., *Multifaceted contributions of Dicer2 to arbovirus transmission by Aedes aegypti*. Cell Rep, 2023. **42**(8): p. 112977.
81. Jasinskiene, N., J. Juhn, and A.A. James, *Microinjection of A. aegypti embryos to obtain transgenic mosquitoes*. J Vis Exp, 2007(5): p. 219.

-GENERAL DISCUSSION-

Conclusions & Perspectives

GENERAL DISCUSSION

In 1909, Sir Robert Boyce, the founder of the Liverpool School of Tropical Medicine, made a bold prediction: the fate of human civilization would be determined by one of two factors: “Mosquito or Man”. More than a century later, it has become evident that the mosquito has had a profound impact on human history – and science. As the historian Timothy C. Winegard observed, “*mosquito-borne diseases have proven far deadlier than manpower, materials or the minds of the most brilliant generals*”. The now deeply researched mosquito has concentrated scientific efforts to develop new weapons in this war opposing mosquitoes and man. As stated in the “Art of war” of Sun Tzu, “*Know the enemy and know yourself, and need not fear the outcome of a hundred battles*”. Whether I know more about myself after reaching the end of the writing of this manuscript is not to be discussed here, however, knowledge about our insect archnemesis has certainly grown exponentially in the last decades. In this specific context, the “enemy” encompasses two entities, mosquitoes and viruses. Therefore, elucidating the obscure secrets of these two allies represents a valuable strategy in the battle against arboviral diseases, with the potential to transform their own resources into a weapon in our favor.

This thesis has been centered on research efforts to describe the molecular interface between the *Aedes aegypti* mosquito and flaviviruses. In this last section, I will discuss the **lessons learnt in the light of the studies conducted in the context of this work, and the future of the investigation of the molecular determinants of mosquito vector competence.**

I- Lessons learnt

A) Chapter 1: *A Vago-like gene enhances dengue and Zika virus dissemination in Aedes aegypti*

The project described in the first chapter intended to study the antiviral effect of the cytokine-like factor Vago -initially identified and characterized in *Drosophila*- in *Ae. aegypti*. However, our phylogenetic study revealed that the Vago-like genes described in mosquitoes had erroneously been designated as Vago homologs. Moreover, our infection data challenge the dogma that members of the Vago gene family are antiviral factors and instead provided evidence that *Ae. aegypti* Vago-like gene 1 (VLG-1) enhanced DENV and ZIKV dissemination in the mosquito’s body. Lessons learnt from this study are two-fold.

First, the well-established **dogma** that Vago-like genes are antiviral cytokine analogs in mosquitoes was in fact supported by very little data obtained in **in vitro systems**. Notably, *in vitro* models do not reproduce virus dissemination between different cells and organs. Our

-GENERAL DISCUSSION-

study highlights the necessity of *in vivo* studies that recapitulate the complexity of the vector-virus system.

Second, our study illustrates that the notion of “**gene homology**” is complex and needs careful examination. In order to call a given gene “a homolog”, a certain degree of sequence similarity, combined with evolutionary evidence that the considered genes derive from a common ancestor, are necessary. In addition, it is essential to perform reciprocal homolog searches for each counterpart to ensure that the most likely homolog match is identified. In the literature that had been published on *Vago* genes in mosquitoes, an incorrect homolog identification combined with the assumption of a conserved function has led to the inaccurate designation of *Vago*-like genes as strict *Vago* homologs and prolonged the notion that *Vago* genes exerted antiviral activity in mosquitoes.

B) Chapter 2: Cytochrome P450 4g15 polymorphism mediates DENV susceptibility in a field-derived *Aedes aegypti* population

The **second chapter** describes a natural resistance phenotype identified in a specific mosquito population from Bakoumba, Gabon, upon DENV infection. It also illustrates how the extensive genetic diversity of natural mosquito populations can be used as a resource for functional studies. The key finding of this body of work is that polymorphisms in the promoter sequence of the identified resistance factor *P450 4g15* underlie, at least in part, resistance to DENV, highlighting another layer of complexity in the description of GxG interactions. This study is the first report of **polymorphism in the promoter of a gene driving phenotypic variation in vector competence** within a population. While this can hinder the quest of a universal resistance factor that can be used as a target for vector control methods, it also provides an opportunity to design fine-tuned strategies specific to a mosquito population or viral pathogen and that minimize the impact on mosquito ecology in the wild.

Arboviruses are unlikely to shape the evolution of vector competence genes. Indeed, because flavivirus infection in mosquitoes has very limited fitness cost [1], and because the proportion of flavivirus-carrying mosquitoes in wild populations is very low even in regions where active transmission is reported [2, 3], strong co-evolution between mosquitoes and viruses is not expected [4]. The polymorphism observed in mosquito genetic factors is likely driven by other processes. For instance, more prevalent pathogens of mosquitoes might be the main evolutionary drivers of diversity in vector competence genes.

Additionally, *P450 4g15* was shown to drive both resistance to DENV as well as resistance to desiccation. Other examples of pleiotropy of molecular factors associated with resistance to

arboviral infection and with response to environmental stress have been described [5, 6]. For instance, a study demonstrated that the peritrophin-coding gene *AePer50* confers protection of the midgut epithelium against desiccation in dry environments and also controls midgut permissiveness to ZIKV [5]. Another study found that nutritional stress enhances susceptibility to DENV because mosquito immune factors also respond to diet-associated stress [6]. This parallel suggests a functional link between **resistance to environmental stress and vector competence**. This hypothesis has significant implications in the context of climate change, suggesting a need for monitoring the emergence of environmental adaptations in mosquitoes that could potentially shape changes in vector competence.

C) Chapter 3: *In vivo characterization of a candidate dengue virus receptor, prohibitin-2, in Aedes aegypti mosquito midguts*

In the **third chapter**, we attempted to confirm the function of the candidate DENV receptor *prohibitin-2* in *Ae. aegypti* midguts. This candidate receptor had been identified based on its interaction with DENV envelope proteins in non-native conditions and in an *in vitro* system [7, 8]. Yet, as mentioned previously, **in vitro models** do not recapitulate the physiological conditions encountered by the virus during the infection process in the mosquito vector and future studies aiming at identifying viral receptors should focus on *in vivo* models. Remarkably, most studies on flavivirus receptor identification in mosquitoes were published over 15 years ago. Since this represents a major knowledge gap in the description of arbovirus transmission by mosquito vectors, it is likely that this illustrates the lack of available *in vivo* interactomic tools which would limit the **risks of detecting irrelevant interactions** between mosquito and virus proteins. Nevertheless, viral receptors are ideal therapeutic targets since interfering with viral invasion before infection is established in the vector would be a promising approach. Consequently, efforts to identify these receptors should not be abandoned but approached with more relevant methodologies. The optimization of *in vivo* tools for direct identification of receptor-ligand interactions, such as TRICEPS or APEX-based proximity labelling [9, 10] could support these attempts.

II- Choosing the right approach and material

This PhD work employed both **targeted and unbiased approaches** to identify molecular determinants of mosquito competence. Targeted approaches are inherently more specific and facilitate the interpretation of results as they are hypothesis-driven. However, they are also subject to limitations in their scope and depend on preexisting knowledge. Unbiased approaches offer a more comprehensive perspective and are more prone to new discoveries. Conversely, they are resource-intensive, can be challenging to interpret, and often require

-GENERAL DISCUSSION-

interdisciplinary expertise. In conclusion, targeted approaches are particularly efficient when prior research established a solid foundation, whereas unbiased approaches provide a broader and often more relevant description of the molecular landscape underlying vector competence mechanisms. Both approaches are complementary and are best when integrated: **unbiased methods** can be employed to generate hypotheses and identify new candidates, which can then be further characterized using **targeted approaches**.

As for **genetic tools**, the development and application of mosquito omics, or “mozomics” [11], such as spatial and single-cell transcriptomics, epigenomics, and metagenomics, will facilitate a comprehensive characterization of the molecular interactions between viral and mosquito factors, offering an **unprecedented level of resolution, spectrum, and approach integration**. For instance, the identification of tissue- and cell-specific markers will facilitate the refinement of reverse genetics strategies using specific drivers of expression. The future of mosquito molecular research lies in advanced omics approaches combined with technologies such as CRISPR/Cas9, as well as interdisciplinary studies, integrative approaches and machine learning to unravel the molecular basis of vector competence.

Finally, laboratory strains of mosquitoes are suboptimal **models** for such studies. They have genetically drifted since their collection from the field [12], years or even sometimes decades ago, and share a uniformized microbiota [13]. It is critical that fundamental research on mosquito immunity includes **field-derived** mosquito population studies, which account for their fantastic genetic diversity. The use of **naturally admixed mosquito populations** will also be instrumental. They are more representative of real-world crossing scenarios and, more importantly, can help address the low recombination rate issue faced in experimental QTL mapping. This is due to the mosaic pattern of ancestry tracks in their genome, which also varies considerably across individuals [14-18]. Additionally, the generation of **panels of inbred mosquito lines** will be greatly informative to characterize numerous phenotypic traits, just like the *Drosophila* genetic reference panel (DGRP) has been foundational in this insect model studies [19].

III- What's more and what's next

The **traditional dogma** posits that arthropod defense against pathogens is based on a broad-spectrum response. However, accumulating evidence of highly specific mosquito-virus interactions contradict this view and underscore the need to challenge insect immunity dogmas.

-GENERAL DISCUSSION-

This thesis work solely focused on genetically encoded drivers of mosquito competence. Yet, growing evidence exist that **other intrinsic factors influence vector competence**. For instance, non-coding genetic elements, or the mosquito microbiome and virome, have a significant effect on their vector competence (as reviewed in [20-22]). The introduction of the endosymbiont bacterium *Wolbachia* into *Aedes aegypti* mosquitoes, which inhibits arbovirus replication and transmission, is an example of how intrinsic factors of vector competence can be exploited for the control of mosquito-borne pathogen transmission [23].

Importantly, **extrinsic factors** such as temperature, humidity, or food availability can impact vector competence [5, 6, 24, 25]. From these observations comes the necessity to account for such parameters in discovery-oriented approaches. For instance, seasonal-like temperature and humidity variations could be incorporated in lab-rearing conditions.

Emerging fields, such as neuroimmunology (the study of the connections between neural tissues, intercellular hormone communication and immunity) and immunometabolism (the study of the interplay between metabolism and immunity) tend to challenge the conventional description of mosquito immunity. Similarly, **ecoimmunology** is an interdisciplinary approach to assess how interactions between host physiology and disease ecology shape immune capacity, *e.g.*, via life history, trained immunity or epigenetic processes. Modeling of the relationships between nutrition, microbiome, interactions with pathogens and behavior, from larval to adult stages, aims to encompass all variables that work in concert to define mosquito immune capacity. As stated before, integrative approaches and predictive modeling are key to a comprehensive understanding of both intrinsic and extrinsic factors of vector competence.

Potentially, the identified host dependency and restriction factors could be used as **biomarkers of vector competence for the assessment of the epidemic risk** associated with specific mosquito populations. The development of diagnostic tools to detect these biomarkers in wild mosquito populations as part of surveillance programs, combined with predictive modeling and followed by intervention strategies, represents a promising integrative approach in the fight against arboviral diseases.

Additionally, this work only focused on the mosquito's side of the vector-virus interface. Yet, **virus-associated genetic variation** has proven to be determining for the mosquito infection phenotype and should not be neglected. To date, there have been few studies that have focused on the viral factors that determine the success and virulence of flavivirus infection in mosquitoes [26-29]. This topic has been explored in the mammalian host [29-31] but remains to be investigated in depth for flavivirus-*Aedes* mosquito interactions. Moreover, experimental

-GENERAL DISCUSSION-

studies are once more not necessarily representative of natural conditions, as the majority of them relies on lab-passaged viruses. Ideally, clinical or field-derived isolates are more likely similar to viral populations found in the wild but cannot be used for extensive long-term lab-based studies.

Overall, the highlights of this work are as follows:

- **Re-evaluation of *Vago*-like genes in insect immunity:** A *Vago*-like gene was found to enhance dengue and Zika virus dissemination in *Ae. aegypti*, contradicting the generalized assumption that insect *Vago*-like genes are antiviral.
- **Genetic diversity and resistance:** Polymorphisms in the promoter sequence of the *P450 4g15* gene were found to mediate resistance to DENV in a field-derived mosquito population, illustrating the impact of genetic diversity on vector competence.
- **Limitations of *in vitro* models:** Our efforts to confirm prohibitin-2 as a dengue virus receptor in mosquito midguts emphasized the need for *in vivo* models to identify relevant viral receptors.
- **Integrated methods for vector competence studies:** This work employed both targeted and unbiased approaches, advocating for their integration to identify and characterize molecular determinants of vector competence.
- **Challenging insect immunity dogmas:** Our findings challenge the traditional dogma of broad-spectrum insect immunity by providing evidence of highly specific mosquito-virus interactions.
- **Holistic approach of vector competence:** A holistic approach integrating genetic, molecular, physiological and ecological variables will offer a more comprehensive understanding of vector competence.

In conclusion, this overview demonstrates that we have only begun to explore the potential of this research field. This thesis work contributes to the generation of fundamental knowledge regarding the molecular interactions between mosquitoes and viruses that underlie vector competence. Ultimately, the integration of advanced genetic tools and multidisciplinary approaches represents a crucial step in the development of novel strategies to combat arboviral diseases. These strategies will ultimately lead to the implementation of innovative measures to mitigate the global impact of mosquito-borne diseases.

REFERENCES

1. Lambrechts, L. and T.W. Scott, *Mode of transmission and the evolution of arbovirus virulence in mosquito vectors*. Proc Biol Sci, 2009. **276**(1660): p. 1369-78.
2. Grubaugh, N.D., et al., *Genomic epidemiology reveals multiple introductions of Zika virus into the United States*. Nature, 2017. **546**(7658): p. 401-405.
3. Gutierrez-Bugallo, G., et al., *Vector-borne transmission and evolution of Zika virus*. Nat Ecol Evol, 2019. **3**(4): p. 561-569.
4. Lambrechts, L. and M.C. Saleh, *Manipulating Mosquito Tolerance for Arbovirus Control*. Cell Host Microbe, 2019. **26**(3): p. 309-313.
5. Accoti, A., et al., *Dehydration induced AePer50 regulates midgut infection in Ae. aegypti*. bioRxiv, 2023.
6. Yan, J., et al., *Nutritional stress compromises mosquito fitness and antiviral immunity, while enhancing dengue virus infection susceptibility*. Commun Biol, 2023. **6**(1): p. 1123.
7. Kuadkitkan, A., et al., *Identification and characterization of prohibitin as a receptor protein mediating DENV-2 entry into insect cells*. Virology, 2010. **406**(1): p. 149-61.
8. Paingankar, M.S., M.D. Gokhale, and D.N. Deobagkar, *Dengue-2-virus-interacting polypeptides involved in mosquito cell infection*. Arch Virol, 2010. **155**(9): p. 1453-61.
9. Frei, A.P., et al., *Direct identification of ligand-receptor interactions on living cells and tissues*. Nat Biotechnol, 2012. **30**(10): p. 997-1001.
10. Xu, Y., X. Fan, and Y. Hu, *In vivo interactome profiling by enzyme-catalyzed proximity labeling*. Cell Biosci, 2021. **11**(1): p. 27.
11. Ruzzante, L., M. Reijnders, and R.M. Waterhouse, *Of Genes and Genomes: Mosquito Evolution and Diversity*. Trends Parasitol, 2019. **35**(1): p. 32-51.
12. Gloria-Soria, A., et al., *Genetic diversity of laboratory strains and implications for research: The case of Aedes aegypti*. PLoS Negl Trop Dis, 2019. **13**(12): p. e0007930.
13. Dickson, L.B., et al., *Diverse laboratory colonies of Aedes aegypti harbor the same adult midgut bacterial microbiome*. Parasit Vectors, 2018. **11**(1): p. 207.
14. Bennett, K.L., et al., *Historical environmental change in Africa drives divergence and admixture of Aedes aegypti mosquitoes: a precursor to successful worldwide colonization?* Mol Ecol, 2016. **25**(17): p. 4337-54.
15. Kotsakiozi, P., et al., *Population structure of a vector of human diseases: Aedes aegypti in its ancestral range, Africa*. Ecol Evol, 2018. **8**(16): p. 7835-7848.
16. Rose, N.H., et al., *Climate and Urbanization Drive Mosquito Preference for Humans*. Curr Biol, 2020. **30**(18): p. 3570-3579 e6.
17. Suarez-Pajes, E., et al., *Genetic Ancestry Inference and Its Application for the Genetic Mapping of Human Diseases*. Int J Mol Sci, 2021. **22**(13).
18. Schaid, D.J., W. Chen, and N.B. Larson, *From genome-wide associations to candidate causal variants by statistical fine-mapping*. Nat Rev Genet, 2018. **19**(8): p. 491-504.
19. Mackay, T.F., et al., *The Drosophila melanogaster Genetic Reference Panel*. Nature, 2012. **482**(7384): p. 173-8.
20. Lewis, J., et al., *Intrinsic factors driving mosquito vector competence and viral evolution: a review*. Front Cell Infect Microbiol, 2023. **13**: p. 1330600.

-GENERAL DISCUSSION-

21. Kramer, L.D. and A.T. Ciota, *Dissecting vectorial capacity for mosquito-borne viruses*. *Curr Opin Virol*, 2015. **15**: p. 112-8.
22. Hardy, J.L., et al., *Intrinsic factors affecting vector competence of mosquitoes for arboviruses*. *Annu Rev Entomol*, 1983. **28**: p. 229-62.
23. Yen, P.S. and A.B. Failloux, *A Review: Wolbachia-Based Population Replacement for Mosquito Control Shares Common Points with Genetically Modified Control Approaches*. *Pathogens*, 2020. **9**(5).
24. Carvajal-Lago, L., et al., *Implications of diet on mosquito life history traits and pathogen transmission*. *Environ Res*, 2021. **195**: p. 110893.
25. Bellone, R. and A.B. Failloux, *The Role of Temperature in Shaping Mosquito-Borne Viruses Transmission*. *Front Microbiol*, 2020. **11**: p. 584846.
26. Fontaine, A., et al., *Epidemiological significance of dengue virus genetic variation in mosquito infection dynamics*. *PLoS Pathog*, 2018. **14**(7): p. e1007187.
27. Weaver, S.C., et al., *Population bottlenecks and founder effects: implications for mosquito-borne arboviral emergence*. *Nat Rev Microbiol*, 2021. **19**(3): p. 184-195.
28. Lequime, S., et al., *Genetic Drift, Purifying Selection and Vector Genotype Shape Dengue Virus Intra-host Genetic Diversity in Mosquitoes*. *PLoS Genet*, 2016. **12**(6): p. e1006111.
29. Liu, J., et al., *Role of mutational reversions and fitness restoration in Zika virus spread to the Americas*. *Nat Commun*, 2021. **12**(1): p. 595.
30. Avila-Perez, G., et al., *A natural polymorphism in Zika virus NS2A protein responsible of virulence in mice*. *Sci Rep*, 2019. **9**(1): p. 19968.
31. Regla-Nava, J.A., et al., *A Zika virus mutation enhances transmission potential and confers escape from protective dengue virus immunity*. *Cell Rep*, 2022. **39**(2): p. 110655.

OTHER SCIENTIFIC WORK

Publications:

Merkling SH, Crist AB, Henrion-Lacritick A, Frangeul L, Couderc E, Gausson V, Blanc H, Bergman A, Baidaliuk A, Romoli O, Saleh MC, Lambrechts L. Multifaceted contributions of *Dicer2* to arbovirus transmission by *Aedes aegypti*. Cell Rep. 2023 Aug 29;42(8):112977 (2023) [10.1016/j.celrep.2023.112977](https://doi.org/10.1016/j.celrep.2023.112977)

In preparation:

Couderc E, Lambrechts L & Merklng SH. Revealing the mosquito's assets: discovery of host molecular factors modulating arbovirus infection in *Aedes aegypti* mosquitoes. (*review, in preparation*)

Merkling SH, Couderc E, Crist AB, Jupatanakul N, Lavina M, Hardy D, Burckbuchler M, Moltini-Conclois I, Fontaine A, Sismeiro O, Legendre R, Varet H, Jiolle D, Paupy C, Marois E, Lambrechts L. Polymorphisms in the cytochrome *P450 4g15* mediate dengue virus susceptibility in a *Aedes aegypti* field-derived population. (*in preparation*)

Vial T, Lopez-Maestre H, Couderc E, Pinaud S, Marti G, Merklng SH. Cellular and metabolic landscape of the midgut and fat body in blood-fed *Aedes aegypti* mosquitoes. (*in preparation*)

Oral communications:

Poster presentation at the Vector Kolymbari meeting, Kolymbari, Greece, July 2024. "A *Vago*-like gene enhances dengue and Zika virus dissemination in *Aedes aegypti*". Couderc E, Crist AB, Daron J, Varet H, van Hout FAH, Miesen P, Palatini U, Dabo S, Vial T, Lambrechts L, Merklng SH.

Oral presentation at the American Society of Tropical Medicine and Hygiene (ASTMH) conference, Chicago, USA, October 2023. "*Vago* genes in *Aedes aegypti* mosquitoes (or how to challenge mosquito immunity dogmas)". Couderc E, Crist AB, Baidaliuk A, Palatini U, Lambrechts L, Merklng SH.

Poster presentation at the Jacques Monod conference « Insect models for infection biology », Roscoff (France), June 2023. "A novel proviral function for *Vago* genes in *Aedes aegypti* mosquitoes upon dengue virus infection". Couderc E, Crist AB, Baidaliuk A, Palatini U, Lambrechts L, Merklng SH.

Poster presentation at the *Journées francophones de Virologie*, Strasbourg (France), April 2022. "Analysis of early resistance to dengue virus in *Aedes aegypti* mosquito midguts". Couderc E, Merklng SH, Lavina M, Crist AB, Simeiro O, Varet H, Legendre R, Jiolle D, Ayala D, Paupy C, Lambrechts L.